THE EFFECT OF JEWELLERY AND THE HUMAN HAND ON SAR AND ANTENNA PERFORMANCE

by

Noor Asmawati Samsuri, MSc

A Doctoral Thesis submitted in partial fulfilment of the requirements for the award of Doctor of Philosophy of Loughborough University

January 2009

Abstract

This thesis investigates the effect of the human hand and metallic jewellery items worn on the human head and hand on SAR and on the antenna radiation patterns at 900 and 1900 MHz. The field excitation is provided by means of a λ/4 monopole antenna on top of a metal box to emulate a simple handset. A planar inverted 'F' antenna (PIFA) is also used for comparison with the monopole. This thesis presents a detailed parametric study utilizing computer simulations via the Transmission Line Matrix (TLM) method and measurements from the DASY4 SAR measurement system. Two different head and hand geometries are considered. Firstly a homogenous spherical head and block-hand were used in the simpler simulation, while the more realistic head and hand models were employed for the detailed study. The hand models include fingers which allow the metallic jewellery rings to be examined.

The human hand has a significant effect on Specific Absorption Rate (SAR) and on the antenna pattern due to energy absorption and possible reflection at the hand dielectric boundary. In addition, the effects of different sizes, orientation, and distance of the metallic loop-like jewellery items relative to the antenna have been investigated. The metallic rings worn on the hand tend to reduce the SAR and could also alter the antenna radiation performance. The wrist worn bangle has very little effect on the results at the frequencies tested due to its position that is relatively far away from the handset antenna. The earrings could significantly influence the SAR and the radiation patterns, but the effects varied depending on the earring's diameter, its position relative to the head, the frequency and the type of antenna in use. The effect of the combination of the hand, the earring and the finger ring only show minor difference on the SAR values and on the antenna radiation patterns.

Measurements of the effects of the hand and metallic jewellery items on SAR were performed inside a Standard anthropomorphic model (SAM) head phantom. A novel liquid hand phantom with realistic fingers has been manufactured, which allow the effect of metallic ring to be further investigated. Measurement results support the simulation results.

Acknowledgements

I am truly indebted to several people for their guidance and valuable support throughout this PhD work.

First and foremost, I would like to express my deepest gratitude to my supervisor Dr. James Flint for his helps, guidance, continuous supports and patience, without which I would not be able to complete this thesis.

I would like to extend my sincere appreciation to all my colleagues and friends herein Loughborough and back-in Malaysia who always there to share every single moment over the past four years. Their advice, friendship and encouragements were an invaluable contribution to this project.

My most sincere goes to my parents and family for their prayer, patience, understanding and encouragement throughout this work. Finally, I express my special thanks to my beloved husband Azeze Harun, who has filled my life with happiness and always there to share the good and bad times, making my life herein Loughborough thoroughly enjoyable. His endless love, support and understanding are very much appreciated.

Last but not least, I would like to thank Associate Prof. Dr. Ngasri Dimon, head of Radio and Communications Department, University of Technology Malaysia for all the support, advice and encouragement he have given me throughout this work. Also thanks to University of Technology Malaysia who provided the financial support over the past four years.

Abbreviations

BSL	Body simulating liquid
CENELEC	European Committee for Electrotechnical Standardization
DAE	Data acquisition electronics
DASY	Dosimetric assessment system
dB	Decibels
EMI	Electromagnetic interference
EMP	Electromagnetic pulse
EOC	Electro-optical converter
ERP	Ear reference point
FCC	Federal Communications Commission
FDTD	Finite-difference time-domain
FEM	Finite Element Method
HSL	Head simulating liquid
ICNIRP	International Commission Non-Ionizing Radiation Protection
MoM	Method of Moment
MRI	Magnetic resonance imaging
PA	DuraForm Polyamide
PCS	Personal communication services
PIFA	Planar inverted 'F' Antenna
RCS	Radar cross-section
RF	Radio frequency
SAM	Standard anthropomorphic model
SAR	Specific Absorption Rate
SLS	Selective laser sintering
TLM	Transmission Line Matrix

Contents

Contents

List of Figures

List of Tables

Chapter 1

Introduction

1.0 Introduction

The use of mobile phones is increasing day by day and yet at the same time some users have had growing concerns about possible health effects due to the electromagnetic field radiated by the antenna. Conventionally, the mobile handset is placed very close to the head and partially masked by the human fingers where a certain amount of electromagnetic energy passes through the head and the hand rather than being directly radiated. Therefore, the validity of the mobile handset antenna characteristics (measured in free space) is placed in doubt due to the presence of the human head and the hand. The issue is complicated further by the presence of additional conductors such as external metallic objects (wire-framed spectacles and hands-free devices) and also metallic implants (surgical pins and jewellery) that may also have effects on the amount of the electromagnetic field radiated by the antenna. Therefore, there is a need to investigate the interaction between the mobile handset, the user and any additional conductors, particularly in the near field of the unit's antenna. Numerous studies have examined the interaction between the electromagnetic fields radiated by the mobile handset, the human head, the hand [1-4], additional conductors such as external objects (wire-framed spectacles, hands-free) [5, 6] and metallic implants (surgical pins, jewellery) [7-9]. In recent years, a number of studies have focused on the effect of metallic jewellery such as earring worn on the ear [8, 9] and implanted metallic loops and pins inside the head [7]. These investigations found that metallic earrings, metallic loops and rings could increase the SAR.

1.1 Objectives of the project

The main objective of this research is to investigate the effect of the human hand and metallic jewellery items worn on the head and the hand on SAR and on the antenna radiation performance. This research involves hand modelling, hand phantom construction, computer simulations and measurements. The objectives can be summarized as follows:

> ➢ To model a realistic hand model for simulations in order to investigate the effect of the hand on SAR and on the antenna performance.

> ➢ To model and manufacture a hand phantom for measurements which allow the effect of metallic ring worn on the finger to be studied.

> ➢ To determine the effect of wearing a metallic earring (with and without a ring) on SAR inside the head and on the antenna performance.

> ➢ To study the effects of the hand and the metallic jewellery items on SAR by means of measurements utilizing a phantom head and hand; and to compare with simulations.

> ➢ To form a conclusion on the effect brought about by the metallic jewellery items; and any possible implications for mobile handset users and also the manufacturers of mobile handsets.

1.2 Hypothesis

The presence of the human hand holding a mobile handset in close proximity to the human head is expected to influence the SAR inside the head. The effects are likely to depend on the antenna type and placement. The presence of metallic jewellery items worn on the human head and hand are expected to introduce additional effects. It is hypothesized that different sizes of the metallic-loop like jewellery items worn on the human head and hand will cause different effects on the SAR and antenna pattern.

1.3 Contributions of the thesis

The effect of the hand holding a mobile handset is of particular importance due to its proximity to the handset-antenna. In this thesis, two different homogeneous hand geometries are included which allow comparison to be made that has not been previously investigated. To begin a simplified homogenous block-hand was used followed by a homogeneous realistic hand model in the latter. The realistic hand model includes fingers which allow the effect of metallic jewellery rings to be investigated.

Two different head models are considered in the simulation study. A simple spherical homogenous head model was used in the earlier section to estimate the effect of the head on the antenna performance and to estimate the amount of energy absorbed in the head itself. The latter studies employ a homogeneous SAM head model and the results are compared to the spherical head. Different shapes of the head models have been shown to be important since it defines the practical head-antenna distance, the head-jewellery distance and the coupling effects, consequently affecting the way the metallic jewellery items interact with the human body and the response to the electromagnetic field, which results in different SAR results.

This thesis also includes the effect of metallic earrings, rings and bangles. None of the previously published research has considered the hand while investigating the effect of metallic jewellery items. Nevertheless, no other published research to date has considered the presence of metallic rings (and a bangle) worn on the hand while investigating the SAR in the head and the antenna performance. The introduction of metallic rings and bangle on the hand is found to cause additional effects. The metallic ring is placed on different fingers for comparison. Different sizes of earrings have also been investigated.

Additionally, two different antennas (a $\lambda/4$ monopole and a PIFA) operating at two different frequencies are employed in this thesis. The antenna is placed in the 'cheek' position as is ordinarily used amongst the majority of users. This work reports novel

results utilizing a PIFA antenna while investigating the effect of metallic jewellery items and thus is fundamentally different from the previous research concerning the effect of the metallic jewellery.

This thesis also includes results of measurements with the hand and metallic jewellery items. A novel liquid hand phantom has been manufactured. The hand phantom is very useful since it strikes an ordinary pose of holding a mobile handset and can be used next to the head phantom. The hand phantom also allows different simulating liquid to be used for measurements of different frequencies. It also includes realistic fingers, which enables the effect of the metallic ring to be measured, which was the main motivation for its construction. SAR measurements with a phantom head wearing an earring together with a phantom hand wearing a ring, is a novel application. Simulation and measurement results of the effect of the hand and metallic jewellery items are compared.

1.4 Overview of the thesis

The thesis comprises of seven chapters and includes both a description of prior art and a detailed computer simulation and measurement campaign.

Chapter 2 outlines a brief summary of the theory of SAR, including the factors affecting the SAR, the standards and the limit guidelines set by expert groups. This chapter also discusses the interaction between the antenna with the human head, the hand and the metallic jewellery items worn on the head and the hand. Some of the human head and hand geometry and the phantom models commonly used are also discussed.

Chapter 3 presents a simulation study of the effect brought about by metallic loop-like jewellery items. A set of simulations are presented to validate the capability and accuracy of Microstripes TLM in dealing with the interaction between the antenna, the human and metallic jewellery items. The results are compared to published results using other commercialized simulation software based on Finite-difference time-

domain (FDTD). In order to investigate the effect brought about by the small ring worn on human fingers, a simple block-hand model with cylindrical fingers was modelled for simulation purposes, whilst a simple block hand phantom was manufactured for measurements. The effects of metallic ring worn on the finger on the field distribution and on SAR inside the hand were investigated.

Chapter 4 shows the effects of the human head, the hand and metallic jewellery items on SAR and on the antenna radiation patterns. A homogeneous spherical head and a block-hand model are employed in this chapter. The latter study includes a block hand model with cylindrical fingers, which allows the effect of metallic rings to be studied. The effects of metallic earrings worn on the ear are presented for different sizes of earring.

Chapter 5 performs the same simulations as in Chapter 4, but the more realistic head (SAM) and hand models are employed in this chapter. The SAM head includes the ears, which allows the earrings to be inserted into the earlobe, representing a more realistic worn position. This chapter presents simulation results of the effect of the hand with both metallic earrings and finger rings on SAR and on the antenna radiation patterns. The simulation results utilizing a PIFA antenna are also included in the study and compared to the monopole.

Chapter 6 shows details of measurements of the effect of the hand and metallic jewellery on SAR inside a SAM head phantom filled with tissue equivalent liquid. The measurement study includes a novel liquid hand phantom with realistic fingers, which allows the effect of metallic ring to be further investigated. The hand phantom construction is also discussed in this chapter. Different sizes of earrings are investigated, whilst the ring is placed on different fingers for comparison. The SAR results from the measurements are compared to simulations.

Finally, Chapter 7 draws conclusions from the research considered in this thesis. Recommendations for future work are also outlined.

1.5 References

[1] S. I. Watanabe, H. Taki, T. Nojima and O. Fujiwara, "Characteristic of the SAR distributions in a head exposed to electromagnetic fields radiated by a hand-held portable radio," *IEEE Transactions on Microwave Theory and Techniques,* vol. 44, pp. 1874 – 1883, Oct. 1996.

[2] M. Francavilla, A. Schiavoni, P. Bertotto and G. Richiardi, "Effect of the hand on cellular phone radiation," *IEE Proceedings on Microwaves, Antennas and Propagation,* vol. 148, pp. 247 – 253, Aug. 2001.

[3] M. Lundmark, R. S. Calvo, P. S. Kildal and C. Orlenius, "A solid hand phantom for mobile phones and results of measurements in reverberation chamber," *Antennas and Propagation Society International Symposium, IEEE,* vol. 1, pp. 719 – 722, 2004.

[4] K. Ogawa, T. Matsuyoshi and K. Monma, "An analysis of the performance of a handset diversity antenna influenced by head, hand and shoulder effects at 900 MHz," *Antennas and Propagation Society International Symposium, IEEE,* vol. 2, pp. 1122 – 1125, July. 1999.

[5] W. Whittow and R. Edwards, "A study of changes to specific absorption rates in the human eye close to perfectly conducting spectacles within the radio frequency range 1.5 to 3.0 GHz," *IEEE Transaction on Antenna and Propagation,* vol. 52, pp. 3207-3212, 2004.

[6] S. E. Troulis, W. G. Scanlon and N. E. Evans, "Effect of 'hands free' leads and spectacles on SAR for a 1.8 GHz cellular handset," *1st Joint IEI/IEE Symposium on Telecommunications Systems Research, Dublin,* pp. 1675-1684, 2001.

[7] H. Virtanen, J. Huttunen, A. Toropainen and R. Lappalainen, "Interaction of mobile phones with superficial passive implants," *Physics in Medicine and Bio.,* vol. 50, pp. 2689-2700, 2005.

[8] W. Whittow, C. J. Panagamuwa, R. Edwards and J. C. Vardaxoglou, "Specific Absorption Rates in the Human Head Due to Circular Metallic Earrings at 1800 MHz," *Antennas and Propagation Conference, LAPC 2007, Loughborough,* pp. 277 – 280, Apr. 2007.

[9] J. Fayos-Fernandes, C. Arranz-Faz, A. Martinez-Gonzalez and D. Sanchez-Hernandez, "Effect of pierced metallic objects on SAR distributions at 900 MHz," *Bioelectromagnetics,* vol. 27, pp. 337-353, 2006.

Chapter 2

Background to the Research

2.0 Introduction

Research into the interaction between the antenna and the human body has been very topical recently. Research to date has been varied and has considered a range of human head and hand models from the simple homogeneous models to the more realistic anatomical models that include various types of different tissues. Different shapes of the head, or the hand models with different tissue properties could significantly affect the antenna performances or the SAR values. In addition, the presence of any metallic objects such as metallic jewellery items in close proximity to the unit's antenna and to the human body may also introduce additional effects. However, the effects can be expected to vary depending on the size of the metallic objects, orientation relative to the antenna, the type of antenna in use and the frequency of excitation. The interaction between the antenna and the human head, hand and metallic jewellery are discussed further in this chapter.

2.1 Specific Absorption Rate (SAR)

The number of mobile phone users has increased substantially and at the same time the level of sophistication and functionality of the mobile handset has also increased. Another recent trend in personal communication services (PCS) has seen the greater integration of different services and capabilities in devices. With the expansion of current use of cellular telephones, there has been a great interest and concern about any possible health effects due to the electromagnetic field radiated from the antenna. Conventionally, the mobile phone is placed close to the face (within the near-field

zone) where a certain amount of the electromagnetic energy is passed through the head and human body rather than being directly radiated. The energy absorbed by the human body is mainly caused by the internal electric and magnetic fields which in turn are converted to heat inside the human body. The exact amount of energy absorbed in the human body is almost inaccurate to calculate due to the complexity in the nature of the interactions. The human body itself is a complex structure and is both are heterogeneous and geometrically complex. The intensity of the energy absorbed in the body also depends on the frequency of excitation, field polarization, the dielectric properties of the exposed body (besides the size and shape) and also the presence of any additional objects in close proximity to the radiation source and the human body [1].

A widely used and generally accepted way to quantify the actual amount of electromagnetic energy absorbed by the human body is the Specific Absorption Rate (SAR). SAR indicates the amount of radio frequency (RF) energy absorbed in a dielectric material per unit time (dt) per unit mass (dm) (Eq. 1). SAR is related to the electric field or the temperature rise (dT) at a given point by Eq. 2:

$$SAR = \frac{d}{dt}\left[\frac{Energy}{dm}\right] \tag{1}$$

$$SAR = \frac{\sigma |E|^2}{\rho} = c\frac{dT}{dt} \tag{2}$$

$|E|$ is the rms electric field magnitude, σ is the conductivity (S/m), ρ is the material mass density (kg/m^3) and c is the specific heat capacity (J/(kg $^\circ$C) . The SAR is usually expressed in Watts per kilogram (W/kg) and is typically quoted in terms of an average value measured over either 1 g or 10 g of tissues.

The SAR can be obtained by mathematical modelling, computer modelling or derived measurement by using a phantom filled with tissue simulating liquid that has properties equivalent to the human tissue for the different required frequencies [2]. An E-field probe is used in the phantom method to measure the electric fields that are induced by a mobile phone which is placed in close proximity to the head/body. The

SAR values are then can be calculated from these measured electric fields by knowing the conductivity and the material mass density of the liquid at any defined frequency of interest. During the measurement, the mobile handset is set to operate at its highest certified power level. However, in normal use, the antenna input power is typically much lower than this value due to active power control at the handset, which is used to conserve battery power. A typical power value for GSM is one-eighth of the maximum transmit power to reach the network [3, 4]. This suggests that in normal usage the actual SAR would be substantially lower than the maximum measured values.

2.1.1 Factors affecting SAR

As stated in the previous section, the intensity of the RF energy absorbed in the human body is highly dependent on the type of antenna used, the frequency of excitation and the antenna location and orientation relative to the base station. The closer the antenna is to the base station, the less power is needed to reach the network, so that less power is absorbed within the body (lower SAR values). Beside that, the size, shape, the dielectric properties of the exposed tissues and transparent objects to RF found in close proximity to the handset antenna and the body can also affect the antenna performance [5] and may also cause changes in SAR. Factors affecting SAR are shown in Figure 2.1-1.

2.1.2 Standards and SAR limits

Maximum permissible exposure limits to the RF energy have been set by several experts' organizations via SAR values[*]. International Commission Non-Ionizing Radiation Protection (ICNIRP 1998) guidelines [7] and IEEE C95.1 (1999) Standard

---

[*] Power densities are conventionally used as well (see ICNIRP guidelines). They also say that at lower frequencies the E or H field maxima should be specified. Power densities are normally used for far-field exposure

[8] outline the measurement techniques/standards for determining the SAR in the head related to the human exposure to electromagnetic fields from mobile communication devices. All cellular phones are tested and the SAR must comply within the safety limit guidelines before being made available to the customers. Different mobile phones will usually have different SAR values. The safety limits are different from country to country. Most standards (EN50360/1, ACA, ARIB) set the SAR limit to 2 W/kg over 10 g mass of tissue while the Federal Communications Commission (FCC-USA) set the limit to 1.6 W/kg over 1 g of mass tissue. Table 2.1-1 represents the basic for both ICNIRP and IEEE standards. In the ICNIRP guidelines, the SAR values are averaged in any 10 g of tissue, while the SAR is averaged over 1 g tissue for the body except the extremities which are averaged over a cube of 10 g tissue [9].
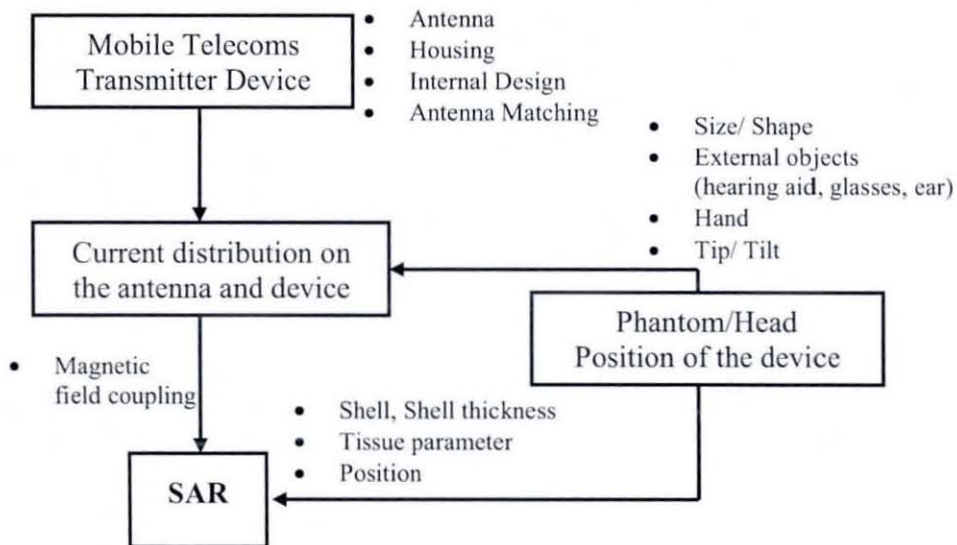
Figure 2.1-1: Factors affecting SAR [6].

Table 2.1-1: Basic SAR Restrictions (W/kg) [9].

Standard	Condition	Frequency	Whole body	Local SAR (Head and trunk)	Local SAR (Limbs)
ICNIRP	Occupation	100 kHz-10 GHz	0.4	10	20
	Gen. Pop	100 kHz-10 GHz	0.08	2	4

Standard	Condition	Frequency	Whole body	Local SAR (Except Extremities)	Local SAR (Extremities)
IEEE	Controlled	100 kHz-6 GHz	0.4	8	20
	Uncontrolled	100 kHz-6 GHz	0.08	1.6	4

Table 2.1-2: Summary of research of the human head/hand-antenna interaction.

Reference	Head	Hand	Method/Technique	Radiating source
Morishita et al. (2000)	Homogeneous boxes and spheres (brain tissue)	Block hand (muscle)	MoM (Zeland Software)	Rectangular loop (1860 MHz)
Jensen and Rahmat-Samii (1994)	Heterogeneous head	Block hand (bone, muscle)	FDTD	Monopole and side mounted PIFA (900 MHz)
Kawai and Ito (2004)	Cubical and spherical (brain), realistic homogeneous head with shell	-	FDTD	0.5λ dipole, monopole, PIFA, 0.5λ dipole with planar reflector (900 MHz, 2 GHz)
Khalatbari et al. (2006)	Homo. sphere (brain), layered sphere (brain, skull, skin), MRI based head	-	FDTD	0.5λ dipole, λ/4 monopole (900, 1800 MHz)
Okionewski and Stuchly (1996)	Homo and layered boxes, sphere and anatomical heads	Block hand (bone, muscle)	FDTD	Monopole antenna (900 MHz)
Keshvari and Lang (2005)	Anatomical heads (adult, children)	-	FDTD	0.47λ dipole antenna (900, 1800, 2450 MHz)
Ruoss (1999)	Homo. Heads (5 shapes)	-	MoM	Dipole, helical monopole (900 MHz)
Jensen and Rahmat-Samii (1995)	Anatomical head, homo. sphere (muscle)	Block hand (bone, muscle)	FDTD	Monopole; side, top and back mounted PIFA (915 MHz)
Burkhardt and Kuster (2000)	Homo. and hetero. realistic head	-	FDTD	Dipole and monopole (900, 1800 MHz)
Watanabe et al. (1996)	Hetero. Head (Japanese)	Realistic hand with thumb crook the radio	FDTD	0.5λ dipole, λ/4 monopole (900, 1500 MHz)
Bernardi et al. (1996)	Inhomogeneous head	Block hand (muscle)	FDTD	Sleeve dipole, whip antenna (900 MHz)
Dautov and Zein (2005)	Realistic homo. head (brain eq.)	-	MoM	λ/4 monopole (900, 1800 MHz)
Lee et al. (2005)	SAM head (homo. tissue eq.)	-	FDTD	Five monopole antennas
Gandhi and Kang (2004)	SAM, anatomical head (Utah, Visible human	-	FDTD	Monopole, helix antenna (835, 1900 MHz)
Toftgard et al. (1994)	Homogeneous sphere (muscle)	Block hand (muscle)	FDTD	Monopole antenna (900, 1900 MHz)
Kim and Rahmat-Samii (1997)	Six-layered sphere	-	MoM, EEM	Dipole antenna (900 MHz)
Kim and Rahmat-Samii (1998)	Anatomical head, six-layered sphere	Block hand	EEM, FDTD	Monopole, side mounted and back mounted PIFA (900, 1900 MHz) Dipole antenna (900, 1500 MHz)

Table 2.1-2: Continue

Reference	Head	Hand	Method/Technique	Radiating source
Hombach et al. (1996) Meier et al. (1997)	Head phantom (homo., hetero.)	-	FIT, FDTD FIT	Dipole antenna (1800 MHz)(1996) Dipole antenna (1800 MHz)(1997)
Koulouridis and Konstantina (2004)	Homo (brain), three-layer sphere (skin, skull, brain), MRI based head (adult, children)	-	MoM, FDTD	Helical dipole (1710 MHz)
Beard and Kainz (2004)	Sam head, anatomical heads (Visible human, Japanese male)	-	FDTD	Generic phone (monopole antenna 835 and 1900 MHz)
Kainz et al. (2005)	Sam head, 14 anatomical heads	-	FDTD	Generic phone (monopole antenna 835 and 1900 MHz)
Francavilla et al. (2001)	Anatomical head	Anatomical realistic shape	FDTD	Commercial phone (900, 1800 MHz bands)
Lundmark et al. (2004)	Head phantom (lossy liquid)	PVC tube filled with lossy liquid	Measurement (reverberation chamber)	Built-in, external, external long antenna (900, 1800 MHz)
Ogawa et al. (1999)	Cylinder (homo.)	Simple parallellepiped	Wire-grid (simulation)	Whip, PIFA antenna (900 MHz)
Li et al. (2007) Li et al. (2008)	SAM head	Inhomo. (skin, muscle, bone), homo. (realistic shape)	FDTD	Four commercial phones (1750 MHz: on 2007), (900, 1750 MHz: on 2008)
Krogerus et al. (2007)	Live test person	Real human hand	Live measurements	Mobile with internal antenna (900, 1800 MHz)
Chavannes et al. (2005)	SAM head	Homo. hand (3 positions on the handset)	FDTD	Motorola handset (1880 MHz)
Rowley and Waterhouse (1999)	Anatomical head (Visible human)	Block hand (bone, muscle)	FDTD	Monopole and shorted patch antenna (1800 MHz)
Zaridze et al. (2003)	SAM head	Homo. hand (no info.)	MAS	Monopole antenna (0.9, 1.8 MHz)
Kivekas et al. (2004)	Anatomical head	Block hand (bone, muscle)	FDTD	Patch antenna (900, 1800 MHz)
Li et al. (2000)	Anatomical head	Block hand	FDTD	Dipole, monopole, side mounted and back mounted PIFA (900 MHz, 1800 MHz)
Iskander et al. (2000)	Anatomical head, include body model (homo. 2/3 of muscle)	-	FDTD	Monopole antenna (900, 1900 MHz) PIFA antenna (900 MHz)
Pedersen (2001)	Simple head phantom (plastic filled with liquid)	Rubber glove hand phantom	Measurement (anechoic room)	Patch, helix antenna (0.9, 1.8 MHz)

2.2 Interaction of electromagnetic fields with the human body and the metallic jewellery

The interaction of electromagnetic fields and human body has been widely studied using various types of head/hand models, methods and also different types of radiating sources (Table 2.1-2). This interaction becomes an important issue that should be considering when designing the antenna for hand-held units [10-12]. When a user is exposed to the RF radiation, the current and electromagnetic fields are induced within the user's body and thus could result in tissue heating due to the dielectric losses [13]. However, the amount of energy transmitted and absorbed in the human body is highly dependent on the frequency of operation and the angle of incident, the orientation of the handset, the distance from the antenna, the shape and size of the body and the dielectric properties of the exposed tissues [14, 15]. In addition, the antenna-tissue coupling could cause antenna detuning, impedance mismatch, the gain loss and pattern degradation [10, 12]. The resonant frequency reduces and the impedance match at resonance deteriorates by the presence of a user [16]. Nevertheless, the presence of the user's body may significantly influence the radiation current distribution on the handset itself resulting in degradation of the antenna performance [12].

In addition, there is, a general fashion amongst users wearing metallic objects such as metallic spectacles, wired hands-free and jewellery on the head and the hand. These metallic objects when worn on human and placed very close to the radiating source have the potential to influence the radiation performance of the handset antenna and may also cause notable effect in SAR. The effects of the wire-framed spectacles or the hands-free wire have been widely investigated [17-21]. In recent years, there has been considerable research effort devoted to the effect of metallic implants such as surgical pins, skull and bone plates, fixtures and earrings [13-15, 22-25]. However, earrings worn in their usual position have received limited attention in the literature, while no work has yet been done regarding the effect of the rings worn on the human hand. Consequently this thesis aims to address these issues.

Figure 2.2-1 shows the general exposure[†] situation experienced by a mobile phone user during ordinary operation.
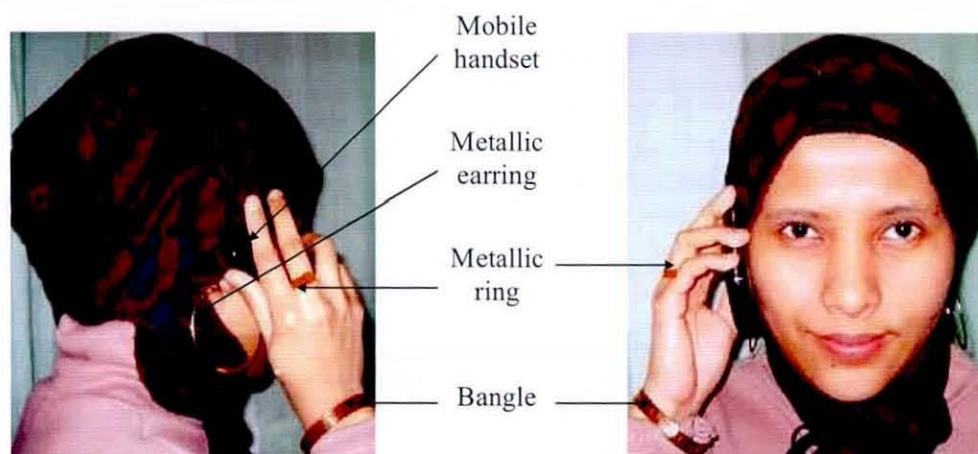
Figure 2.2-1: Mobile handset user wearing a metallic earring (pierces the earlobe), a ring (on the finger) and a bangle (on the wrist).

2.2.1 Modelling of the human head

2.2.1.1 *Human head geometry and effect of the head on the antenna performance and SAR*

Research to date has focused on a range of human head models (see Figure 2.2-2) from the simple homogeneous models with different shapes such as boxes, spheres [13], ovals; with or without the ears, eyes and nose, to the more realistic detailed heterogeneous head models [26] (see Figure 2.2-3) that includes various types of different tissues. Different head geometries with different tissue properties have the potential to give correspondingly different antenna performances or SAR values.

[†] The effect of the head, the hand and metallic jewellery items considered in this thesis

(a)   (b)
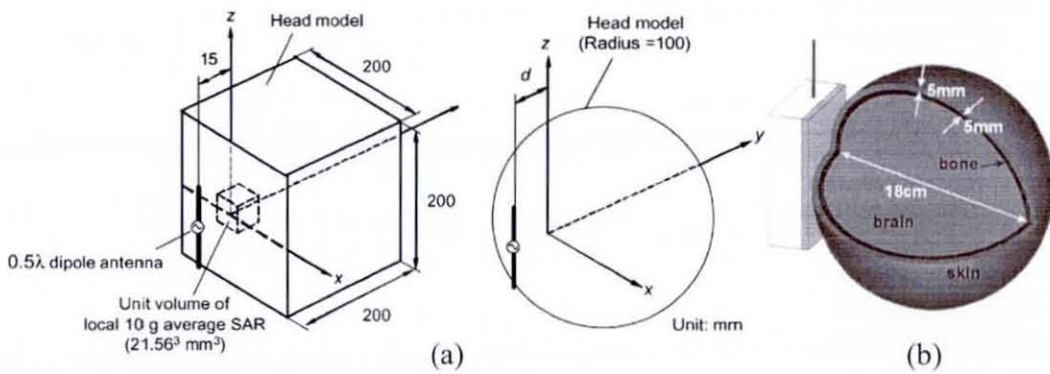
Figure 2.2-2: Simple human head model for simulations: (a) cubical and spherical head [27], (b) layered sphere [3].

(a)   (b)   (c)
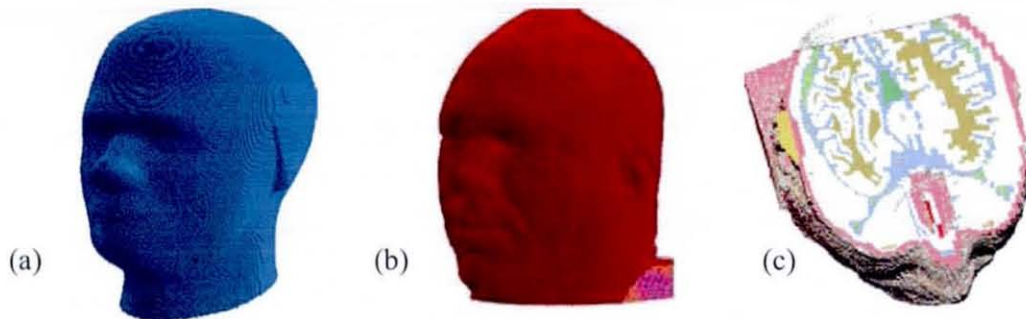
Figure 2.2-3: Realistic head models: (a) SAM head, (b) Visible Human Head [28] and (c) anatomical model of Visible Human Head [29].

In early research works, the human head was primarily modelled as a single tissue simulating liquid sphere [11, 30] or a box [30]. In [30] the box representing the head significantly decreased a monopole antenna's radiation pattern in the direction of the head, giving higher absorbed power in the head and consequently higher SAR as compared to the spherical model. The spherical model in the same study provided reasonably good agreement in the total absorbed power in the head with the relatively low resolution head models investigated in [30]. Ruoss [31] has included five different shapes of the head to investigate the effect of the geometry of the head on SAR. The first three models investigated were simple geometrical shapes, i.e., flat, spherical and ellipsoidal, while the last two model's shapes are more realistic. Ruoss [31] reported that there were only small differences in the averaged 10 g SAR between all head shapes when the antenna was placed at a range of distances from the head surface. In some studies, a multi-layer spherical head has been considered

representing the human head [3, 30, 32, 33]. Okoniewski [30] and Khalatbari [3] employed a three-layered sphere, while Kim and Rahmat-Samii [32] employed a six-layered sphere for investigations (Table 2.1-2). These investigations confirmed that the homogeneous sphere overestimates the SAR values in the head when compared to the multi-layered spherical head.

Nowadays, more realistic head models with different tissues (MRI based) or a homogeneous head with an anatomical head shape are available and been employed in order to investigate the interaction between the handset antenna and the human head [3, 30, 33-37]. Watanabe et al. [34] employ both the homogeneous and heterogeneous head models in their research (Table 2.1-2). Their study reported that the maximum local SAR and the SAR distribution on the surface of the homogeneous model agree well with the heterogeneous model. Hombach et al. [38] and Meier et al. [35] investigated the electromagnetic energy absorption in the human head at 900 and 1800 MHz respectively, by using several different numerical head phantoms based on magnetic resonance imaging (MRI) scans of three different adults and two different homogeneous phantoms. The numerical phantoms differ from each other in terms of shape, size and internal anatomy, while the homogeneous phantoms are different in shape and size. These investigations showed that only small variations existed between SAR values of the different phantoms. It was shown that a homogeneous head of appropriate shape and dielectric parameters is acceptable for exposure evaluations.

In [32], three different configurations of the head models were employed, i.e., a homogeneous spherical head, an anatomical head with different tissues and a homogeneous head with an anatomical head shape. The study was performed by means of FDTD with a dipole antenna as the radiating source located at 20 mm from the ear. The study showed that the dipole's radiation pattern for the three different head models agree well with each other, with only marginal differences measured in the direction of the head. The study also showed very similar results between the three heads on the magnitude of the electric field near the surface of the head. Kim and Rahmat-Samii [32] suggested that the peak SAR in the head can be roughly estimated by using a simple homogeneous spherical head. Although the results from a simple

spherical head model are not particularly accurate, it is sufficient for some validation purposes and provides an easy and a reasonable way of estimating the worst case SAR [15, 31]. Jensen and Rahmat-Samii [39] also confirms that the simple spherical head is an acceptable estimate to approximate the effect of the head. However, an inhomogeneous model is essential to calculate the field distribution within the exposed tissues accurately.

2.2.1.2 Head phantom

Besides the simple spherical head models, heterogeneous or anatomically correct head models, a homogeneous realistic head phantom is also widely used amongst researchers [40, 41]. Most homogeneous head models are given the dielectric property of a brain equivalent liquid. The permittivity and conductivity of the tissue equivalent liquid are dependent on the operating frequency of a mobile handset. The simplified physical phantom adopted by European Committee for Electrotechnical Standardization (CENELEC), FCC (USA), the Association of Radio Industries and Business in Japan, and specified in IEEE SCC34/SC2 and IEC 92209-1 is the SAM head phantom [42]. The SAM (Figure 2.2-4) was built based on the dimensions and shape of a 90th percentile[ψ] of adult male head, published by the U.S.Army [9]. The phantom shell is made of fiberglass with a collapsed ear tapered to the cheek as in a real human head with a handset pressed to it. The SAM head model is used for the standardized SAR measurement procedure of IEEE [43]. Hence, the standard measurement in evaluating the SAR within the head still relies on the homogeneous phantom, since the entire volume must be accessible by the measurement probe [27, 36] and live human head cannot be easily or safely instrumented. For this reason, the compliance testing is done with the head phantom [42, 44]. A homogeneous head model (with appropriate shape and dielectric parameters) also provides better repeatability with respect to the test position than the anatomical head [36, 41].

[ψ] A percentile is a point on a rank-ordered scale, found by dividing a group of observations into parts in order of magnitude from lowest to highest. The nth percentile is the point exceeding n percent of the observations.
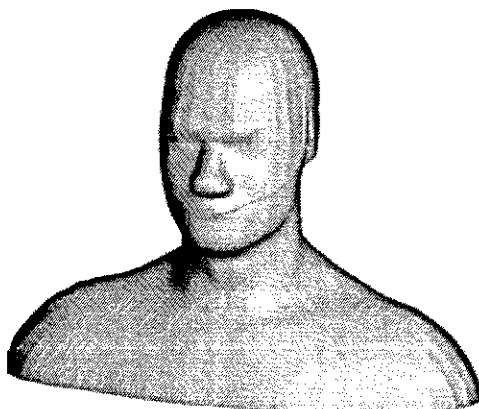
Figure 2.2-4: SAM phantom head for mobile compliance testing according to European Standard EN50361 [45].

Previous research indicates that the SAM could underestimate [46] or overestimate the SAR within the head depending on the experimental conditions as discussed in [28, 42, 44]. It is difficult to compare the results between the published results due to differences in models (include/exclude the pinna), different types of tissues and properties, different types of radiating source and inconsistent positioning of the source relative to the head and the manner in which the SAR is normalized for reporting. The highest SAR is usually found in the pinna due to the proximity of the pinna tissue to the feed point of the mobile antenna. As a result of this high SAR in the pinna, the inclusion or exclusion of tissues near the pinna from the averaging volume will significantly affect the average 1 g or 10 g SAR [44]. In addition small variations in the distance (as small as 1 or 2 mm) between the antenna and the head appeared to change the SAR values quite significantly [42, 44].

2.2.2 Effect of the human hand

Conventionally, the mobile handset is placed very close to the head and partially masked by the human fingers where a certain amount of electromagnetic energy is absorbed rather than been directly radiated. The user's hand especially the thumb frequently strays very close to the antenna, and could potentially be exposed to RF radiation and interact with the electromagnetic field radiated from the mobile handset [47]. Numerous studies have examined the interaction between the electromagnetic

fields radiated by the mobile handset, the human head and the hand [34, 48, 49-53] (Table 2.1-2). The results seem to suggest that the presence of the human hand causes noticeable changes in the antenna performance or to the SAR values within the head. Chavannes et al. [54] also paid special attention to the effect of the hand on the antenna performance in the study. Due to the proximity of the hand to the mobile handset, it is of particular importance to include the hand since the fingers at certain locations could notably affect the antenna performance. Although the CENELEC ES59005 [7] does not include the hand for the mobile phone compliance, it is interesting to evaluate how the hand presence affects the SAR in the head [48].

Okoniewski and Stuchly [30], Pedersen [55] and Excell [47] have highlighted the significance of including a hand together with the head in the investigations as it could significantly affecting both radiation performance and SAR. Okoniewski and Stuchly [30] have concluded that the hand must be included in evaluating the antenna performance and SAR due to the amount of energy absorbed inside the hand. Kuo et al. [56] also consider a hand model to be important in their work. Hence, proper modelling of a handset antenna requires a hand model to hold the handset and be in proximity to the head [56]. Pedersen [55] also signifies the importance of including the hand in evaluating the antenna performance concerning the radiation efficiency.

2.2.2.1 *Human hand geometry and effect of the human hand on the antenna performance and SAR*

There are many different ways to locate a mobile handset using the hand. It is relatively straightforward to determine how users will place their mobile handset relative to the head due to the alignment of the handset earphone to the ear; whereas it is more difficult to predict the precise angle between the phone and the face, the rotation relative to the ear and the position of the fingers and the hand [57]. If the hand wraps around the handset or directly touches the antenna, the antenna characteristics and performances will inevitably be disturbed. The antenna characteristics which have been found to be affected by the hand include the input

impedance [10, 11, 58, 59], the radiation efficiency [11, 55, 60] and the total radiated power [51-53].

The effect of the hand on the antenna performance of two different antennas was investigated in [26]. The hand positions along the antenna were varied in the study. It was shown that the hand effects on the input impedance were marginal unless the hand actually masked the antenna. The effect of various hand positions on SAR inside the hand itself and also inside the head were investigated in [34]. A $\lambda/4$ monopole and $\lambda/2$ dipole antenna were used as the radiating source. The results revealed that the hand effect on the maximum local SAR in the head was only marginal as long as the hand does not cover the antenna.

Boyle [16] from his measurement results away from the head has shown that, much of the reduction in the efficiency is due to the losses in the hand if compared to the free space loss. Rowley and Waterhouse [61] and Su et al. [60] also found the efficiencies dropped for all of the antennas investigated due to the presence of the hand. The efficiencies of shorted patch antennas in the study of [61] were more severely degraded when the hand moved closer to the patch due to current flows and possible physical contact with the antenna structure. In addition, the hand can also modify the antenna radiation pattern but this effect seemed to be strongly dependent on the operating frequency [48]. In [48] the antenna radiation pattern at 902.4 MHz was reduced by more than 10 dB at the angular direction pointing towards the back of the mobile handset, whilst being significantly reduced along the side of the phone that was wrapped by the four fingers at 1715 MHz. Zaridze et al. [62] also considered the human hand (besides the head) in their research. The study showed that the presence of the head caused the system to become more unidirectional due to energy absorption by the head. The study also showed that the introduction of the hand further changed the radiation characteristics of the antenna.

Francavilla et al. [48] also demonstrated the effect of the hand on SAR in the head. The study showed that the influence of the hand on SAR in the head is more notable in the 900 MHz band compared to the 1800 MHz band. The authors concluded that the averaged SAR in the head was only marginally changed by the hand, although the

SAR distribution inside the head does change. In addition, the hand position on the handset (proximate to the head) was found to be one of the factors that caused variation on SAR within the head and the hand itself. A decreasing SAR in the head by the presence of the hand was found in [30] due to the power absorption in the hand. A similar result was found in [63]. In [64], the SAR within the user's head was increased by the presence of the whole human body including the hand and the arm. The highest SAR reported in the study occurred inside the hand. Kuo et al. [65] also included a hand model consisting of a layer of skin, muscle and bone tissues; it had the 'handhold-shape' (with a straight thumb) in their work. The study showed that the hand absorbed approximately 21% of the radiated power from the antenna at 900 MHz and 17% of the power at 1800 MHz.

Most of the investigations to date have employed a very simple block-hand model that does not include any fingers. The block hand model consists of a layer of bone surrounded by a layer of a muscle [10, 26, 30, 47, 61, 63, 66] whereas a layer of skin was included in [18, 47]. In [12], only a layer of muscle was used to represent a block hand model encloses three sides of the handset unit. In [34] a more realistic human hand was presented with the thumb crooked around the handset and a 20 mm gap was introduced between the palm and the handset.
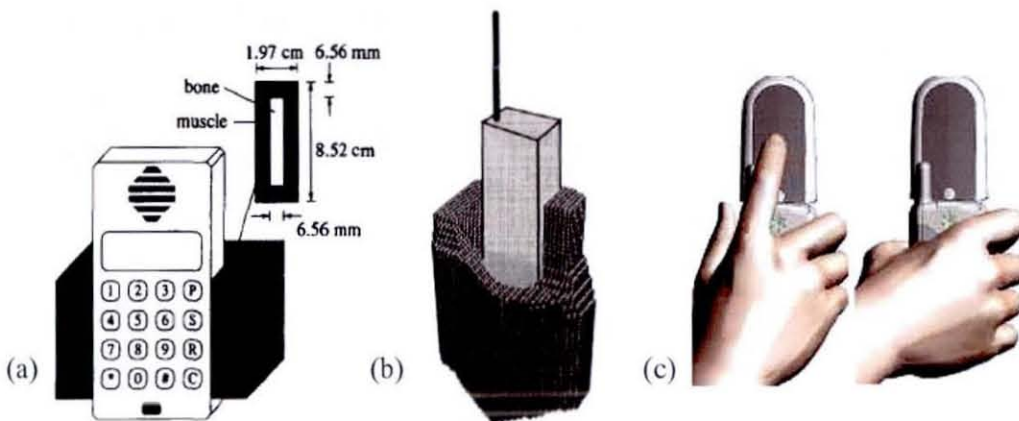
Figure 2.2-5: Human hand models: (a) simple block hand model [39], (b) hand model with the thumbed crooked around the radio [34] and (c) realistic CAD hand model [54].

In some studies, more realistic hand models have been employed [48, 51-54]. The hand in [48] was an anatomical hand modelled of 11 tissues obtained by identifying particular tissue types in a MRI scan data set and applying appropriate material type in the model; while the hand model in [51, 52, 54] consisted of skin, muscle and bone tissues. Li et al. [51, 52] also included a homogenous hand model in their study to determine the effect of different tissue parameters on radiation efficiency and total radiated power. The study has shown only marginal differences between the homogeneous and inhomogeneous hand, so a homogeneous hand can be used to represent a human hand in ordinary usage conditions.

In the current thesis, both the simplified homogeneous block hand and a realistic hand models (with realistic fingers) were employed. The inclusion of the fingers enables the effect of metallic jewellery ring and a bangle to be investigated.

2.2.2.2   Hand phantom for measurements

The head, hand or body phantom can be developed physically or in a numerical model depending on the nature of the proposed study. The phantom chosen should be of a suitable shape, size and it is useful if it has the same anatomical details as the human body. Gabriel [67] has highlighted the importance of considering an anatomical hand phantom that can differentiate between the tissue varieties due to the fact that different tissues have different dielectric properties and they are typically highly dependent on the specified operating frequency. However, Li et al. [51, 52] have found that there were negligible differences between the inhomogeneous and homogeneous hands investigated in their study.
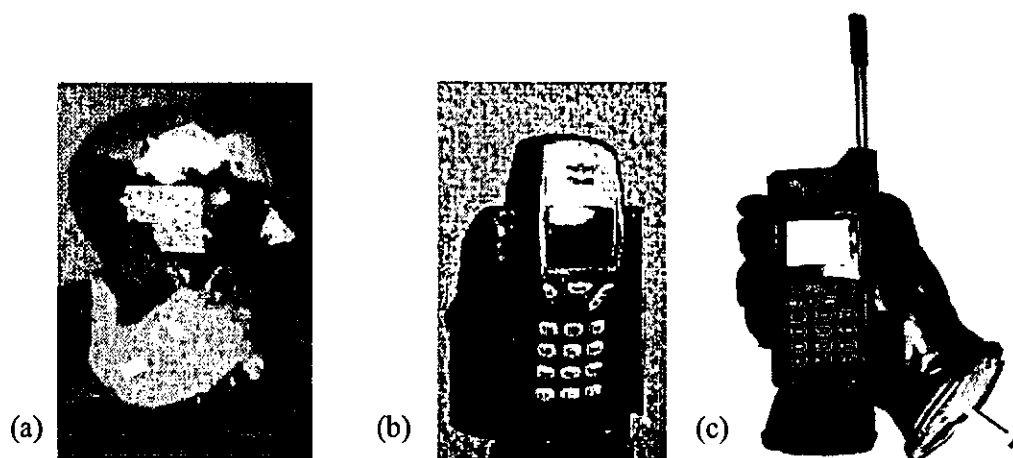
Figure 2.2-6: Human hand phantom for measurements: (a) rubber glove filled with liquid wrapped with transparent tape [55], (b) PVC tube filled with lossy liquid [49] and (c) hand phantom used by [48] with unspecified construction.

A hand phantom made of silicone rubber loaded with carbon fibres was employed in [16, 67]. Boyle [16] suggested that the hand phantom should be placed in various positions representing typical way of holding a mobile handset to allow an accurate phantom measurement on phone-by-phone basis. It is however difficult to have one hand phantom that suits every mobile handset due to its mechanical design [16]. Pedersen [55] uses a thin rubber glove filled with brain/muscle simulating liquid to simulate the effect of the hand holding a mobile handset. A thin transparent tape was wrapped around the hand and fingers to retain its shape during the measurement. Otherwise in [49], the hand phantom was constructed from PVC and filled with the tissue simulating liquid which equivalent to the head tissue liquid whilst in [67], a physical head and hand phantom have been manufactured from synthetic tissues that include some anatomical details of the head and the hand. However, due to the complexity of the heterogeneous phantom model, many research studies make use of the simple homogeneous sphere head and block hand model. These simple models are more practical and can be easily designed and compared with numerical models which used for the simulations. Francavilla et al. [48] also measure the SAR inside an anthropomorphic homogeneous phantom. However, the construction of that specific hand model has not been published in such a way that it can be reproduced.

In this thesis, a realistic homogeneous hand phantom is presented and employed in the measurement for comparison with the simulations. The construction of this model will be further discussed in Chapter 6, together with the measurement process and results.

2.2.3 Effect of the head-antenna separation distance, frequency of excitation and different types of antennas

The mobile handset is typically placed very close to the head near to the left or the right ear, where part of the radiated energy is absorbed by the head and nearby tissues [68]. Small variations in handset-antenna position and orientation relative to the human body could significantly influence the energy absorption and distribution inside the exposed body. In fact, the handset user is normally in the reactive near-field region of the antenna where the electromagnetic field is mostly non-propagating [69] [70]. Therefore the amount of energy absorbed within the head or nearby tissues is mainly due to the electric field induced by the magnetic field generated by the current flowing on the antenna and handset body [66, 69]. The absorbed energy within the body is scattered and attenuated as it propagates through the body tissues [69]. In [68, 71], the antenna was placed at 1.11 mm from the head resulting in significantly higher SAR exceeding the safety guidelines provided by the CENELEC [72] and IEEE C95.1 [73]. The ear is reported as having the largest SAR due to the proximity to the antenna [68].

The dependence of the SAR inside the head on the head-antenna separation distance over two different frequencies was investigated in [33, 34, 74]. The method used by each author mentioned above is provided in Table 2.1-2. These studies showed that the SAR is strongly dependent on the head-antenna separation distance. A significant amount of energy is absorbed in the head when the head is close to the antenna, but the amount of energy absorbed inside the head decreases exponentially when the head-antenna separation distance increases. Similar results were found in [39, 71].

In addition, the amount of energy absorbed inside the human head is also dependent on the type of antennas and the frequency of excitation [34, 74, 75]. Watanabe et al.

[34] and Iskander et al. [74] employed two different antennas, while Li et al. [75] investigated the interaction between the human head and a range of commercial handset antennas (Table 2.1-2) at 900 and 1800 MHz. Li et al. [75] reported that the input impedance and the radiation pattern of the antennas investigated in the study were noticeably influenced by the presence of the head. However, the effects were varied depending on a particular antenna configuration and the frequency of operation. The study also suggested that the energy absorption at 1800 MHz (PCN) is more pronounced compared to 900 MHz (GSM) as the conductivity of the tissues tends to be higher at larger frequency. Hence, the attenuation increases as the frequency increases [75]. Nevertheless, the averaged SAR in the head was higher for the GSM band compared to the PCN frequency band due to the deeper penetration of the fields at GSM frequencies [40, 75]. These studies [40, 75] also showed a notable variation in the highest SAR distribution for the antennas tested. The highest SAR distribution occurs near the ear region for the monopole antenna; for the dipole, the highest SAR distribution is concentrated in the region near the temple, whilst the SAR distribution appears more evenly spread for the IFA antennas.

Thus the effect of the hand on SAR could vary depending on the type of antennas employed within the handset. Rahmat-Samii and Jensen [10] included three antenna configurations in their study, namely the monopole antenna, side-mounted PIFA and back-mounted PIFA. The study showed that over 50% of the total radiated power was absorbed within the head and the hand. Although the back-mounted PIFA antenna significantly reduced the SAR in the head, the SAR in the hand that holding the mobile handset was significantly increased by the side-mounted and back-mounted PIFA. The shorted-patch antenna modelled in [61] produced higher SAR in the hand which appeared due to the current flows on the handset body. In [30], an 85 mm monopole antenna on top of a metal box covered with a 2 mm dielectric insulator was used. It was found that the presence of the hand has helped to decrease the SAR in the head at 915 MHz. Likewise, Gandhi and Kang [76] also found that the hand decreased the peak 1 g SAR since the peak 1 g SAR values increases when the hand is eliminated.

2.2.4 Effect of metallic objects near the human body

The radiation characteristic and performance of a mobile handset could be strongly affected and modified by the presence of any objects in close proximity [15] especially when the size of the objects nearby is comparable to the wavelength of the radiated field [62]. Metallic objects near the mobile handset have the potential to influence the radiation characteristics and thus reduce the radiation efficiency, energy re-distribution and may alter the natural polar pattern [21]. Metallic objects usually found in practice are: external objects (wire-framed spectacles, hands-free) [17-21] and metallic implants (surgical pins, jewellery) [15, 23, 25] (Table 2.2-1).

It is well known that the presence of the human body degrades the antenna performance however; this reduction could be emphasized by wearing metallic objects in close proximity to the antenna [15]. Previous studies (see Table 2.2-1) have shown that the amount of electromagnetic radiation absorption in human tissues could significantly increase and the electromagnetic distributions could noticeably change by the metallic implants or metallic objects. This can be explained by the coupling between the antenna with metallic implants especially those which are particularly close to the antenna position. Hence, a sufficient amount of current induced on the implant's surface could possibly cause the metallic objects to act as weak antenna (producing a secondary electromagnetic field) and therefore could modify the energy distributions and enhance the electromagnetic fields. These may result in excessive local tissue heating [22] and may also modify the SAR values within nearby tissues [21, 24]. However, these effects are strongly dependent on the metallic objects/implants size [23, 24], orientation relative to the antenna, frequency of operation and proximity to the human body [21, 23, 24].

Table 2.2-1: Summary of research on the effect of metallic objects.

Reference	Metallic objects/types	Head	Hand	Method/Technique	Radiating source
Whittow and Edwards (2004)	Spectacles	MRI based (Brooks head)	-	FDTD	Plane wave (1.5-3 GHz), dipole (1.8 GHz)
Edwards and Whittow (2005)	Spectacles	MRI based (Brooks head)	-	FDTD, GA	Plane wave, dipole antenna (1.5-3 GHz)
Troulis et al. (2003)	Hands-free wire	Realistic adult-male body	-	FDTD	Monopole on PEC box (1.8 MHz)
Troulis et al. (2001)	Hands-free, spectacles	Cylindrical muscle, heterogeneous body	-	FDTD	Monopole on a box (1.8 GHz)
Virtanen et al. (2005)	Pins, rings	Cylinder muscle with skin	-	FDTD	$\lambda/4$ monopole on metal box (900, 1800 MHz)
Whittow et al. (2007)	Circular earrings	Homo. cubic phantom, anatomical	-	FDTD	Dipole antenna (1.8 GHz)
Fayos-Fernandes et al. (2006)	Earrings: band and studs	Homo. sphere, 4 tissues anatomical head	-	FIT, FDTD	$\lambda/2$ dipole antenna (900 MHz)
Virtanen et al. (2007)	Earrings, implants	MRI based female head	-	FDTD	0.47λ dipole antenna (900, 1800, 2450 MHz)
McIntosh et al. (2005)	Implant: head plate	Visible human head	-	XFDTD	Plane wave (200, 2500 MHz)
Fleming et al. (1992)	Ankle, knee pins	Cylindrical layered model: skin, muscle, bone	-	FEM, MoM	Plane wave (40, 640, 1250 MHz)
Whittow et al. (2008)	Straight jewellery	Cubic phantom, anatomical-Brooks head	-	FDTD	$\lambda/2$ dipole antenna (900 MHz, 1800 MHz)
Samsuri and Flint (2006)	Rings, bangles	-	Homo. cylinder	TLM	Plane wave
Cooper and Hombach (1998)	Metallic walls	Homo. Sphere	-	FIT	0.45λ dipole antenna (900 MHz)
Homsup et al. (2006)	Metal wall	MRI based head	-	FDTD	Dipole (900, 1800 MHz)
Wang et al. (2004)	Metal ground	Cylindrical (brain tissue)	Cylindrical (muscle)	FI	$\lambda/4$ monopole on metal box (900 MHz)
Panagamuwa et al. (2007)	Metallic pins	SAM head	-	FDTD	Dipole antenna (900, 1800 MHz)

There are two ways of estimating how much effect is being caused by the metallic objects that are the commonly used, namely numerical modelling and thermal modelling techniques. However, most of the studies have shown that there is no significant increase in temperature (no more than 1°C) near the metallic object as discussed in ICNIRP (1998) [13, 22]. It is actually extremely difficult to conduct measurements near to an implant. There is also some contradictory evidence, for example in [13], the temperature in the tissue near a metallic plate was lower than in a similar experiment without the implant. This is due to the high thermal conductivity of the plate and due to the lack of blood circulation and metabolic heat production in the volume occupied by the implant [14].

2.2.4.1 *Metallic objects worn on human body*

Cooper and Hombach [77], Dominguez et al. [78] and Homsup et al. [79] have taken into consideration the effects of a metallic wall in close proximity to a mobile-head and the effect on SAR within the head. The results show that the SAR values are notably higher than the free-space values when the head-handset is a certain distance away from the wall due to the electromagnetic fields being reflected back by the wall (at the back of the handset-head model) [78]. Research in [64] showed that a metallic ground plane could increase the SAR level within the head owing to the reflection from the ground causing constructive interference inside the head. The electromagnetic wave radiated by the antenna may scatter around the head and the body. Thus, the directed wave towards the ground may experience reflection and introduce minor lobes in the antenna radiation pattern. However, the effects of the metallic wall are dependent on its orientation and proximity relative to the head and the antenna [80].

Wire-framed spectacles and hands-free wire are commonly found in close proximity of the handset antenna and user's head. The hands-free wire is widely used together with the mobile handset as it enables the handset antenna to be operated away from user's head, so that in theory the hot spots could be removed from the head region [21]. However, the coupling between the handset antenna and the hands-free wire lead

may increase the energy deposition in the exposed body and therefore could notably increase the SAR. Troulis et al. [18, 21], Whittow and Edwards [17] and Edwards and Whittow [20] included wire-framed spectacles in their investigations by means of a FDTD method. The wire-framed spectacles were reported to cause notable degradation in the radiation efficiency at 1.8 GHz and significant increases in the peak averaged 1 g or 10 g within the head [21]. In addition, the metallic spectacles could generally increase the maximum local SAR and alter the SAR distribution within the head [17, 20]. By adding the spectacles, the maximum SAR appears to be located closer to the spectacle's edges (metal arms) or on the side of the nose. Thus, the greatest increase in SAR owing to the presence of the spectacles is in the nose due to relatively high conductivity tissues contained within (skin, muscle, mucous membrane) [20].

Metallic jewellery worn on or near the human head has begun to attract interest amongst researchers due to the possibility of having a resonant length/size and its location that in vicinity to the radiation exposure [25]. The effect of metallic pins or straight metallic jewellery has been studied by means of FDTD and Dosimetric Assessment System (DASY 4) measurement systems [81, 82]. The metallic pin length and location were varied and the effect of the pins on SAR was compared with the case without pins at 900 and 1800 MHz. At both frequencies, a pin measuring approximately one-third of the wavelength [13, 23] at a certain distance from the phantom surface gives the biggest increase in local and averaged 1 g SAR within the head. The resonant pin generally increased the SAR at the front of the phantom tested, redistributes the energy absorbed in the phantom and focused them close to the metallic pin [82].

Otherwise, in [15], four different aluminum objects that either attached or pierced on the ear were investigated by means of a FDTD and excited by a λ/2 dipole antenna centered at 900 MHz. A homogeneous sphere and a three level head with four different tissues were employed. In pierced cases where the pin enters the tissue of the ear, the metallic material replaces some of the ear cells whilst the metallic object is only touching the ear in the 'attached' cases. In both cases, the dipole antenna feed point was positioned directly above the ear reference point (ERP) at 10 mm distance

from the head's surface. Fayos-Fernandez et al. [15] reported that the pierced metallic object increased the measured peak SAR values in all cases but smaller increased were observed on the peak averaged 1 g SAR values. Fayos-Fernandez et al. [15] suggested that, the increase in SAR occurs in the ear and the volumes contributing most to the peak averaged 1 g SAR (with an increase in SAR) are in the ear itself. However, the probe used for the measurement in the study could not reach the ear phantom surface, resulting in insignificant changed in the averaged SAR values.

2.2.4.2   Metallic loop-like jewellery items worn on human (earring, ring, bangle)

In recent years, a number of studies have focused on the effect of metallic jewellery such as earring hung on the ear [15, 25] and implanted metallic loops and pins inside the head [23]. Whittow et al. [25] have investigated the effect of circular metallic earring at 1800 MHz on SAR within the human head. A $\lambda/2$ dipole near the ear was used as the radiating source and the computation results by means of a FDTD were then compared with the measurements performed using a DASY4 measurement system. Different sizes and positions of circular earrings (copper) were analyzed near to a homogeneous cubic phantom and later, an anatomical realistic head model was employed representing the more realistic condition of human head worn metallic earring. The results with the cubic homogeneous phantom show that circular metallic earring significantly increase the averaged SAR when its circumference is approximately λ wavelength and placed at a range of distances from the phantom surface. Thus, there was a negligible increase in the averaged SAR for all the earring sizes when it touched the phantom. In addition, the maximum SAR appears at the edges of the earring, not at the center. With the anatomically realistic head, the circular earring was inserted into the ear and hung down beside the head, so that the center of the dipole antenna was positioned at 40 mm away from the top of the earring. In this case, the earring increased the averaged 1 g SAR when the circumference was about 0.65 λ due to the close proximity of the head. However, the same earring may affect the SAR differently on different ears as the ears maybe in different shapes and sizes.

Virtanen et al. [23] included three sizes of ring with different thicknesses and a homogeneous cylindrical phantom was employed. For the 30 mm diameter ring, the highest peak SAR occurred when the longest dimension of the ring was oriented parallel to the antenna. Although the peak SAR is highest for the smallest and thinnest ring, the average SAR is however notably highest for the ring with 30 mm of diameter (about 1/3 of the wavelength in the muscle tissue) and when the thickness of the ring increases. In addition, Virtanen et al. [24] numerically investigate an earring that has 42.4 mm outer diameter, 4 mm thick with 1 mm thin part is pierced through the ear lobe. The earring was placed at the lower part of the right ear (on a heterogeneous head) with the dipole antenna feed point is actually in the middle and aligned with the top of the thin part of the earring. This earring has generally enhanced the SAR at 900, 1800 and 2450 MHz. The SAR is highest near to the thin part of the earring which passes through the ear lobe and at the location where part of the earring touches the skin [24].

As the hand is found to give noticeable effects on the antenna radiation performance and could also modify the SAR distribution within the head, the introduction of the metallic ring/bangle worn on the hand is expected to have an additional effect. In order to study the effect brought about by the jewellery rings on SAR, a simplified geometrical representation of a human finger worn a ring and the arm worn a bangle has been presented [83]. The results indicate that the electric-field distribution at the centre of the ring and in between the ring and the dielectric were substantially changed by the dielectric (human fingers or arm) inclusion. However, the measurement campaign carried out during this study suggests that there is no significant effect on SAR due to the presence of the small metallic-loop, although the larger loop does cause an increase in 1 g and 10 g SAR in the 1800 MHz frequency band.

2.3 Conclusions

With the expansion of the current use of cellular telephones, there has been a lot of interest and concern about any possible health effects due to the electromagnetic field

radiated from the antenna. The mobile phone is usually operated extremely close to the head/body where a certain amount of the electromagnetic energy is absorbed inside the human head/body. In addition, the presence of external metallic objects or implants is expected to have further effects on the amount of electromagnetic field radiated by the antenna. Therefore, it will be interesting to investigate the interaction between the mobile handset, the user and any metallic objects, particularly in the near field of the unit's antenna.

Research to date has been extensive and varied and has considered a range of human head models from the simple homogeneous models with different shapes such boxes, spheres, ovals, with or without the ears, eyes and nose to the more realistic detailed heterogeneous head models that include various types of different tissues. Different shapes of the head models with different tissue properties could affect the antenna performances or the SAR values quite differently. In this thesis, a simple spherical homogenous head model will be used in the earlier sections to estimate the effect of the head and the amount of energy absorbed within the head. A spherical head model is said to be better than the box model as it provides results that are in good agreement with a relatively simple but realistic head model. Although the results from a simple spherical head model are not particularly accurate, it is adequate for validation purposes and provides an easy and repeatable way of estimating the worst case SAR. The latter investigations include a homogeneous SAM head model. The SAM head model has been adopted by CENELEC, FCC (USA), the Association of Radio Industries and Business in Japan, and specified in IEEE 1528 and IEC 92209-1 and is also used for standardized SAR measurement procedure. Nevertheless, the homogeneous SAM head model may provide better repeatability with respect to the test position than the anatomical head.

Due to the proximity of the hand to the mobile handset, it is of particular importance to include the hand since the fingers at certain locations could notably affect the antenna performance or SAR within the head. However, most of the investigations to date have employed a very simple block-hand model with homogeneous properties or highly simplified inhomogeneous bone surrounded by a muscle. Some results show only marginal and negligible difference between the homogeneous and

inhomogeneous hand model, therefore in this thesis, a simplified homogenous block-hand and a homogeneous realistic hand model were employed. The realistic hand model (with realistic fingers) employed will allow the effect of metallic jewellery ring and bangle to be worn and placed in different positions for comparison.

Metallic objects near the mobile handset could possibly influence the radiation characteristics thus reducing the radiation efficiency, energy re-distribution and may alter the radiation pattern. However, these effects are dependent on the metallic objects or the implants size, orientation relative to the antenna, frequency of operation and proximity to the human body. Metallic jewellery worn on or near to the human head has started to be an active research topic amongst researchers due to its possibility of having a resonant length/size and its location that in vicinity (at certain distance) of the radiation exposure. In this thesis, metallic loop earrings in different sizes worn on the ear are employed. None of the previously published research has included the hand while investigating the effect of metallic earring worn on the ear on SAR within the head. The hand that holds the handset may alter the effect brought about by the metallic earring on the antenna performance or SAR within the head. Nevertheless, the introduction of the metallic ring or bangle worn on the hand (placed on different fingers) can also be expected to have an additional effect.

Different types of antenna may exhibit different performance characteristics depending on their location relative to the human head and the phone position with respect to the head may vary from one person to another. In this thesis, a monopole antenna on a metal box is used as a radiating source in the 900 and 1900 MHz bands. This antenna provides simplicity in the geometry and can be positioned easily with respect to the head. In the latter model, a PIFA antenna was employed for comparison purposes. The SAR within the head may significantly decrease by the PIFA antenna as it is known to reduce backward radiation toward the user's head. However, the effect of the hand in close proximity may become important. Metallic rings worn on the human fingers may also introduce additional effects and these will be explained. It is also notable that, small variation in the distance (as small as 1 or 2 mm) between the antenna, the head and the hand could change the SAR values quite significantly.

2.4 References

[1]   Harvard. 1997, Absorption of RF radiation. http://www.seas.harvard.edu/
courses/es96/spring1997/web_page/health/absorp.htm. (Last accessed: Mar.
2008)

[2]   D. Manteuffel, A. Bahr, C. Bornkessel, F. Gustrau and I. Wolff. (2002,
Fundamental aspects for the design of low-SAR mobile phones. *IMST GmbH,
Germany*.http://www.empire.de/main/Empire/pdf/publications/2002/dm-ams-
2002.pdf (Last accessed: June 2008)

[3]   S. Khalatbari, D. Sardari, A. A. Mirzaee and H. A. Sadafi, "Calculating SAR in
two Models of the Human Head Exposed to Mobile Phones Radiations at 900
and 1800 MHz," *Progress in Electromagnetic Research Symposium,
PIERS2006, Cambridge, USA,* vol. 2, pp. 104-109, Mar. 2006.

[4]   W. Stewart Sir. (2000, Radiofrequency fields from mobile phone technology.
Independent   Expert   Group   on   Mobile   Phones   (IEGMP),
http://www.iegmp.org.uk/documents/iegmp_4.pdf. (Last accessed: Oct. 2008)

[5]   J. A. Flint and J. C. Vardaxoglou, "Installed performance of printed inverted-F
antennas (IFAs) at 2.45 GHz for Bluetooth and 802.11b," *Microwave and
Optical Technology Letters,* vol. 39, pp. 497-499, Dec. 2003.

[6]   C.   Zombolas.   (2003,   New   compliance   requirements   for   mobile
telecommunications equipment. *EMC Technologies A NATA accredited test
house   for   SAR   measurements   Melbourne,*   Australia.
www.emctech.com.au/sar4/SAR_Article_2003.pdf. (Last accessed: June 2008)

[7]   ICNIRP 1998: Guidelines for limiting exposure to time-varying electric,
magnetic, and electromagnetic fields (up to 300 GHz), *Health Phys.,* vol. 74, pp.
494-522,

[8]   IEEE C95.1 1999: IEEE standard for safety levels with respect to human
exposure to radio frequency electromagnetic fields, 3 kHz to 300 GHz. *Institute
of Electrical and Electronics Engineers, Inc. , Piscataway, NJ*

[9]   K. Fujimoto and J. R. James, *Mobile Antenna Systems Handbook.* ,2nd
ed.Boston, Mass. USA: Artech House: 2001,

[10] Y. Rahmat-Samii and M. A. Jensen, "A study of the electromagnetic coupling
between handset mounted antennas and a human operator," *24th European
Microwave Conference, Cannes, France,* pp. 607-612, 5-8 Sep. 1994.

[11] J. Toftgard, S. N. Hornsleth and J. B. Andersen, "Effects on portable antennas
of the presence of a person," *IEEE Transactions on Antennas and Propagation,*
vol. 41, pp. 739 – 746, June. 1993.

[12] H. Morishita, H. Furuuchi and K. Fujimoto, "Characteristics of a balance-fed
loop antenna system for handsets in the vicinity if human head or hand," *IEEE
Transaction,* pp. 2254-2255, 2000.

[13] R. L. McIntosh, V. Anderson and R. J. McKenzie, "A numercial evaluation of SAR distribution and temperature changes around a metallic plate in the head of a RF exposed worker," *Bioelectromagnetics,* vol. 26, pp. 377-388, 2005.

[14] H. Virtanen, J. Keshvari and R. Lappalainen, "Interaction of radio frequency electromagnetic fields and passive metallic implants – a brief review," *Bioelectromagnetics,* vol. 27, pp. 431-439, 2006.

[15] J. Fayos-Fernandes, C. Arranz-Faz, A. Martinez-Gonzalez and D. Sanchez-Hernandez, "Effect of pierced metallic objects on SAR distributions at 900 MHz," *Bioelectromagnetics,* vol. 27, pp. 337-353, 2006.

[16] K. R. Boyle, "The performance of GSM 900 antennas in the presence of people and phantoms," *Twelfth International Conference on Antennas and Propagation, (ICAP 2003),* vol. 1, pp. 35 – 38, Mar.- Apr. 2003.

[17] W. Whittow and R. Edwards, "A study of changes to specific absorption rates in the human eye close to perfectly conducting spectacles within the radio frequency range 1.5 to 3.0 GHz," *IEEE Transaction on Antenna and Propagation,* vol. 52, pp. 3207-3212, 2004.

[18] S. E. Troulis, N. E. Evans, W. G. Scanlon and G. Trombino, "Influence of wire-framed spectacles on specific absorption rate within human head for 450 MHz personal radio handsets," *Electronics Letters,* vol. 39, 12 Nov. 2003 (a).

[19] S. E. Troulis, W. G. Scanlon and N. E. Evans, "Effect of a hands-free on specific absorption rate for a waist-mounted 1.8 GHz cellular telephone handset," *Physics in Medicine and Bio.,* vol. 48, pp. 1675-1684, 2003 (b).

[20] R. M. Edwards and W. G. Whittow, "Applications of a Genetic Algorithm for Identification of Maxima in Specific Absorption Rates in the Human Eye Close to Perfectly Conducting Spectacles," *IEEE Proceedings, Science, Measurement and Technology,* vol. 152, pp. 89-96, May. 2005.

[21] S. E. Troulis, W. G. Scanlon and N. E. Evans, "Effect of 'hands free' leads and spectacles on SAR for a 1.8 GHz cellular handset," *1st Joint IEI/IEE Symposium on Telecommunications Systems Research, Dublin,* pp. 1675-1684, 2001.

[22] A. H. J. Fleming, V. Lubinas and K. H. Joyner, "Calculation of Electric Fields in Tissue Near Metallic Implants," *Asia-Pacific Microwave Conference, APMC 92, Adelaide,* vol. 1, pp. 229 – 232, Aug. 1992.

[23] H. Virtanen, J. Huttunen, A. Toropainen and R. Lappalainen, "Interaction of mobile phones with superficial passive implants," *Physics in Medicine and Bio.,* vol. 50, pp. 2689-2700, 2005.

[24] H. Virtanen, J. Keshvari and R. Lappalainen, "The effect of authentic metallic implants on the SAR distribution of the head exposed to 900, 1800 and 2450 MHz dipole near field," *Physics Medicine and Bio.,* vol. 52, pp. 1221-1236, Feb. 2007.

[25] W. Whittow, C. J. Panagamuwa, R. Edwards and J. C. Vardaxoglou, "Specific Absorption Rates in the Human Head Due to Circular Metallic Earrings at 1800 MHz," *Antennas and Propagation Conference, LAPC 2007, Loughborough,* pp. 277 – 280, 2-3 April. 2007.

[26] M. A. Jensen and Y. Rahmat-Samii, "The electromagnetic interaction between biological tissue and antennas on a transceiver handset," *IEEE,* pp. 367-370, 1994.

[27] H. Kawai and K. Ito, "Simple evaluation method of estimating local average SAR," *IEEE Transactions on Microwave Theory and Techniques,* vol. 52, pp. 2021 – 2029, Aug. 2004.

[28] W. Kainz, A. Christ, T. Kellom, S. Seidman, N. Nikoloski, B. Beard and N. Kuster, "Dosimetric comparison of the specific anthropomorphic mannequin (SAM) to 14 anatomical head models using a novel definition for the mobile phone positioning," *Physics in Medicine and Bio.,* vol. 50, pp. 3423-3445, 2005.

[29] J. Keshvari and S. Lang, "Comparison of radio frequency energy absorption in ear and eye region of children and adults at 900, 1800 and 2450 MHz," *Physics in Medicine and Bio.,* vol. 50, pp. 4355-4369, 2005.

[30] M. Okoniewski and M. A. Stuchly, "A study of the handset antenna and human body interaction," *IEEE Transactions on Microwave Theory and Techniques,* vol. 44, pp. 1855-1864, Oct. 1996.

[31] H. O. Ruoss, "Influence of the shape of the head model on the maximum averaged SAR value," *IEE Seminar on Electromagnetic Assessment and Antenna Design Relating to Health Implications of Mobile Phones,* pp. 7/1 - 7/5, 28 June. 1999.

[32] K. W. Kim and Y. Rahmat-Samii, "Antenna and humans in personal communications: an engineering approach to the interaction evaluation," *IEEE Proceeding in Medicine and Biology Society, Chicago,* pp. 2488-2491, Oct. 1997.

[33] K. W. Kim and Y. Rahmat-Samii, "EM interactions between handheld antennas and human: Anatomical head vs. multi-layered spherical head," in *IEEE-APS Conference on Antennas and Propagation for Wireless Communications, Waltham, Mass.* 1998, pp. 69-72.

[34] S. I. Watanabe, H. Taki, T. Nojima and O. Fujiwara, "Characteristic of the SAR distributions in a head exposed to electromagnetic fields radiated by a hand-held portable radio," *IEEE Transactions on Microwave Theory and Techniques,* vol. 44, pp. 1874 – 1883, Oct. 1996.

[35] K. Meier, V. Hombach, R. Kastle, R. Y. S. Tay and N. Kuster, "The dependence of electromagnetic energy absorption upon human-head modeling at 1800 MHz," *IEEE Transaction on Microwave Theory and Techniques,* vol. 45, pp. 2058-2062, Nov. 1997.

[36] M. Burkhardt and N. Kuster, "Appropriate modeling of the ear for compliance testing of handheld MTE with SAR safety limits at 900/1800 MHz," *IEEE Transactions on Microwave Theory and Techniques,* vol. 48, pp. 1927 – 1934, Nov. 2000.

[37] S. Koulouridis and K. S. Nikita, "Study of the coupling between human head and cellular phone helical antennas," *IEEE Transactions on Electromagnetic Compatibility,* vol. 46, pp. 62 – 70, Feb. 2004.

[38] V. Hombach, K. Meier, M. Burkhardt, E. Kuhn and N. Kuster, "The dependence of EM energy absorption upon human head modeling at 900 MHz," *IEEE Transaction on Microwave Theory and Techniques,* vol. 44, pp. 1865-1873, Oct. 1996.

[39] M. A. Jensen and Y. Rahmat-Samii, "EM interaction of handset antennas and a human in personal communications," *Proceeding of the IEEE,* vol. 83, pp. 7-17, Jan. 1995.

[40] O. S. Dautov and A. E. M. Zein, "Application of FEKO program to the analysis of SAR on human head modeling at 900 and 1800 MHz from a handset antenna," *The 6th International Symposium on Electromagnetic Compatibility and Electromagnetic Ecology, IEEE,* pp. 274 – 277, June. 2005.

[41] A. K. Lee, H. D. Choi, J. I. Choi and J. K. Pack, "The scaled SAM models and SAR for handset exposure at 835 MHz," *MTT-S International Microwave Symposium Digest, IEEE,* pp. 1323-1326, 12-17 June. 2005.

[42] B. B. Beard, W. Kainz, T. Onishi, T. Iyama, S. Watanabe, O. Fujiwara, J. Wang, G. Bit-Babik, A. Faraone, J. Wiart, A. Christ, N. Kuster, A. K. Lee, H. Kroeze, M. Siegbahn, J. Keshvari, H. Abrishamkar, W. Simon, D. Manteuffel and N. Nikoloski, "Comparisons of computed mobile phone induced SAR in the SAM phantom to that in anatomically correct models of the human head," *IEEE Transactions on Electromagnetic Compatibility,* vol. 48, pp. 397 – 407, May. 2006.

[43] IEEE std. 1528-2003, IEEE recommended practice for determining the peak-spatial average specific absorption rate (SAR) in the human head from wireless communications devices: Measurement techniques.

[44] B. B. Beard and W. Kainz. (2004, Review and standardization of cell phone exposure calculations using the SAM phantom and anatomically correct head models: *Bio. Medical Engineering Online.* pp. 1-10. http://www.biomedical-engineering-online.com/content/3/1/34. (Last accessed: Jan. 2009)

[45] European Standard EN 50361 2001: Basic standard for the measurement of specific absorption rate related to human exposure to electromagnetic fields from mobile phones (300 MHz-3 GHz), *CENELEC, Brussels,* July. 2001.

[46] O. P. Gandhi and G. Kang, "Inaccuracies of a plastic "pinna" SAM for SAR testing of cellular telephones against IEEE and ICNIRP safety guidelines," *IEEE Transactions on Microwave Theory and Techniques,* vol. 52, pp. 2004 – 2012, Aug. 2004.

[47] P. S. Excell, "Modelling of handsets, antennas, heads and hands in the FDTD method, Design of Mobile Handset Antennas for Optimal Performance in the Presence of Biological Tissue," *IEE Colloquium,* pp. 7/1 - 7/4, Jan. 1997.

[48] M. Francavilla, A. Schiavoni, P. Bertotto and G. Richiardi, "Effect of the hand on cellular phone radiation," *IEE Proceedings on Microwaves, Antennas and Propagation,* vol. 148, pp. 247 – 253, Aug. 2001.

[49] M. Lundmark, R. S. Calvo, P. S. Kildal and C. Orlenius, "A solid hand phantom for mobile phones and results of measurements in reverberation chamber," *Antennas and Propagation Society International Symposium, IEEE,* vol. 1, pp. 719 – 722, 2004.

[50] K. Ogawa, T. Matsuyoshi and K. Monma, "An analysis of the performance of a handset diversity antenna influenced by head, hand and shoulder effects at 900 MHz," *Antennas and Propagation Society International Symposium, IEEE,* vol. 2, pp. 1122 – 1125, July. 1999.

[51] C. H. Li, E. Ofli, N. Chavannes and N. Kuster, "The effects of hand phantom on mobile phone antenna OTA performance," *The 2nd European Conference on Antenna and Propagation (EUCAP 2007),* Nov. 2007.

[52] C. H. Li, E. Ofli, N. Chavannes, E. Cherubini, H. U. Gerber and N. Kuster, "Effects of Hand Phantom and Different Use Patterns on Mobile Phone Antenna Radiation Performance," *IEEE International Symposium on Antennas and Propagation, San Diego, California,* 5-12 July. 2008.

[53] J. Krogerus, J. Toivanen, C. Icheln and P. Vainikainen, "Effect of the Human Body on Total Radiated Power and the 3-D Radiation Pattern of Mobile Handsets," *IEEE Transactions on Instrumentation and Measurement,* vol. 56, pp. 2375 – 2385, Dec. 2007.

[54] N. Chavannes, P. Futter, R. Tay, K. Pokovic and N. Kuster, "Reliable prediction of MTE performance under real usage conditions using FDTD," *Proceeding of ICECOM 05, Dubrovnik,* Oct. 2005.

[55] G. F. Pedersen, "Phantoms for radiation measurements of mobile phones Personal Indoor and Mobile Radio Communications," *12th IEEE International Symposium,* vol. 1, pp. C-95 - C-99, 30 Sept.-3 Oct. 2001.

[56] L. C. Kuo, Y. C. Kan and H. R. Chuang, "Analysis of a 900/1800 MHz dual-band gap loop antenna on a handset with head and hand model," *Journal of Electromagnetic Waves and Applications,* vol. 21, pp. 107-122, 2007.

[57] G. F. Pedersen and J. B. Andersen, "Integrated antennas for hand-held telephones with low absorption," *IEEE 44th Vehicular Technology Conference,* vol. 3, pp. 1537 – 1541, 8-10 June. 1994.

[58] K. R. Boyle and L. P. Ligthart, "Radiating and Balanced mode analysis of user interaction with PIFAs," *Proceeding of the IEEE Antennas and Propagation Society International Symposium, Washington DC,* vol. 2B, pp. 511-514, July. 2005.

[59] K. R. Boyle, Y. Yuan and L. P. Ligthart, "Analysis of mobile phone antenna impedance variations with user proximity," *IEEE Transactions on Antennas and Propagation,* vol. 55, pp. 364-272, Feb. 2007.

[60] C. M. Su, C. H. Wu, K. L. Wong, S. H. Yeh and C. L. Tang, "User's hand effects on EMC internal GSM/DCS dual-band mobile phone antenna," *Microwave and Optical Technology Letters,* vol. 48, pp. 1563-1569, Aug. 2006.

[61] J. T. Rowley and R. B. Waterhouse, "Performance of shorted microstrip patch antennas for mobile communications handsets at 1800 MHz," *IEEE Transactions on Antennas and Propagation,* vol. 475, pp. 815 – 822, May. 1999.

[62] R. S. Zaridze, K. N. Tavzarashvili and G. N. Ghvedashvili, "Electromagnetic analysis of the distributed structures applied to EMC and SAR estimation problems," *IEEE Antennas and Propagation Society International Symposium,* vol. 2, pp. 1049 – 1052, 22-27 June. 2003.

[63] O. Kivekas, J. Ollikainen, T. Lehtiniemi and P. Vainikainen, "Bandwidth, SAR, and efficiency of internal mobile phone antennas," *IEEE Transaction on Electromagnetic Compatibility,* vol. 46, pp. 71-86, Feb. 2004.

[64] Z. Wang, X. Chen and C. G. Parini, "Effects of the ground and the human body on the performance of a handset," *IEE Proceeding on Microwaves, Antenna and Propagation,* vol. 151, pp. 131-134, Apr. 2004.

[65] L. C. Kuo and H. R. Chuang, "Design of a 900/1800 MHz dual-band loop antenna mounted on a handset considering the human hand and head effects," *Antennas and Propagation Society International Symposium, IEEE,* vol. 3, pp. 701 – 704, 2003.

[66] C. M. Kuo and C. W. Kuo, "SAR distribution and temperature increase in the human head for mobile communication," *Antennas and Propagation Society International Symposium, IEEE,* vol. 2, pp. 1025 – 1028, 22-27 June. 2003.

[67] C. Gabriel, "Phantom models for antenna design and exposure assessment," *IEE Colloqium on Design of Mobile Antennas for Optimal Performance in the Presence of Biological Tissue,* pp. 6/1-6/5, Jan. 1997.

[68] A. O. Rodrigues, L. R. P. Malta, R. Borsali, R. B. Takai and R. Conhalato, "SAR calculations in an anatomically realistic model of the head of cellular phone users," *The Institution of Electrical Engineers, IEE,* 2002.

[69] A. Sargent and C. Zombolas. SAR testing of IEEE 802.11a/b/g devices. http://www.ce-mag.com/archive/05/07/zombo2.html.BAKpp. (Last accessed: 27 Feb. 2008)

[70] M. A. Stuchly, M. Rahman, M. Potter and T. Williams, "Modeling antenna close to the human body," *Aerospace Conference Proceedings, IEEE,* vol. 5, pp. 83-89, 18-25 Mar. 2000.

[71] O. A. Saraereh, M. Jayawardene, P. McEvoy and J. C. Vardaxoglou, "Simulation and experimental SAR and efficiency study for a dual-band PIFA handset antenna (GSM 900 / DCS 1800) at varied distances from a phantom head," *Antenna Measurements and SAR, AMS 2004, IEE,* pp. 5 – 8, 25-26 May. 2004.

[72] CENELEC ENV 50166-2," *Brussels,* 1995.

[73] IEEE standard C95.1 1995. *IEEE, New York*

[74] M. F. Iskander, Z. Yun and R. Quintero-Illera, "Polarization and human body effects on the microwave absorption in a human head exposed to radiation from handheld devices," *IEEE Transaction on Microwave Theory and Techniques,* vol. 48, pp. 1979-1987, Nov. 2000.

[75] L. W. Li, P. S. Kooi, M. S. Leong, H. M. Chan and T. S. Yeo. (2000, July). Antenna patterns & input impedance of handset antennas and SARs in human head: A comparative study using FDTD. *Extended Report of Journal of Electromagnetic Waves and Applications.* pp.987-1000. http://www.ece.nus.edu.sg/stfpage/elelilw/Handset.htm. (Last accessed: 29 May 2008)

[76] O. P. Gandhi and G. Kang, "Some present problems and a proposed experimental phantom for SAR compliance testing of cellular telephones at 835 and 1900 MHz," *Physics in Medicine and Biology,* vol. 47, pp. 1501-1518, 2002.

[77] J. Cooper and V. Hombach, "The specific absorption rate in a spherical head model from a dipole with metallic walls nearby," *IEEE Transactions on Electromagnetic Compatibility,* vol. 40, pp. 377 – 382, Nov. 1998.

[78] H. Dominguez, A. Raizer and W. P. Carpes Jr., "Electromagnetic fields radiated by a cellular phone in close proximity to metallic walls," *IEEE Transactions on Magnetics,* vol. 38, pp. 793 – 796, Mar. 2002.

[79] N. Homsup and T. Jariyanorawiss, "FDTD Simulations of a Mobile Phone Operating near a Metal Wall," *International Symposium on Communications and Information Technologies, ISCIT '06,* pp. 332 – 335, Oct.- Sept. 2006.

[80] P. Bernardi, M. Cavagnaro and S. Pisa, "Evaluation of the SAR distribution in the human head for cellular phones used in a partially closed environment," *IEEE Transactions on Electromagnetic Compatibility,* vol. 38, pp. 357 – 366, Aug. 1996.

[81] C. J. Panagamuwa, W. G. Whittow, R. M. Edwards and J. C. Vardaxoglou, "A study of the effects of metallic pins on SAR using a Specific Anthropomorphic Mannequin (SAM) head phantom," *The Second European Conference on Antenna and Propagation, EuCAP2007, Edinburgh, United Kingdom,* Nov. 2007.

[82] W. G. Whittow, C. J. Panagamuwa, R. M. Edwards and J. C. Vardaxoglou, "On the effects of straight metallic jewellery on the specific absorption rates resulting from face-illuminating radio communication devices at popular cellular frequencies," *Physics in Medicine and Bio.,* vol. 53, pp. 1167-1182, Feb. 2008.

[83] N. A. Samsuri and J. A. Flint, "On the effect of jewelry rings on specific absorption rate (SAR)," *Antennas and Propagation Conference, LAPC 2006, Loughborough,* pp. 421 – 424, 11-12 Apr. 2006.

Chapter 3

Metallic Loop-like Jewellery Items and Validation to the TLM Model

3.0 Introduction

In this chapter, a simulation study focusing on the effect brought about by metallic loop-like jewellery items is presented. The simulations will also provides validation for the capability and accuracy of the TLM modelling method (as implemented in the commercial solver Microstripes) compared to published results using other commercialized simulating software based on FDTD. The effect of different sizes and orientation of the metallic loop-like jewellery items relative to the monopole antenna are investigated. The metallic jewellery is also given different metal properties for comparison. In order to investigate the effect brought about by the small ring worn on human fingers, a simple block-hand model with cylindrical fingers was modelled. The ring was place on different fingers in the simulations for comparison. Finally, a simple hand phantom is manufactured and measurements were performed. The measurement results are then compared with simulations.

3.1 Numerical modelling

Most of previously published studies have employed FDTD by [1] such as in [2-6]; Method of Moment (MoM) [7] and Finite Element Method (FEM) [8] to estimate the effect of human body on the antenna performance and on SAR. In addition to the above-mentioned methods, Babli et al. [9] and Dominguez et al. [10] employed the TLM method in their investigations on the interaction of the electromagnetic fields with dielectric bodies and to calculate the SAR in the head exposed to a mobile

handset close to the metallic wall. The investigations in this thesis also employ the TLM method in evaluating the antenna performance and SAR, in the presence of the head, the hand and metallic jewellery items in the vicinity of the radiating source.

The TLM method is a numerical modelling technique for solving Maxwell's equations for the electromagnetic fields in space and time [10, 11]. In this technique, the time is divided into discrete time steps whilst the space is divided into cells. The time step is automatically found by the size of the smallest cell and the properties of that cell. Each cell is modelled as the intersection of 12-orthogonal transmission lines that combined several shunt and series nodes [12, 13]. Hence, in TLM, there exists a direct correspondence between the field components with voltages and currents on the transmission lines [13, 14]. Therefore, voltage pulses that travel along the lines scatter at the center of the node and results in reflected pulses that are incident on the adjacent nodes. At each time step, the E-fields and H-fields are calculated directly from the voltages and currents on the set of the transmission lines. The scattering matrix (form by the incident and reflected voltages) can be modified to account for dielectric/magnetic materials, radiating and conducting boundaries [13].

The TLM approach is implemented in Microstripes [15], one of the electromagnetic simulation software packages that solve the fields via the TLM method. All the results presented and discussed in this thesis are obtained through simulations using MicroStripes V7.0. Microstripes has been employed to design intricate antenna structures, assess installed performance, optimize RFID tags, predict absorption of electromagnetic fields in human tissues, determine radar cross-section (RCS), EMI/EMP and lightning effects on vehicles, ships and aircraft. Microstripes has a sophisticated graphical interface, which can handle CAD data and the solver has many extensions to the basic TLM method. For example, it incorporates a fast meshing algorithm with a multi-grid technique in the solver and it also has a sub-cell wire model.

The TLM Symmetrical Condensed Node (SCN) is presented in Figure 3.1-1. The geometric model is modelled in the Build window, assigned with corresponding materials and excited with specified source (via either a port or free space excitation).

The required output type was defined while the workspace and the mesh around the geometric model is generated. In terms of meshing, the mesh size is highly dependent on the frequency of operation and the dielectric material used in the model. However, Microstripes has enabled the automatic meshing algorithm which ensures the mesh is fine enough consequently eliminates the need for such fine tuning, thus allowing automatically generated meshes to be used for nearly all simulations. The cell sizes can be modified to ensure more efficient and accurate mesh but care must be taken as this may significantly affect the computation time/size and accuracy. Hence, the computation time is proportional to the total number of cells in the model. Longer computation time due to larger number of cells can be reduced by using cell lumping which lumped small cells together to form larger cells.
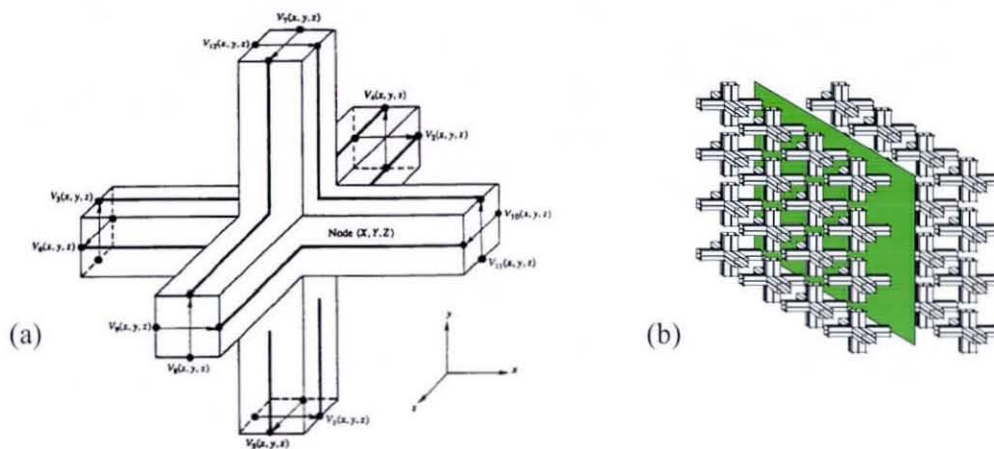
Figure 3.1-1: (a) TLM node (SCN) [12] and (b) TLM meshed volume with a fixed thin boundary [16].

Microstripes is a time domain TLM solver. At the end of the simulations, the time-domain file is produced and Fourier Transform is used to generate the frequency-domain results (S-parameters, input impedance, SWR). With a small number of measurement points, the entire transient response is captured in one simulation and the results are obtained via Fourier Transform. However, to generate a SAR map at a particular frequency, a lot of measurement points are needed. In addition, Microstripes also capable to solve all frequencies of interest (up to 99 frequencies) in a single calculation and therefore provides the full broadband response of the system in one simulation cycle. However, this takes up RAM in the computer (it has to hold 1 matrix in memory for the whole simulation per frequency). Hence, the more

frequencies chosen, the more memory is consumed. For an individual data point, the memory is not that important because at each time step the solver writes the E and H field to the disk. The electromagnetic fields, surface currents, wire currents and radiation patterns (including efficiencies) results are visualized in full 3-D. Moreover, the specific absorption rate (SAR) and the averaged 1 g/10 g SAR (W/kg) in any lossy medium at any requested frequencies can be obtained and generated by only one time-domain simulation.

3.2 Commercially-available metallic hoop-earring sizes

There are many earring shapes available and worn on the human ear. Some of them are stud in the ear and some are pierced. The effects of metallic loop/hoop/circular have been studied by other published research; for example in [17, 18]. In the current thesis, metallic hoop/loop earring shapes are employed and investigated further. The commercially available sizes of the hoop/loop metallic earring are summarized in Table 3.2-1. Hence, a commercial earring is 1.5, 2 or 3 mm thick, but a typical loop thickness is found to be 2 mm (Figure 3.2-); therefore the thickness of earrings (of different external diameters) investigated in the current thesis are set to 2 mm.

Thickness
(minor diameter)
2 mm

Table 3.2-1: The commercial earring sizes and their external diameter in wavelength (λ) corresponding to the wavelength of specified frequencies.

earring external
diameter
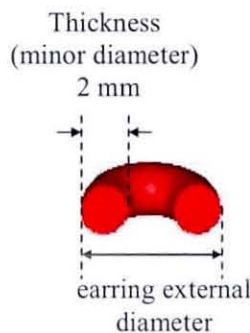
Figure 3.2-1: The earring dimensions.

Diameter (mm)	900 MHz	1800 MHz	1900 MHz	2450 MHz
20	0.06λ	0.12λ	0.13λ	0.16λ
25	0.08λ	0.15λ	0.16λ	0.20λ
30	0.09λ	0.18λ	0.19λ	0.24λ
35	0.11λ	0.21λ	0.22λ	0.29λ
40	0.12λ	0.24λ	0.25λ	0.33λ
45	0.14λ	0.27λ	0.28λ	0.37λ
50	0.15λ	0.30λ	0.32λ	0.41λ
70	0.21λ	0.42λ	0.44λ	0.57λ
80	0.24λ	0.48λ	0.51λ	0.65λ
90	0.27λ	0.54λ	0.57λ	0.73λ

3.3 Commercial metallic rings and bangles sizes

The fit of the ring will differ from person to person. Table A.1 in the Appendix A summarized the ring sizes commercially available in several different countries. Different countries have different ways of representing the size. In the UK and Australia, letters of the alphabets one used and this will be the standard referred to in this thesis.

Bangle sizes and fits tend to be even more variable than rings because a deciding factor on size choice is the ability of the wearer to pass their hand through the center. Hence, bangles are much looser than rings on most people. Consequently, the diameter of the bangle is required as two people may have the same wrist size, yet differences in the size of their hands differentiate their bangle sizes. Table A.2 in the Appendix A illustrates the relationship between the standard diameters of certain bangle sizes, with the correlated inner circumference. The bangle diameters are generally supplied in increments of 1/16 of an inch.

3.4 Validation to the TLM model

This thesis presents results that attempt to quantify the effect of metallic jewellery when worn on human head and hand using TLM method when compared with the FDTD method to show the accuracy of the TLM tool in evaluating the antenna performance and SAR. The human head is represented as a homogeneous cubic box filled with head simulating liquid (HSL) at 1800 MHz with a relative permittivity (ε_r) of 40.48 and a conductivity (σ) of 1.37 S/m. The head phantom is covered with a 2 mm thick layer fibreglass with the ε_r is set to 3.5 and the conductivity is 0 S/m. Although the simple box homogeneous phantom is not realistic and may overestimate the SAR values [19], it is however a useful and repeatable method in estimating the effect brought about by the presence of the metallic objects near biological tissues/bodies. The results obtained by the homogeneous cubic model may represent a worst-case scenario in investigating the effects of circular metallic items [17].

The model consists of a 74 mm long dipole antenna as a radiating source resonating at 1800 MHz. The distance from the dipole antenna to the surface of the phantom is 40 mm (Figure 3.4-1). The results presented in [17] were simulated by FDTD. These models were replicated and the simulations were performed by means of TLM, Microstripes (V.7) simulation software. The model has been modified in length and was chosen to be large enough to ensure enough penetration depth for the electromagnetic energy. It was proven by carrying out a convergence test that the depth allowed in the simulation was adequate for the electromagnetic waves to decay to a suitable value before reaching the numerical boundary of the simulation.
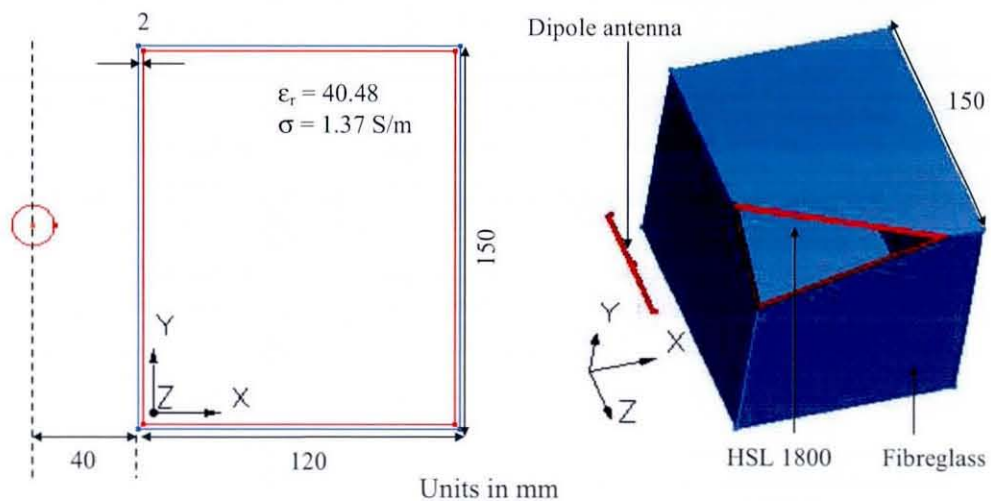
Figure 3.4-1: Phantom dimension at 40 mm from a dipole antenna at 1800 MHz.

In [17], the circular earring (with different sizes) was placed at various distances from the homogeneous cubic phantom surface starting from 0 mm to 16 mm with the step size of 4 mm. However, the metallic loop in this study is placed at only 0, 4, 8 and 12 mm from the cubic phantom surface (Figure 3.4-2) as this is assumed to be suitable enough to show the accuracy of TLM method in providing the same effect as other simulation tools (with the same model properties and conditions). In each case, the loops were given the conductivity equal to the conductivity of copper. The metallic loops dimensions employed in the current section are as in Table 3.4-1.
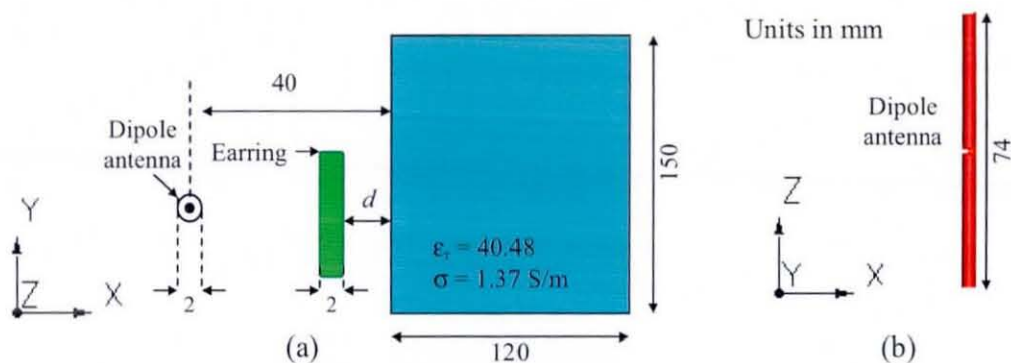
Figure 3.4-2: (a) Metallic loop jewellery placed at d distances from the phantom (d = 0, 4, 8 and 12 mm) and (b) a dipole antenna dimension.

Table 3.4-1: Metallic loop jewellery sizes employed in the simulations (1800 MHz).

Circumference of loop (wavelength λ)	External diameter (mm)
No loop	-
0.7	37.0
0.8	42.4
0.9	47.6
0.95	50.2
1.0	53.0
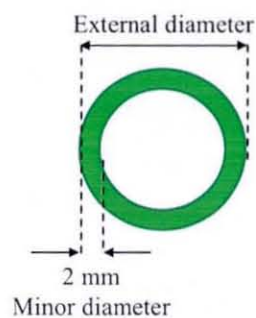
3.4.1 Validation results

Simulation results of the averaged 1 g SAR obtained by the TLM and as published in [17] are shown in Figure 3.4-3. It can be seen that both results are agree well in shape. There are only slight variations in the values due to the possibility of different meshing size on the antenna and the phantom models, or probably on the loop model itself. The effect of changing wavelength is variable. The averaged 1 g SAR in the head is significantly increased by the circular metallic earring when the circumference is approximately one-wavelength and at certain distance from the phantom surface. In this case, the largest increase with the λ wavelength is observed at 12 mm from the phantom. With a dipole antenna oriented in the z-direction (see Figure 3.4-2), the currents around the ring are at the greatest on the sides of the ring and the least on the top and bottom sections of the ring. These currents induce magnetic fields in a similar pattern around the ring. In terms of SAR distribution, Figure 3.4-4 shows the SAR distribution for the λ wavelength ring at 12 mm from the phantom. The maximum

SAR in the head appears at the edges of the circular earring not at the center of the earring and again, agrees well with [17]. When the electromagnetic field impinges on metallic object, the field is scattered and the metallic objects may redistribute the incident RF energy around them. This could lead to a significant SAR concentration around certain part of the object and corresponding SAR reduction in other areas. As the results presented here agreed well and in shape with the results presented in [17], therefore it provides evidence that TLM is useful enough and could estimate the interaction between the antenna, the head/hand and metallic jewellery items in close proximity. In addition, the results presented in Table 1 in [17] also indicated that the result produces by Microstripes (TLM) are comparable and in good agreement with other commercial software.
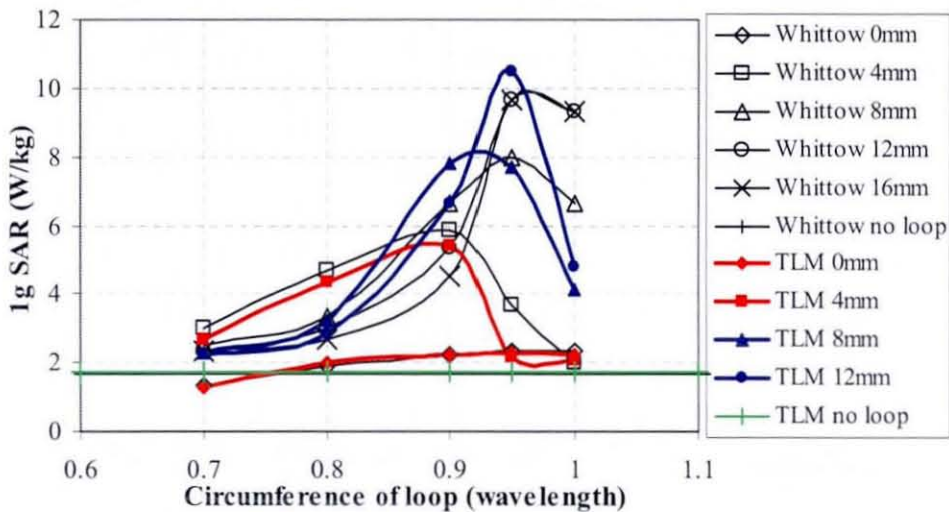
Figure 3.4-3: TLM simulations of different loops sizes at various distances from a cubic phantom. The TLM simulation results are validated against published results in [17].
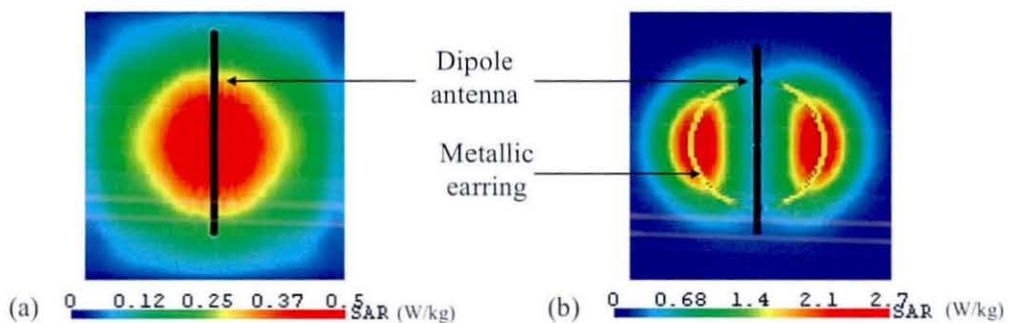
Figure 3.4-4: The maximum SAR in the head (a) without metallic-loop and (b) with metallic-loop (appears at the edges of the circular earring, not at the center of the earring).

3.5 A monopole antenna as radiating source

Different types of antenna may exhibit different performance characteristics depending on their location relative to the human head. The phone position relative to the head may vary from one person to another. As mentioned in Chapter 2, a monopole antenna on a metal box is employed as a radiating source in this thesis. This device has a simple structure and could be positioned easily with respect to the head. The validation of TLM model as discussed in the above Section 3.4 is replicated in this section but the dipole antenna is replaced with a $\lambda/4$ monopole antenna on top a metal box ($20 \times 50 \times 90$ mm) operating at 1800 MHz. The monopole antenna is kept at 40 mm distance from the surface of the cubic phantom whilst the antenna feed point is still at the center of the loop (Figure 3.5-1). Figure 3.5-2 shows the difference between the results utilizing a dipole and a monopole antenna as the radiating source at 1800 MHz. The results show the same trend where significant increase in the averaged 1 g SAR in the head is found when the circumference of the circular metallic earring is approximately one-wavelength and at a range of distances from the phantom surface. However, the monopole antenna produces lower averaged 1 g SAR values although the same distance and sizes of loops are employed. This would agree with [20] that different antenna may exhibit different performance and therefore could also affect the SAR values quite differently [21-24].
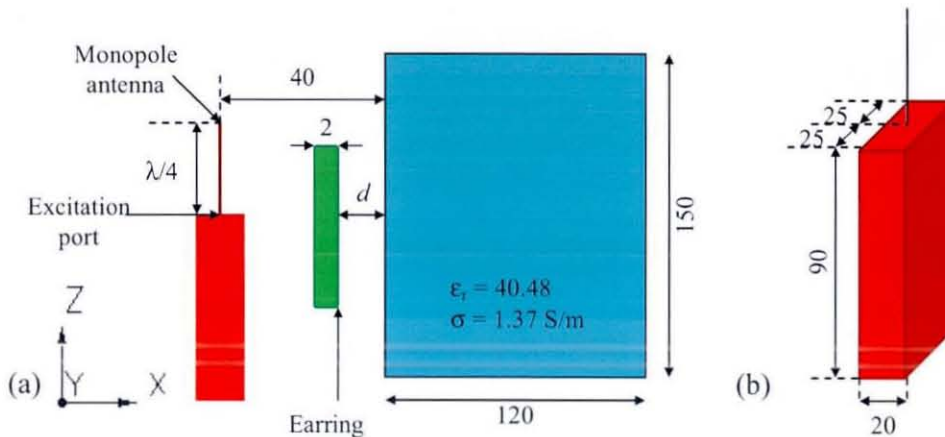
Figure 3.5-1: (a) Simulation setup for the handset-loop model and (b) monopole antenna on top of a metal box dimension, (units in mm). d is a distance from the phantom.
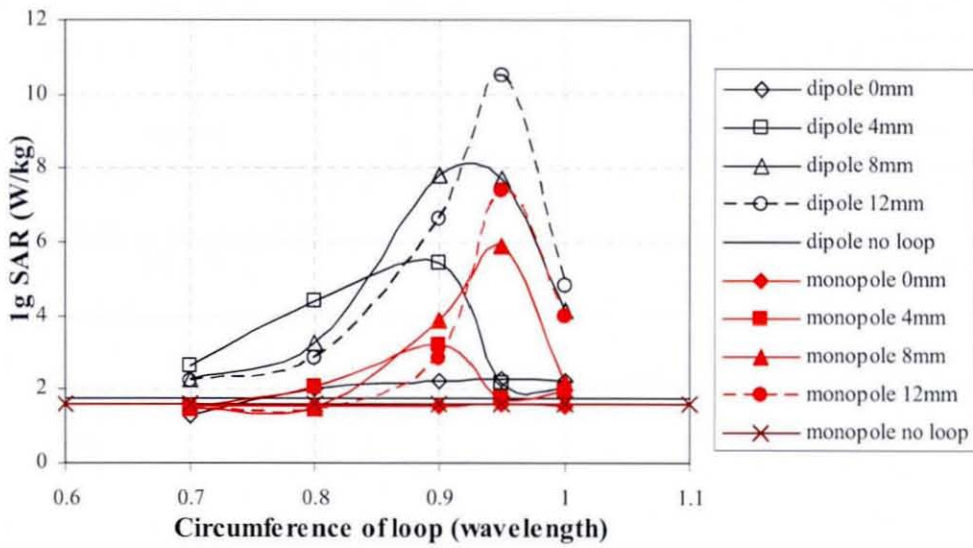
Figure 3.5-2: The averaged 1 g SAR values for the dipole and the monopole antenna at 1800 MHz.

3.5.1 Realistic phantom-antenna separation distance

The mobile handset is typically placed very close to the head near the left or the right ear, where part of the radiated energy is absorbed by the head and nearby tissues [25]. Small variations in antenna-nearby objects position and orientation could significantly influence the energy absorption and distribution within the exposed body. The dipole and monopole antenna feed point employed in [17, 18, 26] was placed at about the center of the earring. However, to allow a more realistic condition of operating a mobile handset, the monopole antenna in the current experiments is placed at 20 mm from the surface of the cubic phantom for frequencies of 900 MHz and 1800 MHz. A loop of different sizes was kept at 4 mm distance from the phantom surface with its top level with the feed point of the monopole antenna (top case) (see Figure 3.5-3 (a)), while the monopole feed point is placed behind the center of the loop in the middle case (see Figure 3.5-3 (a)). At 900 MHz, the relative permittivity (ε_r) of the HSL is set to 41.5 with conductivity (σ) of 0.97 S/m.

Figure 3.5-3 (b) shows the effect of positioning the monopole antenna feed point in the middle of the loop and at the loop's top (see Figure 3.5-3 (a)), both at 900 and

1800 MHz. The results of a dipole antenna at 1800 MHz are also shown for comparison with the monopole. It can be seen that the position of the antenna feed point relative to the metallic loop near the phantom noticeably alters the averaged 1 g SAR values especially for the loop with circumference of 0.9λ. Significant changes are observed with the monopole antenna on top of metallic box at both 900 MHz and 1800 MHz cases.

(a)

(b)
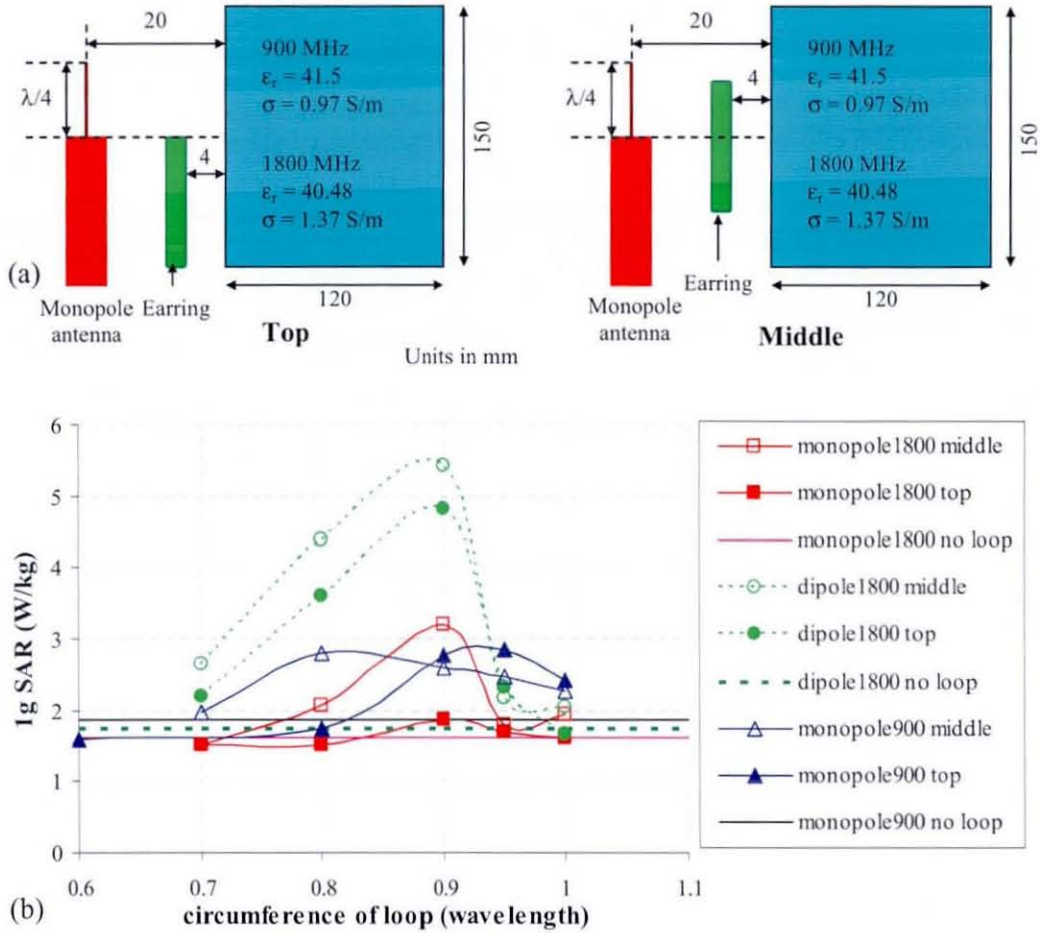
Figure 3.5-3: (a) Different antenna feed point position relative to the metallic loop and (b) the averaged 1 g SAR in the cubic phantom at 900 and 1800 MHz. Metallic loop was placed at 4 mm from the phantom in all cases.

In the next investigation, the monopole antenna was placed at different distances (d), namely at 20, 25 and 40 mm from the phantom's surface. The metallic loop of 2 mm length and thickness was fixed at 4 mm from the phantom surface (see Figure 3.5-5 (a)). As expected, the averaged SAR increases significantly when the radiating source was placed closer to the phantom [27, 28]. The results are shown in Figure 3.5-4. The

3-11

highest averaged 1 g SAR is observed when the antenna was placed at 20 mm from the phantom compared to 25 and 40 mm. However, the effect of the metallic loops placed at 4 mm from the phantom could vary depending on their sizes relative to the wavelength and the operating frequency.
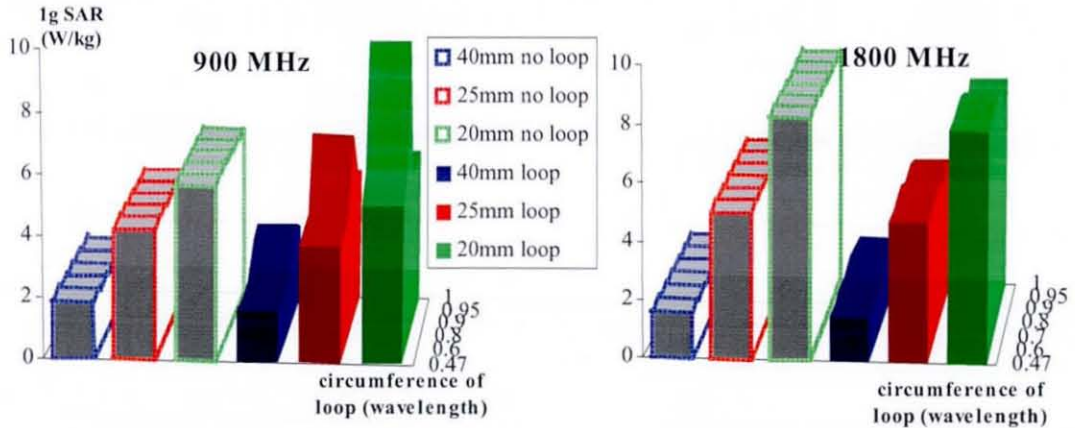
Figure 3.5-4: The effect of different antenna distances from the phantom surface, with and without metallic loop at 900 MHz and 1800 MHz. These graphs correspond to the simulations defined by Figure 3.5-5 (a).

Next, the monopole antenna feed point is placed at 20 mm from the phantom surface and the length of the loop (*l*) is changed to 5 mm whilst the thickness is kept 2 mm (see Figure 3.5-5 (b)). In this case, the effect of the metallic loop length on SAR was observed. Following these experiments, the effect of a metallic loop when placed behind the antenna was investigated. The metallic loop with both 2 and 5 mm length (*l*) were oriented perpendicular (horizontal) to the handset body and the phantom; and placed at 12 and 24 mm (*d*) behind the antenna (see Figure 3.5-5 (c)). This orientation would represent the case of wearing a ring on the human finger. The loop's length and diameters were also varied. The latter model includes both the loop in the front and behind of the antenna feed point (see Figure 3.5-5 (d)). These may represent the case when both earring and ring worn in close proximity to the head and the antenna. The ring (loop behind the antenna) in this case was 5 mm in length and placed at 12 and 24 mm distance (*d*) behind the antenna, while the earring was 2 mm in length and fixed at 4 mm from the phantom surface. The results for the above mentioned cases are shown in Figure 3.5-6 to Figure 3.5-7.

Earring loop

d

900 MHz
$\varepsilon_r = 41.5$
$\sigma = 0.97$ S/m

$\lambda/4$

2

4

150

1800 MHz
$\varepsilon_r = 40.48$
$\sigma = 1.37$ S/m

Monopole Earring
antenna

120

(a)

Thick earring loop

20

900 MHz
$\varepsilon_r = 41.5$
$\sigma = 0.97$ S/m

$\lambda/4$

5

4

150

1800 MHz
$\varepsilon_r = 40.48$
$\sigma = 1.37$ S/m

Monopole Earring
antenna

120

(b)

Z

Y   X

Finger ring

20

900 MHz
$\varepsilon_r = 41.5$
$\sigma = 0.97$ S/m

$\lambda/4$

l

Ring

d

150

1800 MHz
$\varepsilon_r = 40.48$
$\sigma = 1.37$ S/m

Monopole
antenna

120

(c)

Finger and ear ring

20

900 MHz
$\varepsilon_r = 41.5$
$\sigma = 0.97$ S/m

$\lambda/4$

2

2

4

5

Ring

d

150

1800 MHz
$\varepsilon_r = 40.48$
$\sigma = 1.37$ S/m

Monopole Earring
antenna

120

(d)

Figure 3.5-5: Simulations of different loop sizes, orientation and distances from the antenna:

(a) a simulation of different loop sizes at a range of distances (d) from a cubic phantom with the top of the loop level with the antenna feed point;

(b) the monopole feed point and was fixed at 20 mm from the phantom surface, the loop is fixed 4 mm from the phantom surface and its length (l) was varied (2 and 5 mm);

(c) the loop is oriented perpendicular to the handset body and placed at (d) distance behind the antenna feed point, the loop length (l) was varied between 2 and 5 mm; and

(d) the loop in the front (2 mm length) and behind (5 mm length) the antenna are included.

The results presented in Figure 3.5-6 and Figure 3.5-7 are for the monopole antenna placed 20 mm from the phantom surface. The antenna feed point is level with the top of the metallic earring placed in front of the antenna (parallel to the phantom); but in series with the ring positioned behind the antenna (perpendicular to the phantom surface). The results presented in [18] have found that the metallic earrings, metallic loops and rings have an effect on SAR. However, the study showed that these effects were dependent on the metallic objects/implants size, orientation relative to the antenna, frequency of operation and proximity to the human body.

In the current simulations (see Figure 3.5-5), the averaged 1 g SAR at 1800 MHz generally decreases in the presence of a metallic loop at 4 mm from the phantom surface (see Figure 3.5-6). However, the average 1 g SAR values at 900 MHz are significantly increased when the loop circumference is in the range of 0.6-0.8λ. In addition, metallic loops placed 12 and 24 mm behind the antenna have generally a lower averaged 1 g SAR regardless of the length (2 or 5 mm) at both frequencies tested.
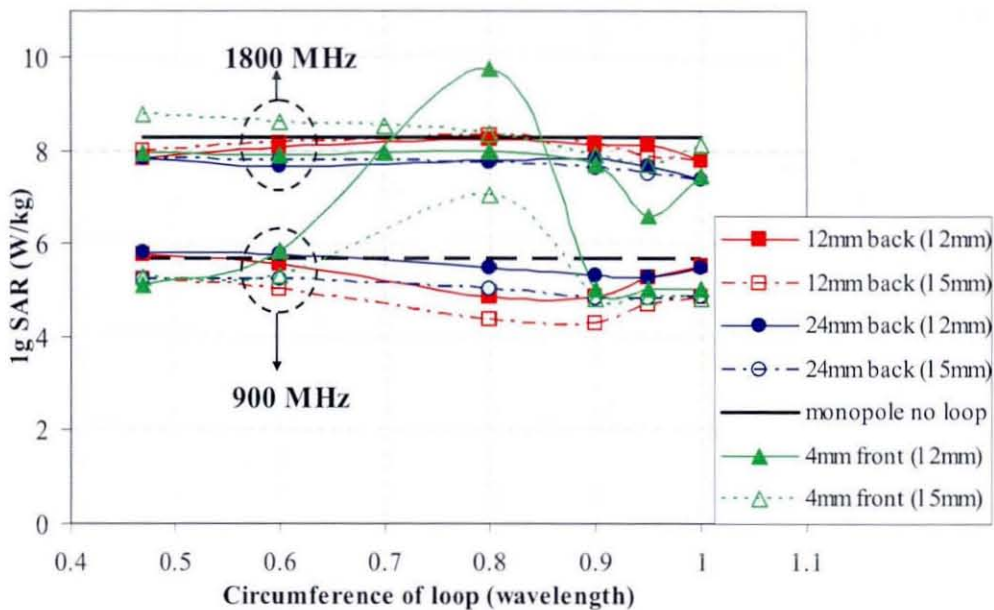
Figure 3.5-6: Metallic loop thickness, position and orientation effect on the averaged 1 g SAR at 900 MHz and 1800 MHz. This graph corresponds to the case defined in Figure 3.5-5 (b and c).

Virtanen et al. [26] suggested that a metallic object positioned parallel to the antenna may results in notably higher SAR. However, from the results of the current simulation in this thesis (see Figure 3.5-6) it was found that metallic loop that is perpendicular to the antenna and the phantom surface, and placed behind the antenna could possibly helps to reduce the SAR inside the phantom. Beside that, metallic ring (behind the antenna) could alter the averaged 1 g SAR resulted by the presence of metallic earring (4 mm in front of the phantom) (see Figure 3.5-7). The changes on the averaged 1 g SAR due to the ring (behind the antenna) indicates considerable coupling between the antenna with both the metallic loops of the front and behind the antenna although the effect is quite small However, the phantom model employed in this simulation was highly simplified; while the metallic earrings or rings position are completely approximated to the corresponding flat phantom. Hence, the correct positioning of the ring on the finger and the earring on the ear (in the simulation) is very important as the presence of the human head and the hand may introduce different affect on SAR values. The effect by the presence of metallic loops may therefore be varied depending on the size, orientation relative to the antenna, frequency of operation and the proximity to the corresponding body.
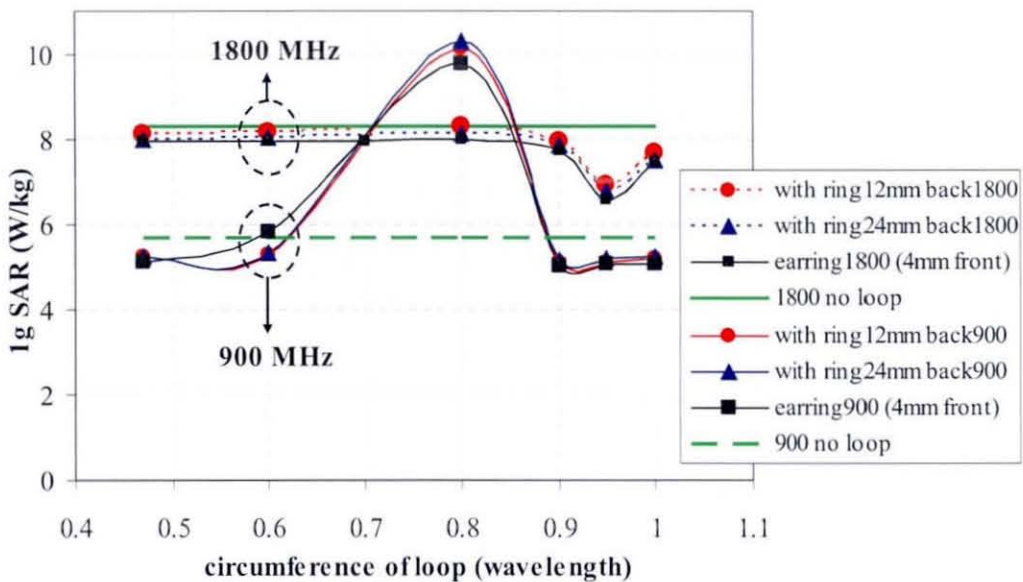
Figure 3.5-7: The effect of metallic ring (at 12 or 24 mm behind the antenna) and the earring (4 mm from the phantom) present on the averaged 1 g SAR within the phantom. This graph corresponds to the case defined in Figure 3.5-5 (d).

3.5.2 Effect of metal types

So far, the simulations have been presented for copper; however few jewellery items are made of copper. The reason for choosing this material was to enable economical experimental verification, where possible. In practice a range of metals such as Silver (Ag), Titanium (Ti), Gold (Au), Platinum (Pt) and, more recently, Palladium (Pd) are used. To investigate the effect of different materials used for jewellery on SAR at 900 MHz and 1800 MHz, besides copper (Cu), the loop in this section was given the properties of Silver (Ag) and Platinum (Pt). However, there are only marginal differences between conductivities of these metallic properties, so that the effect cause by this variation on SAR in the head is almost negligible (see Figure 3.5-8).
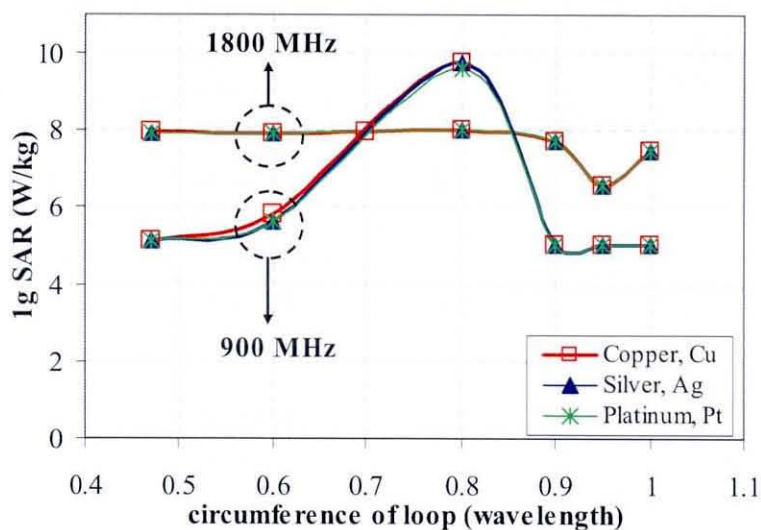
Figure 3.5-8: Different metallic loop material effect on the averaged 1 g SAR results.

3.6 A study on the effect of metallic ring worn on human fingers using a very simplified homogenous cylindrical model

In order to quantify the effect of the jewellery (rings and bangles) worn on the human hand and wrist, a series of simulations utilizing TLM were performed using a simplified homogeneous cylindrical model representing human finger or arm. A range of rings and bangle sizes were modelled both with and without dielectric present. The geometrical configurations employed in the simulation study are shown in Figure 3.6-1. In order to provide simple validation of the model, the resonant frequencies of the rings in free space (see Figure 3.6-1 (a)) were first verified with analytical expressions. The simulated frequency is within about 6% of the theoretical value, which seems reasonable given that the simulation includes the effects of realistic materials, finite thickness of the rings and since it also includes some errors due to the discretisation effects of the meshing process.
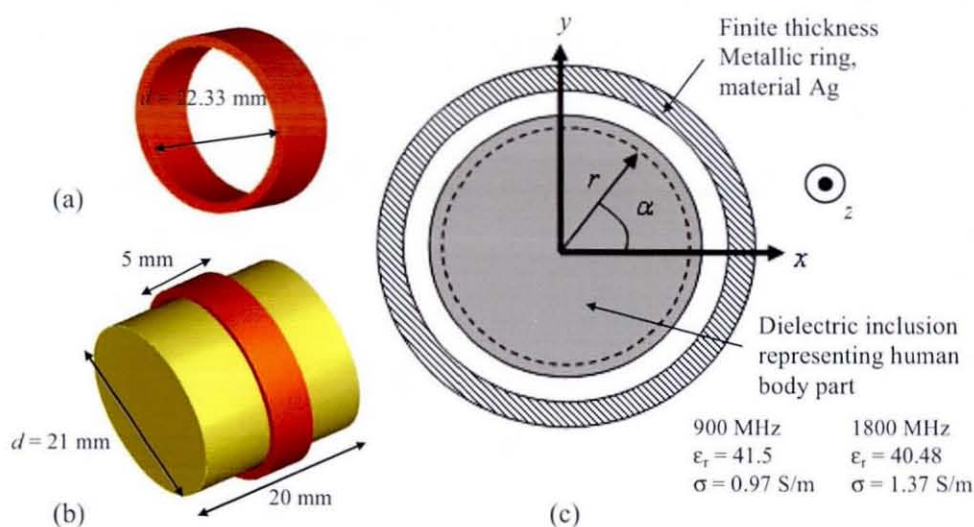
Figure 3.6-1: (a) Ring or bangle in free space, (b) ring or bangle with dielectric material (representing jewellery worn on the human hand) and (c) definition of the model parameters. The sizes shown are for the ring size Z½.

The resonant frequency for different metallic rings/bangles sizes are shown in Figure 3.6-2. A homogenous dielectric inclusion was then introduced to represent a ring

worn on the finger or a bangle worn on the wrist (Figure 3.6-1 (b)). The (frequency dependent) parameters used in the dielectric were the same as those for standard tissue equivalent liquids. In each case the excitation was provided by means of a plane wave with unit magnitude electric field originating from the +z direction and polarised in $\alpha = 0$ (Figure 3.6-1 (c)). The results are shown in Figure 3.6-3.

(a)

(b)
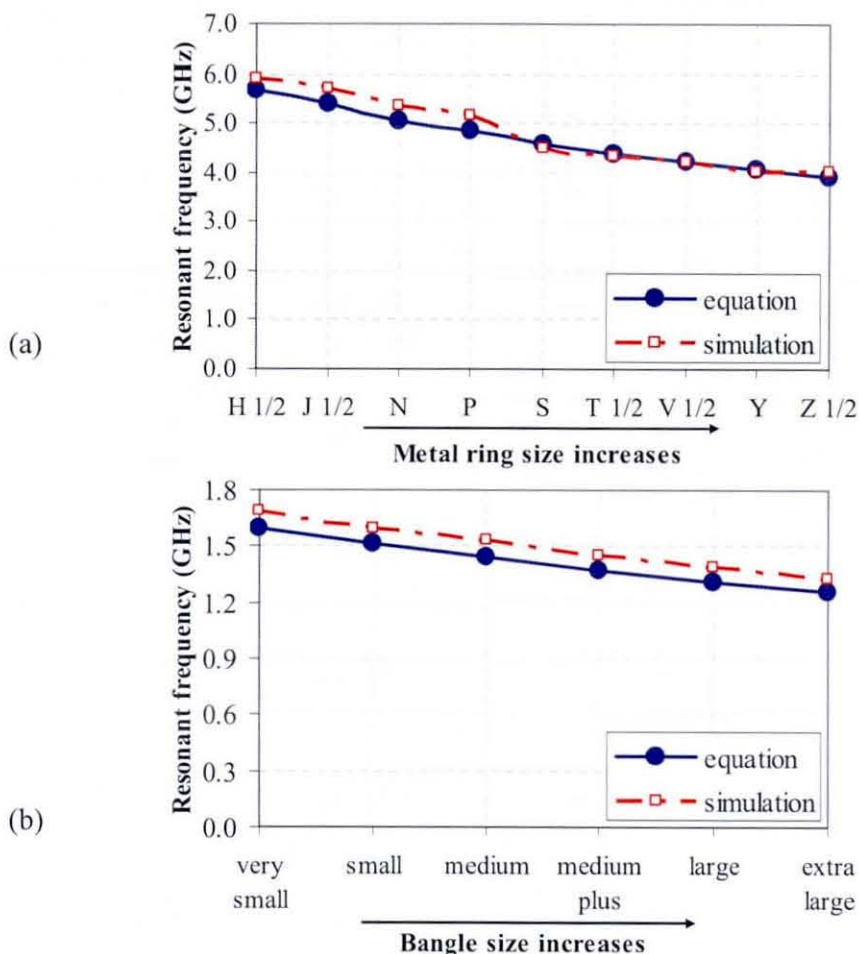
Figure 3.6-2: The (a) rings and (b) bangles resonant frequencies relative to the loop sizes (no dielectric inclusion).

From Figure 3.6-2, as expected, the larger rings have the lower resonant frequencies and it was found that only the larger bangles are liable to exhibit any resonant behavior in the mobile frequency bands of interest (900 or 1800 MHz). The introduction of the dielectric into the model further complicates matters since the resonance is both shifted in frequency and is heavily damped due to dielectric losses. In order to study the changes brought about by dielectric loading a series of plots were obtained for the electric field magnitude inside the ring. Due to the geometrical

symmetry, it was convenient to use the polar coordinate system of Figure 3.6-1 (c) and to plot the electric field as a function of α for $-180° \leq \alpha \leq 180°$. The calculations were made for various combinations of the ring and the dielectric inclusion. The electric field values were computed for regions just inside and just outside the dielectric for comparison purposes. In the simulations with both dielectric and the ring, there was a small gap deliberately introduced in between the two of approximately 0.67 mm. A typical result for a ring size Z½ is shown in Figure 3.6-3. In each case the excitation was provided by means of a plane wave with unit magnitude electric field originating from the +z direction.
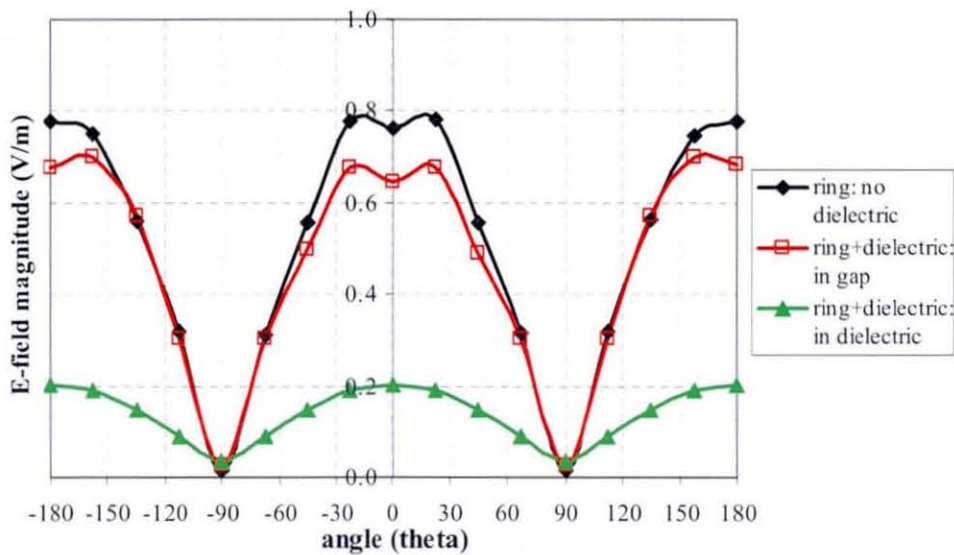
Figure 3.6-3: Electric field magnitude simulated in the gap and inside the dielectric with and without the dielectric inclusion at 900 MHz.

The electric field amplitude of the ring Z½ at 900 MHz is significantly damped with the hand present due to dielectric loading in this orientation reducing the electric field both at the centre of the ring and in the gap between the ring and the dielectric (Figure 3.6-3). The simulation results seem to suggest that the SAR value in the finger is marginally altered by the loop. However, the model is greatly simplified and a more detailed model incorporating a nearby radiator and a realistic hand phantom would be needed in order to fully verify this result. In addition, the model only considers the effect of a dielectric passing through the centre of a ring. For a finger-worn ring, there may be an effect on objects directly adjacent to the ring, such as the other fingers or the head.

3.7 A study on the effect of metallic ring worn on human fingers using a simple scannable block hand phantom

As the models presented in Section 3.6 are highly simplified, this section introduces another simple geometrical representation of a human hand that includes the fingers, which permit a metallic ring to be worn on the finger. The electric field distribution within the finger (without ring) was measured using a phantom and compared with the case when the ring is worn in an isolated finger. The measurement results were then compared with simulations with different properties of simulating liquid used in the hand model. The geometrical configurations employed in the measurement and the simulation studies are shown in Figure 3.7-1 and Figure 3.7-2. The handset was taken to be a metallic box ($90 \times 16 \times 44$ mm) with a $\lambda/4$ monopole antenna on top of it. Measurements were carried out using a DASY 4 system. The hand phantom was constructed from ABS plastic (3 mm thick) and filled with HSL at 900 MHz and 1800 MHz (Table 3.7-1).

The field distribution within fingers 1, 2 and 3 were measured along z-direction in x and y-plane. Due to the size of the probe body, only about 4 mm distance can be measured in the x and y-plane within each finger (refer to the solid-black dots in Figure 3.7-2). A metallic ring was introduced into the measurement set-up (worn on finger 2) in order to examine any change in the electric field magnitude within the fingers. In each case, the excitation was provided by means of a CW source at 900 MHz and 1800 MHz. All results in this section are normalized to 0.25 W of power. The same geometrical configurations as the measurement are then replicated in the simulations. The effects of a ring worn on human hand were simulated using Microstripes TLM. The ABS plastic relative permittivity was set to 3 with a conductivity of ~ 0 S/m. The ring investigated was modelled as copper with a radius of 16 mm, 2 mm thick and 5 mm wide. The simulation results were then compared with the measurements. Further study on the effect brought about by the ring is performed by extending the measurement points closer enough to the edge of the inner finger diameter (refer to the red line-dots in Figure 3.7-2). These points were not reachable by the probe in the measurements. Three scenarios were then considered in

simulations: (i) set the inner hand with the head liquid properties, (ii) set the inner hand with muscle properties (named 'muscle' in the result) and (iii) reduce the thickness of the ABS to 0.1 mm and then set the inner hand with muscle properties (named 'homo' in the results). The muscle properties (ε_r, σ) used in the hand model were the same as those for the standard tissue equivalent liquids recommended by the IEEE Std. 1528 and FCC [29].

Table 3.7-1: Head tissue simulating liquid (HSL) parameters filled in the hand phantom [29].

HSL	Permittivity, ε_r	Conductivity (S/m)
900 MHz	41.28	0.96
1800 MHz	40.48	1.37

(a)   (b)
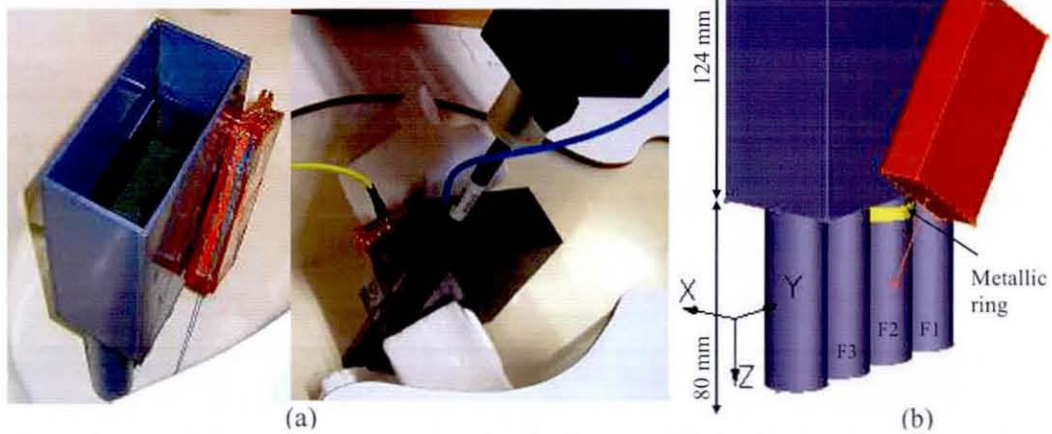
Figure 3.7-1: (a) Measurement setup: a hand phantom filled with head tissue simulating liquid, excited by means of CW source at 900 and 1800 MHz, and (b) simulation setup: a hand phantom filled with head/muscle properties, with a ring worn on finger 2.
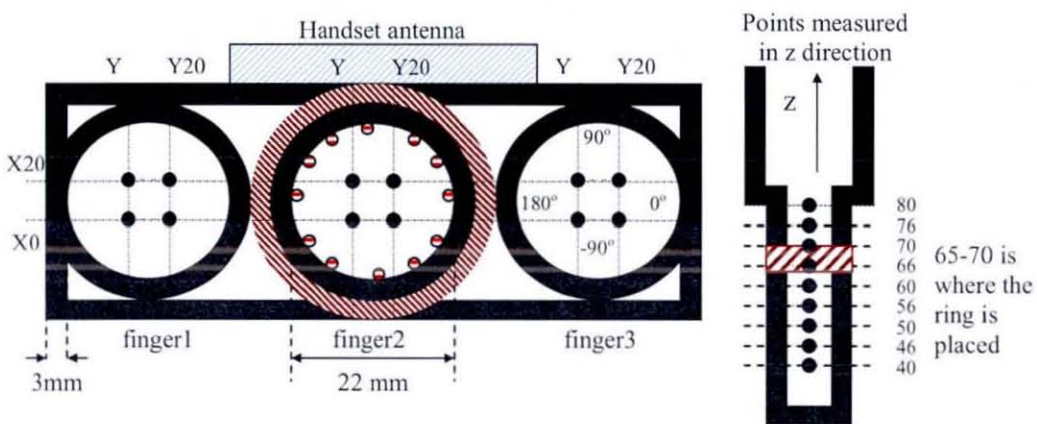
Figure 3.7-2: Points measured in the measurement and simulations (●) and the extended points set in the latter simulations (⊖).

3.7.1 Simulation and measurement results

In order to study the changes brought about by the ring inclusion, a series of plots were obtained for the electric field magnitude inside the fingers. Figure 3.7-3 illustrates the electric field magnitude changes by the ring within finger 2 at 900 MHz and 1800 MHz. The black vertical lines represent the position where the ring is placed. The ring appears to give only a minor effect on the E-field magnitude along z-direction at 900 MHz but significantly increases from the bottom (point 65) to the top (point 70) of the ring at 1800 MHz. However, the hand phantom shell is quite thick and the points measured were far in the center, the ring effects are expected to be more noticeable when the measured points are place closer to the edge of the inner finger.

Figure 3.7-3: E-field (V/m) along z-axis in finger 2 for the simulation and the measurement.

The latter results present the extended simulations with the measured points were placed closer to the edge of the inner finger (see Figure 3.7-2). The results shown in Figure 3.7-4 are for the E-field magnitude around the ring at point 65 in the finger 2. The ring does significantly alter the E- field magnitude especially at the points that were very close to the antenna ($0^o < \theta < 180^o$). The same phenomenon was observed for the hand phantom filled with 'muscle' and 'homo' properties. In addition, the ring worn on the finger 2 can also affect the E-field magnitude inside the adjacent fingers. The E-field magnitudes in the adjacent fingers (finger 1 and 3) are shown in Figure 3.7-5. The results shown are for the points along z-direction at $\theta = 0^o$ within finger 1 and $\theta = 180^o$ in the finger 3 at 900 MHz and 1800 MHz. The 1 g and 10 g SAR inside the hand with different tissue properties at both frequencies are demonstrated in Figure 3.7-6.
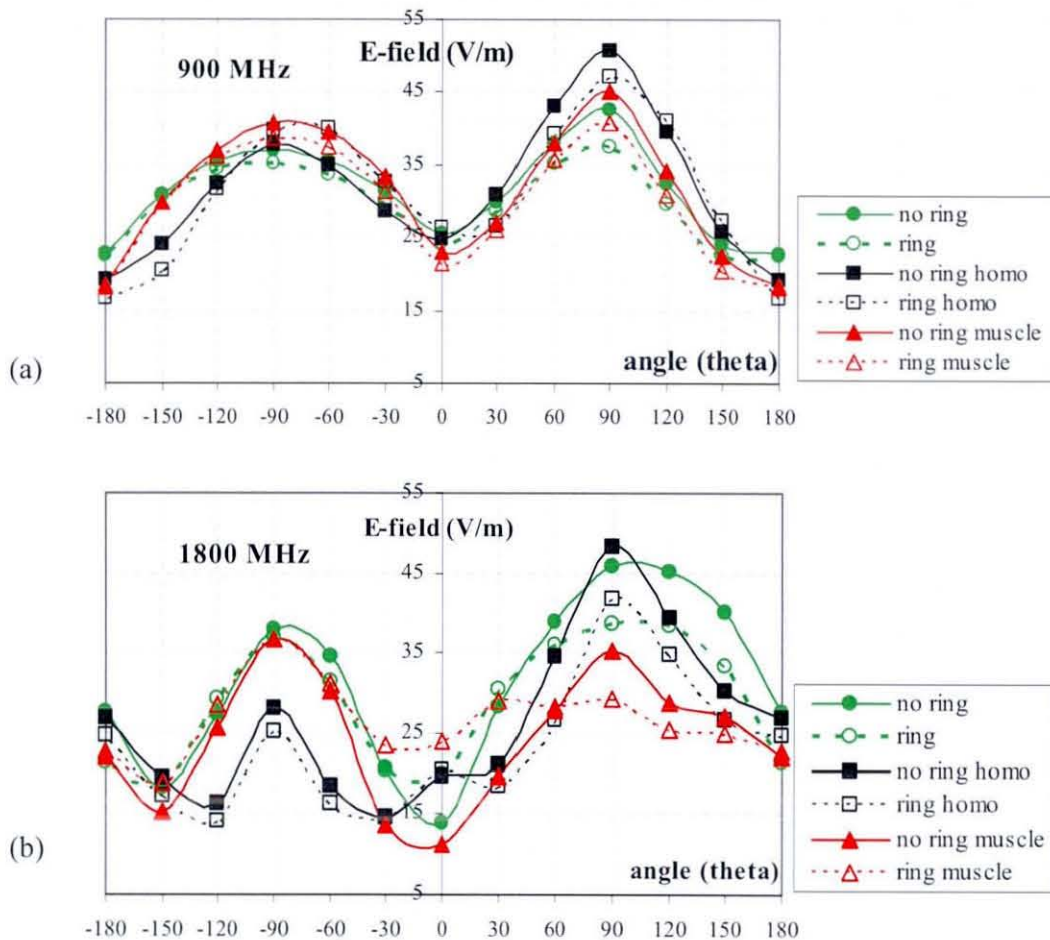
Figure 3.7-4: E-field (V/m) magnitude inside the finger 2, around the points where the ring is worn.
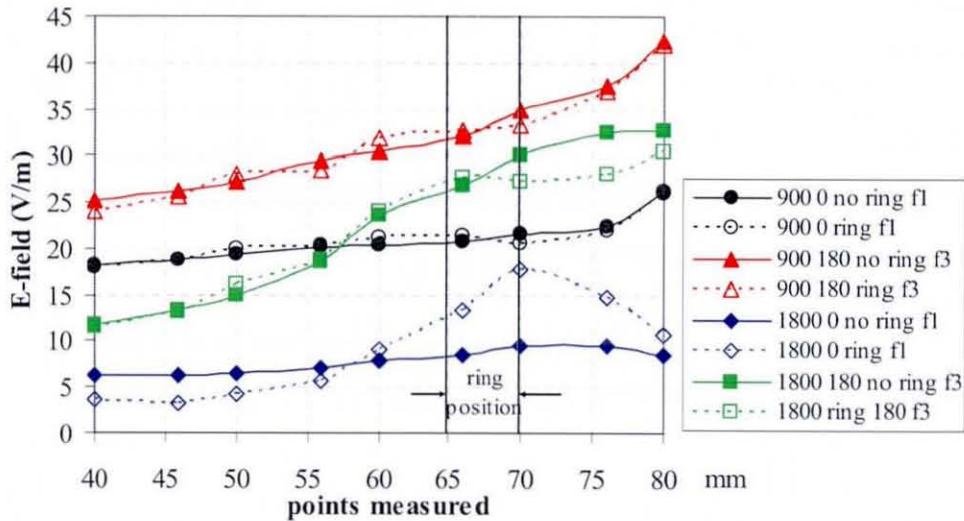
Figure 3.7-5: The E-field magnitude changes in the finger 1 and the finger 3 due to the ring worn on finger 2.
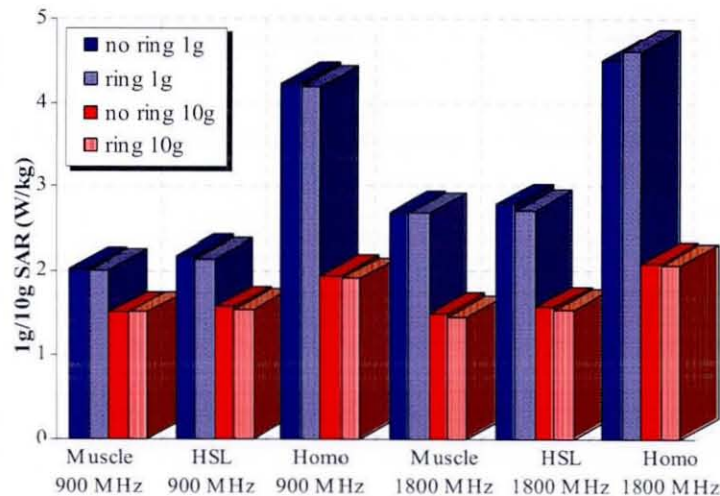
Figure 3.7-6: The simulated averaged 1 g and 10 g SAR inside the hand at 900 MHz and 1800 MHz for different tissue properties tested.

From the results shown in Figure 3.7-3 to Figure 3.7-5, the metallic ring only marginally affects the E-field magnitude within the fingers at 900 MHz but the effect was more noticeable at 1800 MHz. The metallic ring worn on one finger can also affect the E-field magnitude in the adjacent fingers at both frequencies investigated. The ring could potentially introduce additional effects as the ring could experience local enhancement of the electromagnetic field near the metallic object. Figure 3.7-6 shows that the ring does not seem to be having much effect on the SAR, but there are changes. As the metallic ring worn on the human hand does cause noticeable changes

in the E-field distribution and SAR inside the hand itself, it could also affect the SAR values inside the head when included in a complete simulation model. Hence, it is worth considering the metallic jewellery worn on the human hand when measuring the SAR. Nevertheless, it should be noted that there is a general trend for higher frequency communication devices and the influence of metallic rings may be more significant due to resonance effects.

3.8 Conclusions

In the first part of the chapter, the TLM method and Microstripes simulation software were discussed. The validity and accuracy of Microstripes (TLM) have been compared to the published results using other commercialized simulating software (FDTD). Next, series of simulations results were presented which included the effect of different size, orientation, and the location of metallic loops (ring/earring) relative to the antenna and the phantom. The results in this chapter were based on a particular simplified phantom, which does not provide any information about the real shape of the human head (with the inclusion of the ear). In addition, the exposure was only provided by means of two types of transmitter (dipole and monopole antenna). Nevertheless, this study enables conclusions to be made that generally valid within reasonable and specified limits. However, the results shown were very useful in understanding what effect that metallic jewellery worn on human might have on SAR.

The simulation results in this chapter have shown that the metallic loop of a certain size relative to the wavelength and placed at some distance from the radiating source could significantly affect the SAR. In addition, the metallic ring placed behind the antenna could alter the averaged 1 g SAR due to the presence of a metallic earring (4 mm in front of the phantom), although the effect is quite small. The results also showed that the presence of jewellery ring worn on the human hand could influence the SAR. However, the influence on the result is affected by the proximity of the ring to the handset antenna and also the coupling effect between the antenna and the dielectric within the hand model. Due to RF field scattering, the metallic loops (earring, ring or bangle) could potentially exhibit resonance effects as the can

redistribute the incident RF energy around them and experience local enhancement of the electromagnetic field near the metallic object. However, the position of the metallic jewellery items on the finger or on the ear is of great importance as the human head and the hand may have a different affect on SAR. The effect of the metallic loop may be varied depending on its diameter, orientation and proximity to the antenna and the human body, and the frequency of operation. Therefore, it is worth considering the metallic jewellery worn on the human hand when measuring the SAR. The fact that the higher frequency has a greater influence may be relevant to current trends in personal mobile communications. The next chapter will present simulation results of SAR inside a homogeneous spherical head model in the presence of a block-hand model and metallic loop-like jewellery items.

3.9 References

[1]   K. S. Yee, "Numerical solution of initial boundary value problems involving Maxwell's equations in isotropic media," *IEEE Transaction on Antenna and Propagation,* vol. 14, pp. 302-307, 1966.

[2]   C. M. Kuo and C. W. Kuo, "SAR distribution and temperature increase in the human head for mobile communication," *Antennas and Propagation Society International Symposium, IEEE,* vol. 2, pp. 1025 – 1028, 22-27 June. 2003.

[3]   S. I. Watanabe, H. Taki, T. Nojima and O. Fujiwara, "Characteristic of the SAR distributions in a head exposed to electromagnetic fields radiated by a hand-held portable radio," *IEEE Transactions on Microwave Theory and Techniques,* vol. 44, pp. 1874 – 1883, Oct. 1996.

[4]   A. K. Lee, H. D. Choi, J. I. Choi and J. K. Pack, "The scaled SAM models and SAR for handset exposure at 835 MHz," *MTT-S International Microwave Symposium Digest, IEEE,* pp. 1323-1326, 12-17 June. 2005.

[5]   O. P. Gandhi and G. Kang, "Some present problems and a proposed experimental phantom for SAR compliance testing of cellular telephones at 835 and 1900 MHz," *Physics in Medicine and Bio.,* vol. 47, pp. 1501-1518, 2002.

[6]   J. Keshvari and S. Lang, "Comparison of radio frequency energy absorption in ear and eye region of children and adults at 900, 1800 and 2450 MHz," *Physics in Medicine and Bio.,* vol. 50, pp. 4355-4369, 2005.

[7]   O. S. Dautov and A. E. M. Zein, "Application of FEKO program to the analysis of SAR on human head modeling at 900 and 1800 MHz from a handset antenna," *The 6th International Symposium on Electromagnetic Compatibility and Electromagnetic Ecology, IEEE,* pp. 274 – 277, 21-24 June. 2005.

[8]   M. Kacarska, L. Ololoska-Gagoska, S. Loskovska and L. Grcev, "Visualization of induced currents and SAR in human's head in cellular telecommunications," *Antennas and Propagation Society International Symposium, IEEE,* vol. 2, pp. 1012 – 1015, 11-16 July. 1999.

[9]   I. E. Babli, A. Sebak and N. Simons, "Application of the TLM method to the interaction of EM fields with dispersive dielectric bodies," *IEE Proceeding on Microwaves, Antennas and Propagation,* vol. 147, no. 3, pp. 211-217, 2000.

[10] H. Dominguez, A. Raizer and W. P. Carpes Jr., "Electromagnetic fields radiated by a cellular phone in close proximity to metallic walls," *IEEE Transactions on Magnetics,* vol. 38, pp. 793 – 796, Mar. 2002.

[11] D. Lukashevich, A. Cangellaris and P. Russer, "Transmission line matrix method reduced order modeling," *Microwave Symposium Digest, 2003 IEEE MTT-S International,* vol. 2, pp. 1125 - 1128, 8-13 June. 2003.

[12] C. Christopoulos, "The historical development of TLM," *IEE Colloquium on Transmission Line Matrix Modelling – TLM,* pp. 1/1 - 1/4, 18 Oct. 1991.

[13] A. Centeno, "A comparison of numerical dispersion in FDTD and TLM algorithms," *Asia-Pacific Conference on Applied Electromagnetics, APACE 2003,* pp. 128 - 131, 12-14 Aug. 2003.

[14] W. J. R. Hoefer, "The Transmission-Line Matrix Method--Theory and Applications," *IEEE Transactions on Microwave Theory and Techniques,* vol. 33, pp. 882 – 893, Oct. 1985.

[15] CST microstripes. http://www.cst.com/Content/Products/MST/Overview.aspx. (Last accessed: Jan. 2009)

[16] Flomerics. http://www.flomerics.com/news/news_details.jsp?newsId=402. (Last accessed: Jan. 2005)

[17] W. Whittow, C. J. Panagamuwa, R. Edwards and J. C. Vardaxoglou, "Specific Absorption Rates in the Human Head Due to Circular Metallic Earrings at 1800 MHz," *Antennas and Propagation Conference, LAPC 2007, Loughborough,* pp. 277 – 280, 2-3 April. 2007.

[18] H. Virtanen, J. Keshvari and R. Lappalainen, "The effect of authentic metallic implants on the SAR distribution of the head exposed to 900, 1800 and 2450 MHz dipole near field," *Physics Medicine and Bio.,* vol. 52, pp. 1221-1236, Feb. 2007.

[19] W. G. Whittow, C. J. Panagamuwa, R. M. Edwards and J. C. Vardaxoglou, "On the effects of straight metallic jewellery on the specific absorption rates resulting from face-illuminating radio communication devices at popular cellular frequencies," *Physics in Medicine and Bio.,* vol. 53, pp. 1167-1182, Feb. 2008.

[20] M. Lundmark, R. S. Calvo, P. S. Kildal and C. Orlenius, "A solid hand phantom for mobile phones and results of measurements in reverberation chamber," *Antennas and Propagation Society International Symposium, IEEE,* vol. 1, pp. 719 – 722, 20-25 June. 2004.

[21] L. W. Li, P. S. Kooi, M. S. Leong, H. M. Chan and T. S. Yeo. (2000, July). Antenna patterns & input impedance of handset antennas and SARs in human head: A comparative study using FDTD. *Extended report of Journal of Electromagnetic   Waves   and   Applications,* http://www.ece.nus.edu.sg/stfpage/elelilw/Handset.html4pp.987-1000.   (Last accessed: 29 May 2008)

[22] L. W. Li, P. S. Kooi, M. S. Leong, H. M. Chan and T. S. Yeo, "FDTD analysis of electromagnetic interactions between handset antennas and human head," *Asia Pacific Microwave Conference,* 1189-1192. 1997.

[23] Y. Rahmat-Samii, "Novel antennas for personal communications including biological effects," *Proceedings of Microwave and Optoelectronics Conference, 1995 SBMO/IEEE MTT-S International,* vol. 1, pp. 295-308, 24-27 July. 1995.

[24] M. A. Jensen and Y. Rahmat-Samii, "EM interaction of handset antennas and a human in personal communications," *Proceeding of the IEEE,* vol. 83, pp. 7-17, Jan. 1995.

[25] A. O. Rodrigues, L. R. P. Malta, R. Borsali, R. B. Takai and R. Conhalato, "SAR calculations in an anatomically realistic model of the head of cellular phone users," *The Institution of Electrical Engineers, IEE,* 2002.

[26] H. Virtanen, J. Huttunen, A. Toropainen and R. Lappalainen, "Interaction of mobile phones with superficial passive implants," *Physics in Medicine and Bio.,* vol. 50, pp. 2689-2700, 2005.

[27] M. F. Iskander, Z. Yun and R. Q. Illera, "Polarization and human body effects on the microwave absorption in a human head exposed to radiation from handheld devices," *IEEE Transactions on Microwave Theory and Techniques,* vol. 48, pp. 1979-1987, 2000.

[28] O. A. Saraereh, M. Jayawardene, P. McEvoy and J. C. Vardaxoglou, "Simulation and experimental SAR and efficiency study for a dual-band PIFA handset antenna (GSM 900 / DCS 1800) at varied distances from a phantom head," *Antenna Measurements and SAR, AMS 2004,* pp. 5 – 8, 25-26 May. 2004.

[29] M. Y. Kanda, M. Ballen, S. Salins, C. K. Chou and Q. Balzano, "Formulation and characterization of tissue equivalent liquids used for RF densitometry and dosimetry measurements," *IEEE Transaction on Microwave Theory and Techniques,* vol. 52, pp. 2046 – 2056, Aug. 2004.

Chapter 4

The Effect of a Homogeneous Spherical Head, a Block Hand Model and Jewellery on SAR and Antenna Performance

4.0 Introduction

As explained in Chapter 3, metallic loops placed at some distances from the antenna and the cubic phantom can have a notable effect on the SAR values inside the phantom. This chapter will further investigate the effect of the hand and metallic loop-like jewellery items worn on the human head and the hand on SAR and on the antenna performance. The previous chapter used a very simple cubic phantom, but a more realistic configuration will be considered in this chapter.

A simple homogeneous spherical head and a block-hand model are employed in this chapter. The latter study includes a block hand model with cylindrical fingers, which allow the effect of metallic rings to be studied. The ring is placed on different fingers for comparison. In addition, this chapter also includes the effect of wearing metallic rings on the side of the head on SAR. Results are presented for different sizes of earring. The effects are also shown in combination with the effect of different positions of the ring on the hand at two different frequencies (900 MHz and 1900 MHz). The latter section in this chapter will show results of the effect of the simple head model, the block-hand model, the earrings and the rings on the antenna radiation patterns.

4.1 Antenna, spherical head and block-hand models

4.1.1 Antenna and handset model

Simulations were performed by means of Microstripes (TLM) for the 900 MHz and
1900 MHz bands. The handset was modelled as a $\lambda/4$ monopole antenna mounted on
top of a metal box. The monopole antenna is center-fed at its end on the top the metal
box (see Figure 4.1-1). The antenna length was adjusted so it was resonant at the
required frequency. The reason of using this type of antenna is due to its simplicity (in
the structure) and repeatability; it could be positioned easily with respect to the head
and allows easy comparison with measurements. The handset body was modelled as
metal with no dielectric cover since research by Lee et al. [1] suggests that dielectric
covering on the antenna or the handset has no significant effect on SAR in this
scenario.
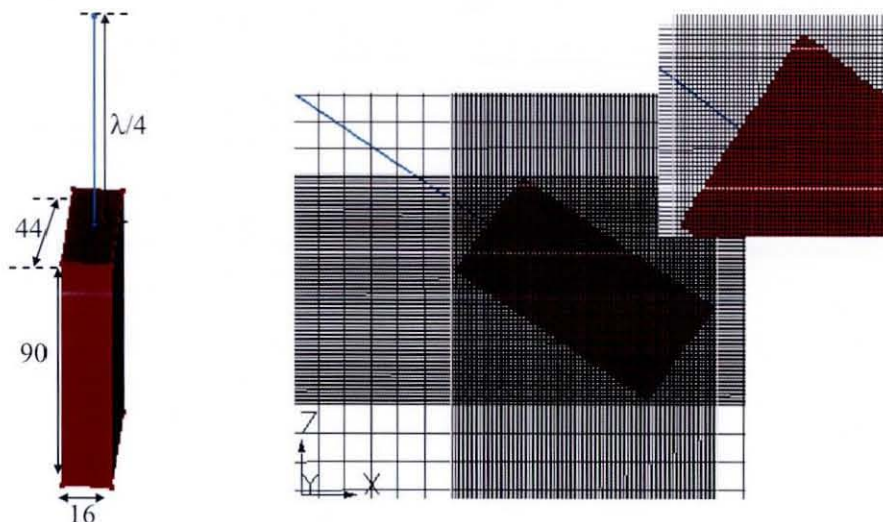
Figure 4.1-1: A $\lambda/4$ monopole antenna by itself; is center- fed at its end on the top of a metal
box, which dimension 90×16×44 mm.

In terms of the orientation of the handset-antenna relative to the head, the head model
used by [2-4] was rotated (rather than the handset) in order to avoid problems with
mesh stair-casing affecting the handset model. The stair-casing has the potential to
change the wire antenna's electrical length, thus shifting its resonant frequency [5].

However, in the current thesis, the handset body needs to be rotated due to the difficulty of modeling a hand and there were practical problems with the meshing which will be discussed in Chapter 5 later. The angled handset-antenna orientation (see Figure 4.1-1) is assumed to be the 'free-space' case and the cell sizes along the handset-model were kept the same throughout all the simulation cases considered in this chapter. In this simple spherical head configuration, the ERP[†] is assumed to be at the center on the right hand side of the spherical head model (Figure 4.1-2).
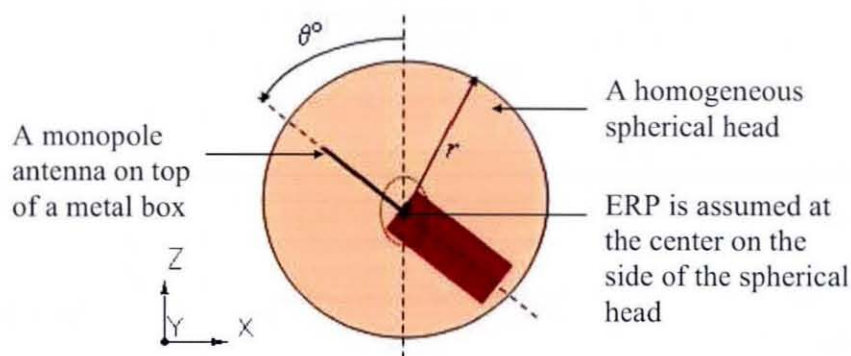
Figure 4.1-2: A handset-antenna model and its position relative to the spherical head. r is the radius of the spherical head.

4.1.2 The block-hand model

In this chapter, a simple homogeneous block-hand is modelled in order to investigate any effects that the hand alone might have on SAR and on the antenna radiation performance (Figure 4.1-3 (a)). As proposed by Morishita et al. [6] the hand model in this chapter is wrapped around the three sides of the handset and the effects of the hand positions relative to the antenna are also considered. Li et al. [7, 8] found only a marginal effect and negligible difference in the results of a homogenous and an inhomogeneous hand model and hence a homogeneous hand model has been assumed. The hand model is filled with tissue simulating liquid equivalent with the muscle properties at 900 MHz or 1900 MHz, (see Table 4.1-1) (as recommended by IEEE Std. 1528 [9] and FCC [10]). The latter study of the current chapter will employ

---

[†] ERP is a specific reference used to align a test device to the head phantom. For the SAM head phantom, the ERP (left and right) is located 1.5 cm above the centre of the ear canal entrance [10]

a block-hand model that includes cylindrical fingers, which enables the effect of metallic rings to be investigated (Figure 4.1-3 (b)).
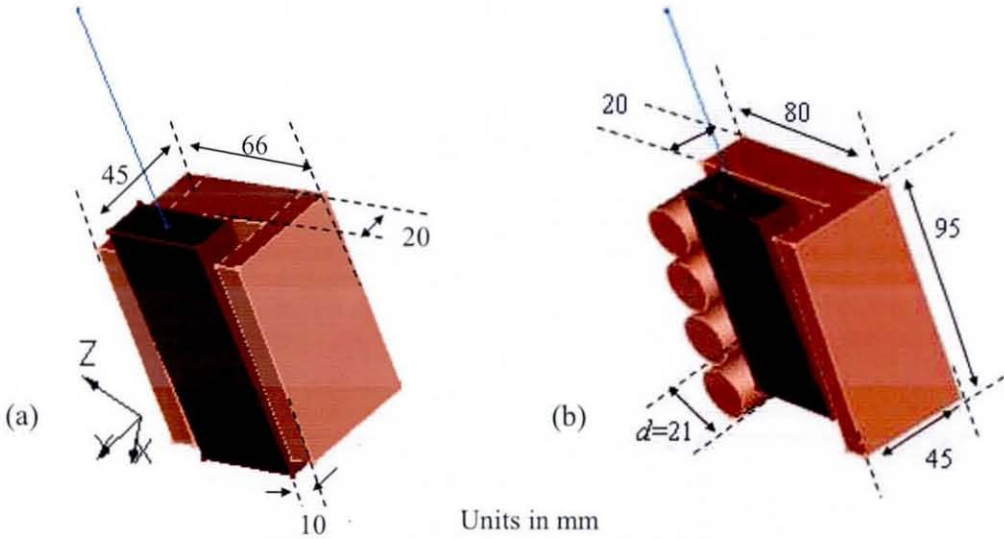
Figure 4.1-3: Simple homogeneous block hand model (a) without cylindrical fingers and (b) with cylindrical fingers. (*d*=diameter)

Table 4.1-1: Dielectric properties for the head and the hand at 900 MHz and 1900 MHz [11].

Frequency	900 MHz		1900 MHz	
Model	ε_r	σ (S/m)	ε_r	σ (S/m)
Head (HSL)	41.5	0.97	40	1.4
Hand (Body tissue)	55	1.05	53.3	1.52

4.1.3 The spherical head model

Simplified geometries incorporating a single tissue type are adequate in many circumstances [12], and require only moderate computational effort in terms of modelling and processing time. The head model used in this chapter is a simple homogeneous spherical head with the radius (*r*) set to 105.5 mm (as in [13]) (see Figure 4.1-2). The spherical head is modelled with head simulating liquid as defined already in Table 4.1-1. The materials chosen are equivalent to the tissue simulating liquids available for the measurements. These properties are also used for the realistic head and the hand model in Chapter 5 and Chapter 6 later.

4.1.4 Normalization

The SAR results presented in this thesis were obtained directly from the computer software and calibrated to the value of power delivered at the output of the antenna. This value accounted for the reflected power due to the antenna mismatch [14]. The value of the forward power into the system is accessed through the (.io) file and tagged as 'Power IN' in the simulation results. Note that a typical handset would have a delivered power of 0.25 W and 0.125 W at 900 MHz and 1900 MHz respectively. These values are about 1/8 of the mobile phone's permitted maximum transmitted power under its real operating conditions [15, 16]. These power values were used to normalize the SAR values obtained from the computer simulations and measurements in this thesis.

4.2 The effect of metallic ring worn on the hand on SAR (within the hand)

4.2.1 Different hand model shape and size affect on SAR

In this section, a block-hand model (see Figure 4.1-3) is placed at certain distances (h) from the feed-point of the monopole antenna in order to investigate the effect of the hand holding the handset. The results for the block-hand model are compared with the hand model that includes cylindrical fingers on it (Figure 4.1-3 (b)). The head model was not considered in this section.

The effects of the block-hand (with and without cylindrical fingers) holding the handset at 900 and 1900 MHz are shown in Figure 4.2-1. Figure 4.2-1 also includes a block-hand with smaller cylindrical fingers (d=17 mm) for comparison. The dashed lines with symbols represent the effect of the hand at 900 MHz, while the solid lines with symbols are for the effect at 1900 MHz. Figure 4.2-1 demonstrates that the averaged 1 g SAR inside the hand is only marginally influenced when the hand is placed on the bottom part of the handset ($-h$). As the hand begins to cover part of the

antenna ($h>0$), the averaged 1 g SAR values significantly increase (by more than 50%) compared with the case when the hand does not shield the antenna ($h<0$). This appears to be the case at both 900 and 1900 MHz. These results show the same trend as the results in [2]. For the same simulation but adding the cylindrical fingers further changes in the SAR can be observed. The effect brought about by all three different block-hand models investigated show agreement in the trend. Consequently only the block-hand model with cylindrical fingers (d=21 mm) will be employed in the next simulations as it enable the effect of metallic rings to be studied.
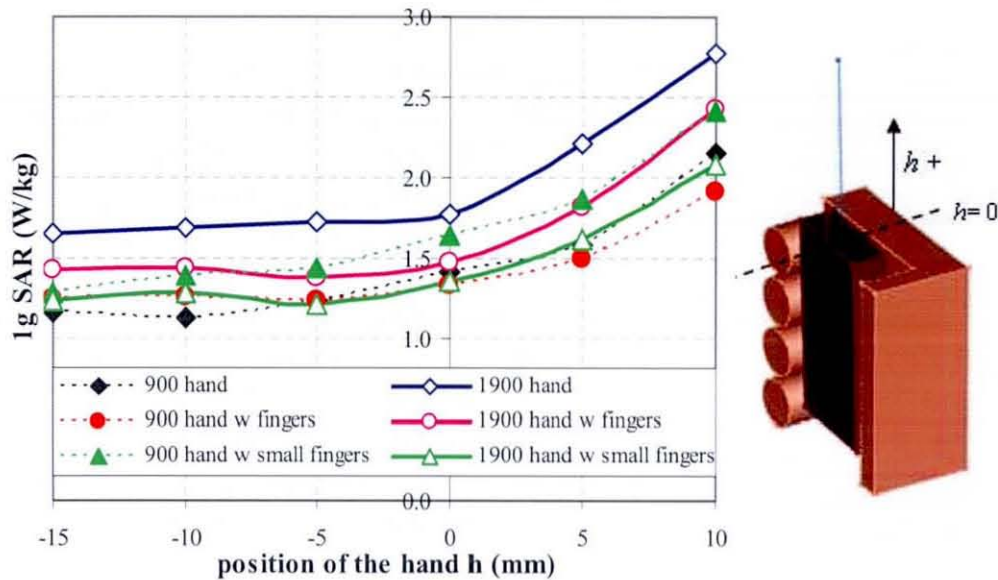
Figure 4.2-1 : The averaged 1 g SAR inside the hand versus the hand position 'h' from the antenna feed point. (Result are normalized to 0.25 W at 900 MHz and 0.125 W at 1900 MHz)

4.2.2 The effect of metallic rings worn on the hand on SAR

In order to investigate the effect of the metallic ring worn on the human finger on SAR (inside the hand), a metallic ring was placed on specified fingers named index (i), middle (m) and ring (r) finger (Figure 4.2-2 (a)). As the results presented in Chapter 3 showed no important difference between different types of metal (copper, silver and platinum), so that the metallic rings in this chapter are modelled as copper. The geometric representation of the metallic ring employed in this chapter is shown in Figure 4.2-2 (b).
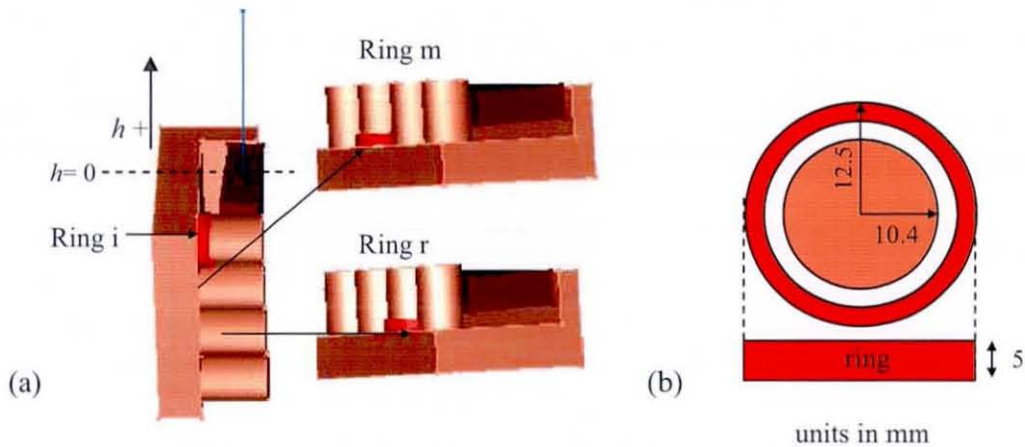
Figure 4.2-2: (a) The metallic ring worn on different fingers and (b) a geometric representation of the ring worn on the specified finger.

Figure 4.2-3 shows the effect of the various metallic rings on the averaged 1 g SAR in the hand at 900 and 1900 MHz. The hand model was placed at $h=0$ and $h=10$ mm with respect to the monopole antenna feed point (see Figure 4.2-1). The ring was placed on different fingers for comparison. The solid and the dashed lines represent the case of the hand without the ring whilst the columns represented the effect of the ring. Figure 4.2-3 suggests that a ring worn on the finger could alter the averaged 1 g SAR inside the hand at both frequencies tested, but the effect varies depending on which finger the ring been placed. Generally, an increase was seen in the averaged 1 g SAR in the hand at 900 MHz, and a decrease in the averaged 1 g SAR at 1900 MHz for the metallic rings investigated in this case. In addition, Figure 4.2-3 (b) shows that metallic rings are unlikely to significantly affect the averaged 10 g SAR values inside the hand at either frequency. The averaged 1 g SAR in the hand was significantly increased when the hand shaded part of the antenna at $h=10$ mm, however this particular position, whilst not completely infeasible, would be quite an unusual and inconvenient operating position. The hand will be placed at the 'normal' $h=0$ position in the next simulations.
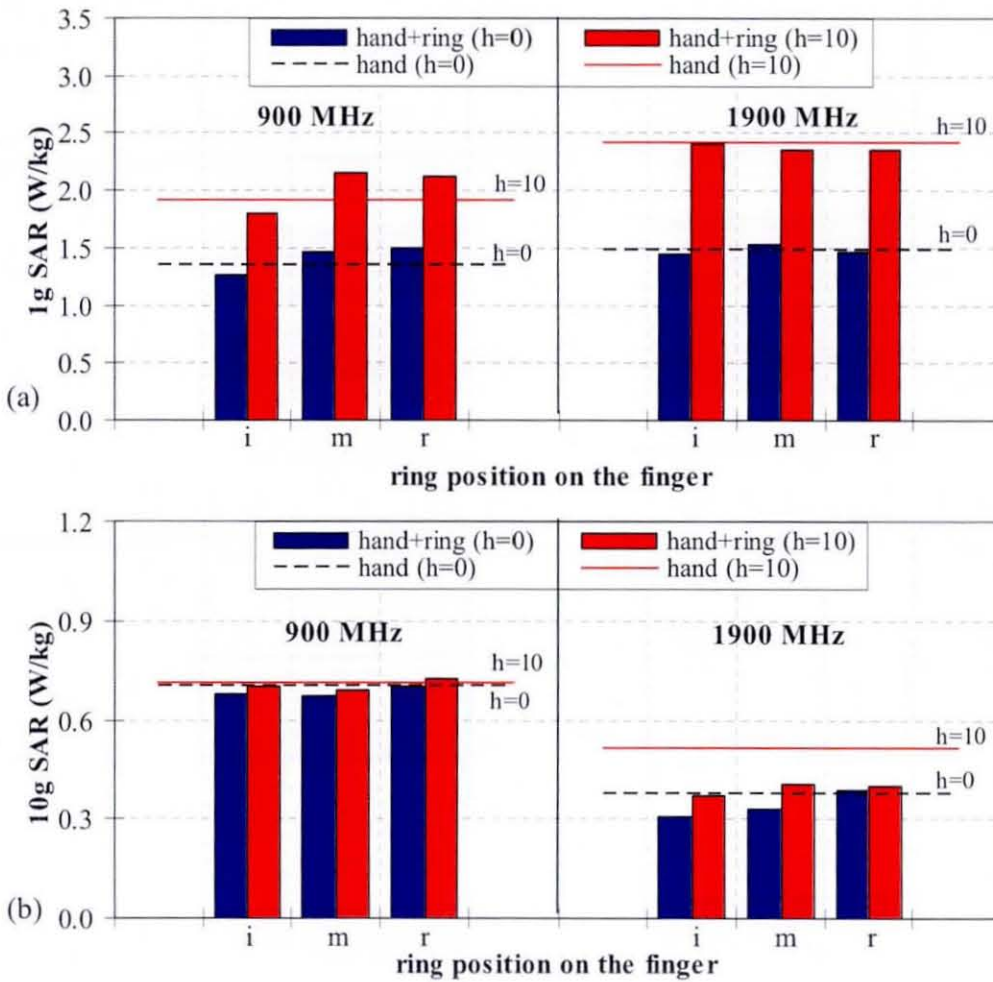
Figure 4.2-3: The averaged (a) 1 g and (b) 10 g SAR inside the hand with and without the rings. The hand model is placed at $h=0$ and $h=10$ mm.

Figure 4.2-4 illustrates the peak SAR distribution inside the hand at 900 MHz and 1900 MHz. The peak SAR distributions presented in this thesis are shown on a logarithmic scale (dB) to give a clearer picture of the SAR distributions owing to the presence of metallic jewellery on each case investigated. The 0 dB point is taken as the SAR in the computational cell with the maximum computed value. The value for each figure is normalized to the peak voxel value for the particular plane. For this simulation, the maximum SAR generally appears on the closest part of the hand to the antenna and the handset body at both frequencies when no ring is worn. However, when the ring is added into the model (see Figure 4.2-4), the SAR is enhanced at the edge of the ring on the finger wearing the ring and also on a small part on the adjacent fingers. Nevertheless, it can be seen that the metal ring has stronger effect at 900 MHz

compared to 1900 MHz. At 900 MHz, the SAR is still enhanced around the ring on the ring finger that is far away from the antenna; hence the fields at lower frequency penetrate deeper than at larger frequency [17, 18].
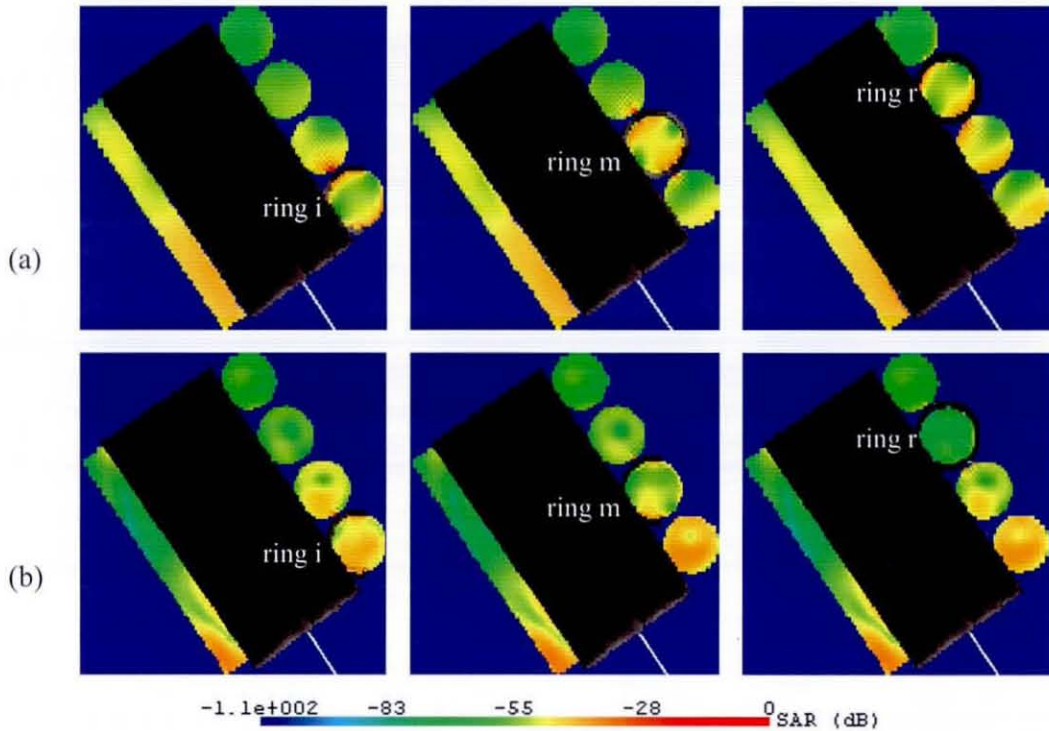
Figure 4.2-4: The maximum SAR distribution within the hand at (a) 900 MHz and (b) 1900 MHz.

Although measuring the SAR inside the hand seems to be less important since there are no sensitive tissues inside the hand as in the head (i.e. eye, brain). However, the previously published research has shown that the hand absorbed part of the energy radiated by the antenna [19] and could significantly modify the SAR within the head [2, 20-22]. Hence, the result in this section has confirmed that metallic rings worn on the fingers can notably alter the averaged 1 g SAR inside the hand. Therefore, it is expected that the metallic ring worn on the hand could also have effects on the SAR values inside the head. As a result, the metallic ring will be included in the following simulations while investigating the effect of the hand and the metallic loop-like jewellery (earring and ring) on SAR within the head.

4.3 The effect of the spherical head, the hand and the metallic jewellery on SAR (in the head) and on the antenna performance

4.3.1 The effect of the hand and the metallic rings worn on the hand on the SAR values inside the head

Jensen and Rahmat-Samii [12], Fayos-Fernandes et al. [13], Okionewski and Stuchly [23] and Ruoss [24] have shown that a simple spherical head is very useful for estimating the effects of SAR. In this chapter, the simple homogeneous spherical head discussed in Section 4.1.3 is employed to investigate the effect of the hand and the metallic jewellery items on SAR. The mobile handset (see Figure 4.1-1) is placed very close to the right hand side of the head, above the ERP (see Figure 4.1-2). To investigate the effect of the hand on SAR values inside the head, a block-hand model with cylindrical fingers (as employed in the earlier section) is added into the simulation model. The hand holds the handset in the cheek position with its top level with the antenna feed point ($h=0$) (Figure 4.3-1 (b)). The head and the hand model resolution is set to $\lambda_{min}/10$, where λ_{min} is the wavelength within the dielectric material having the highest permittivity (dielectric constant). The SAR results presented in this section are normalized to 0.25 W at 900 MHz and 0.125 W at 1900 MHz.
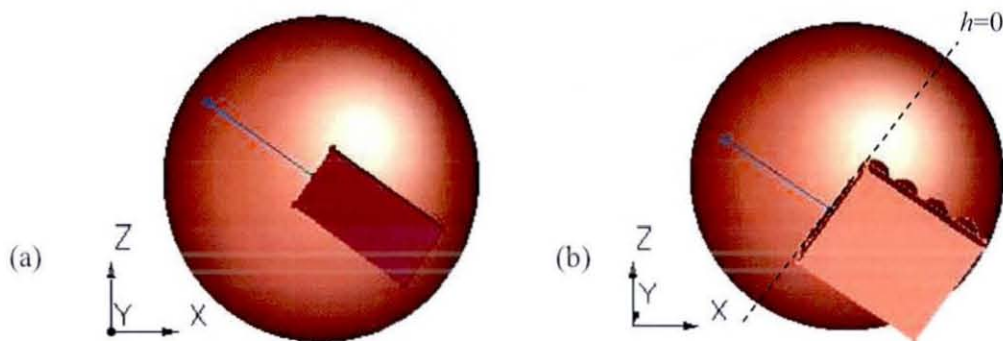
Figure 4.3-1: A homogeneous spherical head model with a mobile handset placed very close to the right side of the head in the 'cheek' position, (a) without the hand and (b) with the hand model.

The averaged 1 g and 10 g SAR results inside the head with and without the hand are shown in Table 4.3-1. Generally the averaged 1 g and 10 g SAR values rose as the frequency was increased due to higher conductivity and thus absorption in tissues. It can be seen that the average 1 g and 10 g SAR values within the head are decreased when the hand is added into the simulation for 900 MHz. A similar trend was found in [23]. However, Table 4.3-1 shows that the averaged 1 g and 10 g SAR inside the head were increased when compared to no hand for an antenna operating at 1900 MHz. The increased in SAR at 1900 MHz can be explained partly by the reflection at the hand-dielectric boundary.

Table 4.3-1: The averaged 1 g and 10 g SAR in the spherical head, with and without the hand (without ring).

Frequency	900 MHz		1900 MHz	
SAR (W/kg)	Head only	With hand	Head only	With hand
1 g	5.59	5.30	6.64	7.53
10 g	2.69	2.59	2.97	3.36

Furthermore, to account for the effect brought about by a metallic ring on SAR in the head, the metallic rings (i, m and r) as employed in Section 4.2.2 are added to the hand model (see Figure 4.3-2). The ring dimensions and configurations for this experiment are the same as in Figure 4.2-2 (b). The peak SAR and the averaged SAR (1 g and 10 g) in the head were determined and compared with no rings. The ring is placed on different fingers for a comparison at two different frequencies. The effects of the hand wearing a ring are illustrated in Figure 4.3-3. The straight line represents the head by itself, the broken line with symbols represents the head and hand, while the effect of the rings are represented by the columns.
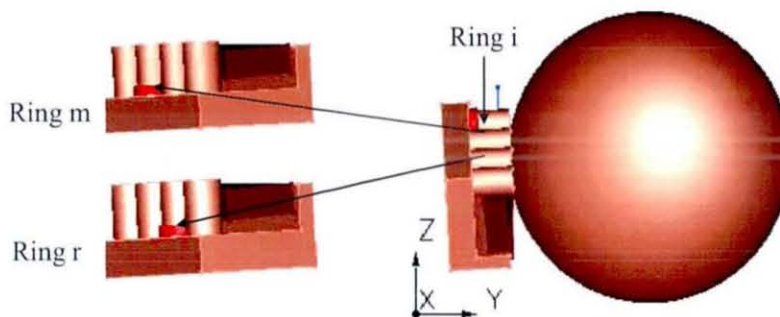
Figure 4.3-2: A metallic ring worn on different fingers close to the spherical head.
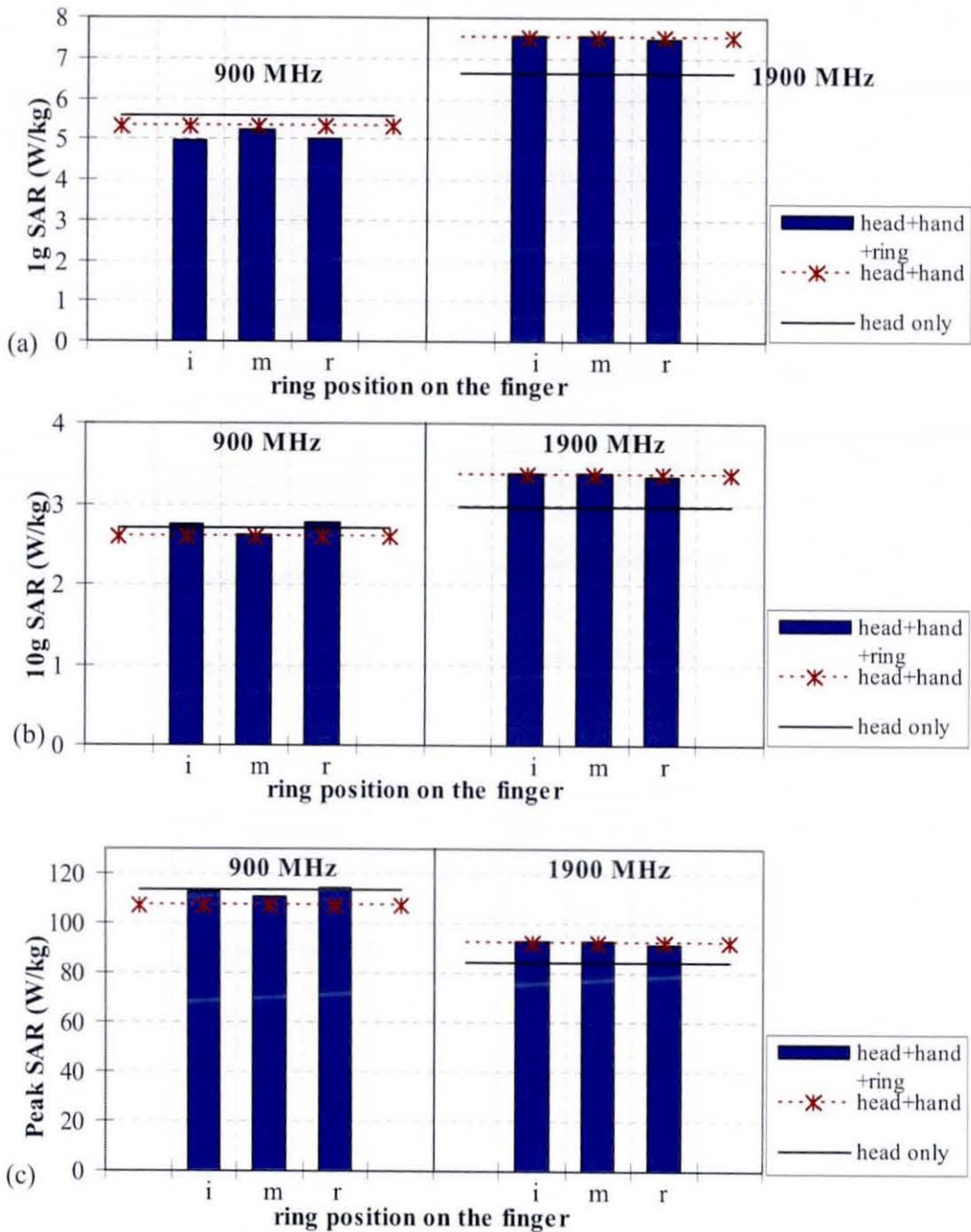
Figure 4.3-3: The effect of metallic rings worn on human fingers at 900 MHz (left) and 1900 MHz (right) on the (a) averaged 1 g, (b) averaged 10 g and (c) peak SAR in the head.

Figure 4.3-3 shows that the influence of the rings on the averaged 1 g SAR in the head is much more significant at 900 MHz than at 1900 MHz where the effect of the rings on the averaged 1 g SAR is minimal. At 900 MHz, the two positions of the ring on the hand decrease the averaged 1 g SAR in the head by approximately 7%. However, the

averaged 10 g SAR values inside the head do not change considerably owing to the presence of the rings worn on the hand at both frequencies (Figure 4.3-3 (b)). Although the average 1 g and 10 g SAR are usually considered in investigating the amount of energy absorbed in the head, the peak SAR values in smaller scale may be important and should be considered [13, 25]. The effect of the ring worn on the hand on the peak SAR values in the head are presented in Figure 4.3-3 (c). Note that the peak SAR in the head is increased at 900 MHz when compared to the case of just the head and hand. This may be due to the coupling effect between the radiated fields with the dielectric bodies and the metallic rings, although the effect on the averaged SAR is only marginal. However the rings are unlikely to influence the peak SAR in the head at 1900 MHz.

4.3.2 The effect of metallic loop-like earrings worn on the ear on SAR inside the head

The effects of metallic earrings on SAR have been investigated in [13, 17, 26, 27]. These investigations found that metallic earrings when worn close to a radiating source may cause a notable enhancement in SAR. However, none of the above mentioned studies have accounted for the effect of the hand that holds the handset in ordinary use.

In this section, the effects of metallic jewellery (earrings and rings) on SAR inside the head are investigated. The earrings with an outer diameter of 25, 30, 40, 50, 80 and 90 mm are made of copper, while the size of the ring employed in this section is the same as in the previous experiments (Figure 4.2-2 (b)). To investigate the effect of metallic jewellery, three different scenarios were examined (as in Figure 4.3-4); (a) the addition of metallic earrings to the head model (no hand), (b) the inclusion of metallic earrings to the head and hand model and (c) the inclusion of metallic earrings and ring to the head and hand model. In practice, an earring is usually pierced into the earlobe. However, for this simulation, the edge of the earrings was attached and in direct contact to the right hand side of the head (not been inserted into the earlobe) (see Figure 4.3-4 (a)). For the scenarios b and c, a block-hand (with cylindrical

fingers) was used. Meanwhile, results in Figure 4.3-3 showed that the difference of the ring position on the hand has only a very minor effect on the SAR inside the head; therefore the ring in this experiment (for scenario c) is placed only on the index finger. In all scenarios considered here, the block-hand model and the mobile handset dimension and configuration are the same as employed in previous section. The frequency dependent parameters (ε_r, σ) used for the spherical head and the hand are the same as those for the standard tissue equivalent liquids (as in Table 4.1-1). Nevertheless, as in the previous cases, the SAR results presented in this section are normalized to 0.25 W at 900 MHz and 0.125 W at 1900 MHz.
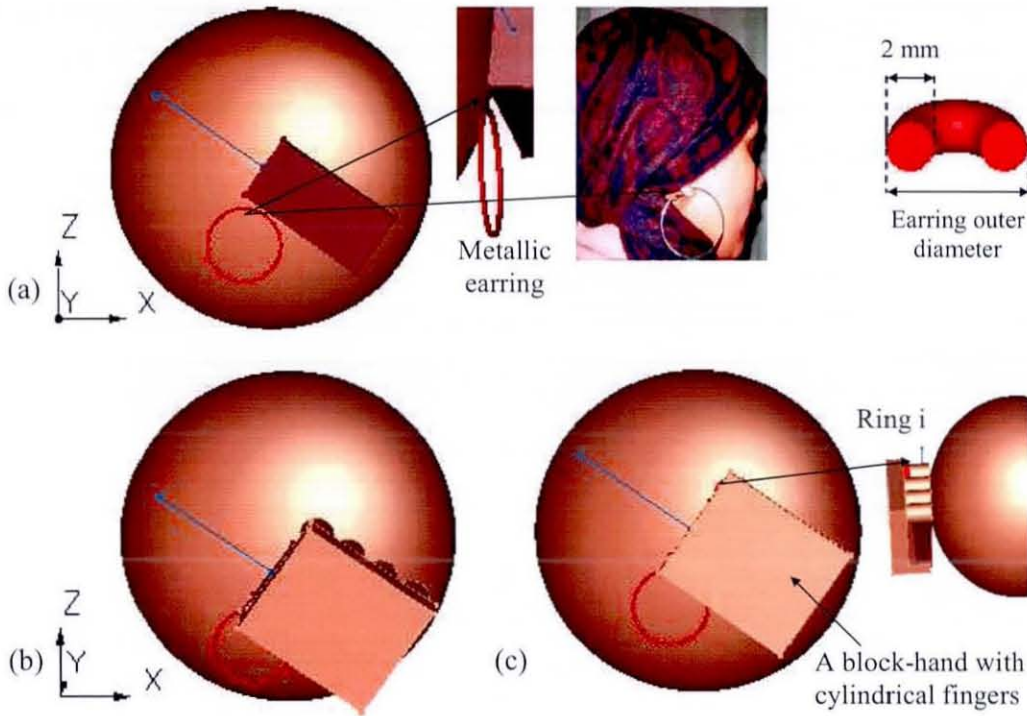
Figure 4.3-4: Three scenarios considered in the simulations. The metallic earring is attached to the right side of the head, (a) without the hand, (b) with the hand holding the mobile handset and (c) with the hand wearing a ring on the index finger.

The results for the averaged SAR (1 g and 10 g) for all scenarios investigated (see Figure 4.3-4) are illustrated in Figure 4.3-5. As expected the hand and metallic jewellery affected the averaged SAR in the head, but the effect is varied dependent on the diameter of the earring and the frequency of excitation.

Figure 4.3-5 and Figure 4.3-6 shows that the peak and the averaged 1 g SAR in the head is generally increased by the earrings at 900 MHz and decreased at 1900 MHz. The inclusion of the hand decreases the averaged 1 g SAR in the head at 900 MHz by approximately 9% compared to the 'no hand' case. However, the hand in this configuration can also increase the averaged 1 g SAR in the head at the higher frequency considered in this study. It therefore appears to be important that the hand is included in the model.
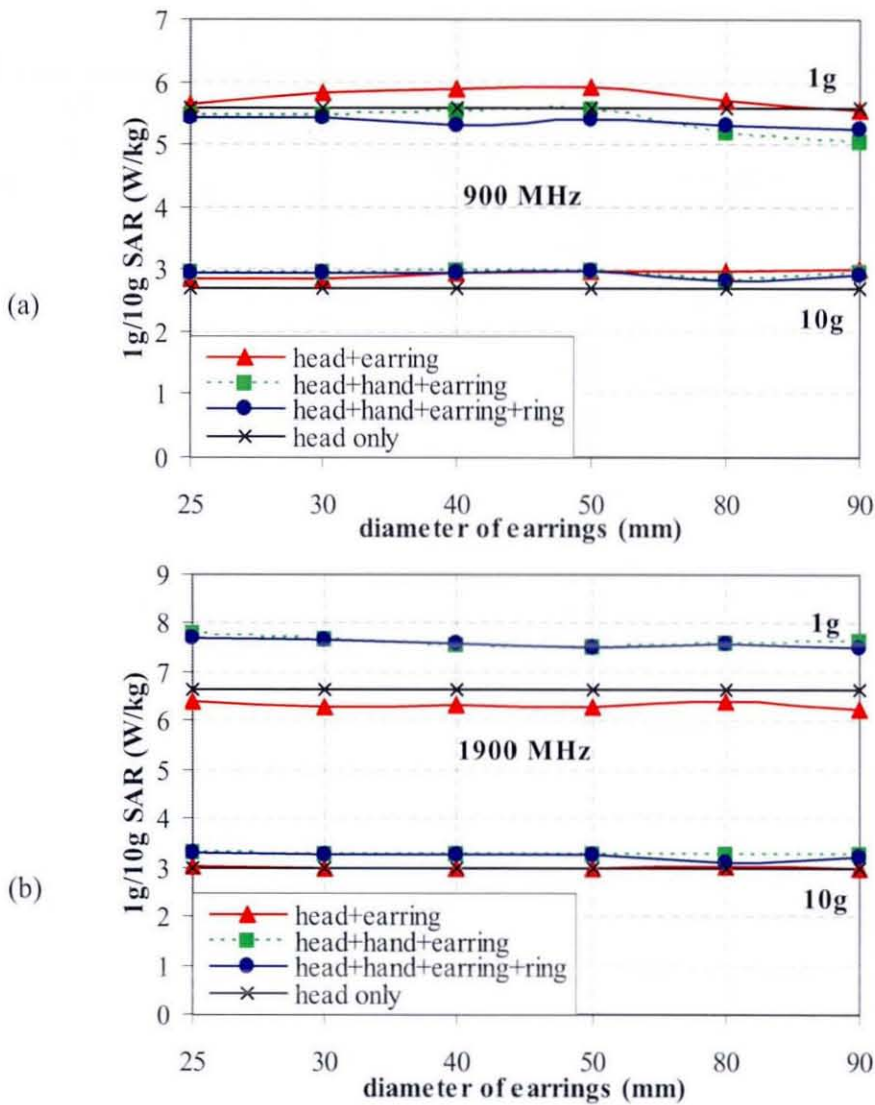
Figure 4.3-5: The effect of the hand and the jewellery on the averaged 1 g and 10 g SAR in the head at (a) 900 MHz and (b) 1900 MHz.

The graphs (Figure 4.3-5 and Figure 4.3-6) also include the same simulation with a ring worn on the index finger (scenario c). As for the results in Figure 4.3-3, adding a ring to the hand and head-earring model notably decreased the averaged 1 g SAR in the head at 900 MHz when compared to the case of just the head and earrings; but the effect at 1900 MHz is insignificant. The increase and decrease in the peak and the averaged 1 g SAR in the head is may be due to energy absorption by the head and the hand, the reflection at the dielectric boundaries and also due to the complexity of the interaction between multiple metallic items and the electromagnetic energy. Nevertheless, an increase and decrease in the peak and the averaged 1 g SAR inside the head have been demonstrated; however the change in the averaged 10 g SAR owing to the presence of the rings worn on the hand at both frequencies is very marginal.
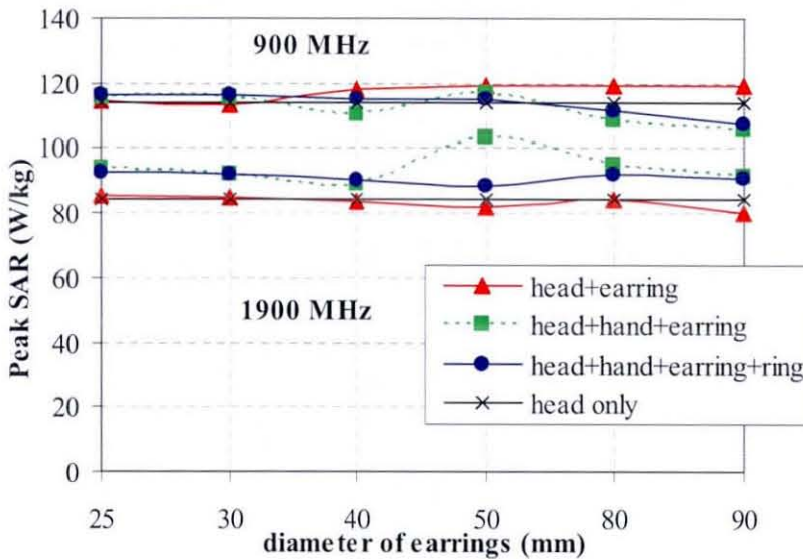
Figure 4.3-6: The effect of the hand and the jewellery on the peak SAR in the head at 900 MHz and 1900 MHz.

Figure 4.3-7 represents the effects that the earring might have on the peak SAR distribution inside the spherical head for 900 MHz and 1900 MHz. The SAR distributions shown are taken from the yz-plane, while the small circle with a broken line represents the plot (xz-plane) where adding earrings increased the SAR (inset). It can be seen from Figure 4.3-6 that all the sizes of earrings investigated give a similar

effect in the peak SAR. Therefore only the effect of the earring with a diameter of 90 mm is shown in Figure 4.3-7. A comparison between Figure 4.3-7 (a) and (b) (also Figure 4.3-7 (c) and (d)) clearly showed that when a metallic objects like an earring lies close to the radiating source, it affects the radiated field and the SAR distribution. Due to RF field scattering, the metallic objects may redistribute the incident field around them. This leads to higher absorption near the earring compared to the same tissue volume with no earring. From Figure 4.3-7, the SAR was enhanced in the area where the earring touches the head at both simulated frequencies. The effect of earrings is more pronounced at 900 MHz than at 1900 MHz. However, no noticeable enhancement was seen deeper in the head due to the earrings, especially at 1900 MHz.
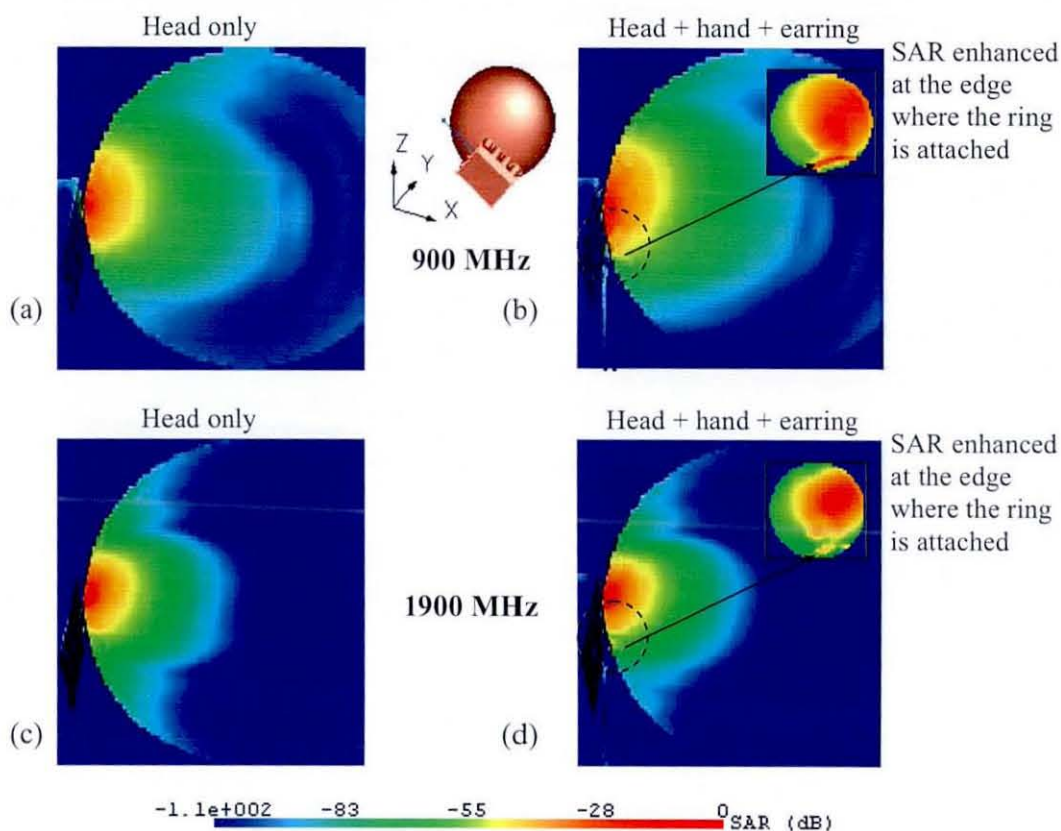
Figure 4.3-7: The peak SAR distribution inside the spherical head for 900 MHz (a and b) and 1900 MHz (c and d). An earring is added to the model in (b) and (d).

4.3.3 The effect of the head, the hand and metallic jewellery on the antenna radiation pattern and efficiencies

4.3.3.1 Effect of the head and the hand

In this section, the effect of the head, the hand, the earrings and rings on the antenna radiation pattern (gain pattern) for 900 MHz and 1900 MHz were examined. The antenna radiation pattern in free-space was calculated with the handset-antenna oriented at a natural speaking angle (see Figure 4.1-1). Figure 4.3-8 shows radiation patterns (calculated in the yz-plane) for a $\lambda/4$ monopole antenna in isolation, near the spherical head and with the addition of a block-hand model at 900 MHz (left) and 1900 MHz (right). The radiation patterns for the xy-plane are shown in the Appendix B for a comparison.

Figure 4.3-8 shows that the monopole in free-space has an omni-directional radiation pattern. However an asymmetric monopole radiation pattern was observed at 1900 MHz due to the increased electrical length of the metal box relative to the monopole. In the presence of the head, the monopole's radiation pattern is significantly influenced in the direction of the head (y-direction) due to energy absorption inside the head. The inclusion of the block hand causes a significant difference in y-direction, and the difference is higher at 1900 MHz than at 900 MHz.
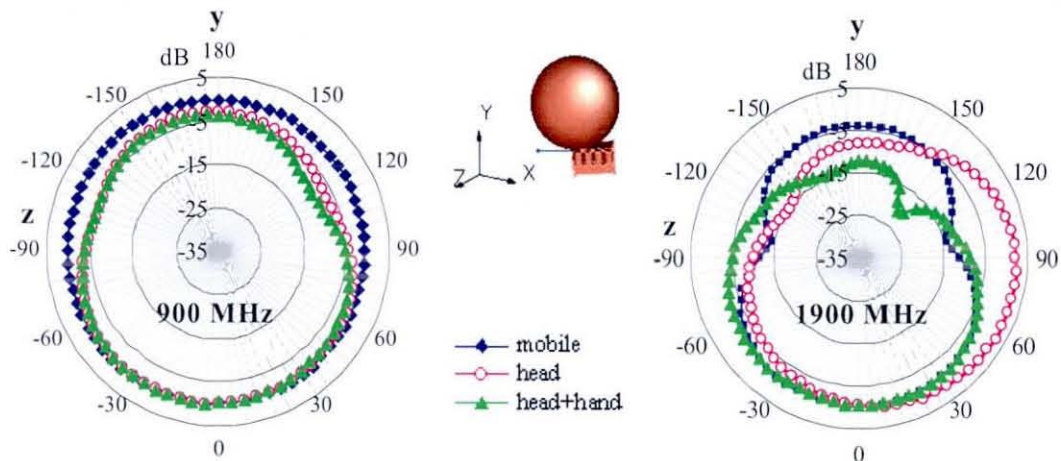
Figure 4.3-8: The antenna radiation pattern at 900 MHz (left) and 1900 MHz (right) with and without the head and the hand (yz-plane).

4.3.3.2   Effect of a metallic ring

Figure 4.3-9 shows the effect of the hand wearing a metallic ring on the radiation pattern at both 900 MHz (left) and 1900 MHz (right). The ring was simulated on different fingers for comparison. It can be seen from the figure that all the three positions of ring investigated give similar effects on the radiation pattern if compared to the case of just the head and hand. These results seem to suggest that metallic rings worn on the hand will be less likely to perturb the antenna radiation performance at the frequencies tested. The effect of the ring is insignificant due to the circumference of rings being relatively small compared to the wavelength and also the orientation and the ring position with respect to the antenna.
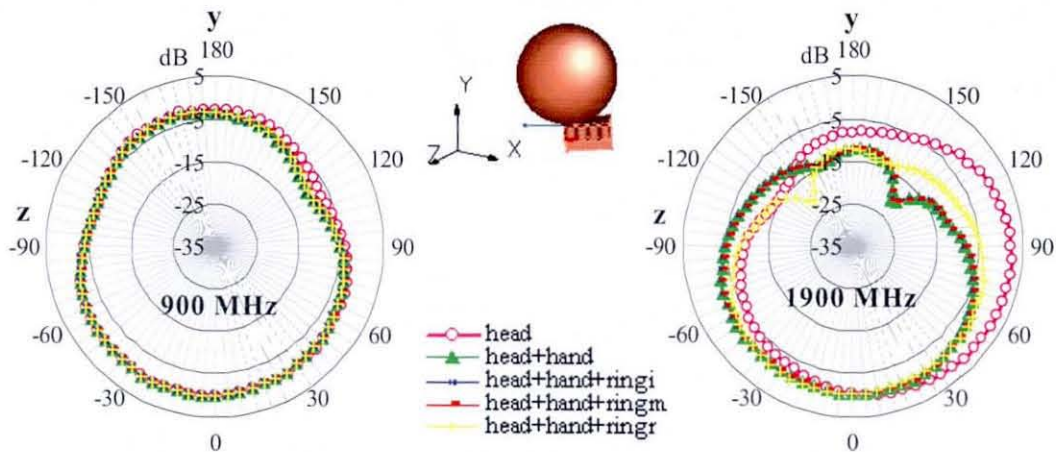
Figure 4.3-9: The radiation pattern at 900 MHz (left) and 1900 MHz (right) with the head and hand. A metallic ring is worn on different fingers for comparison (yz-plane).

4.3.3.3   Effect of metallic earrings

Considering the effect of metallic earrings on the antenna radiation pattern, Fayos-Fernandez et al. [13] found that there are small differences between radiation patterns due to metallic piercing in the ear. They also concluded that the presence of metallic objects especially that are pierced could emphasize the reduction on the antenna performance due to the presence of the user's body. However, Fayos-Fernandez et al. [13] used different shapes and sizes of metallic earrings and the effect of the user's hand was not considered in the paper. In the current chapter, the effects of different

sizes of metallic-loop like earrings at two different frequencies were examined. The
latter models in this simulation included a block-hand model to represent an ordinary
way of operating a mobile handset. In all cases, the edge of the earring is attached on
the right hand side of the spherical head (see Figure 4.3-4 (a)).

Figure 4.3-10 (a) shows results of various different sizes of earrings over two different
frequencies investigated. Smaller earrings with a diameter of 25, 30 and 40 mm show
very similar and insignificant effects on the antenna radiation pattern at both
frequencies, so that only the effect of the earring with a diameter of 30 mm
(representing smaller earrings) shown in Figure 4.3-10. Meanwhile, larger earrings in
this configuration (diameter$\geq$ 50 mm) could alter the radiation pattern by 1 dB (in -z
direction) at 900 MHz when compared to the case of just the head and hand (Figure
4.3-10 (b)). However no important effect of the earring was observed at 1900 MHz
(Figure 4.3-10 (b)). Figure 4.3-11 includes the same earring with a ring worn on the
hand, but neither the earring nor the ring has a significant effect in the radiation
pattern at 900 MHz and 1900 MHz if the hand is present. This means that it is
important that the hand is included while investigating the antenna radiation
performance.

Figure 4.3-12 shows the radiation efficiencies of the system when the metallic rings or
earrings were added to the spherical head and hand model. Placement of the mobile
handset close to the spherical head results in an efficiency drop by 5% compared to no
head. The hand when included into the system produced further degradation of the
radiation efficiencies at both 900 MHz and 1900 MHz. The presence of a metallic
ring or earring show only marginal difference to the radiation efficiency of the
system. Only localized SAR seems to be affected by the rings or the earrings whilst
no important effect was observed on the radiation pattern and the efficiency. This
suggests no large overall effect by the metallic rings and earrings worn on the human
head and hand.
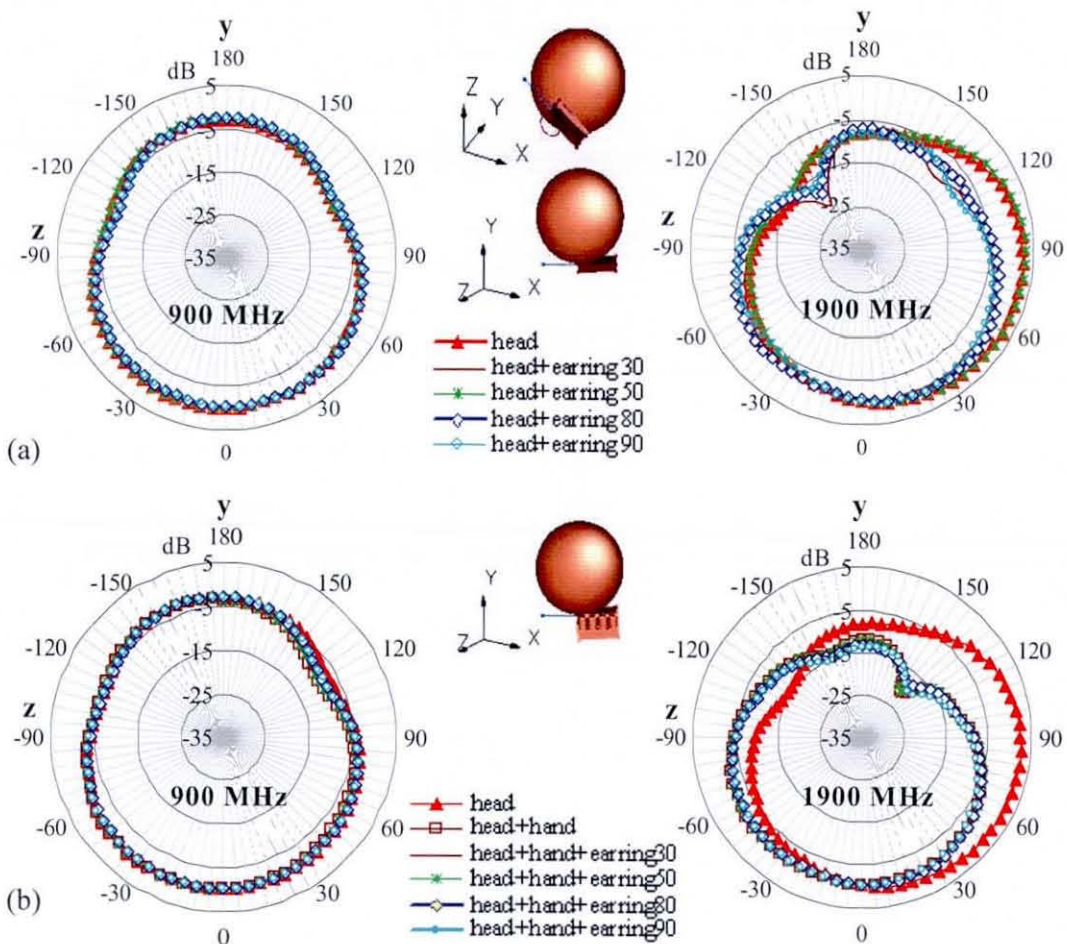
Figure 4.3-10: Radiation patterns for a monopole antenna at 900 MHz (left) and 1900 MHz (right) when placed close to the spherical head. Metallic earrings attached on the right hand side of the head (a) without the hand, (b) with the hand (yz-plane).
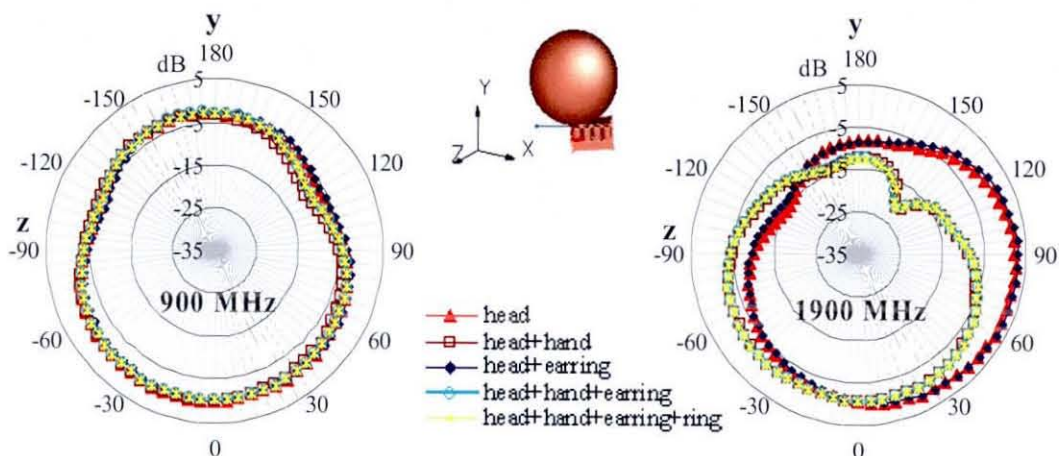
Figure 4.3-11: Radiation patterns for a monopole antenna at 900 MHz (left) and 1900 MHz (right) when placed close to the spherical head. In this simulation, the effect of the combination of the earring and ring were investigated (yz-plane).
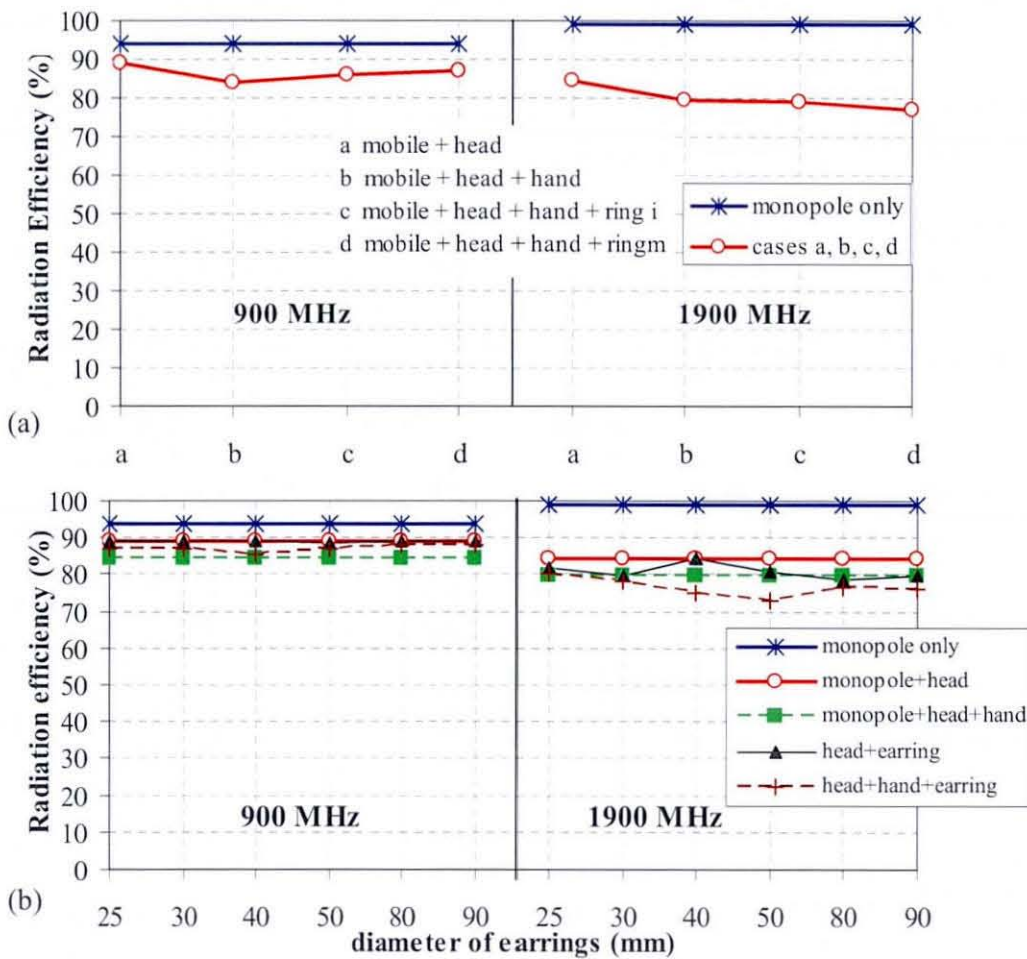
Figure 4.3-12: Radiation efficiencies for a monopole antenna at 900 MHz (left) and 1900 MHz (right) for the case of (a) metallic rings and (b) the metallic earrings worn on the spherical head.

4.4 Conclusions

In conclusion, this study has successfully shown some possible effects brought about by metallic jewellery worn on human head and hand on SAR within the head. A simple spherical homogeneous head and block-hand model have been employed, which are adequate to estimate the modelled antenna performances and to approximate the effect of the head [12]. However, these effects vary depending on the size, orientation, frequency of operation and the presence or absence of the hand.

The small rings worn on the hand appear to have additional effects on the averaged 1 g SAR inside the head and on the antenna radiation pattern. The rings decreased the averaged 1 g SAR in the head by around 7% but the rings do not seem significant to the averaged 1 g SAR in the head at 1900 MHz. In addition, the rings in this configuration marginally change the antenna radiation performance but the effect appears to be insignificant. It seems likely that this is because the size of the ring is relatively small compared to the wavelength and its relative orientation and location to the radiation source makes coupling unfavorable in the situations investigated.

Generally, the earrings in this configuration increased the averaged 1 g SAR in the head by 6% at 900 MHz and decreased it by 6% at 1900 MHz. However, the earrings are unlikely to be significant to the SAR values inside the head when the hand is added to the model. The hand can significantly alter the averaged 1g SAR inside the head at both frequencies tested. Therefore it is important to include the hand while investigating the effect of metallic jewellery on SAR and the antenna performance. In addition, larger earrings of diameter $\geq$ 50 mm in this configuration could increase the antenna directivity by 1 dB at 900 MHz, but no important effect of the earring was observed at 1900 MHz especially when the hand is present.

In addition, the radiation efficiency of the system decreased when the head and the hand were included at both 900 MHz and 1900 MHz. However, the presence of a metallic ring or earring shows insignificant difference to the radiation efficiency of the system. Coupling the handset antenna to the metallic rings or earrings only showed localized effect on SAR, no important effect was observed on the radiation pattern and the efficiency suggests no large overall effect by the metallic rings and earrings worn on the human head and hand.

Nevertheless, the results in this chapter employed only a simple shape of the human head and hand. The more realistic head (SAM) and hand model will be employed in Chapter 5. The SAM head includes the ears, which allows the earrings to pierce the earlobe, representing a more realistic worn position. Although the head shape does not significantly alter the absorption, it appears to be important since it defines the practical antenna distance with respect to the head surface [28]; thus it might also

affect the head-jewellery distance and the SAR values inside the head. Moreover, a simple block-hand in this chapter includes very simple cylindrical fingers, which is only wrapped around the three sides of the handset body. However, in reality, the fingers of mobile users frequently stray near the back side of the antenna and it is potentially of great interest to investigate what effect this would have on the results both with and without the ring.

4.5 References

[1]   A. K. Lee, H. D. Choi, J. I. Choi and J. K. Pack, "The scaled SAM models and SAR for handset exposure at 835 MHz," *MTT-S International Microwave Symposium Digest, IEEE,* pp. 1323-1326, 12-17 June. 2005.

[2]   S. I. Watanabe, H. Taki, T. Nojima and O. Fujiwara, "Characteristic of the SAR distributions in a head exposed to electromagnetic fields radiated by a hand-held portable radio," *IEEE Transactions on Microwave Theory and Techniques,* vol. 44, pp. 1874 – 1883, Oct. 1996.

[3]   J. T. Rowley and R. B. Waterhouse, "Performance of shorted microstrip patch antennas for mobile communications handsets at 1800 MHz," *IEEE Transactions on Antennas and Propagation,* vol. 47, pp. 815 – 822, May. 1999.

[4]   B. B. Beard and W. Kainz. (2004, Review and standardization of cell phone exposure calculations using the SAM phantom and anatomically correct head models: *BioMedical Engineering,* pp. 1-10. http://www.biomedical-engineering-online.com/content/3/1/34. (Last accessed: Jan. 2009).

[5]   P. S. Excell, "Modelling of handsets, antennas, heads and hands in the FDTD method," *IEE Colloquium on Design of Mobile Handset Antennas for Optimal Performance in the Presence of Biological Tissue,* pp. 7/1 - 7/4, 20 Jan. 1997.

[6]   H. Morishita, H. Furuuchi and K. Fujimoto, "Characteristics of a balance-fed loop antenna system for handsets in the vicinity if human head or hand," *IEEE Transaction,* pp. 2254-2255, 2000.

[7]   C. H. Li, E. Ofli, N. Chavannes and N. Kuster, "The effects of hand phantom on mobile phone antenna OTA performance," *The 2nd European Conference on Antenna and Propagation (EUCAP 2007),* Nov. 2007.

[8]   C. H. Li, E. Ofli, N. Chavannes, E. Cherubini, H. U. Gerber and N. Kuster, "Effects of Hand Phantom and Different Use Patterns on Mobile Phone Antenna Radiation Performance," *IEEE International Symposium on Antennas and Propagation, San Diego, California,* 5-12 July. 2008.

[9]   IEEE std. 1528-2003, IEEE recommended practice for determining the peak-spatial average specific absorption rate (SAR) in the human head from wireless communications devices: Measurement techniques.

[10]   D. L. Means and K. W. Chan, "Evaluating compliance with FCC guidelines for human exposure to radiofrequency electromagnetic fields-Additional information for evaluating compliance of mobile and portable devices with FCC limits for human exposure to radiofrequency emissions," *Office of Engineering and Technology FCC, Washington DC,* vol. Supplement C (Edition 01-01) to OET Bulletin 65, June. 2001.

[11]   M. Y. Kanda, M. Ballen, S. Salins, C. K. Chou and Q. Balzano, "Formulation and characterization of tissue equivalent liquids used for RF densitometry and dosimetry measurements," *IEEE Transaction on Microwave Theory and Techniques,* vol. 52, pp. 2046 – 2056, Aug. 2004.

[12]   M. A. Jensen and Y. Rahmat-Samii, "EM interaction of handset antennas and a human in personal communications," *Proceeding of the IEEE,* vol. 83, pp. 7-17, Jan. 1995.

[13]   J. Fayos-Fernandes, C. Arranz-Faz, A. Martinez-Gonzalez and D. Sanchez-Hernandez, "Effect of pierced metallic objects on SAR distributions at 900 MHz," *Bioelectromagnetics,* vol. 27, pp. 337-353, 2006.

[14]   R. Aitmehdi. SAR calculation of a dual band helical antenna mounted in a mobile handset using a SAM homogeneous phantom. *Flomerics,* http://www.flomerics.com/microstripes/applications/sar/index.jsp., pp. 10, (Last accessed: Apr. 2007).

[15]   S. Khalatbari, D. Sardari, A. A. Mirzaee and H. A. Sadafi, "Calculating SAR in two Models of the Human Head Exposed to Mobile Phones Radiations at 900 and 1800 MHz," *Progress in Electromagnetic Research Symposium, PIERS2006, Cambridge, USA,* vol. 2, pp. 104-109, 26-29 Mar. 2006.

[16]   W. Stewart, Sir, 2000, Radiofrequency fields from mobile phone technology. Independent Expert Group on Mobile Phones (IEGMP), http://www.iegmp.org.uk/documents/iegmp_4.pdf, (Last accessed: Jan. 2009).

[17]   H. Virtanen, J. Keshvari and R. Lappalainen, "The effect of authentic metallic implants on the SAR distribution of the head exposed to 900, 1800 and 2450 MHz dipole near field," *Physics Medicine and Bio.,* vol. 52, pp. 1221-1236, Feb. 2007.

[18]   L. W. Li, P. S. Kooi, M. S. Leong, H. M. Chan and T. S. Yeo. (2000, July). Antenna patterns & input impedance of handset antennas and SARs in human head: A comparative study using FDTD, *Extended report of Journal of Electromagnetic Waves and Applications,* vol. 14, pp. 987-1000, http://www.ece.nus.edu.sg/stfpage/elelilw/Handset.htm, (Last accessed: 29 May 2008).

[19] L. C. Kuo and H. R. Chuang, "Design of a 900/1800 MHz dual-band loop antenna mounted on a handset considering the human hand and head effects," *Antennas and Propagation Society International Symposium, IEEE,* vol. 3, pp. 701 – 704, 2003.

[20] M. Francavilla, A. Schiavoni, P. Bertotto and G. Richiardi, "Effect of the hand on cellular phone radiation," *IEE Proceedings on Microwaves, Antennas and Propagation,* vol. 48, pp. 247 – 253, Aug. 2001.

[21] M. Lundmark, R. S. Calvo, P. S. Kildal and C. Orlenius, "A solid hand phantom for mobile phones and results of measurements in reverberation chamber," *Antennas and Propagation Society International Symposium, IEEE,* vol. 1, pp. 719 – 722, 20-25 June. 2004.

[22] K. Ogawa, T. Matsuyoshi and K. Monma, "An analysis of the performance of a handset diversity antenna influenced by head, hand and shoulder effects at 900 MHz," *Antennas and Propagation Society International Symposium, IEEE,* vol. 2, pp. 1122 – 1125, 11-16 July. 1999.

[23] M. Okoniewski and M. A. Stuchly, "A study of the handset antenna and human body interaction," *IEEE Transaction on Microwave Theory and Techniques,* vol. 44, pp. 1855-1864, 1996.

[24] H. O. Ruoss, "Influence of the shape of the head model on the maximum averaged SAR value," *IEE Seminar on Electromagnetic Assessment and Antenna Design Relating to Health Implications of Mobile Phones,* pp. 7/1 - 7/5, 28 June. 1999.

[25] P. Bernardi, M. Cavagnaro and S. Pisa, "Evaluation of the SAR distribution in the human head for cellular phones used in a partially closed environment," *IEEE Transactions on Electromagnetic Compatibility,* vol. 38, pp. 357 – 366, Aug. 1996.

[26] W. Whittow, C. J. Panagamuwa, R. Edwards and J. C. Vardaxoglou, "Specific Absorption Rates in the Human Head Due to Circular Metallic Earrings at 1800 MHz," *Antennas and Propagation Conference, LAPC 2007, Loughborough,* pp. 277 – 280, 2-3 April. 2007.

[27] W. G. Whittow, C. J. Panagamuwa, R. M. Edwards and J. C. Vardaxoglou, "On the effects of straight metallic jewellery on the specific absorption rates resulting from face-illuminating radio communication devices at popular cellular frequencies," *Physics in Medicine and Bio.,* vol. 53, pp. 1167-1182, Feb. 2008.

[28] N. Kuster. 1998, Current status of dosimetry techniques and results, *Swiss Federal Institute of Technology Zurich 8092 Zurich, Switzerland,* pp. 1-20, www.itis.ethz.ch/publi/IBC_KUSTER2.pdf, (Last accessed: 17 Nov. 2008).

Chapter 5

Realistic Homogeneous Head and Hand Models, with and without Metallic Loop-like Jewellery Items

5.0 Introduction

In this chapter, the same methods as employed in Chapter 4 are applied to a more realistic human head and hand geometry. A homogenous SAM head and a realistic hand model that includes fingers are developed. Besides investigating the effect of the presence of the hand, the inclusion of realistic fingers enables more subtle effects of the metallic ring to be studied. In addition, the effect of a metallic earring placed beside the ear is also studied. Simulations results presented in this chapter include the effect of the hand and both fingers and earrings on SAR inside the head. Antenna radiation patterns at two different frequencies (900 MHz and 1900 MHz) are also studied in this context. In an attempt to improve the realism of the situation a PIFA antenna is included in the study and compared to the monopole.

5.1   Antenna, SAM head and realistic hand models

5.1.1 Antenna models (Monopole and PIFA antenna)

The simulations were carried out using Microstripes (TLM) at 900 and 1900 MHz. The first simulations in this chapter employ a $\lambda/4$ monopole antenna on top of a metal box, which has the same dimension as the handset-antenna model employed in Chapter 4 (Figure 5.1-2 (a)). For comparison, the latter simulations use a dual-band PIFA antenna as the radiating source. PIFA antennas are a popular choice for internal

mobile handset antennas due to their low-cost, low-profile and because the free-space
radiation pattern shows a lower gain in the direction of the head [1, 2]. A typical gain
for both a λ/4 monopole and a PIFA antennas are 2-6 dB and 0-3 dBi respectively.
The PIFA is generally considered to be a narrow band device and the gain is similar to
a λ/4 monopole antenna. Previous studies [3, 4] have shown that the PIFA antenna
could significantly reduce the SAR in the head compared to the λ/4 monopole
antenna, however the effect of the hand that hold the handset becomes important due
to the hand proximity to the antenna position [3, 5]. Therefore, the inclusion of a
metallic ring on the hand is expected to cause additional effects on the PIFA radiation
performance and on SAR inside the head. In both cases (monopole and PIFA
antenna), the distance between the feed point of the antenna and the SAM head
phantom surface is fixed at 8.3 mm. The dimensions of the PIFA's radiating elements
(based on the model in [6]) were changed to achieve resonance at around 908.45 MHz
and 1915 MHz respectively (the actual resonant frequencies of the λ/4 monopole
antenna) (see S11 plot in Figure 5.1-1). The PIFA antenna dimensions employed in
this study are shown in Figure 5.1-2 (b). In addition, the hand model is placed at the
same position (distance and orientation) relative to the head in both antennas cases.
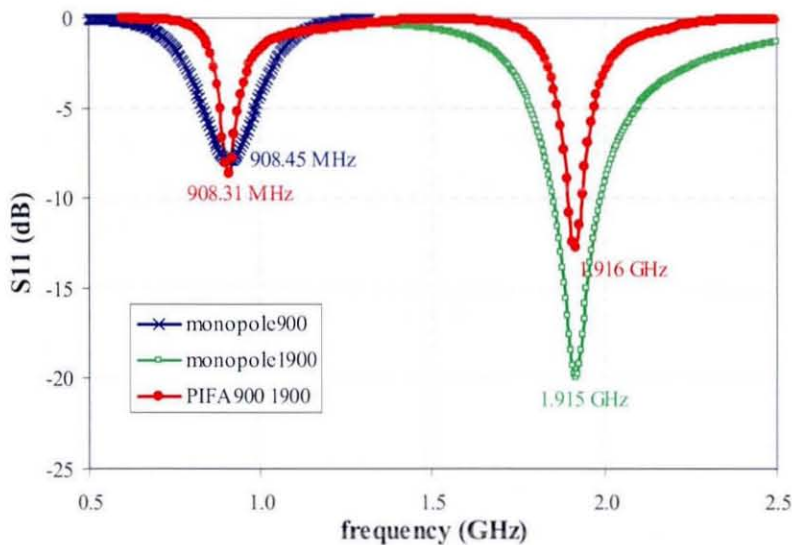
Figure 5.1-1: Simulated return loss performance of the monopole and the PIFA antenna
employed in this chapter.
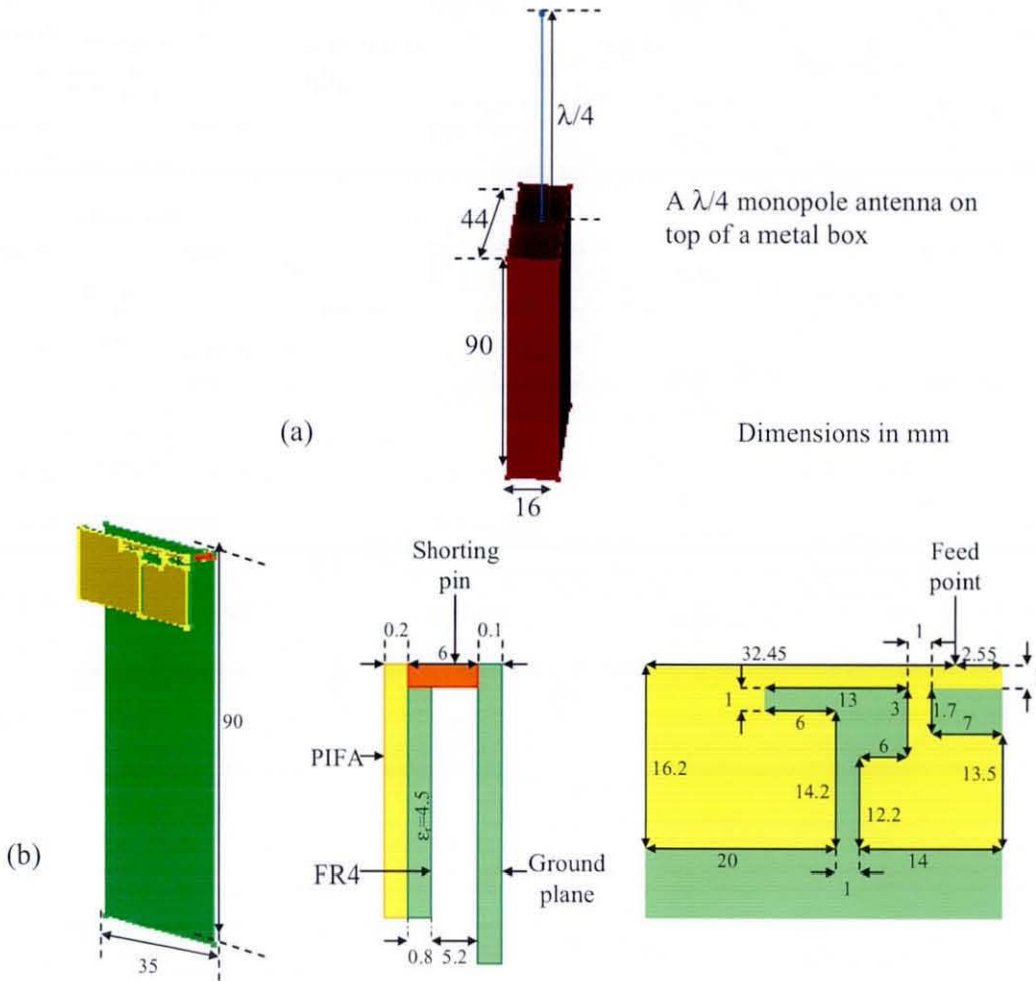
Figure 5.1-2: (a) A monopole antenna on top of metallic box and (b) a PIFA antenna employed for the simulations in this chapter.

5.1.2 A realistic human hand model

In use a handset will typically be orientated at a particular angle with respect to the head. The hand will also usually apply an undefined force to the handset which will compress the human pinna (outer ear) [5]. Different positioning of the handset will undoubtedly cause different effects on the radiation performance and on SAR. The realistic hand employed in the current thesis was obtained from a commercial CAD model [7], which had a grip suitable for incorporating the handset unit. In order to place the handset, the CAD data was manipulated by making comparison with published sources [8, 9] and by studying the results of an online poll conducted by the

author of this thesis. However, the result obtained from the survey is not definitive since there are different operational conditions between users. Moreover, to minimize the number of simulation runs, only the right hand holding the handset and the right hand-side of the head situation will be considered for investigations. In addition, the handset body for this investigation needs to be orientated at a particular angle (as mentioned in the earlier chapter) due to the difficulty of modelling the hand. The hand orientation showed in Figure 5.1-3 (b) is the best position of the hand can be modelled to avoid unintended 'grooves' resulted by translating and rotating the hand, whilst further rotation on the realistic hand model may further distort the joints between the fingers and the palm. Hence, complex CAD data often has unjoined surfaces which can only be partially repaired in numerical electromagnetic interfaces. Meanwhile, the meshing process is very sensitive to this problem, which can only be repaired by a specialized fixing software tool. However, these problems have been overcome by minimizing the amount of CAD manipulation and by carefully checking the mesh files for holes. The material properties of the hand model are as in Table 4.1-1.
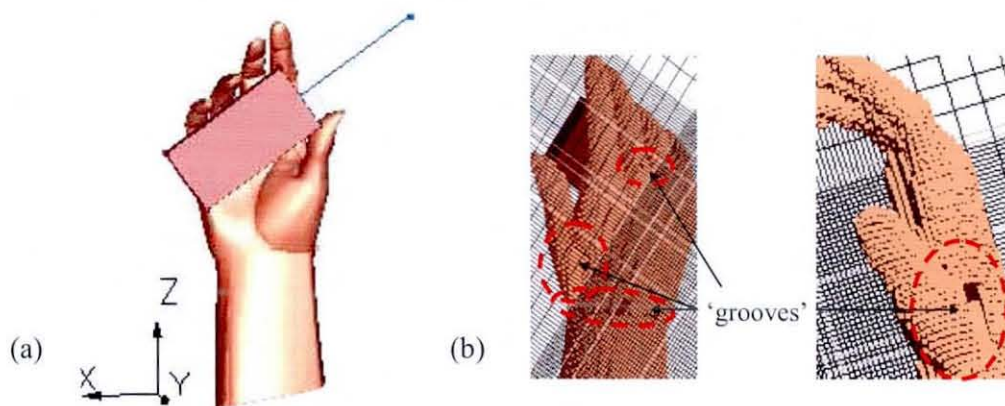
Figure 5.1-3: (a) A realistic hand model holds a mobile handset and (b) unintended 'grooves' resulted by further translating and rotating the hand model.

5.1.3 The SAM head model

Although complex anatomical phantoms have mostly been employed in simulating the human head, the standard experimental procedures still relies on the homogeneous phantom [10, 11]. In this thesis, the standard homogeneous SAM head CAD model has been employed in the simulation study (Figure 5.1-4). The mass density of brain

and muscle tissues is assumed to be 1000 kg/m^3 as given in IEEE Standard 1528 [12].
The frequency dependent parameters (ε_r, σ) used in the SAM head and the hand are
the same as those for the standard tissue equivalent liquids employed in Chapter 4 (as
in Table 4.1-1). The head and the hand model resolution was set to the maximum cell
size of $\lambda_{min}/10$, where λ_{min} is the wavelength within the dielectric material that having
the highest permittivity (dielectric constant). The SAR results presented in this section
are normalized to 0.25 W at 900 MHz and 0.125 W at 1900 MHz.
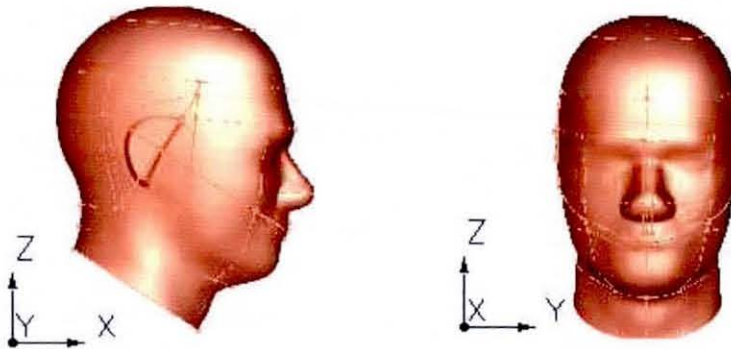
Figure 5.1-4: The SAM head model employed in the simulations.

5.2 The effect of a metallic ring worn on the hand on SAR in the hand (no head)

5.2.1 The effect of the hand with the ring and bangle present on SAR

In Chapter 4, a simple block-hand was employed which incorporated very simple
cylindrical fingers wrapped around three sides of the handset body. However, in
practice the fingers of mobile users frequently stray near to the back side of the
antenna and it is of great interest to investigate what effect this would have on the
results. In the current chapter, the hand is placed at a fixed position relative to the
antenna and the SAR inside the hand is investigated considering the presence and the
absence of metallic ring and bangle (worn on the finger and wrist respectively) (see
Figure 5.2-1). The dashed lines represent the cut away plane for the SAR distributions

inside the hand that will be demonstrated later. The results for a monopole antenna
will be compared with a PIFA antenna at both 900 MHz and 1900 MHz.
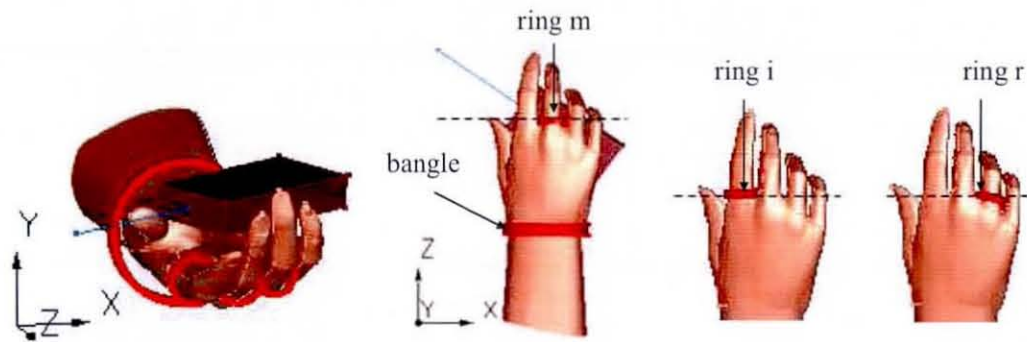
Figure 5.2-1: A realistic hand model holds the handset unit (monopole or PIFA antenna) with
metallic ring worn on different fingers for comparison. The dashed lines are the cutaway
planes for the peak SAR distributions in Figure 5.2-4 and Figure 5.2-5 later.
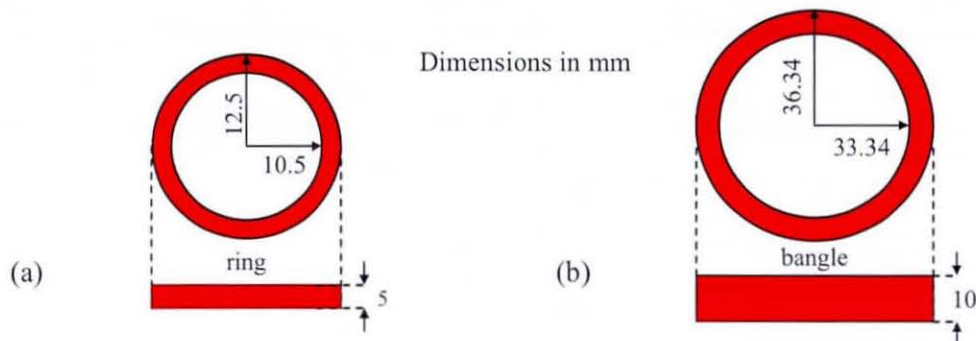
Figure 5.2-2: The metallic (a) ring and (b) bangle dimensions employed in this chapter.

As has already been suggested, the SAR could vary depending on the type of antenna
employed within the handset [13]. Rahmat-Samii and Jensen [13], Francavilla et al.
[14], Kuo and Chuang [15] have considered the SAR in the hand besides the SAR in
the head and the highest SAR was found inside the hand because it holds the handset
whilst operating [16]. The results presented in the current chapter will provide a fuller
understanding of how much energy is absorbed inside the hand that holds the handset
when the head is absent. This situation might be found if a person was using the
handset as a speakerphone for example. The inclusion of a metallic ring and bangle on
the hand into the simulation model (mobile-head) will further estimates any changes
in the amount of energy absorbed in the hand, which could also affect the SAR values
inside the head. The metallic ring is given the material properties of copper. The ring

is worn on the index (i), middle (m), ring (r) finger and the latter worn on the three fingers at the same time (imr) for comparison (Figure 5.2-1).

Figure 5.2-3 shows results of how different ring positions on the hand (with or without a bangle) affect the SAR in the hand at 900 MHz and 1900 MHz. The geometrical representation of the ring and bangle are as Figure 5.2-2. Ring i and ring m use the same dimension shown in Figure 5.2-2 (a) whilst the ring r is smaller with the inner and outer radius of 9.8 and 11.8 mm respectively, due to the ring finger being smaller than the index and middle finger.

Figure 5.2-3 shows that the averaged 1 g SAR inside the hand at 900 and 1900 MHz is notably altered by the ring, but the effect is varies depending on the type of antenna in use and on which finger the ring been placed. There were both positive and negative differences in SAR observed at both frequencies investigated in this case when a monopole antenna is employed as the radiating source. However, the change in SAR in the hand is more pronounced when a PIFA antenna is used as the radiating source. With a PIFA antenna (right hand side of Figure 5.2-3), the ring worn on the fingers (with or without the bangle) increased the averaged 1 g SAR in most of the cases investigated. This is expected since the PIFA antenna is mounted facing the fingers, thus the small metallic rings worn on the fingers are in very close proximity to the antenna and are liable to influence the SAR significantly. The strongest effect is found with the ring worn on middle finger, which increases the SAR by more than 27% at 900 MHz and 13% at 1900 MHz respectively. It is therefore important to include the ring on the hand in the model as it may alter the SAR in the hand itself and could also affect the SAR in the head.

In addition, besides the small ring worn on the fingers, Figure 5.2-3 also includes the effect of a bangle worn on the wrist. However, the presence of the bangle does not show any significant effects on this configuration due to the fact that the bangle is positioned a significant distance away from the unit's antenna. The effect of the rings on the averaged 10 g SAR values at 900 MHz and 1900 MHz for both antennas was found to be insignificant and therefore the results are not presented in the current section.
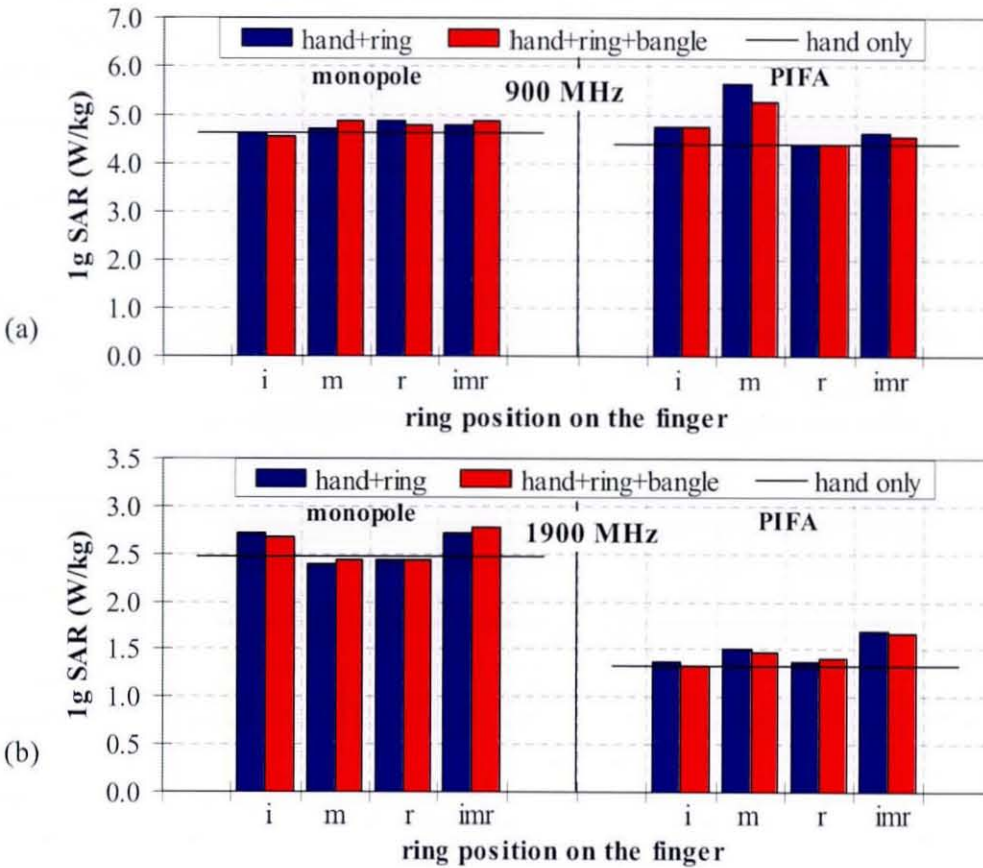
Figure 5.2-3: The averaged 1 g SAR in the hand with the ring and bangle worn on the hand at
(a) 900 MHz and (b) 1900 MHz when the head is absent. A λ/4 monopole (left) and a PIFA
(right) antenna were used as the radiating source.

5.2.2 Peak SAR distributions in the hand with and without the rings present

Figure 5.2-4 and Figure 5.2-5 demonstrate the effect of the ring on the peak SAR
distribution inside the hand at 900 MHz and 1900 MHz for both the monopole and the
PIFA antennas. The SAR distributions shown are on the same xy-plane but the plots
are in different cut-level depending on which finger the ring is worn on (see the
dashed lines on the hand in Figure 5.2-1). Note that the cut plane for the no ring case
is the same as the ring i case. As in Chapter 4, the peak SAR distributions presented in
this chapter are also shown in logarithmic scale (dB) to give a clearer picture of the

SAR distribution owing to the presence of metallic jewellery on each case investigated. The value for each figure is normalized to the peak voxel value for the particular cut plane. A metallic ring has a potential to redistribute the incident RF energy around the ring, leading to SAR concentration at some points and corresponding SAR reduction in the other points.
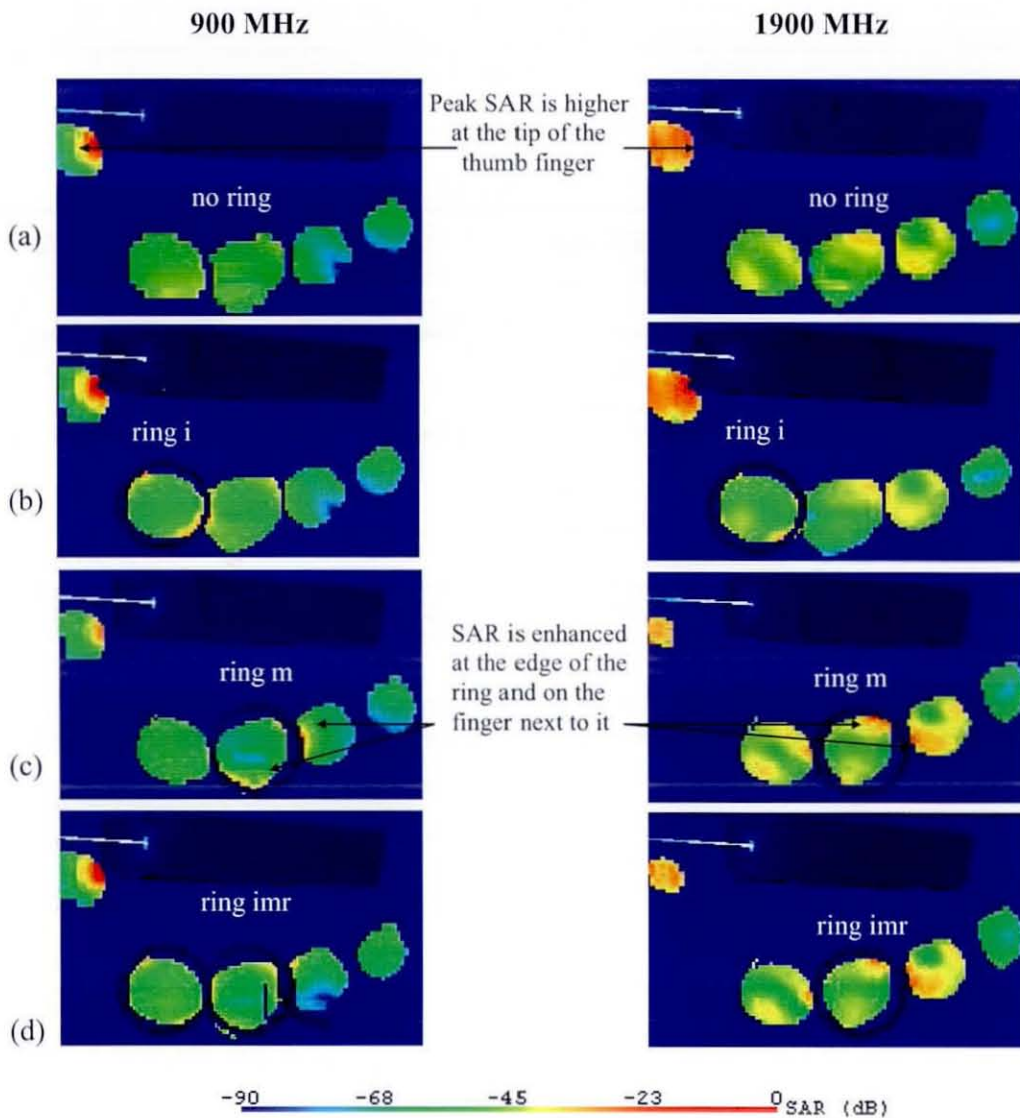
900 MHz   **1900 MHz**

Figure 5.2-4: The SAR distribution inside the hand for a monopole antenna on the xy-plane (see Figure 5.2-1) at 900 MHz (left) and 1900 MHz (right). The ring is worn on different finger for comparisons (a) no ring, (b) index finger, (c) middle finger and (d) on index, middle and ring finger.
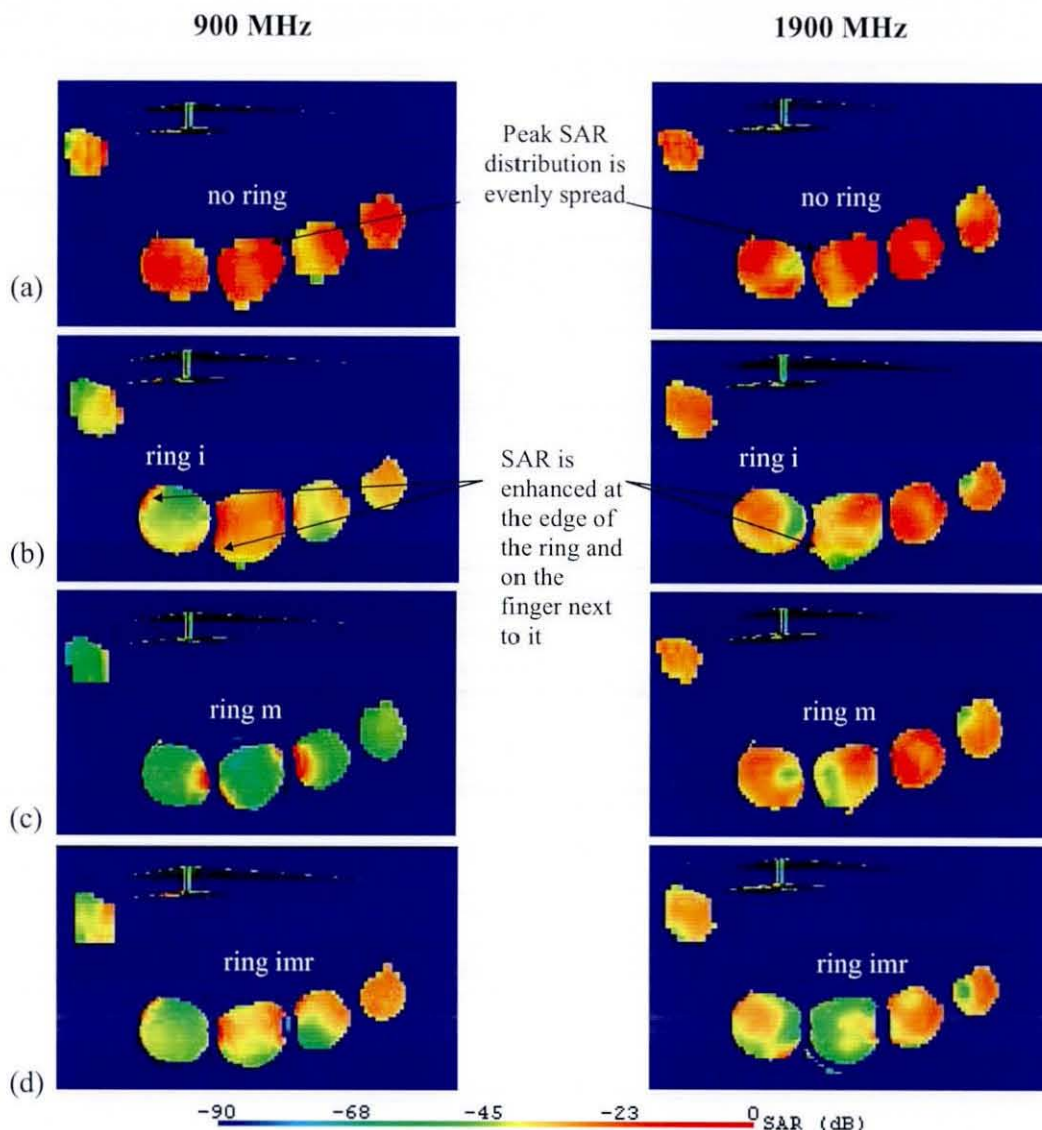
900 MHz   **1900 MHz**

Figure 5.2-5: The SAR distribution inside the hand for a PIFA antenna on the xy-plane (see Figure 5.2-1) at 900 MHz (left) and 1900 MHz (right). The ring is modelled on different fingers for comparison (a) no ring, (b) index finger, (c) middle finger and (d) on index, middle and ring finger.

Figure 5.2-5 shows that the PIFA illuminates the fingers much more uniformly than the monopole (Figure 5.2-4). Since the dB scale is relative there is no reference level to compare. In both cases (monopole and PIFA antenna), the maximum SAR generally appears on the closest fingers to the antenna and the handset body when no ring is worn. For the monopole antenna, the highest SAR distribution appears at the edge of the fingers where they touch the handset body especially on the tip of the

thumb finger, whereas for the PIFA antenna, the SAR distribution is uniformly spread over the five fingers. When the ring is added into the simulations, the SAR values are enhanced and occur at the edge of the ring on the finger wearing the ring and also on a small part on the adjacent fingers. As the ring could modify the SAR distribution in the hand, it could also affect the SAR distributions in the head.

5.3   The SAM head, the hand and metallic jewellery affect on SAR (in the head) and on the antenna performance

5.3.1 The hand and metallic ring worn on the hand affect on SAR values within the head

The results in [8, 14, 17-21] have shown that the presence of the human hand causes noticeable changes in the antenna performance and to the SAR values within the head. Therefore, it is of great interest to evaluate how the hand presence could affect the SAR inside the head [14]. In this section, the monopole antenna or the PIFA antenna is placed in the 'cheek' position as is ordinarily used amongst the majority of users [22] (see Figure 5.3-1). To investigate the effect of the hand on SAR values inside the head, a realistic hand model is included in the simulation model. It is assumed that the hand holds the handset very close to the right hand side of the head surface (see Figure 5.3-2 (a)), and the handset-antenna is placed above the ERP (Figure 5.3-1). In the latter simulations, the rings are included (Figure 5.3-2 (b)) to investigate the effects of wearing a ring and bangle on SAR values inside the head. The ring is placed on different fingers (i, m, r) for comparison as in the previous simulations. The ring and bangle dimensions are the same as in Figure 5.2-2. As discussed in Section 5.1.3, the frequency dependent parameters (ε_r, σ) used in the spherical head and the block-hand are the same as those for the standard tissue equivalent liquids. The same considerations were made when selecting the mesh dimensions as in the previous case.
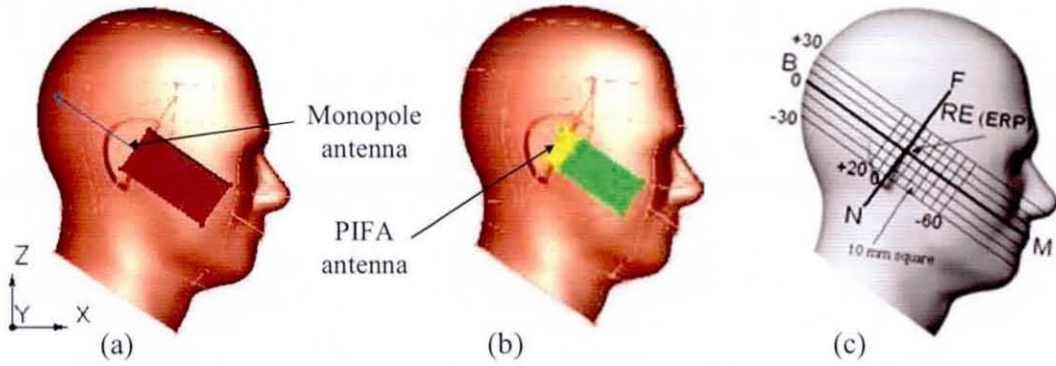
Figure 5.3-1: The SAM head model with a mobile handset placed in the 'cheek' position beside the right hand side of the head. A (a) monopole antenna, (b) PIFA antenna is used as the radiating source, and (c) the ERP on the SAM head [12].
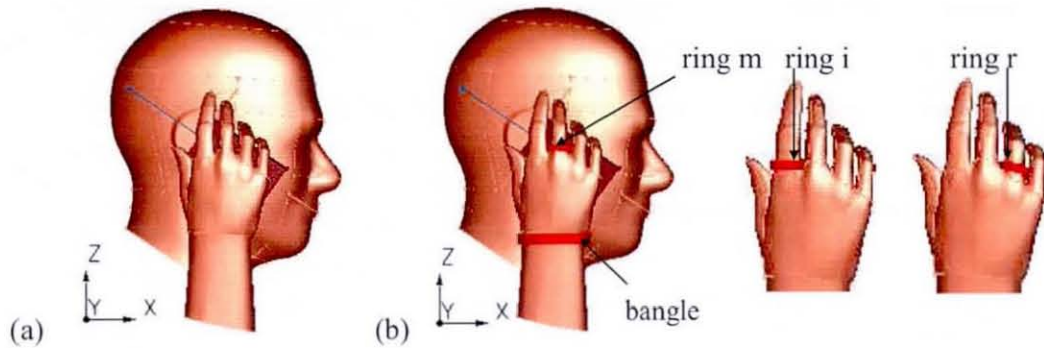
Figure 5.3-2: The SAM head model with a mobile handset placed in the 'cheek' position beside the right hand side of the head (a) with the hand and (b) with the ring worn on different fingers (with or without bangle).

The effects of the hand wearing a metallic ring to the averaged 1 g SAR and the peak SAR values within the SAM head are illustrated in Figure 5.3-3 and Figure 5.3-4. The straight line shows SAR in the head without the hand and the ring, the dashed line is for the SAR in the presence of the hand, whilst the columns represent the SAR with both the hand and the ring. Figure 5.3-3 shows the averaged 1 g SAR in the head with a monopole antenna as the radiating source. The hand model notably decreases the averaged 1 g SAR in the head at 900 MHz and increases it at 1900 MHz. For the same simulation but adding a ring to the hand, the averaged 1 g SAR in the head is decreased by approximately 7% at both frequencies (compared to the case of just the head and hand). These results (in this configuration) seem to suggest that the metallic ring worn on the hand reduces the amount of energy absorbed in the head at 900 MHz

and 1900 MHz. In all cases, the bangle has only marginal effects on the results due to the fact that the position of the bangle is far from the unit's antenna and the mobile-head model. The peak SAR values inside the head in Figure 5.3-3 (b) shows the same trend as the averaged 1 g SAR values in the head.

Figure 5.3-3: (a) The averaged 1 g SAR and (b) the peak SAR inside the head for a monopole antenna at 900 MHz (left) and 1900 MHz (right). A metallic ring is worn on different fingers (with and without bangle) for comparison.

Figure 5.3-4 shows the SAR results with a PIFA antenna as the radiating source. The averaged 1 g SAR in the head (with the hand) has similar characteristic to the results of the monopole antenna at 900 MHz, but only marginally changes at 1900 MHz. The inclusion of a metal ring on the finger decreases the averaged 1 g SAR in the head by 8% at 900 MHz. However, the ring in this configuration significantly increases the averaged 1 g SAR in the head at 1900 MHz when compared to the head-hand only model.
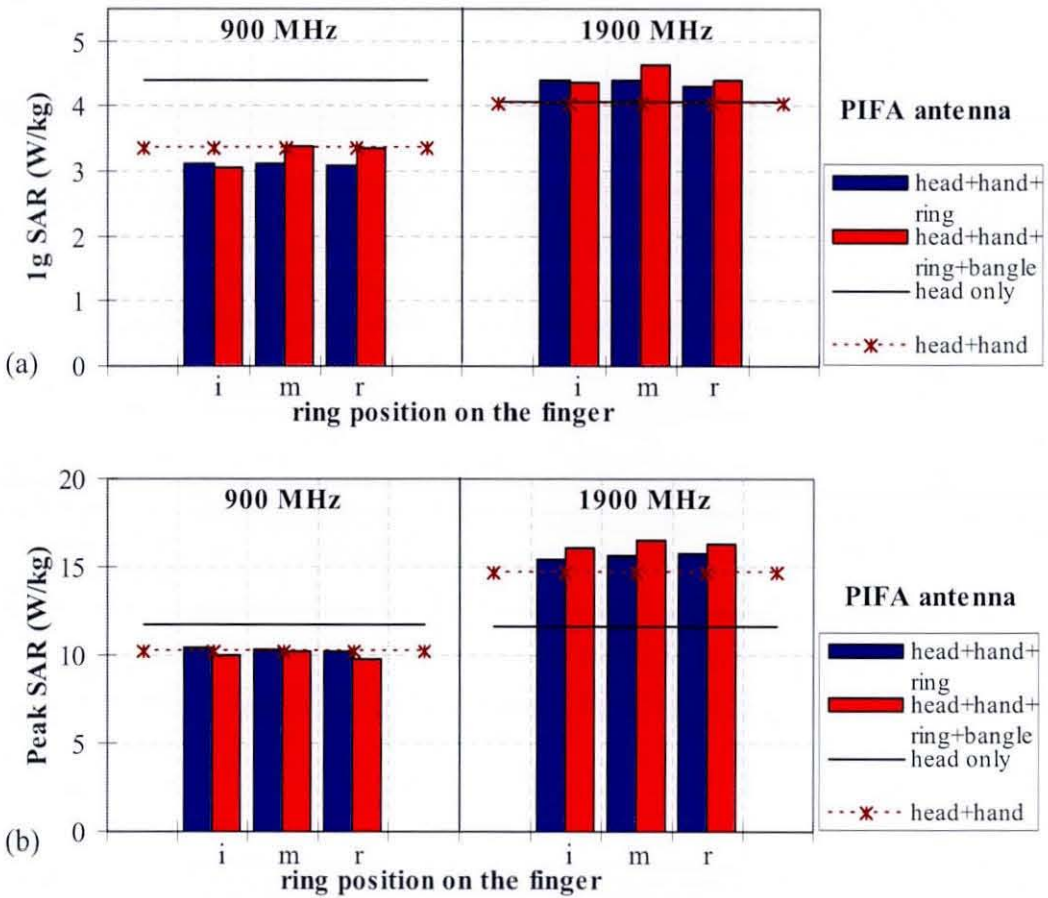
Figure 5.3-4: (a) The averaged 1 g SAR and (b) the peak SAR in the head for a PIFA antenna at 900 MHz (left) and 1900 MHz (right). A metallic ring is worn on different fingers (with and without bangle) for comparison.

Figure 5.3-3 and Figure 5.3-4 show there is a notable difference in SAR in the head caused by the hand and the inclusion of metallic ring on the hand, therefore both the hand and the ring should be included in the model while investigating the SAR. The ring worn on the hand in this configuration could help to reduce the SAR in the head at 900 MHz. However, the effect clearly varies depending on the frequency and the type of antenna in used. The rings worn on the hand may also increase the averaged 1 g SAR in the head, particularly at higher frequency (in this case at 1900 MHz) when an internal antenna i.e. a PIFA antenna is used as the radiating source. In addition, the inclusion of larger ring, such as bangle on the wrist can cause additional effects on the results but the effect is less important due to its remote position.

5.3.2 The effect of metallic loop-like earrings on SAR

As in Chapter 4, three scenarios are considered in order to investigate the effect of wearing metallic earrings on the SAR values inside the head. The scenarios are (a) metallic loop earring worn on the head, (b) metallic earring worn on the head in the presence of a hand (holding the mobile handset), and (c) metallic earring worn on the head with both the hand and the metallic ring worn on the middle finger (with and without the bangle).

To begin, metallic earrings with the material modelled as copper with a diameter (d) of 25, 30, 40, 50, 80 and 90 mm were included in the simulation model (mobile-head). In contrast to the previous chapter, the earring passes through the ear. This is made possible by the more accurate morphological model of the human (Figure 5.3-5 (a)). A realistic hand model was also included (Figure 5.3-5 (b)) to investigate the effects of the hand and an earring on the SAR values inside the head. Finally, the hand model with a metal ring worn on the middle finger (m) (with and without bangle) was included into the simulation models (Figure 5.3-5 (c)), in order to assess the effect brought about by the hand and the three metallic jewellery items on SAR. As in previous cases, the SAR results presented in this section are normalized to 0.25 W at 900 MHz and 0.125 W at 1900 MHz.
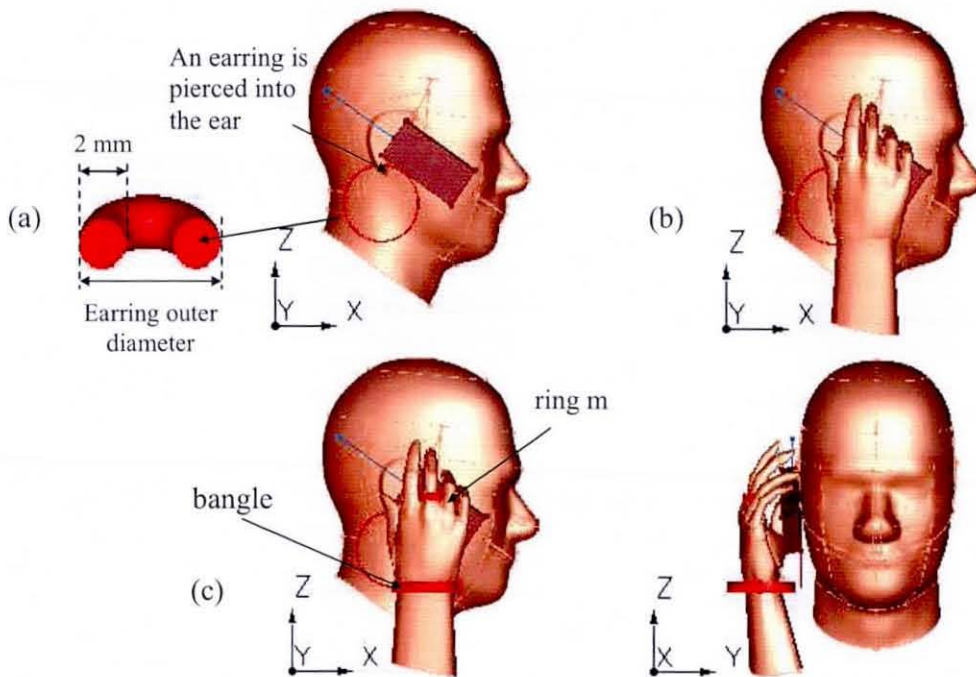
Figure 5.3-5: Three scenarios considered in evaluating the effect on the hand and metallic jewellery items on SAR in the head. The edge of the metallic earring is pierced into the earlobe, (a) without the hand, (b) with the hand holds the mobile handset and (c) with both the hand and the ring (with or without a bangle).

5.3.2.1 *Results of metallic earrings with monopole antenna excitation*

In this section three scenarios as shown in Figure 5.3-5 are investigated with a monopole antenna as the radiating source. The two different parameters investigated were the averaged 1 g SAR and the peak SAR in the head at 900 and 1900 MHz. Figure 5.3-6 shows results of various different sizes of earrings with or without the hand effects on SAR in the head. Only two sizes of earrings were used for the combination case, i.e. a diameter of 50 and 80 mm at 900 MHz, and the earring with a diameter of 40 and 50 mm at 1900 MHz. These earrings sizes were chosen since these were the most affected sizes in this configuration.
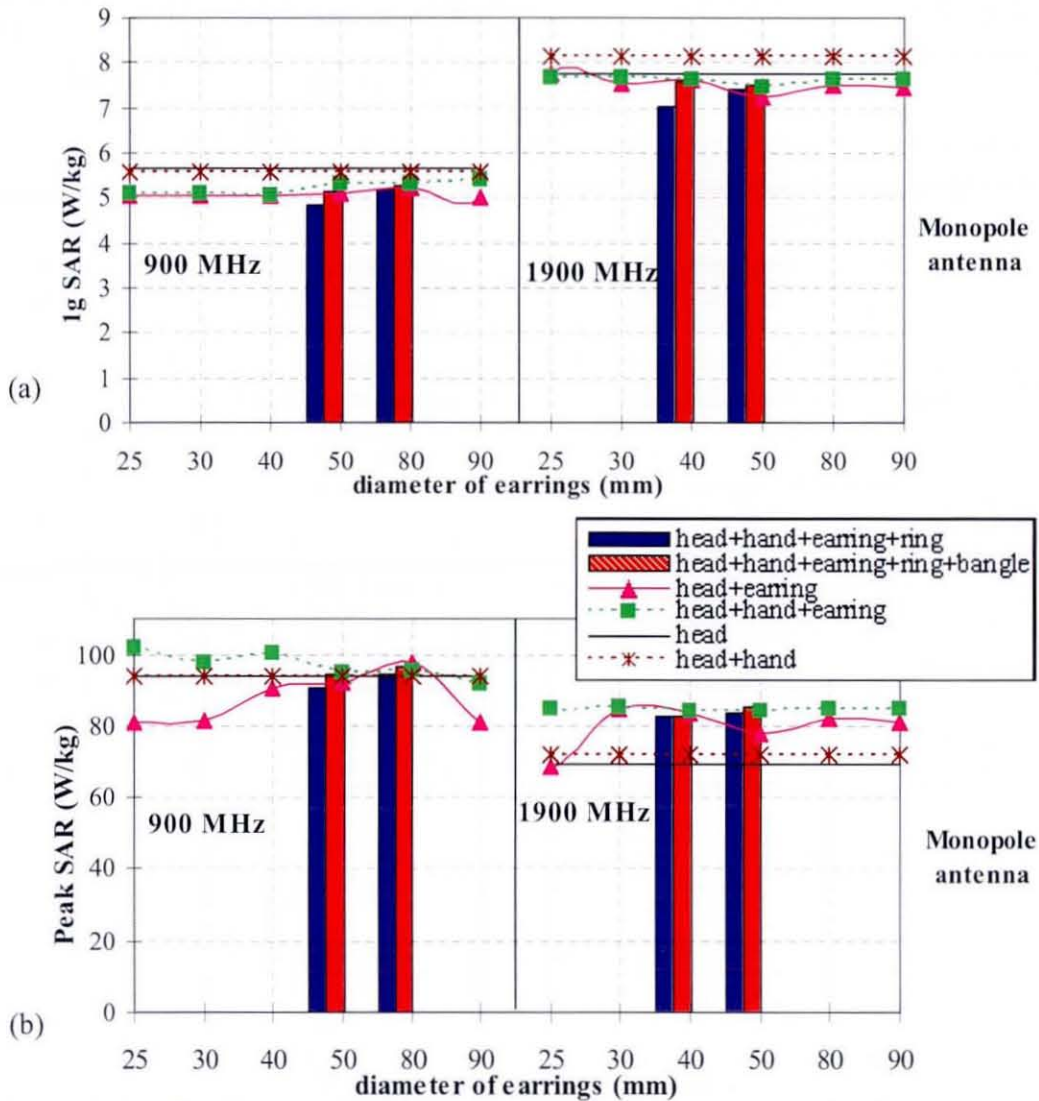
Figure 5.3-6: The (a) averaged 1 g and (b) peak SAR in the head for a monopole antenna at 900 MHz (left) and 1900 MHz (right). The earrings penetrate the earlobe in the model.

Figure 5.3-6 (a) shows the effect of the earrings on the averaged 1 g SAR in the head at 900 and 1900 MHz. The results seem to suggest that the earrings piercing the earlobe (in this configuration) seem to significantly decrease the averaged 1 g SAR in the head at both frequencies regardless of the earrings diameter. The hand when added into the model alters the averaged 1 g SAR due to increased dielectric loading, absorption and also due to the reflection at the hand-dielectric boundary. Generally, the combination of the hand, an earring and a ring (worn on the middle finger) further decreased the averaged 1 g SAR values (when compared to head-hand-earring cases) at both frequencies tested.

Figure 5.3-6 (b) shows the peak SAR in the head at 1900 MHz is generally increased
by the metallic earring (with or without a ring), although the averaged 1 g SAR in the
head is decreased. This difference can be explained by the fact that the peak SAR in
the head is enhanced near to the edge of the earring. The surface currents flowing on
the metallic earring appear to be carried on into the dielectric of the ear, causing large
increase in the local SAR values (see Figure 5.3-7 for the visualization of the SAR).
However, since this is a highly localised effect, the mass averaged SAR values do not
show this effect (there is no important increase deeper in the head). Figure 5.3-7
shows the effect of the earring on the SAR distribution in xz-plane for the earring
with a diameter of 80 mm and 50 mm at 900 and 1900 MHz respectively.
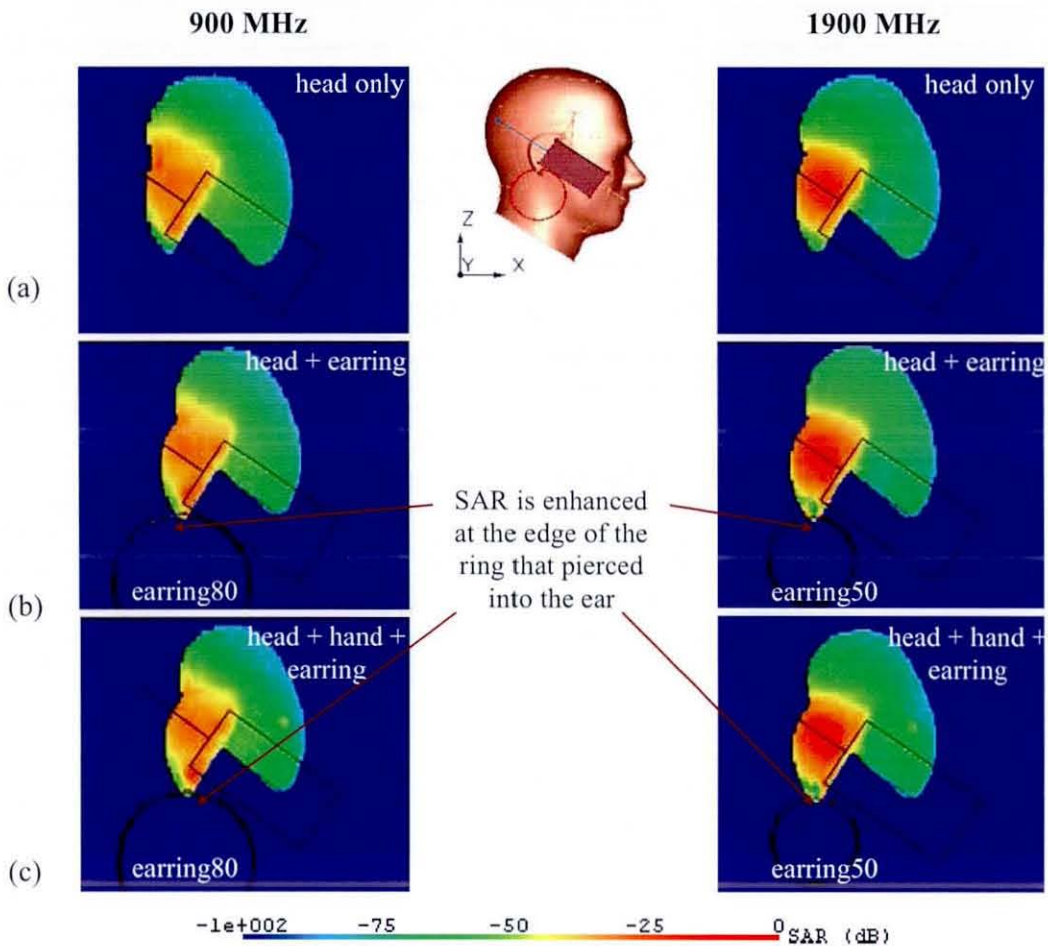
Figure 5.3-7: The peak SAR distribution inside the head for a monopole antenna at 900 MHz
(left) and 1900 MHz (right); (a) head only, (b) an earring is worn and (c) head worn earring
with the hand present.

5.3.2.2   Results of metallic earrings with PIFA antenna excitation

Figure 5.3-8 shows the effect of metallic earrings on SAR for three scenarios as in
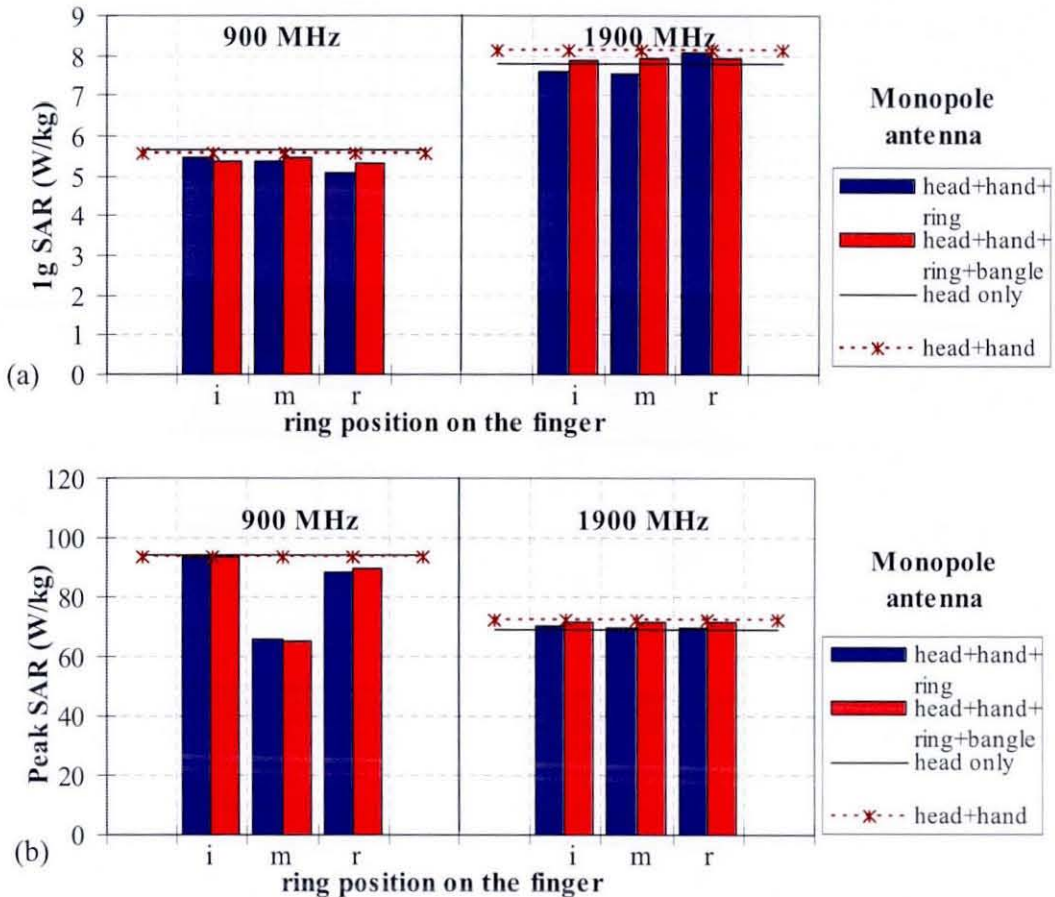Figure 5.3-5, but with a PIFA antenna (see Figure 5.1-1 (b)) as the radiating source.
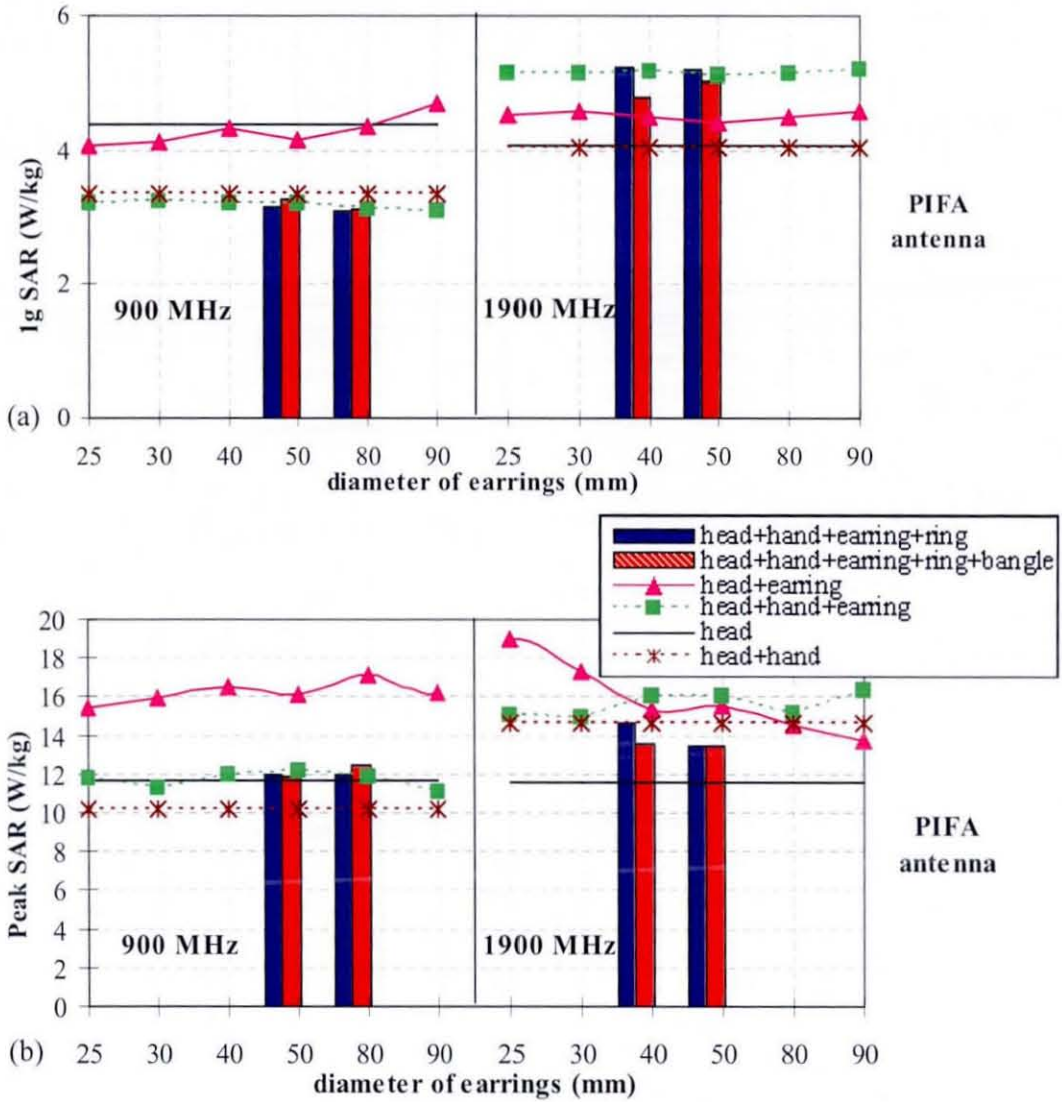
Figure 5.3-8: The (a) averaged 1 g and (b) the peak SAR in the head for a PIFA antenna at
900 MHz (left) and 1900 MHz (right). The earrings penetrate the earlobe in the model.

Figure 5.3-8 shows that the earrings marginally decrease the averaged 1 g SAR in the
head at 900 MHz, but increase it by 15% at 1900 MHz. The inclusion of the hand
significantly decreases the averaged 1 g SAR in the head at 900 MHz when compared
to head-earring case. However, the hand when added into the head-earring model

further increased the averaged 1 g SAR at 1900 MHz compared with no hand. The graph also shows that the combination of the hand and both the earring and the ring generally show minor effect on the SAR values (compared to the head-hand-earring cases) at both frequencies. The earrings effect is less significant when the hand is included in the simulation model. The hand can alter the SAR more substantially with the PIFA antenna (when compared to monopole antenna) due to dielectric loading, energy absorption and reflection at the hand dielectric boundary, since the hand situated very close to the large area of the PIFA antenna. However, the earrings can significantly increase the peak SAR in the head near to the edge of the earring at the point where it penetrates the earlobe (see Figure 5.3-9).
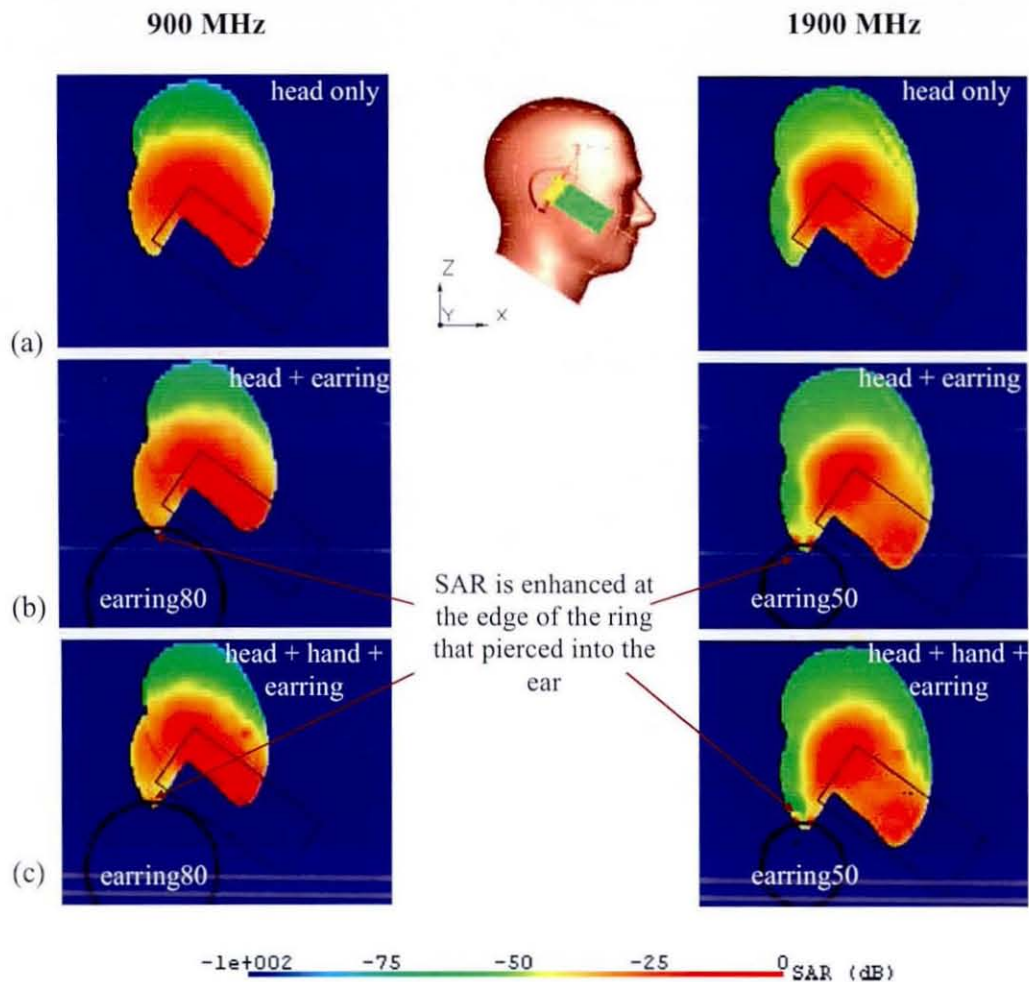
Figure 5.3-9: The SAR distribution inside the head for a PIFA antenna at 900 MHz (left) and 1900 MHz (right); (a) head only, (b) an earring is worn and (c) head worn earring with the hand present.

Figure 5.3-6 to Figure 5.3-9 show that the earrings examined of these configurations (Figure 5.3-5) decrease and increase the averaged 1 g SAR in the head, but the effect is strongly dependent on the frequency, the type of antenna in use and any additional objects in close proximity to the earring. Wearing an earring by itself regardless of the diameter seems to decrease the averaged 1 g SAR in the head at 900 MHz for both antennas investigated. However, the results suggest that care should be taken, as the averaged 1 g SAR in the head is increased by approximately 15% when the earring is worn at 1900 MHz with the PIFA antenna as the radiating source. The combination of the hand with an earring and the ring decreased the averaged 1 g SAR in the head at 900 MHz by approximately 14% with the monopole antenna and 28% with the PIFA antenna respectively (compared to just the head). However, this combination can also increase the averaged 1 g SAR in the head by approximately 28%, particularly at 1900 MHz when a PIFA antenna is used as the radiating source.

5.3.3 The effect of the human head and hand-worn metallic jewellery on antenna radiation pattern and efficiencies

5.3.3.1   *Radiation patterns for λ/4 monopole antenna*

As in Chapter 4, the antenna radiation pattern (gain pattern) in free-space was calculated with the handset-antenna oriented at a natural speaking angle (see Figure 5.3-1). Figure 5.3-10 to Figure 5.3-12 show radiation patterns (calculated in the yz-plane) for a λ/4 monopole antenna in isolation, near the SAM head and with the addition of a realistic hand model at 900 MHz (left) and 1900 MHz (right). The radiation patterns for the xy-plane are shown in the Appendix C.1 for a comparison.

Figure 5.3-10 shows the effect of the head and the hand on the radiation patterns at 900 and 1900 MHz. The antenna radiation pattern at both frequencies has a 'dipole-like' pattern in free-space. In the presence of the head, the monopole's radiation pattern is significantly influenced along the direction of the head (y-direction) due to

significant amount of energy absorbed by the head. The hand when added into the model further modified the radiation pattern since the hand that holds the handset body has absorbs and reflects part of the radiated energy. The shadow effect by the presence of the hand in the y-direction is about 1 dB at 900 MHz and 6 dB at 1900 MHz respectively.

Figure 5.3-10: A monopole antenna radiation patterns at 900 MHz (left) and 1900 MHz (right) with and without the head and the hand (yz-plane).

Figure 5.3-11: A monopole antenna radiation patterns at 900 MHz (left) and 1900 MHz (right) with and without the head and the hand worn a ring (with and without the bangle) (yz-plane).

Figure 5.3-11 shows the monopole's radiation pattern in the presence of the head-hand model with a metallic ring worn on the finger and a bangle worn on the wrist at 900 MHz (left) and 1900 MHz (right). The ring was simulated on different fingers for

comparison. As the plot with the ring worn on the index finger is as similar as the ring worn on the middle and the ring finger, only the effect of the ring worn on middle finger is shown in this section (Figure 5.3-11). It can be seen that the ring worn on the finger (with bangle) has only very minor effect on the antenna radiation pattern (at both frequencies) if compared to the case of just the head and hand. This phenomenon is in good agreement with the results presented in Chapter 4, which uses the spherical head and the block-hand model. There are only minor differences in the radiation pattern shape from the simplified case due to the different geometries employed. Neither the ring nor the bangle worn on the hand (in this configuration) has a significant effect on the monopole's radiation pattern. This means that metallic jewellery worn on the hand appears unlikely to affect the monopole performance when compared to the case of just the head and hand.

Figure 5.3-12 shows results of different sizes of metallic earrings on the monopole's radiation pattern at 900 MHz (left) and 1900 MHz (right). All cases of smaller earrings with a diameter of 25, 30 and 40 mm show a very similar effect on the antenna radiation pattern, so only the effect of the earring with a diameter of 30 mm is presented in Figure 5.3-12. The effect of these smaller earrings on the radiation pattern at both frequencies is of little significance; however the larger earrings of diameter 50, 80 and 90 mm noticeably alter the radiation pattern. This is particularly noticeable in the -z direction. The inclusion of the hand (Figure 5.3-12 (b)) cause a significant difference on the radiation pattern, particularly at 1900 MHz; however, wearing the larger earrings (with the hand present) seem to improve monopole's radiation performance in the –z direction (where the earring was positioned relative to the antenna and the head model).

The combination of the earring worn on the ear with the ring and bangle worn on the hand was also considered and the results are shown in Figure 5.3-12 (c). Only the results for the earring with a diameter of 80 mm at 900 MHz and 50 mm at 1900 MHz are illustrated in Figure 5.3-12 (c). The combination of the earring with the ring and bangle has only a minor effect on the radiation pattern at 900 MHz. However, a larger effect was found when all three metallic jewellery items were added to the head-hand model at 1900 MHz, when compared to the case of just the earring.
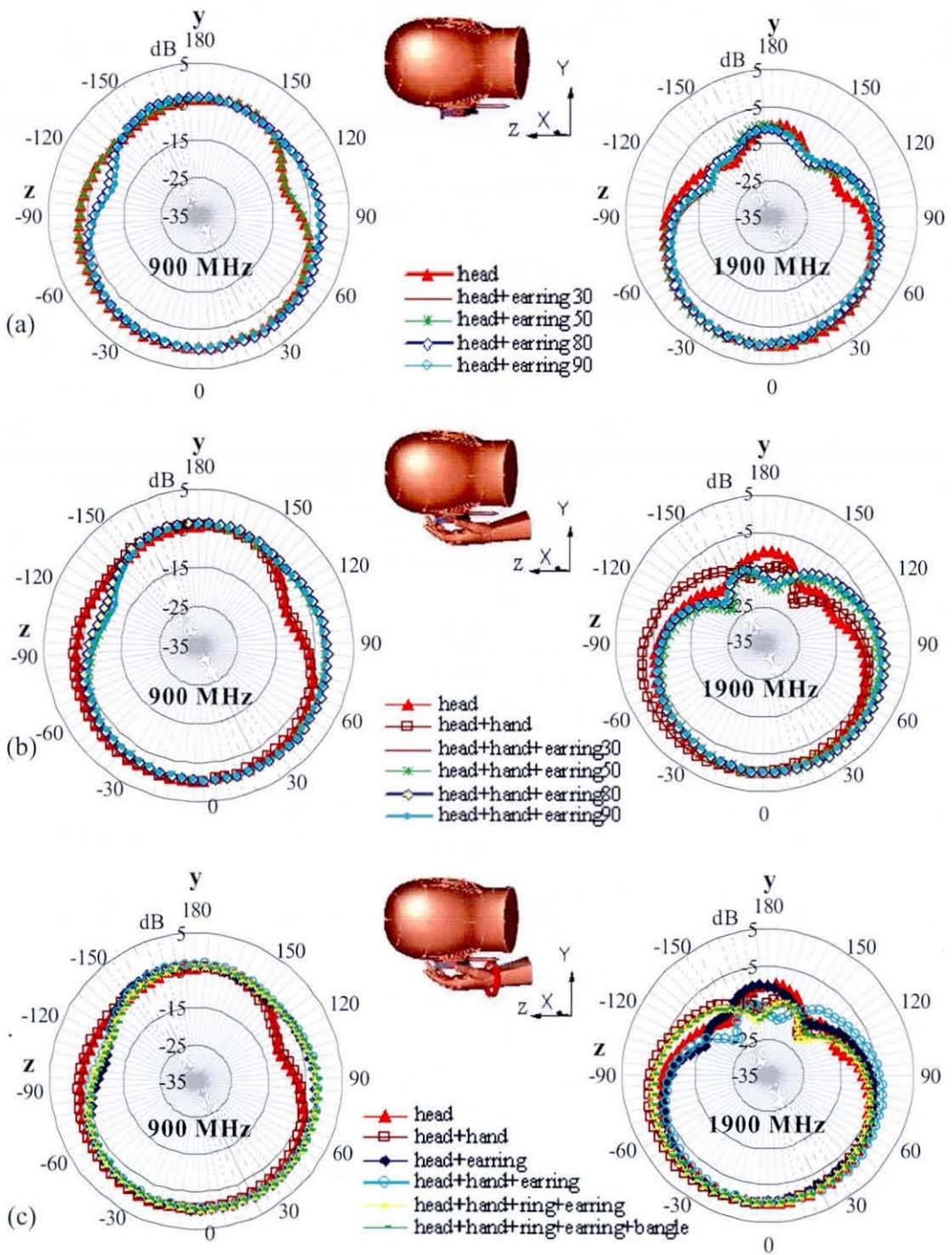
Figure 5.3-12: Radiation patterns for a monopole antenna at 900 MHz (left) and 1900 MHz (right) when place close to the SAM head (yz-plane). The earrings penetrate the earlobe in the model (a) without the hand, (b) with the hand and (c) with the hand wearing a ring and the bangle.

5.3.3.2   *Radiation patterns for a PIFA antenna*

The same scenarios as the monopole antenna with and without the presence of the
head, the hand and metallic jewellery are repeated in this section but a PIFA was used
as the radiating source. The PIFA antenna radiation patterns are taken from the yz-
plane and the radiation patterns in free-space at 900 MHz (left) and 1900 MHz (right)
are shown in Figure 5.3-13. The radiation patterns for the xy-plane are shown in the
Appendix C.2 for a comparison. Figure 5.3-13 shows that the PIFA radiation pattern
in free space is symmetrical and close to omni-directional at both frequencies tested.
However, the presence of the user's head significantly reduces the PIFA radiation
pattern in the y-direction, which results in about 8 dB and 10 dB differences at
900 MHz and 1900 MHz respectively. Moreover, the hand when included into the
simulation further modifies the antenna radiation patterns, but the effect is varied
depending on the frequency.
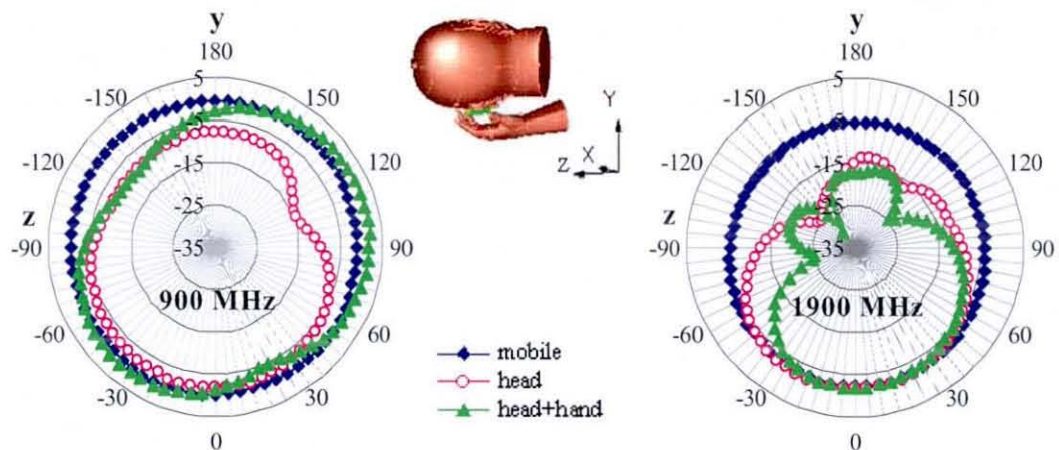
Figure 5.3-13: A PIFA radiation patterns at 900 MHz (left) and 1900 MHz (right) with and
without the head and the hand (yz-plane).

Figure 5.3-14 shows the PIFA radiation plots at 900 MHz (left) and 1900 MHz (right)
when a metallic ring and a bangle were included in the head-hand model. The
radiation patterns with the ring (with and without the bangle) have very similar
patterns as in the case with just the head and hand. As in the monopole antenna cases,
only the effect of the ring worn on the middle finger is presented in Figure 5.3-14.
There are only minor effects brought by the inclusion of the ring on the hand, which

results in about 2 dB difference at θ = -120° to -140° and at θ = 15° to 30° at
900 MHz. However, the ring effect at 1900 MHz is insignificant.
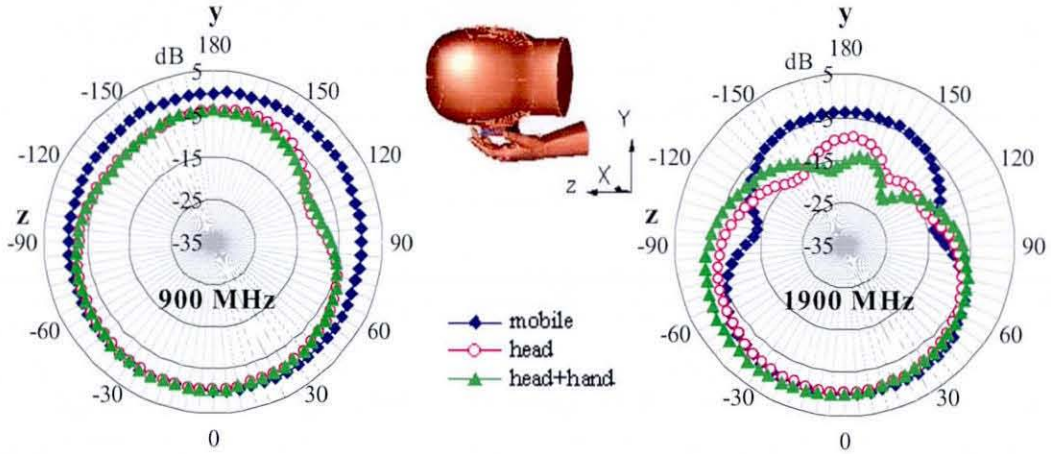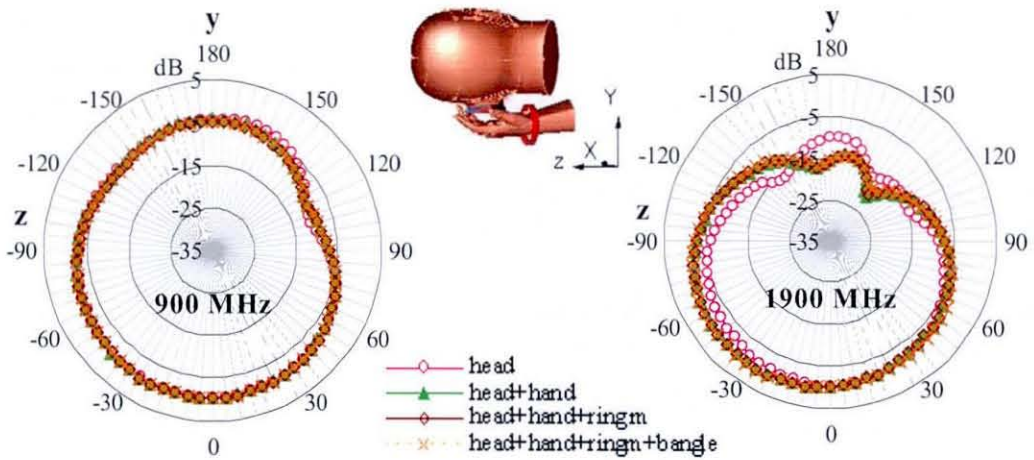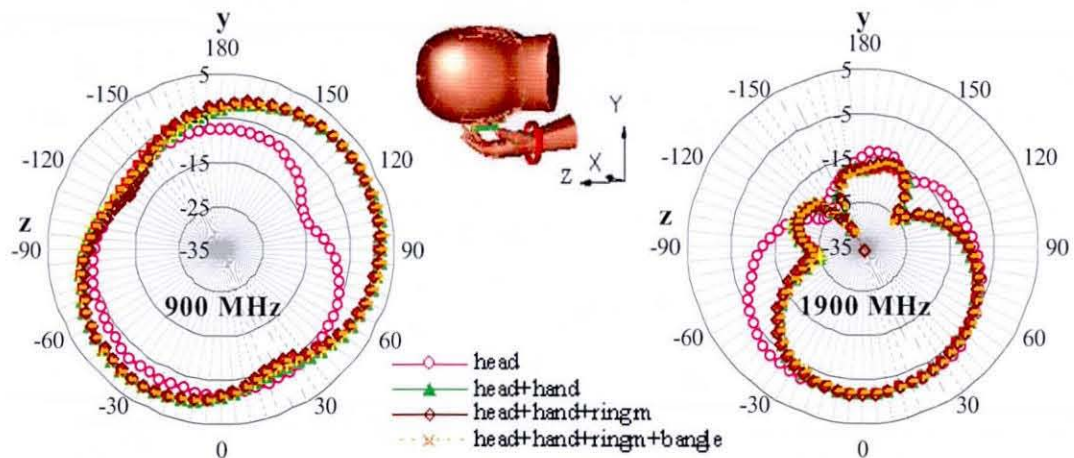

Figure 5.3-14: A PIFA radiation patterns at 900 MHz (left) and 1900 MHz (right) with and
without the head and the hand worn a ring (with and without the bangle) (yz-plane).

Figure 5.3-15 shows results of different sizes of metallic earrings on the PIFA's
radiation pattern at 900 MHz (left) and 1900 MHz (right). In all the tested cases, the
edge of the earring is pierced into the earlobe on the right hand side of the SAM head.
Figure 5.3-15 (a) shows that the inclusion of larger earrings with a diameter of 50, 80
and 90 mm notably alters the radiation pattern at 1900 MHz (when the hand is
absent); however the effect of an earring is less significant with the hand present. At
900 MHz, some variations on the patterns were observed with the smaller earrings,
but the most significant effect is observed with an earring having a diameter of 90 mm
(with and without the hand). A relatively large difference in the radiation pattern is
observed in the θ = -90° to -150° region compared to the case of just the head and just
the head and hand. Figure 5.3-15 (c) includes the same earring with the ring and
bangle worn on the hand. The combination of all three metallic jewellery items can
clearly alter the radiation pattern in a certain direction at 900 MHz but overall appears
to have less effect at 1900 MHz.
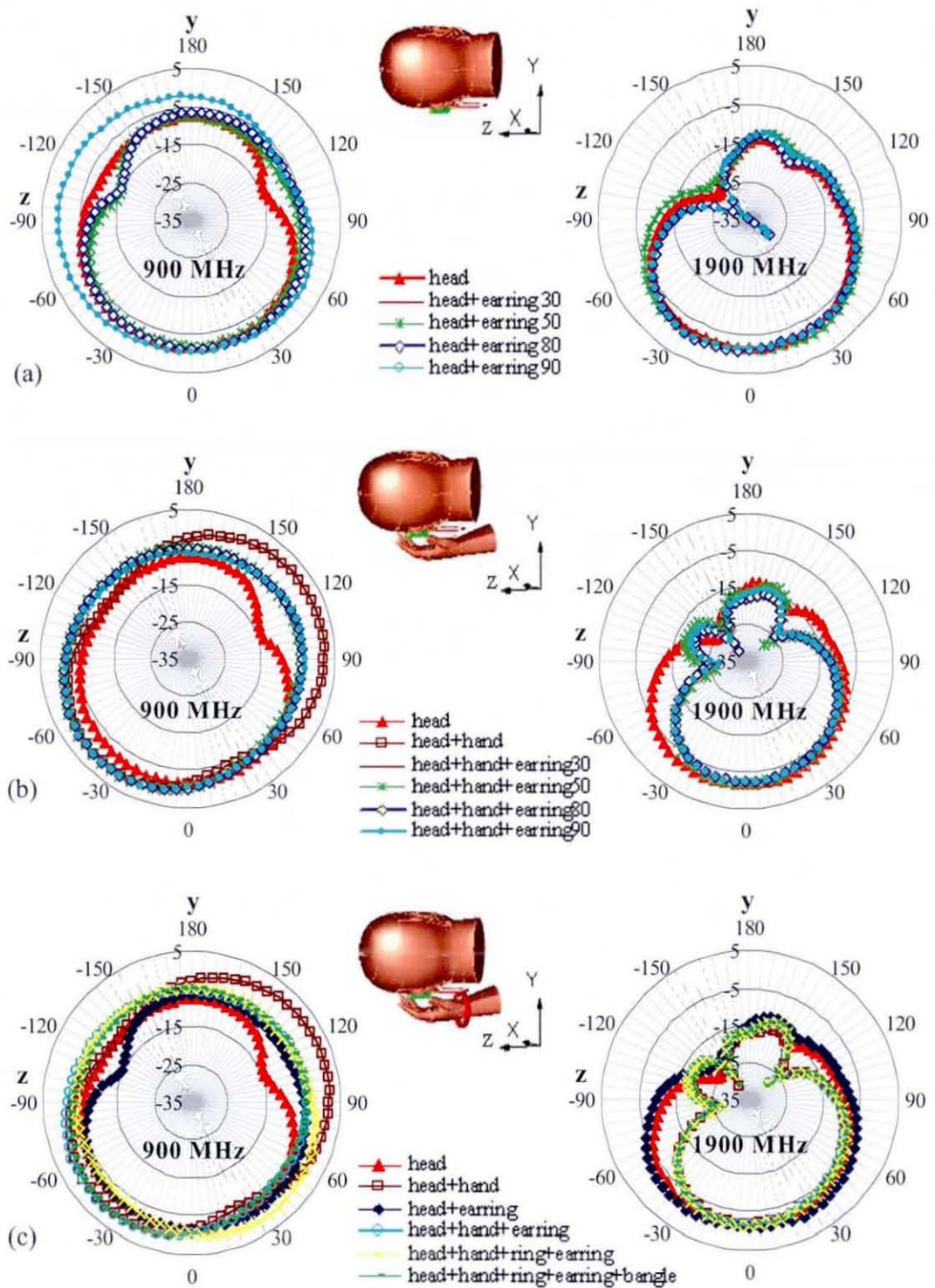
Figure 5.3-15: Radiation patterns for a PIFA antenna at 900 MHz (left) and 1900 MHz (right) when place close to the SAM head (yz-plane). The earrings penetrate the earlobe in the model (a) without the hand, (b) with the hand and (c) with the hand wearing a ring and the bangle.

Figure 5.3-16 shows the radiation efficiencies of the system when the metallic rings or
the earrings were included to the SAM head and hand model at 900 and 1900 MHz
with a monopole and a PIFA antenna as the radiating sources. Generally the radiation
efficiency of the system decreased significantly when the mobile handset was
positioned closed to the SAM head and hand. The presence of a metallic ring or an
earring alters the radiation efficiency of the system but the effect strongly dependant
on the frequency, type of antenna in use and the inclusion of the human hand. As in
Chapter 4, the metallic rings and earrings investigated in this thesis generally show
less significant effect especially when the hand is included in the simulation model.
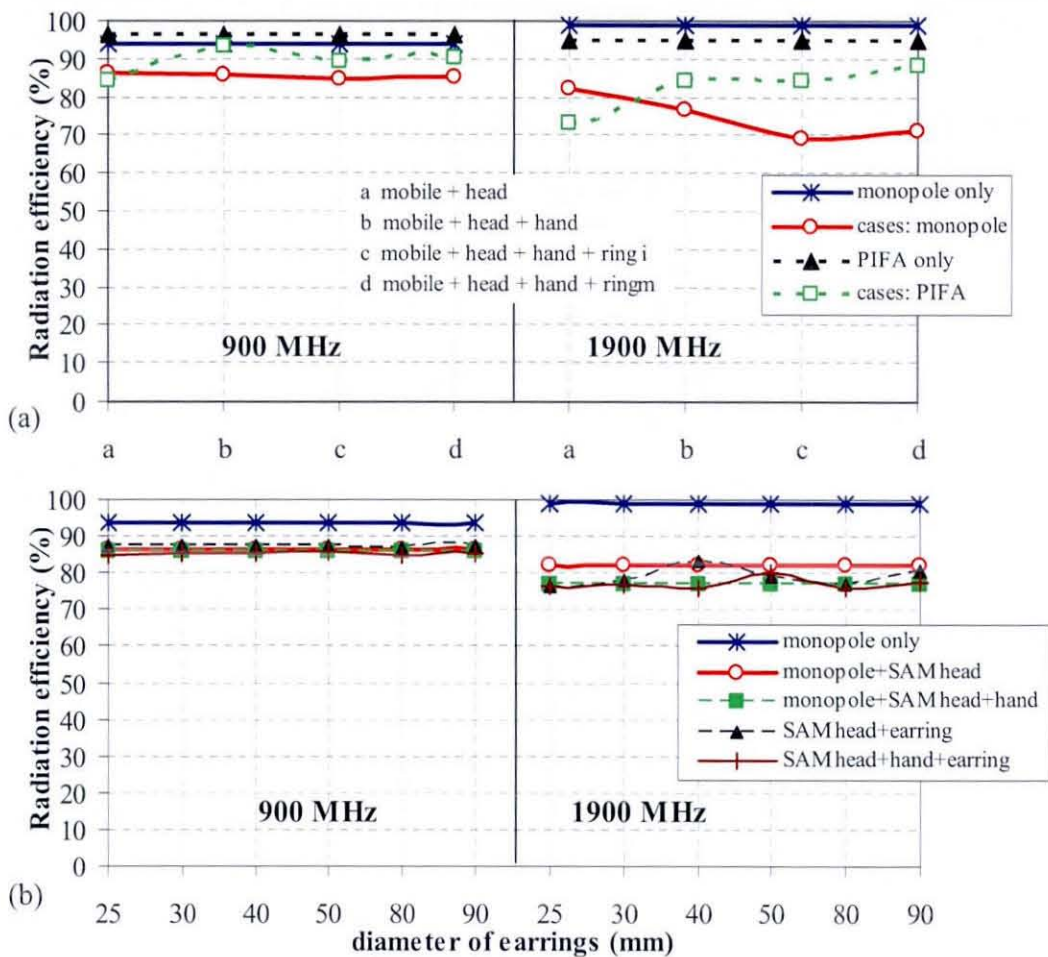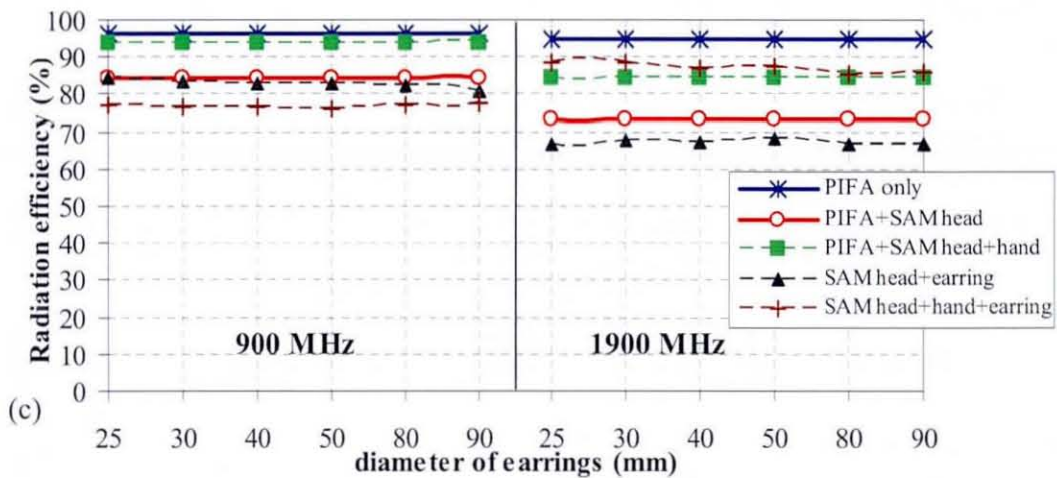
Figure 5.3-16: Radiation efficiencies for a monopole and a PIFA antenna at 900 MHz (left) and 1900 MHz (right) for the case of (a) metallic rings, and (b and c) the metallic earrings worn on the SAM head.

5.4 Conclusions

It is well known that the head and the hand have an influence on handset antenna performance and on SAR. This chapter has indicated that the metallic loop-like jewellery items worn on the head and the hand have an additional effect. However, the magnitude of influence on the results is strongly dependent on the proximity of the jewellery items to the antenna, the jewellery size and orientation relative to the antenna, the excitation frequency and the type of antenna in use. As in Chapter 4, the results in this chapter are considered novel since no other research to date has considered the presence of metallic rings (and a bangle) worn on the hand while investigating the SAR in the head and the antenna performance. In addition, the presence of the hand that holds the handset has not been reported while investigating the metallic earrings effect on SAR.

For both antennas investigated, the presence of the head has significantly altered the antenna radiation pattern along the direction of the head (y-direction) and the radiation efficiency of the system due to the significant amount of energy absorbed and reflected by the head. The hand, when added, further modifies the radiation

patterns and efficiencies at both frequencies investigated. The hand has also introduced a very strong effect into the SAR values compared to 'no hand', especially when an internal antenna was used as the radiating source. This may be due to the amount of energy absorbed and reflected at the hand dielectric boundary and since the hand is usually placed very close to the main radiating element in the PIFA antenna. This would suggest that it is important that the hand is modelled and included in evaluating the antenna radiation performance and SAR.

Neither the ring nor the bangle worn on the hand has an important effect on the monopole or the PIFA radiation pattern and efficiency at 900 or 1900 MHz due the size and orientation of the ring relative to the unit's antenna. Wearing a ring could also be beneficial since it helped to reduce the amount of energy absorbed in the head at 900 MHz. However, the ring may also increase the averaged 1 g SAR in the head particularly at the higher frequency. Larger diameter loops found in the bangle should be expected to have more significant effect due to its resonant frequency being much closer to the handset operating bands. However, the results have shown that the bangle appears to be less important due to the fact that the position of the bangle is far away from the unit's antenna.

The earrings when pierced into the earlobe can alter the antenna radiation performance, but the effect will be very variable depending on the earring diameter (especially when the earring diameter is the same or larger than 1/3 of the free-space wavelength), the type of antenna and the frequency in use, and also the presence of the hand. The earrings have a potential to increase the averaged 1 g SAR in the head by approximately 15% at 1900 MHz. The combination of the hand with an earring and a ring could decreases the averaged 1 g SAR in the head by 28% at 900 MHz and increase it by 28% at 1900 MHz when compared to just the head case. The metallic rings/earrings could potentially exhibit resonance effects and experience local enhancement of the electromagnetic field near the metallic object. However the metallic rings or earrings in this configuration appear to have no significant effects especially when a hand model was included in the simulation model.

5.5 References

[1]   L. W. Li, P. S. Kooi, M. S. Leong, H. M. Chan and T. S. Yeo, "FDTD analysis
      of electromagnetic interactions between handset antennas and human head,"
      Asia Pacific Microwave Conference, pp. 1189-1192, 1997.

[2]   D. G. Choi, C. S. Shin, N. Kim and H. S. Shin, "Design and SAR analysis of
      broadband PIFA with triple band," *Progress in Electromagnetic Research
      Symposium, PIERS2005, Hangzhou, China,* vol. 1, pp. 290-293, Aug. 2005.

[3]   M. A. Jensen and Y. Rahmat-Samii, "EM interaction of handset antennas and a
      human in personal communications," *Proceeding IEEE,* vol. 83, pp. 7-17, Jan.
      1995.

[4]   J. T. Rowley, R. B. Waterhouse and K. H. Joyner, "FDTD handset antenna
      modeling at 1800 MHz for electrical performance and SAR results," *The 2nd
      International Conference on Bioelectromagnetism, Melbourne, Australia,* pp.
      87-88, Feb. 1998.

[5]   P. S. Excell, "Modelling of handsets, antennas, heads and hands in the FDTD
      method," *IEE Colloquium on Design of Mobile Handset Antennas for Optimal
      Performance in the Presence of Biological Tissue,* pp. 7/1 - 7/4, 20 Jan. 1997.

[6]   M. F. Abedin and M. Ali, "Modifying the ground plane and its effect on Planar
      Inverted-F Antennas (PIFAs) for mobile phone handsets," *IEEE Antenna and
      Wireless Propagation Letters,* vol. 2, pp. 226-229, 2003.

[7]   3dcadbrowser. http://www.3dcadbrowser.com, (Last accessed: June 2008).

[8]   C. H. Li, E. Ofli, N. Chavannes and N. Kuster, "The effects of hand phantom on
      mobile phone antenna OTA performance," *The 2nd European Conference on
      Antenna and Propagation (EUCAP 2007),* Nov. 2007.

[9]   N. Chavannes, P. Futter, R. Tay, K. Pokovic and N. Kuster, "Reliable prediction
      of MTE performance under real usage conditions using FDTD," *Proceeding of
      ICECOM 05, Dubrovnik,* 12-14 Oct. 2005.

[10] H. Kawai and K. Ito, "Simple evaluation method of estimating local average
      SAR," *IEEE Transactions on Microwave Theory and Techniques,* vol. 52, pp.
      2021 – 2029, Aug. 2004.

[11] M. Burkhardt and N. Kuster, "Appropriate modeling of the ear for compliance
      testing of handheld MTE with SAR safety limits at 900/1800 MHz," *IEEE
      Transactions on Microwave Theory and Techniques,* vol. 48, pp. 1927 – 1934,
      Nov. 2000.

[12] IEEE std. 1528-2003, IEEE recommended practice for determining the peak-
      spatial average specific absorption rate (SAR) in the human head from wireless
      communications devices: Measurement techniques.

[13] Y. Rahmat-Samii and M. A. Jensen, "A study of the electromagnetic coupling between handset mounted antennas and a human operator," *24th European Microwave Conference, Cannes, France,* pp. 607-612, 5-8 Sep. 1994.

[14] M. Francavilla, A. Schiavoni, P. Bertotto and G. Richiardi, "Effect of the hand on cellular phone radiation," *IEE Proceedings on Microwaves, Antennas and Propagation,* vol. 148, pp. 247 – 253, Aug. 2001.

[15] L. C. Kuo and H. R. Chuang, "Design of a 900/1800 MHz dual-band loop antenna mounted on a handset considering the human hand and head effects," *Antennas and Propagation Society International Symposium, IEEE,* vol. 3, pp. 701 – 704, 2003.

[16] Z. Wang, X. Chen and C. G. Parini, "Effects of the ground and the human body on the performance of a handset," *IEE Proceeding on Microwaves, Antenna and Propagation,* vol. 151, pp. 131-134, April. 2004.

[17] S. I. Watanabe, H. Taki, T. Nojima and O. Fujiwara, "Characteristic of the SAR distributions in a head exposed to electromagnetic fields radiated by a hand-held portable radio," *IEEE Transactions on Microwave Theory and Techniques,* vol. 44, pp. 1874 – 1883, Oct. 1996.

[18] M. Lundmark, R. S. Calvo, P. S. Kildal and C. Orlenius, "A solid hand phantom for mobile phones and results of measurements in reverberation chamber," *Antennas and Propagation Society International Symposium, IEEE,* vol. 1, pp. 719 – 722, 2004.

[19] K. Ogawa, T. Matsuyoshi and K. Monma, "An analysis of the performance of a handset diversity antenna influenced by head, hand and shoulder effects at 900 MHz," *Antennas and Propagation Society International Symposium, IEEE,* vol. 2, pp. 1122 – 1125, 11-16 July. 1999.

[20] C. H. Li, E. Ofli, N. Chavannes, E. Cherubini, H. U. Gerber and N. Kuster, "Effects of Hand Phantom and Different Use Patterns on Mobile Phone Antenna Radiation Performance," *IEEE International Symposium on Antennas and Propagation, San Diego, California,* 5-12 July. 2008.

[21] J. Krogerus, J. Toivanen, C. Icheln and P. Vainikainen, "Effect of the Human Body on Total Radiated Power and the 3-D Radiation Pattern of Mobile Handsets," *IEEE Transactions on Instrumentation and Measurement,* vol. 56, pp. 2375 – 2385, Dec. 2007.

[22] W. Kainz, A. Christ, T. Kellom, S. Seidman, N. Nikoloski, B. Beard and N. Kuster, "Dosimetric comparison of the specific anthropomorphic mannequin (SAM) to 14 anatomical head models using a novel definition for the mobile phone positioning," *Physics in Medicine and Bio.,* vol. 50, pp. 3423-3445, 2005.

Chapter 6

Hand Phantom Construction and SAR Measurement Results

6.0 Introduction

This chapter aims to address the effect of the hand and metallic loop-like jewellery on SAR inside a SAM head via measurements rather than just simulations. The measurement includes a novel liquid hand phantom with realistic fingers, which allow the effect of metallic ring to be further investigated. The SAR results from the measurements will be compared to simulations.

It has already been shown that the hand does have an effect on the handset. However the aim of this chapter is to examine if these effects could have a measureable impact on a standard SAR test. In this chapter, a realistic liquid hand phantom will be presented, which has been successfully constructed and employed in SAR measurements together with a SAM head phantom. The SAR measurements presented were performed with the SPEAG DASY 4 system [1] and a replica of a mobile handset as employed in Chapter 4 and Chapter 5 was constructed and used as the radiating source. Metallic loop-like jewellery (earring and rings) made of copper are added to the experimental setups. Moreover, the effect of the metallic jewellery and the hand are examined and the measurement results are compared to the simulations.

6.1   Phantoms and metallic loops for measurements

6.1.1 The SAM head phantom

The standard measurement in evaluating SAR inside the head still relies on the homogeneous phantom. The homogeneous phantom also has the benefit that the entire volume is accessible by the measurement probe [2, 3]. Therefore, the most convenient and practical method of estimating the SAR in the head is by using a homogeneous head phantom [4, 5], which also provides better repeatability with respect to the test position than the anatomical head [3, 6].

In this chapter, the SAM head phantom will be employed (Figure 6.1-1) for SAR measurements. The standard phantom is made of fibreglass with a relative permittivity of ~3. The phantom's thickness is 2 mm over most of the interior surface, but 6 mm thick at the compressed ear location. The SAM head model is filled with the dielectric material discussed earlier in the thesis, choosing the correct material for the frequency of interest (Table 6.1-1) [1, 8].

Table 6.1-1: The dielectric properties of the simulating liquids for the head and the hand at 900 MHz and 1900 MHz [1, 8].

Frequency	900 MHz		1900 MHz	
Model	ε_r	σ (S/m)	ε_r	σ (S/m)
Head (HSL)	41.5	0.97	40	1.4
Hand (BSL)	55	1.05	53.3	1.52

Right head side   Left head side

Twin SAM head phantom   Head simulating
made of fiberglass, $\varepsilon_r = 3$ liquids (HSL)
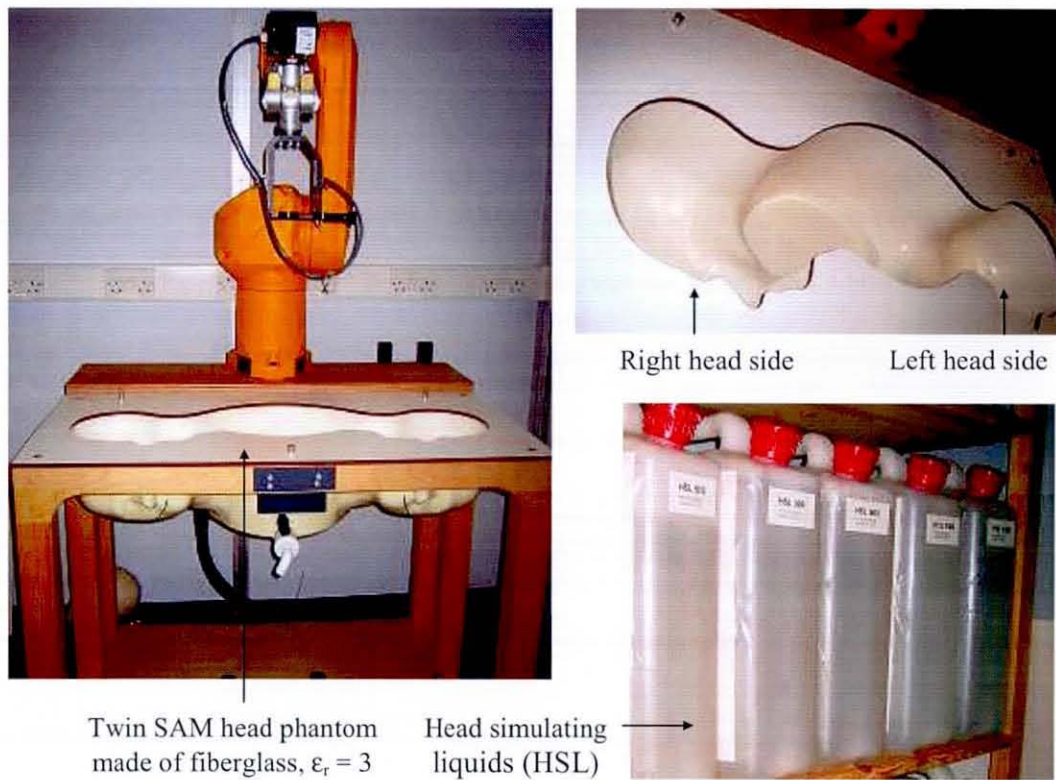
Figure 6.1-1: The SAM head phantom and the head simulating liquid (HSL) employed in the SAR measurements. Only the right head phantom was used for measurements in this chapter.

6.1.2 Hand phantom for measurement

Handsets are typically tested without a hand, which usually results in an overestimation of the SAR in the head (more energy is absorbed in the head phantom [7, 8]. A standardized hand model is not currently available due to the large number of possible finger positions and different practices of holding the handset makes it difficult to specify a standard "hand phantom". This is why the effect of the hand not been considered in [7].

As has been extensively discussed already, the hand does affect the SAR values, and yet there has been little reported research effort placed on constructing a phantom for it. There are several examples of hand phantoms, such as in [9-11]. The study in [9]

has shown a strong loss contribution by the hand. The hand phantom in this paper is made of silicone rubber loaded with carbon fibres, by Indexsar Ltd. Boyle [9] suggested that the hand phantom should be placed in various positions representing typical way of holding a mobile handset to allow an accurate phantom measurement on phone-by-phone basis. However, it is difficult to have a hand phantom that suits each mobile handset design due to physical differences in the construction.

The hand model in [10] was constructed from PVC and filled with tissue simulating liquid which is equivalent to the head tissue liquid, whilst in [12] a physical head and hand phantom have been manufactured from synthetic tissues that include some anatomical details of the head and the hand. The latest hand phantom introduced by Gabriel [11] is made of carbon-loaded silicones. However, due to the complexity of the heterogeneous phantom model, a substantial amount of research is still uses the simple homogeneous sphere head and block hand models. These simple models are more practical and can be more easily designed and compared with numerical models. Although the CENELEC [13] and the IEEE Std. 1528 [7] have not currently included the hand for the mobile phone compliance, it is interesting to evaluate how the hand presence could affect the SAR in the head [14].

In this thesis, a homogeneous hand phantom has been successfully manufactured and has been employed in the measurements representing a realistic way of holding a mobile handset (Figure 6.1-2). The sizes of the hand phantom (including the fingers) are comparable to the sizes of the hand anthropomorphic data of US Army (1991) [15]. The hand phantom construction is discussed in Section 6.1.2.1. The hand phantom is filled with the body simulating liquid (BSL), for the frequency of interest.
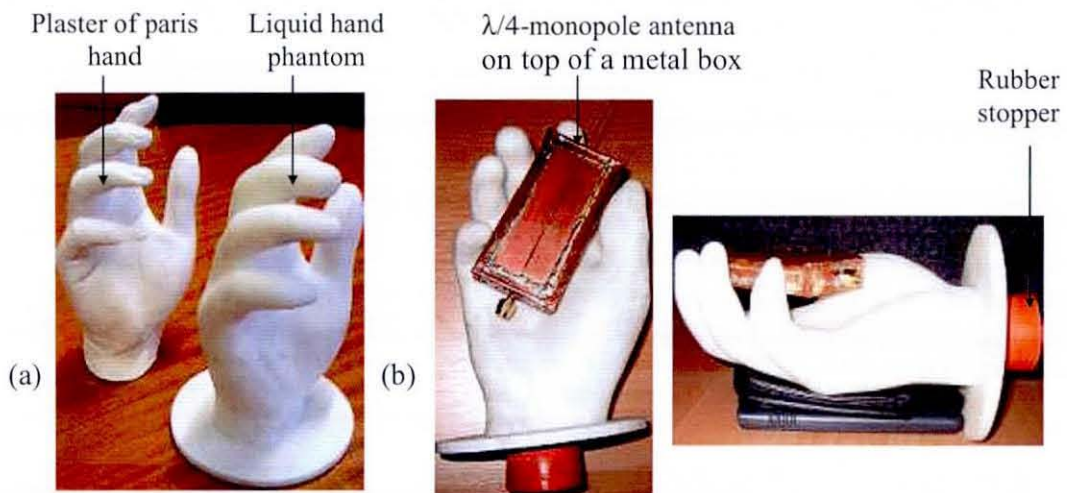
Figure 6.1-2: The (a) constructed hand phantom employed in the SAR measurements and (b) hand phantom holds the handset unit.

6.1.2.1   The hand phantom construction

To begin, the hand and finger sizes of 15 people selected randomly from the locality and of mixed gender were measured. The dimensions of each person's fingers were recorded (in Appendix D.1) and the data set was compared statistically with the US Army Hand Anthropometry (1991) [15]. An individual from the group of 15 was found to have nearly similar averages to the US Army Size set. Statistical data is presented in the Table D.3 (Appendix D.1) to support this selection. The individual agreed to have his hand cast using a two-stage process prior to digitization. The casting was essential to capture a very accurate CAD model because small movements in the hand generate errors during laser scanning.

The hand casting technique utilized dental alginate powder and Plaster of Paris. The scanning was carried out using a *Roland Picza Scanner* that was available in the Wolfson School of Mechanical and Manufacturing, Loughborough University. During the moulding process (shown in the Appendix D.2) the right hand was inserted into the alginate, whilst the left hand held a handset in a natural pose. This is very useful technique because there is no visual feedback when the hand is immersed in the alginate. Thus when the left hand strikes the intended pose, the human brain is able to

make the right hand mirror it with reasonable accuracy[*]. Following the moulding of the hand, the hand itself was extracted from the curved alginate and the cavity was filled with plaster to form a cast. The end result from the casting is shown in Figure 6.1-2. The cast hand model was scanned and the 3D data was prepared for the manufacturing process, which utilized a *Selective Laser Sintering* (SLS) machine [16]. The SLS is an additive rapid manufacturing technique that uses a high power laser to fuse together small particles of plastic, metal, or ceramic powders into a mass representing the desired 3-dimensional object. The manufactured hand phantom was made of *DuraForm Polyamide* (PA) [17] (also shown in Appendix D), nylon material with 2.5 mm wall thickness and a dielectric constant of approximately 2.9 (see Figure 6.1-2).

The manufactured hand phantom is useful since it strikes an ordinary pose of holding a mobile handset and can be used next to the head phantom. It also provides high repeatability due to its fixed shape and the ability to 'hold' the handset unit. The hand phantom also allows different simulating liquid to be applied for measuring different frequencies. In addition to that, the hand phantom includes realistic fingers, which enable the effect of the metallic ring present on SAR to be measured, which was the main motivation for its construction.

6.1.3 Metallic loop like jewellery for measurements

To allow comparison between the measurement results and the simulations, the same sizes of earrings as in Chapter 4 and Chapter 5 were adopted in the measurements. However, copper earrings with an inner diameter of 2 mm were not available during the measurements, so an inner diameter of 3 mm was used (Figure 6.1-3). The copper earring in this study is attached to the outer surface on the right hand side of the SAM

---

[*] Different person clearly have different ability to perform this. Most people find that they can perform this mirroring without practice, though it is a skill which can be improved with practice. The subject used for the model in this thesis was considered skilled.

head phantom. A metallic ring was also included in the measurements. The ring width was 5 mm, whilst its outer diameter was about 30 mm to fit with the finger of the hand phantom.
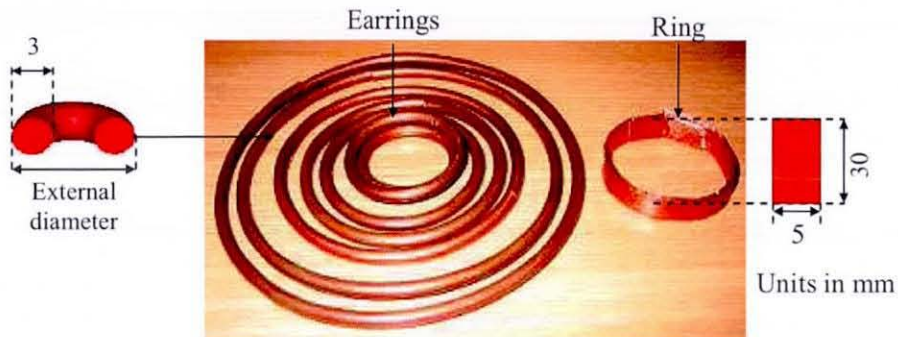
Figure 6.1-3: Copper earrings (left) and ring (right) dimensions employed in this chapter.

6.2 DASY 4 measurement system and procedures

6.2.1 The DASY 4 measurement system setup

The measurements in this study were performed by means of the DASY 4 system. This system comprises of mechanical arm to position an isotropic electric field probe inside the SAM head phantom, a shell phantom, tissue simulating liquid and software that controls the robot and processes the measured data. The DASY 4 measurement system setup is as shown in Figure 6.2-1. The highest SAR typically occurs near the surface of the SAM phantom and is not usually measurable by an electric field probe since its sensor is located 2-4 mm behind the probe tip. Therefore, an extrapolation algorithm is included in the software which enables the deepest measured points in the phantom surface to be estimated [1]. Likewise, an interpolation algorithm is also available to provide finer mesh in the measured results [1, 18]. In determining the SAR, area scans were performed with a coarse measurement grid (at least 10 mm) in order to determine the approximate location of the hot-spots or the peak SAR values. So-called zoom scans were also carried out over a much finer measurement grid at locations identified as having high SAR. The output of the process was a set of 1 g or

10 g averaged SAR values. The DASY4 measurements were evaluated and the results visualized with the SEMCAD, post-processor software.

Electro-optical converter (EOC) box

Data acquisition electronics (DAE)

Robot arms

Dosimetric probe

Server

Twin SAM phantom

DASY4 software and SEMCAD post processing tools
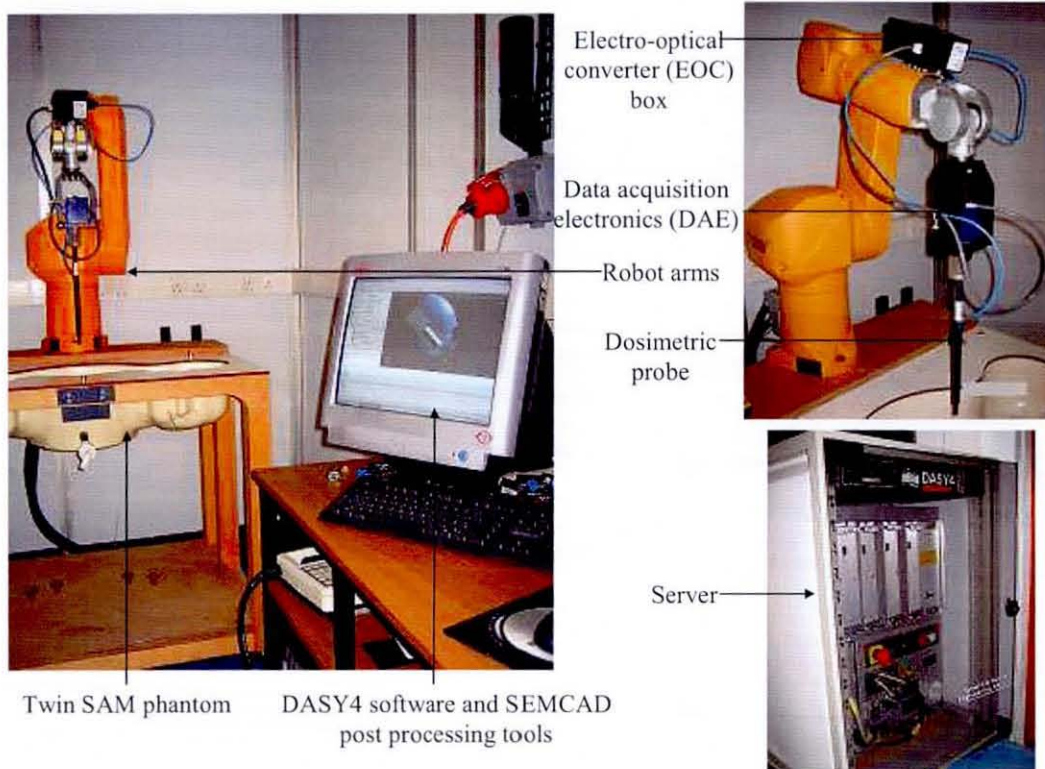
Figure 6.2-1: The DASY 4 measurement system setup [1].

6.2.2 Measurement procedures

In this chapter, a replica of a mobile handset as employed in Chapter 4 and 5 is developed with a $\lambda/4$ monopole antenna fed at its center on top of a conducting box (see Figure 6.2-2 (a)). The antenna was powered by a CW source at both 900 MHz and 1900 MHz and the amplitude of the input power was measured using a power meter prior to each measurement being performed. In this work, the handset antenna is placed in the 'cheek' position as ordinarily used amongst the majority of users (see Figure 6.2-2 (b)) [7, 13, 19]. In order to investigate the effect brought about by the metallic earring worn on the ear, a metallic loop (of different diameters) as discussed in Section 6.2 was attached to the edge of the ear (see Figure 6.2-2 (c)), representing a realistic condition of human wearing an earring. Note that at this stage no hand

phantom was in place. Cotton threads and a clear sticky tape were used to attach the loop. The amount of additional material was kept to an absolute minimum to minimize any detuning effects. In the latter measurements, the manufactured hand phantom was included in order to investigate what effects the hand may have on SAR values inside the head (with or without an earring).

In the next set of measurements the hand phantom was placed underneath the head and holds the handset (see Figure 6.2-3). In addition to that, each of the finger positions beneath the phantom surface was marked to ensure that the hand was at the same position throughout the measurements. Meanwhile, the effect of the metallic ring worn on the human finger was also investigated (with or without the earring). The metallic ring was placed on different fingers for comparison.
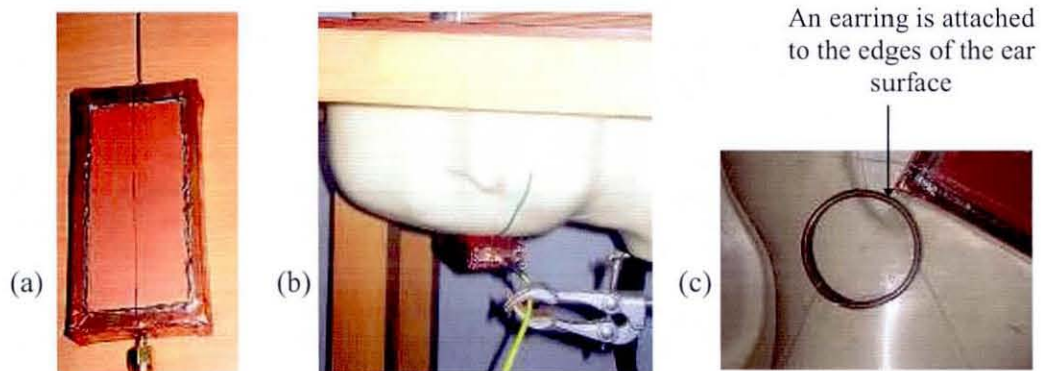
Figure 6.2-2: (a) The handset antenna model employed in the measurements, (b) the handset placed in the cheek position beneath the head phantom and (c) the earring attached at the edges of the outer ear surface on the phantom.

(a)   (b)

Metallic ring

(c)

Marked with points to
ensure the hand was
placed at the same
position throughout the
measurements
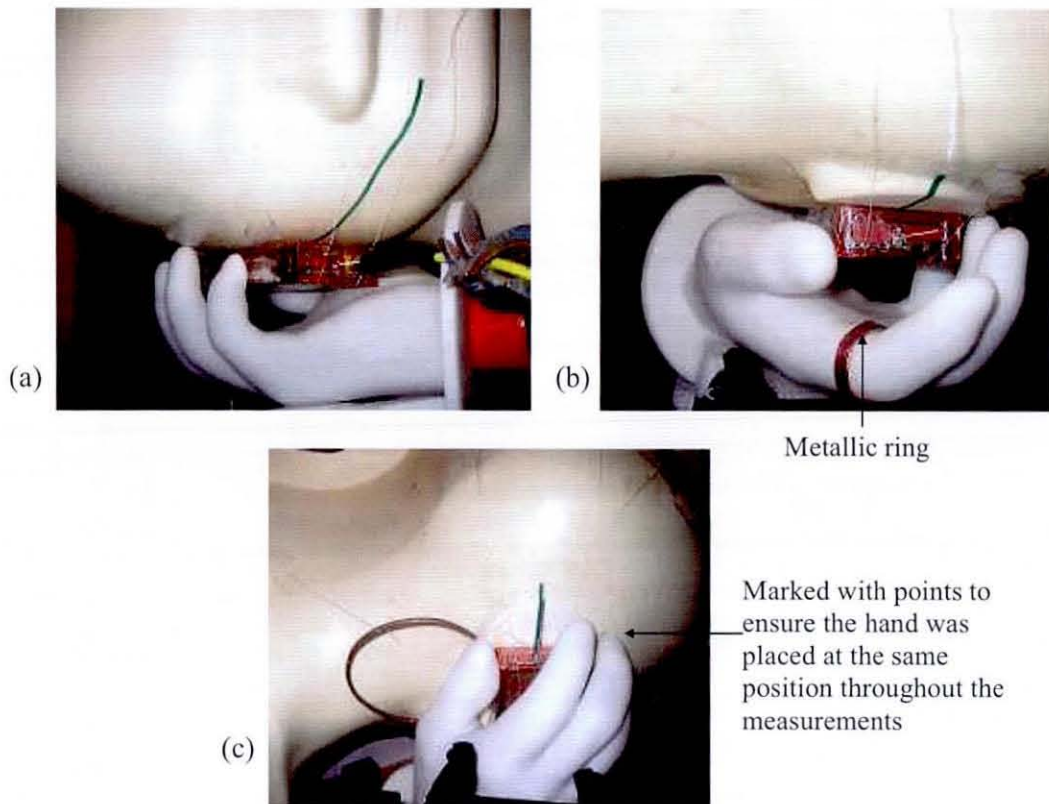
Figure 6.2-3: The measurements scenarios: (a) the hand phantom filled with body simulating liquid (BSL) was placed underneath the head holding the handset, (b) a metallic ring worn on the index finger and (c) the earring attached at the edge of the ear surface with the presence of the hand. In all cases, the head was filled with head simulating liquid (HSL).

6.2.3 SAR measurement results

The $\lambda/4$ antenna was fed at its center by a CW source at both 900 MHz and 1900 MHz. The recorded SAR values were normalized to 0.25 W and 0.125 W at 900 MHz and 1900 MHz respectively. The simulations results were also included in the figures for comparison with the measurements.

Figure 6.2-4 shows the effect of metallic earrings on the averaged 1 g SAR in the head at 900 MHz. Generally, the trend of the effect of the metallic earrings is in reasonably good agreement with the simulation results. However, there are

discrepancies between the two results in which the amplitude of the simulated averaged 1 g SAR in the head is more than twice the measured averaged 1 g SAR value. This difference was expected since the head model employed in the simulation does not include the outer dielectric shell, so the handset body was positioned in very close proximity to the head surface (see Figure 6.2-7 (a)). With this geometry, the simulated SAR in the head will be higher than the measurement. Hence, small variation in the distance (as small as 1 or 2 mm) between the antenna and the head could change the SAR values quite significantly [4, 5].
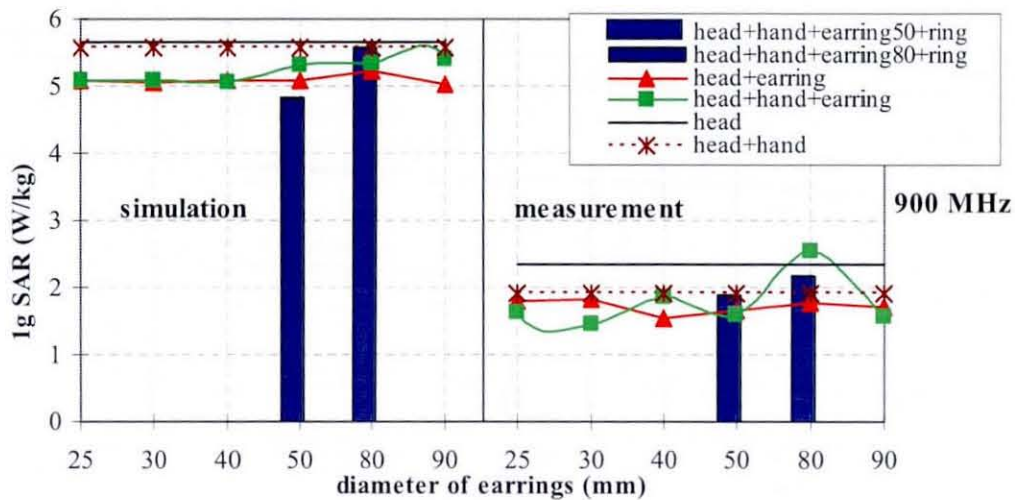
Figure 6.2-4: The simulations and measurement results of the averaged 1 g SAR in the head, with or without the hand and the jewellery at 900 MHz.

Figure 6.2-4 also includes the effect of the hand, the earring and the ring. The hand by itself with the earrings, regardless of the earring diameter, decreases the averaged 1 g SAR in the head if compared to the case of just the head. Generally, the hand when added to the head-earring model decreases the averaged 1 g SAR in the head. However, there are discrepancies between the measured and simulated results incorporating the hand phantom, which will be explained in Section 6.2.4 later. In addition, it is good to simulate the same model as the measurement setup. However this procedure cannot be performed due to the difficulties and limitation of handling the same models in different software packages (Microstripes vs SEMCAD).
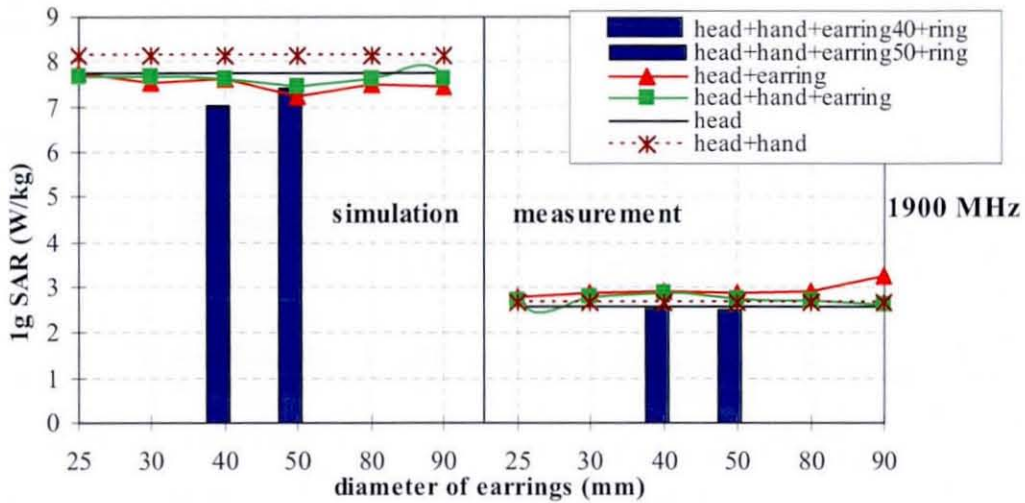
Figure 6.2-5: The simulation and measurement results of the averaged 1 g SAR in the head, with or without the hand and the jewellery at 1900 MHz.

Figure 6.2-5 shows the head, the hand and metallic jewellery effect on the averaged 1 g SAR in the head at 1900 MHz. As at 900 MHz, the magnitude of the simulated averaged 1 g SAR in the head is more than twice the measured one. The hand notably increases the averaged 1 g SAR values in the head compared to the 'no hand' case, which is in good agreement with the simulation results. Conversely, there are some differences between the measurements and the simulations on the effects of the earring with or without the hand. The earrings reduce the averaged 1 g SAR in the head in the simulations but increase it in the measurements. However, the trend of increased SAR at 1900 MHz can be seen on the simulated peak SAR values in the previous chapter (see Figure 5.3-6), while the averaged 1 g SAR showed no increase. The SAR is locally enhanced in close proximity to where the earring pierces the earlobe, but no important enhancement is observed deeper in the head. In addition, the difference of the antenna-dielectric and the earring-dielectric distance between the measurement and simulation model can also affect the earring response to the electromagnetic field radiated by the antenna.

Comparing the effects of the metallic ring worn on the hand on the averaged 1 g SAR in the head (see Figure 6.2-6), shows a good agreement, particularly on the trend. The difference on the amplitude is similar as been discussed above. The inclusion of the hand decreases the averaged 1 g SAR in the head at 900 MHz, but increases it at 1900 MHz. Figure 6.2-6 also shows that the hand wearing a ring in this configuration can notably decrease the averaged 1 g SAR in the head at both frequencies investigated.
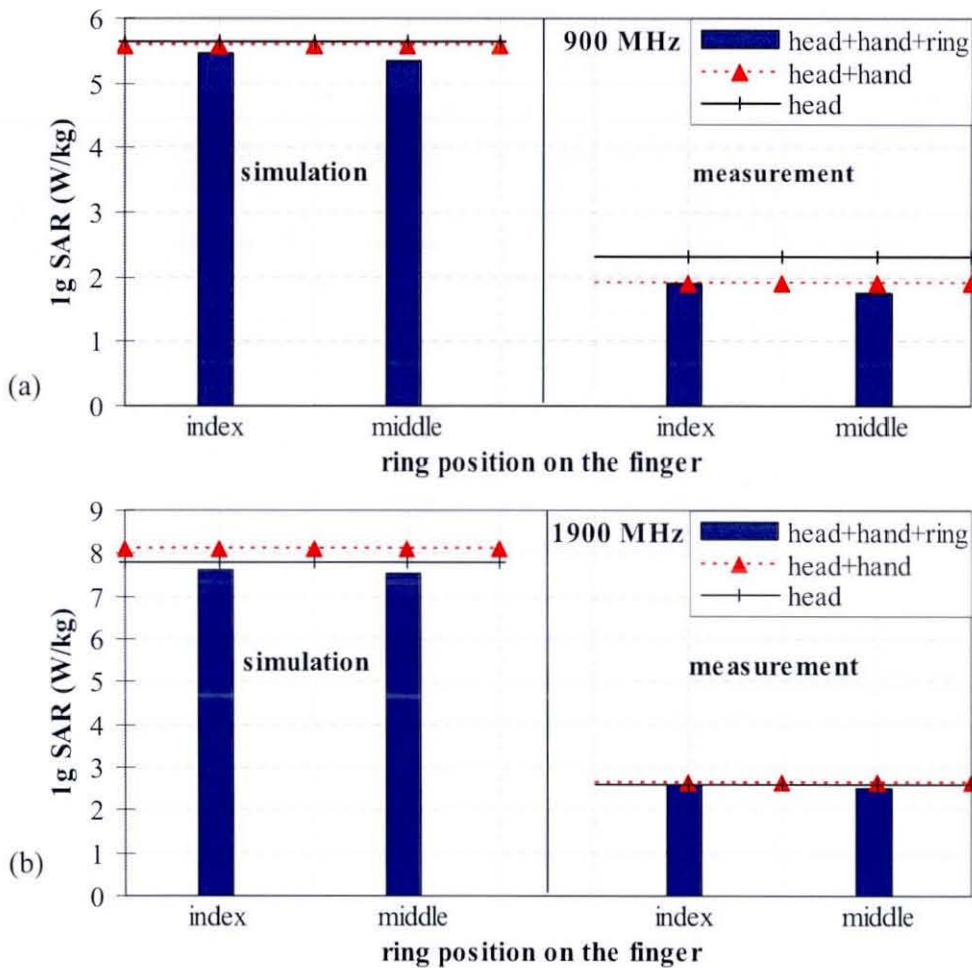
Figure 6.2-6: Simulation and measurement results of the averaged 1 g SAR in the head, with and without the hand, the ring and the combination of both an earring worn on the ear and a ring worn on the hand at (a) 900 MHz and (b) 1900 MHz.

6.2.4 Measurement result discussions

In general, the trend of the effect of the hand, the earring and the ring shows agreement with the simulations at 900 MHz (see Figure 6.2-4 and Figure 6.2-6). However, there are significant differences on the amplitude of the averaged 1 g SAR between the two methods which are worthy of further investigation. The simulated averaged 1 g SAR values in the head were higher than the measured values by more than 50%. The differences in the measurement results are more pronounced at 1900 MHz compared to 900 MHz. The discrepancies between both methods are often due to the uncertainty related to SAR measurements [20].

There are differences between the geometry of the head, the hand and the jewellery models employed in both methods. There are also large differences between the simulation and the measurement in terms of the distance between the antenna-head, antenna-hand and antenna-head-jewellery. The SAM head model employed in the simulations does not include any outer shell and thus the handset body is oriented in the cheek position and placed very close to the compressed ear (see Figure 6.2-7 (a)). However, the SAM head phantom employed in the measurements includes 2 mm shell thickness with about 6 mm shell thickness on the compressed ear region (Figure 6.2-7 (b)), which separates the handset antenna from the simulating liquid.

Additionally, the size of the hand phantom employed in the measurements was bigger than the simulation model due to the inclusion of around 2.5 mm thick wall on the hand phantom; but no outer shell was included in the simulation model. The hand phantom shape was also not as similar as the simulation model; so this causes the fingers position of the hand phantom relative to the antenna differs slightly compared to the simulation. Nevertheless, the hand phantom used in the measurement at 900 MHz was filled with BSL of 1900 MHz because the body fluid of 900 MHz is currently not available in the lab. This different may has an effect on the SAR value since the dielectric properties of the liquid were different for different frequency.

In addition to that, the metallic earring employed in the simulations has 2 mm of internal diameter and was pierced directly into the earlobe (dielectric). Otherwise, the earring in the measurements was 3 mm of internal diameter (see Figure 6.1-3) and was attached (not pierced) to the outer surface of the phantoms' ear, which was about 6 mm distance from the liquid. Although the earring thickness does not show important effect on the SAR results in Chapter 3, the separation distance between the earring and the dielectric employed in the measurements may modify the current distribution on the surface of the metallic earring, thus influencing the earring response to the field radiated from the antenna, which may therefore affect the SAR values.
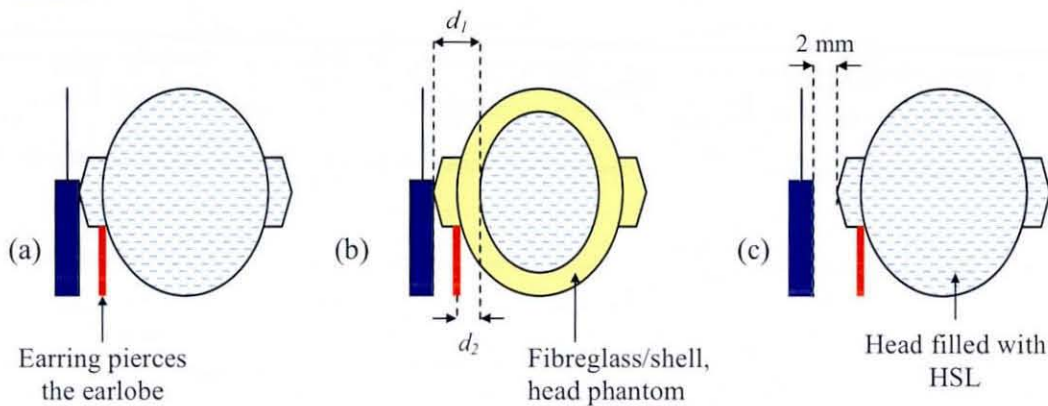
Figure 6.2-7: Simplified representation of the geometry employed in the (a) simulation in Chapter 4 (spherical head) and Chapter 5 (SAM head), (b) measurement (SAM head phantom) and (c) modified simulation with 2 mm gap. d_1: shell thickness at the compressed ear region, d_2: shell thickness of 2 mm.

Moreover, analysis on the results of the peak SAR distribution at 900 MHz revealed that the simulated peak SAR occurs behind the ear, but the peak SAR in the measurement was found behind the ear and the cheek on which the handset-antenna was placed. This may therefore lead to the difference in the maximum SAR values found between the two methods that can also alter averaged SAR results. Thus, the above mentioned differences could cause discrepancies in the results, as these factors may affect the coupling, the way the metallic jewellery interact and response to the electromagnetic field, which results in different SAR results.

6.2.5 Further simulations

The results in previous section show discrepancies between the simulation and the measurement results. In order to allow comparison with the measurements, further simulations were performed by modifying some details on the models employed in the simulations. In this section, the same SAM head and realistic hand model were used, but the head was translated by 2 mm in y-direction, so that there was a more representative 2 mm gap between the head-handset models. The earring of 3 mm diameter was also placed at 2 mm distance from the head surface and was not inserted into the dielectric as in the previous simulation models (Figure 6.2-8). The hand model at 900 MHz was given the properties of muscle at 1900 MHz (as employed in the measurements), whilst the dielectric for the hand model at 1900 MHz remains the same as in the earlier simulations. However, the same hand model (as in earlier simulations) was used in the following investigation and no outer shell was added to the hand model. There were problems producing an analysis model from the available CAD data, but at least the model produced (with 2 mm gap between the head-antenna) was better than before.
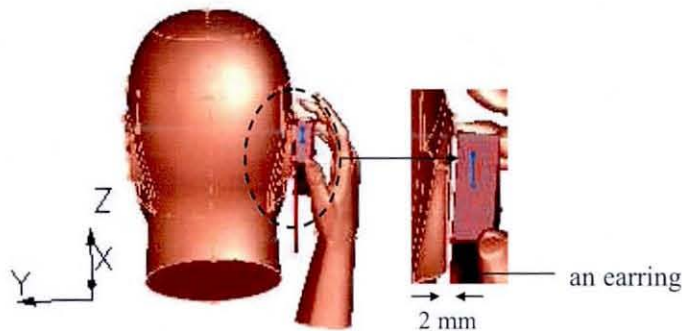
Figure 6.2-8: The hand holds the handset at 2 mm distance from the ear surface. An earring is also place at 2 mm distance from the ear considering the shell thickness of the head phantom in the measurements.

Figure 6.2-9 represents results of the modified simulation model (2 mm gap) and the effect that the hand and the jewellery may have on the averaged 1 g SAR inside the head. The lines with solid symbols represent the measurement results, whilst the simulation results (with 2 mm gap) are represented by the lines with hollow symbols.

Generally, the simulations (modified model) show good agreement with the measurement results, at both 900 and 1900 MHz (see Figure 6.2-9). The trend and the amplitude of the averaged 1 g SAR in the head, considering the effect of the hand and the metallic earrings looks reasonable. At 2 mm distance from the dielectric, an earring with a diameter of about $1/4$-λ of the corresponding frequencies (900 MHz) significantly increased the averaged 1 g SAR in the head. The hand when added into the simulation further modified the averaged 1 g SAR but the effect was varied with the diameter of an earring being worn.

The simulations with the modified model (Figure 6.2-9) compared to the previous model (Figure 6.2-4 to Figure 6.2-5) have shown that the proximity of the head and the metallic jewellery to the radiating source is very significant. Certain sizes of earring may significantly increase the averaged 1 g SAR when its diameter is close to resonance and when it is placed at certain distance from the head-antenna. Although the simulation results of the modified model show better correlation with the measurements, there are still discrepancies between the simulations and the measurements. Possible reasons for these differences are the head-antenna and earring-head distance (2 mm in the modified model vs. 6 mm in the measurement), the hand model geometry (with/without the outer shell) and also the computational cell sizes employed in both methods. The cell sizes employed in the measurement is different from the simulations. In the simulation a cell size of at least $\lambda min^{\dagger}/10$ was set inside the head and hand, and smaller cell sizes were considered in the antenna and the metallic jewellery region. Otherwise in the DASY4 measurements 10 mm and 5 mm grid step size were used for the area scan and the zoom scan respectively. Thus due to this difference, the maxima point determined in the simulation may not being scanned by the probe and yet may produces different averaged SAR results.

---

† λ_{min} is the wavelength within the dielectric material that having the highest permittivity (dielectric constant).
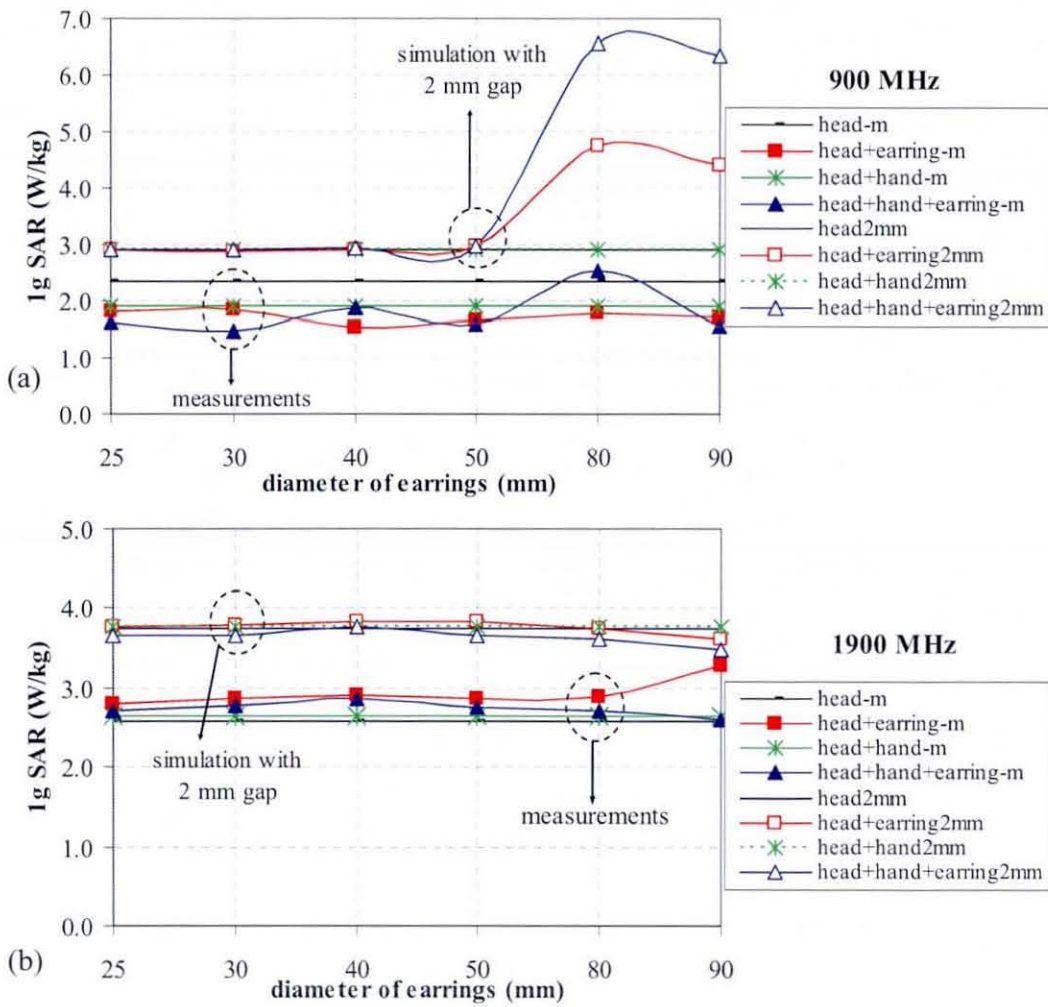
Figure 6.2-9: The averaged 1 g SAR in the head by the presence of the hand and metallic earring at (a) 900 MHz and (b) 1900 MHz. The head is at 2 mm distance from the handset body.

Figure 6.2-10 shows the peak SAR distribution of the modified simulation models (with 2 mm gap between the head-handset). Figure 6.2-10 show good agreement with the distribution obtained from the measurement (as discussed in Section 6.2.4), where the peak SAR was found behind the ear and on the cheek region with no earring. An earring, when present, enhanced the SAR values near to the region where the earring is placed. The hand when added to the head-earring model notably changed the peak SAR distribution due to the absorption and reflection at the hand dielectric boundary.

900 MHz   **1900 MHz**

(a)   Maximum SAR
                       occur at the back of
                       the ear and on the
                       cheek area where
                       the handset-antenna
                       is placed

(b)

(c)   SAR is enhanced at
                       the edge of the ear
                       that is close to the
                       place where the
                       earring is placed

(d)

Figure 6.2-10: The simulated SAR distribution inside the head for the modified simulation models at 900 MHz (left) and 1900 MHz (right); (a) head only, (b) head with hand, (c) head worn earring without the hand and (d) head worn earring with the hand present. A monopole antenna was used as the radiating source.

6.3 Conclusions

In this chapter, a realistic liquid hand phantom has been successfully constructed representing a realistic way of holding a mobile handset and employed in the SAR measurements together with the SAM head phantom. The manufactured hand phantom is advantageous since it strikes an ordinary pose of holding a mobile handset next to the head phantom. It also provides high repeatability due to its fixed shape and the ability to hold most the handset unit. In addition to that, the hand phantom also allows different simulating liquid to be used. It also includes realistic fingers, which enable the effect of the metallic ring present on SAR to be measured.

This chapter has compared the measurement results with two sets of simulations. No direct comparison between both methods can be fully investigated due to inherent modelling limitation, the discrepancies due to the uncertainty related to SAR measurements and additional factors as have been discussed in Section 6.2.4 and Section 6.2.5. The results showed that the metallic earring increased the averaged 1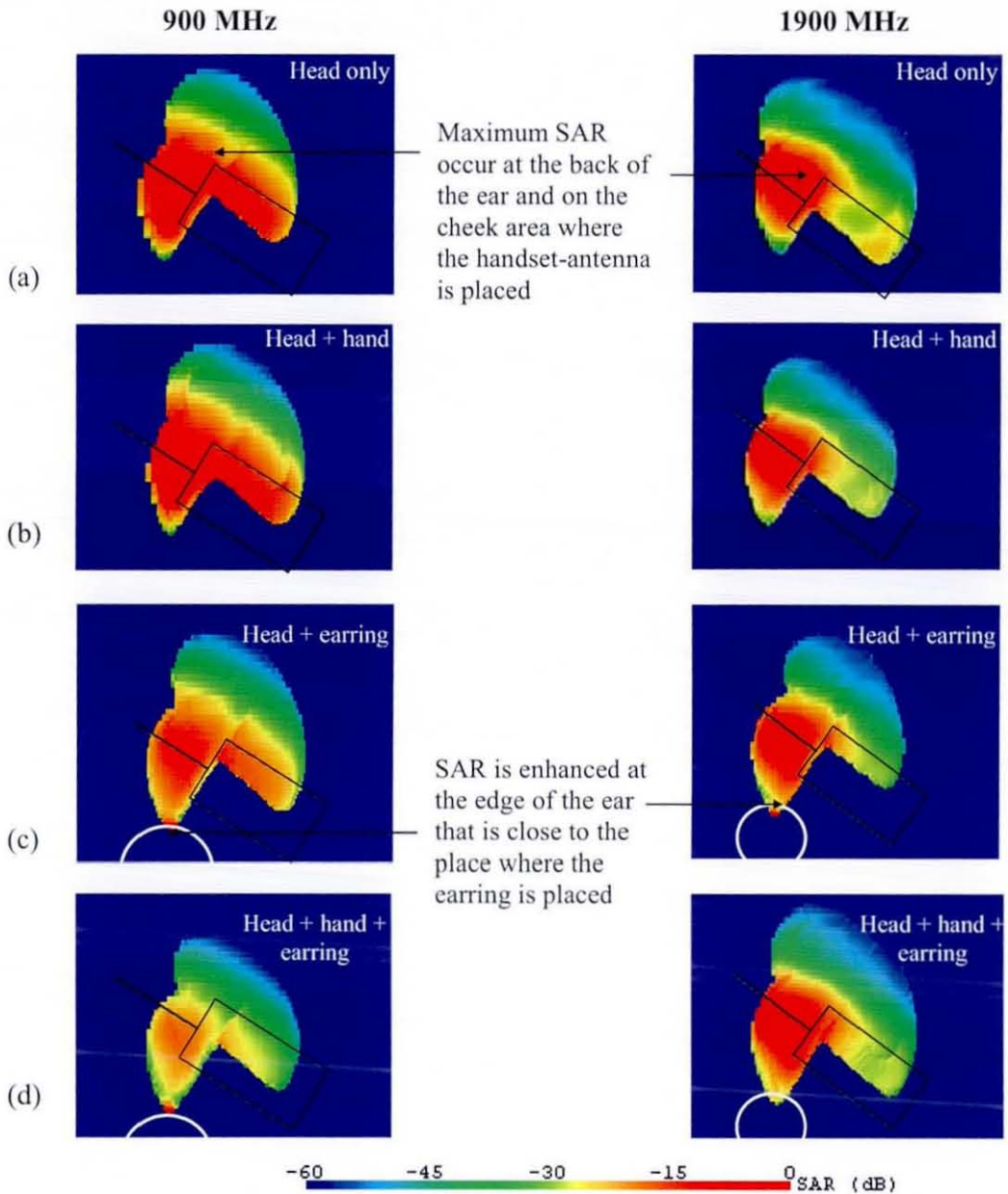 g SAR by 60% when its diameter is around 1/4 of the free space wavelength. However, the effect of metallic earring on SAR is highly dependent on its position relative to the head, the head-antenna distance and the presence of any additional objects in close proximity (i.e. hand, ring) especially at higher frequency. The hand, when added to the model, tends to increase or decrease the SAR depending on the frequency. There is good agreement between measurement and computer model. Wearing a metallic ring on the finger seems to be advantageous as it is appears to decrease the averaged 1 g SAR in the head. This supports the conclusions in Chapter 4 and 5.

Care should be taken when modelling the handset, the head, the hand and the metallic objects. The distances between these subjects to the radiating source are very important, since small differences in the distance may significantly alter the SAR. For example, the introduction of just 2 mm gap between the head-antenna and head-earring appears to lead to more than 50% difference in the results, and could also affect the metallic jewellery behavior and response to the electromagnetic energy radiated from the antenna.

6.4   References

[1]   SPEAG, "DASY4 System Handbook, V4.5," *Zurich, Switzerland,* 2005.

[2]   H. Kawai and K. Ito, "Simple evaluation method of estimating local average SAR," *IEEE Transactions on Microwave Theory and Techniques,* vol. 52, pp. 2021 – 2029, Aug. 2004.

[3]   M. Burkhardt and N. Kuster, "Appropriate modeling of the ear for compliance testing of handheld MTE with SAR safety limits at 900/1800 MHz," *IEEE Transactions on Microwave Theory and Techniques,* vol. 48, pp. 1927 – 1934, Nov. 2000.

[4]   B. B. Beard and W. Kainz, "Review and standardization of cell phone exposure calculations using the SAM phantom and anatomically correct head models," *BioMedical Engineering Online,* pp. 1-10, 2004.

[5]   B. B. Beard, W. Kainz, T. Onishi, T. Iyama, S. Watanabe, O. Fujiwara, J. Wang, G. Bit-Babik, A. Faraone, J. Wiart, A. Christ, N. Kuster, A. K. Lee, H. Kroeze, M. Siegbahn, J. Keshvari, H. Abrishamkar, W. Simon, D. Manteuffel and N. Nikoloski, "Comparisons of computed mobile phone induced SAR in the SAM phantom to that in anatomically correct models of the human head," *IEEE Transactions on Electromagnetic Compatibility,* vol. 48, pp. 397 – 407, May. 2006.

[6]   A. K. Lee, H. D. Choi, J. I. Choi and J. K. Pack, "The scaled SAM models and SAR for handset exposure at 835 MHz," *MTT-S International Microwave Symposium Digest, IEEE,* pp. 1323-1326, 12-17 June. 2005.

[7]   IEEE Std. 1528-2003, IEEE Recommended Practice for Determining the Peak-Spatial Average Specific Absorption Rate (SAR) in the Human Head from Wireless Communications Devices: Measurement Techniques.

[8]   D. L. Means and K. W. Chan, "Evaluating compliance with FCC guidelines for human exposure to radiofrequency electromagnetic fields-Additional information for evaluating compliance of mobile and portable devices with FCC limits for human exposure to radiofrequency emissions," *Supplement C (Edition 01-01) to OET Bulletin 65, Office of Engineering and Technology FCC, Washington DC,* June. 2001.

[9]   K. R. Boyle, "The performance of GSM 900 antennas in the presence of people and phantoms," *Twelfth International Conference on Antennas and Propagation, (ICAP 2003),* vol. 1, pp. 35 – 38, 31 Mar.-3 Apr. 2003.

[10] M. Lundmark, R. S. Calvo, P. S. Kildal and C. Orlenius, "A solid hand phantom for mobile phones and results of measurements in reverberation chamber," *Antennas and Propagation Society International Symposium, IEEE,* vol. 1, pp. 719 – 722, 20-25 June. 2004.

[11] C. Gabriel, "Tissue equivalent material for hand phantoms," *Physics in Medicine and Bio.,* vol. 52, pp. 4205-4210, 2007.

[12] C. Gabriel, "Phantom models for antenna design and exposure assessment," *IEE Colloqium on Design of Mobile Antennas for Optimal Performance in the Presence of Biological Tissue,* pp. 6/1-6/5, Jan. 1997.

[13] CENELEC. 2000. EN 50361, Basic Standard for the measurement of specific absorption rate related to human exposure to electromagnetic fields from mobile phones (300 MHz-3GHz), *European Standard, Brussels.*

[14] M. Francavilla, A. Schiavoni, P. Bertotto and G. Richiardi, "Effect of the hand on cellular phone radiation," *IEE Proceedings on Microwaves, Antennas and Propagation,* vol. 148, pp. 247 – 253, Aug. 2001.

[15] T. M. Greiner. (Dec. 1991, Hand anthropometry of U.S. army personnel. *Army Natick Research Development and Engineering Center, MA,* http://handle.dtic.mil/100.2/ADA244533. (Last accessed: .Jan. 2009).

[16] SLS system by 3D systems, http://www.3dsystems.com/products/sls/index.asp. (Last accessed: Jan. 2009).

[17] Mar. 2005, DuraForm PA & GF plastics for use with all SLS systems, http://www.acucast.com/pdf/DS-DuraForm_LS_mat-US_Engl_0405.pdf. (Last accessed: Jan. 2009)

[18] J. Fayos-Fernandes, C. Arranz-Faz, A. Martinez-Gonzalez and D. Sanchez-Hernandez, "Effect of pierced metallic objects on SAR distributions at 900 MHz," *Bioelectromagnetics,* vol. 27, pp. 337-353, 2006.

[19] W. Kainz, A. Christ, T. Kellom, S. Seidman, N. Nikoloski, B. Beard and N. Kuster, "Dosimetric comparison of the specific anthropomorphic mannequin (SAM) to 14 anatomical head models using a novel definition for the mobile phone positioning," *Physics in Medicine and Bio.,* vol. 50, pp. 3423-3445, 2005.

[20] A. Schiavoni, P. Bertotto, G. Richiardi and P. Bielli, "SAR generated by commercial cellular phones- Phone modeling, head modeling and measurements." *IEEE Transaction on Microwave Theory and Techniques,* vol. 48, pp. 2064-2071, 2000.

Chapter 7

Conclusions

7.0 Introduction

This thesis has investigated the interaction between the handset antennas and the human head, the hand and also additional metallic jewellery items worn on the human head and hand. The thesis provides details of the research topic by mean of computer simulations and measurements. In this chapter, the completed works are summarized and some suggestions are presented for future research.

7.1 Summary of research and results

This thesis has investigated the effect of the human hand and metallic jewellery items on SAR and on the antenna radiation performance over two different frequencies. In Chapter 3, the capability and accuracy of Microstripes in dealing with the interaction between the antenna, the human and metallic loop-like jewellery items has been validated against the published results of other commercialized simulating software (FDTD). Good agreement was observed between both methods, thus provides evidence that TLM is suitable to estimate the interaction between the antenna, the head/hand and metallic jewellery items. The effects of different sizes, orientations, and distances of the metallic loop-like jewelery items relative to the monopole antenna on a cubic phantom were investigated. The effect of different metal properties was also investigated. Based on the results, it can be concluded that metallic loops have additional influence on SAR in the phantom (beside the effect of the human head and hand). However, the effect is highly dependent on their size, orientation and distance relative to the unit's antenna, the frequency and the type of antenna in use.

The effect of the metallic loop is not strongly dependent on the material of the loops. The metallic ring placed behind the antenna does seem to alter the mass averaged SAR, although the effect is quite small.

The effect of metallic jewellery items on SAR and on the antenna performance have been further investigated utilizing a simple homogeneous spherical head and a block hand models in Chapter 4, whilst a more realistic head (SAM) and hand models were employed in Chapter 5. A $\lambda/4$ monopole antenna on top of a metal box has been used as the radiating source in both chapters; a dual-band PIFA was also included in Chapter 5 for comparison to the monopole. Different diameters of earrings were considered and the ring was placed on different fingers for comparison.

7.1.1 Effects on SAR

This thesis has shown the effect of the two different hand geometries on SAR and on the antenna radiation patterns (of a $\lambda/4$ monopole and a PIFA antennas). The effect of the hand position relative to the antenna was also investigated using a homogeneous block hand model. The averaged 1 g SAR inside the hand was significantly increased when the hand shaded part of the antenna, however this particular position, would be quite an unusual and inconvenient operating position. In ordinary use position, the hand notably decreases the SAR in the head at 900 MHz due to the energy absorption. However, the hand increases the SAR at 1900 MHz and this is partly explained by the reflection at the hand-dielectric boundary.

In addition, the hand models in this thesis include fingers which enable the effect of metallic rings to be examined. The rings can notably alter the SAR in the hand itself, therefore could also affect the SAR inside the head. Note that the effect of the ring on the SAR values inside the hand and the head has not been previously reported in the literature. For both the head models considered, metallic rings can both increase or decrease the SAR inside the head depending on the frequency of excitation and the type of antenna in use. Generally, results indicate that metallic rings decrease the averaged 1 g SAR in the head by more than 5% at 900 MHz when compared to the

'no ring' case. Larger diameter loops found in the bangle should be expected to have more significant effect due to resonant frequency being more likely to be much closer to the handset operating bands. However, the results have shown that the bangle appears to be less important due to the fact that the bangle is positioned a significant distance away from the unit's antenna.

The effects of metallic earrings worn on the ear are presented for different sizes of earrings. The effect of metallic earrings has been found to be very dependent on the earring's position relative to the head model, the frequency of excitation and the type of antenna in use. Note that the effect of pierced earring on the SAM head is very different to the effect of the attached earring on the spherical head model. Considering an ordinary worn condition (pierced earrings), results indicate that the earrings in this configuration decreased the averaged 1 g SAR in the head at 900 MHz but the amplitude is dependent on the earrings diameter. The earrings also have the potential to increase the highest SAR figure in the head by approximately 15% at 1900 MHz. The hand when added to the head-earring model alters the averaged 1 g SAR due to increased dielectric loading, absorption and also due to the reflection at the hand-dielectric boundary. Results also show that the hand becomes more significant with a PIFA antenna as the radiating source due to the position of the hand is substantially closer to the radiating elements of the PIFA antenna. The effect of the combination of the hand, the earring and the finger ring only show minor difference on the SAR values (compared to the head-hand-earring cases) at both frequencies tested.

7.1.2 Effects on the antenna radiation patterns and efficiencies

The effect of the head, hand and metallic jewellery items on the antenna radiation patterns are also presented in this thesis. In the presence of the head, the antenna radiation pattern was significantly influenced along the direction of the head (y-direction) due to a quite large fraction of the energy being absorbed by the head. The hand when added to the model (head only) further modified the radiation pattern since the hand that holds the handset body absorbs and reflects part of the radiated energy. Adding metallic rings to the hand shows only minor effects on the radiation pattern

for the frequencies considered in this thesis. There was also found to be very little difference for the results between the ring positions on the fingers. It seems likely that this is because the size of the ring is relatively small compared to the wavelength and its relative orientation and location to the radiation source makes coupling unfavorable in the situations investigated. The earrings when pierced into the earlobe can alter the antenna radiation performance, but the effect will be variable depending on the earring's diameter, the type of antenna and the frequency in use, and also the presence of the hand. Smaller earrings with diameters of 25, 30 and 40 mm show very similar and mostly insignificant effects on the antenna radiation pattern. However, larger earrings with a diameter of 1/4-1/3 of the wavelength do noticeably alter the radiation pattern, particularly in the direction where the earring is placed (in z-direction of this configuration). The combination of all three metallic jewellery items can also alter the radiation pattern a little, but overall the effect appears to be less significant.

Placement of the mobile handset close to the head results in an efficiency dropped by 9% and 17% compared to no head at 900 and 1900 MHz respectively for a monopole antenna as the radiating source, while 22% and 13% 900 and 1900 MHz respectively when a PIFA antenna was used as the radiating source. The hand when included into the system further alters the radiation efficiencies at both 900 MHz and 1900 MHz. The inclusion of a metallic ring or earring show only marginal difference to the radiation efficiency of the system. Only localized SAR seems to be affected by the rings or the earrings whilst no important effect was observed on the radiation pattern and the efficiency suggests no large overall effect by the metallic rings and earrings especially when the hand is included in the simulation model.

7.1.3 SAR measurements

The effect of the hand and metallic jewellery items were also investigated using the DASY4 measurement system. A novel liquid hand phantom with fingers was manufactured which allows the effect of metallic rings to be further investigated. The manufactured hand phantom is very useful since it strikes an ordinary pose of holding

a mobile handset and can be used next to the head phantom. It also provides high repeatability due to its fixed shape and the ability to 'hold' the handset unit. The hand phantom also allows different tissue simulating liquids to be applied for measuring different frequencies. As in the earlier simulations, different sizes of earrings were used in the measurement, whilst the ring is placed on different fingers for comparison. Generally, the trend of the effect of the hand, the earring and the ring shows agreement with the simulations; however there are significant differences in the amplitude of the averaged 1 g SAR between the two methods which have been discussed in detail in Chapter 6. Further simulations were made by introducing a realistic 2 mm distance between the antenna and the head further supports the conclusion in Chapter 4 and 5.

7.1.4 Final conclusions

From these results, it can be concluded that wearing metallic rings on the human hand could possibly be beneficial to the users of a mobile handset as it seems to decrease the amount of energy absorbed inside the human head. Meanwhile, both the rings and the bangle are unlikely to affect the antenna radiation performance to any large extent, unless they are close to the radiating element. Wearing a smaller earring has very little effect on SAR and on the antenna performance, whereas the earrings of diameter 1/4-1/3 of the wavelength (of the corresponding frequency) could notably alter the antenna radiation pattern and could also lead to enhance the local SAR near to edge where the earring pierces the earlobe. However, no increased in SAR deeper in the head due to the metallic earring is in evidence. These results may also benefit to the manufacturers of mobile handset and the jewellers since the results do not seem to suggest a significant problem with the SAR values and fields only being affected slightly by the presence of the metallic ring and earrings. However, care should be taken since there is a general trend for higher frequency communication devices and the influence of metallic jewellery items may be more significant due to resonance effects. Nevertheless, the thesis has showed that the human hand could significantly modify the antenna radiation patterns and the SAR. Hence, there is a general trend of internal handset antenna for communication devices, thus PIFA antennas are a

popular choice due to their low-cost, low-profile and because the free-space radiation pattern shows a lower gain in the direction of the head. Consequently, the effect of the hand could be very significant due to the hand and fingers situated very close to the large area of the PIFA radiating elements. Therefore, it is important that the hand is considered during the antenna design and the compliance testing.

7.2   Future works recommendation

This thesis has produced original work, containing several new results which to the author's knowledge have not previously been reported in the literature. Based on this research study, there are still a lot of areas that seem worthy of study for future investigations.

Further works can be done to investigate the effect of metallic jewellery items worn on the human body by utilising the more up to date commercial model of a mobile handset as the radiating source. This can be a representation of a real-world in-use condition since the realistic mobile handset model may define the correct head-antenna, hand-antenna and jewellery-antenna distance in an ordinary use. The effect of metallic jewellery items can also be further studied over a wide range of frequencies; hence there is a general trend for higher frequency communication devices and the effect of metallic jewellery items may be more significant due to resonance effects.

In this thesis, a novel liquid hand phantom has been manufactured for the measurements, whereas different hand model was used in the computer simulations due to the difficulty of producing an analysis model from the available CAD data. Further works can be done to overcome this problem, since it is very useful if an identical model of the hand is used in both methods to allow more precise comparisons between the simulations and measurements.

There are a number of studies which have focused on the effect of metallic spectacles, metallic implants and metallic jewellery items (earrings, nose rings, rings and

eyebrow piercing). However, none of them has considered the human hand. As the hand has been found to significantly affect the antenna radiation performance and SAR; further research of the effects of the above mentioned metallic objects can be carried out by considering the presence of the human hand holding the handset unit. Thus, it may be interesting to investigate how the hand could modify the effect brought about by the metallic spectacles or the metallic implants.

List of Publications

[1] N. A. Samsuri and J. A. Flint, "On the effect of jewelry rings on specific absorption rate (SAR)," *Antennas and Propagation Conference, LAPC 2006, Loughborough,* pp. 421 – 424, 11-12 Apr. 2006.

[2] N. A. Samsuri and J. A. Flint, "The effect of loop-like jewellery items worn on human hand on SAR for a 900 MHz cellular handset," *5th European Workshop on Conformal Antennas (EWCA07), Bristol,* 10-11 Sept. 2007.

[3] N. A. Samsuri and J. A. Flint, "A study on the effect of a metallic ring worn on human fingers using a simple scannable block hand phantom (SAR)," *Antennas and Propagation Conference, LAPC 2008, Loughborough,* pp. 285 – 288, 17-18 Mar. 2008.

[4] N. A. Samsuri and J. A. Flint, "A study on the effect of loop-like jewellery items worn on human hand on Specific Absorption Rate (SAR) at 1900 MHz," *Antennas and Propagation Conference, LAPC 2008, Loughborough,* pp. 297 – 300, 17-18 Mar. 2008.

Appendix A

Table A.1: Different sizes of finger rings commercially available over different countries.

Diam. in mm	Circumf. in mm	US Size	British / Aust.	French	German	Japanese	Swiss
11.95	-	1/2	A	-	-	-	-
12.37	38.9	1	B	-	-	1	-
12.78	40.2	1 1/2	C	-	-	-	-
13.00	40.8	1 3/4	C 1/2	-	-	-	-
13.21	41.5	2	D	41 1/2	13 1/2	2	1 1/2
13.61	42.7	2 1/2	E	42 3/4	13 3/4	3	2 3/4
13.83	43.4	2 3/4	E 1/2	-	-	-	-
14.05	44.0	3	F	44	14	4	4
14.36	44.9	3 3/8	G	45 1/4	-	5	5 1/4
14.65	45.9	3 3/4	H	46 1/2	-	-	6 1/2
14.86	46.5	4	H 1/2	-	15	7	-
15.04	47.1	4 1/4	I	47 3/4	-	-	7 3/4
15.27	47.8	4 1/2	I ½	-	15 1/4	8	-
15.40	48.1	4 5/8	J	49	15 1/2	-	9
15.70	49.0	5	J ½	-	15 3/4	9	-
15.80	49.3	5 1/8	K	50	-	-	10
160.0	50.0	5 3/8	K 1/2	-	-	10	-
16.10	50.3	5 1/2	L	51 3/4	16	-	11 3/4
16.41	51.3	5 7/8	L 1/2	-	-	-	-
16.51	51.5	6	M	52 3/4	16 1/2	12	12 3/4
16.92	52.8	6 1/2	N	54	17	13	14
17.13	53.4	6 3/4	N 1/2	-	-	-	-
17.35	54.0	7	O	55 1/4	17 1/4	14	15 1/4
17.45	54.7	7 1/4	O 1/2	-	-	-	-
17.75	55.3	7 1/2	P	56 1/2	17 3/4	15	16 1/2
18.19	56.6	8	Q	57 3/4	18	16	17 3/4
18.61	58.4	8 5/8	R	59	-	-	19
19.10	59.4	9 1/8	S	60 1/4	-	-	20 1/4
19.51	60.6	9 5/8	T	61 1/2	-	-	21 ½
19.84	61.6	10	T 1/2	-	20	20	-
20.02	62.2	10 1/4	U	62 3/4	-	21	22 3/4
20.32	63.1	10 5/8	V	63	-	-	23 3/4
20.68	64.1	11	V 1/2	-	20 3/4	23	-
20.76	64.3	11 1/8	W	65	-	-	25
21.18	65.7	11 5/8	X	66 1/4	-	-	26 1/4
21.49	66.6	12	Y	67 1/2	21 1/4	25	27 ½
21.69	67.2	12 1/4	Y 1/2	-	-	-	-
21.89	67.9	12 1/2	Z	68 3/4	21 3/4	26	28 3/4
22.10	68.5	12 3/4	Z 1/2	-	-	-	-
22.33	69.1	13	-	-	22	27	-

Table A.2: Different sizes of bangles.

Item	Size	Diameter (inch)	Circumference (inch)
		Bangles	Bracelets
Bangle/Bracelet	Very Small	2-2/16"	6.67"
Bangle/Bracelet	Small	2-4/16"	7.06"
Bangle/Bracelet	Medium	2-6/16"	7.45"
Bangle/Bracelet	Medium Plus	2-8/16"	7.85"
Bangle/Bracelet	Large	2-10/16"	8.24"
Bangle/Bracelet	Extra Large	2-12/16"	8.63"
Men's Bangle or Kara	Large	2-14/16"	9.02"
Men's Bangle or Kara	Extra Large	3.0"	9.42

Appendix B

Radiation patterns for a monopole antenna (xy-plane)
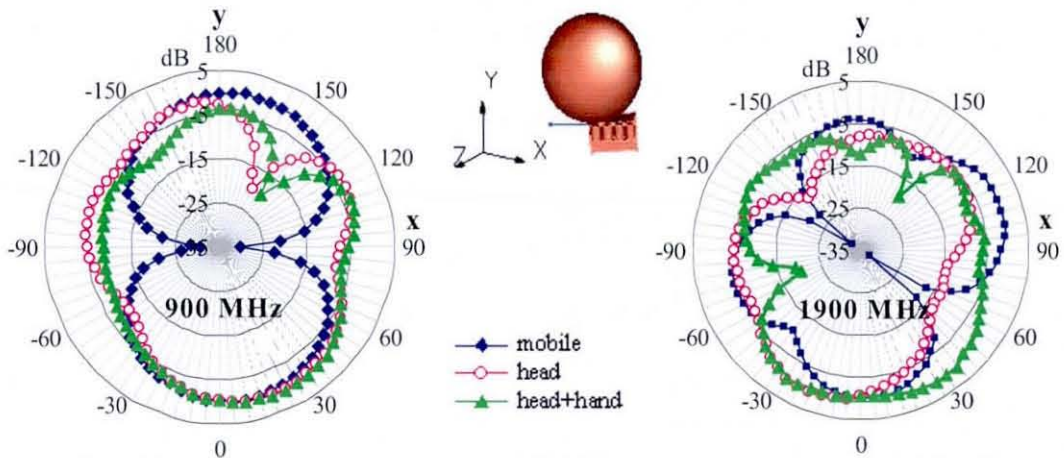## (Chapter 4)

Figure B.1: The antenna radiation pattern at 900 MHz (left) and 1900 MHz (right) with and without the head and the hand (xy-plane).
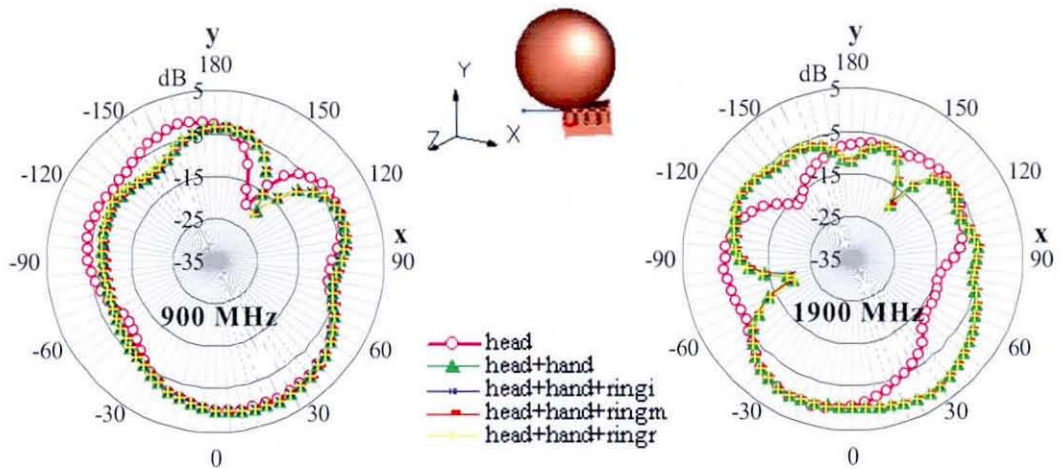

Figure B.2: The radiation pattern at 900 MHz (left) and 1900 MHz (right) with the head and hand. A metallic ring is worn on different fingers for comparison (xy-plane).
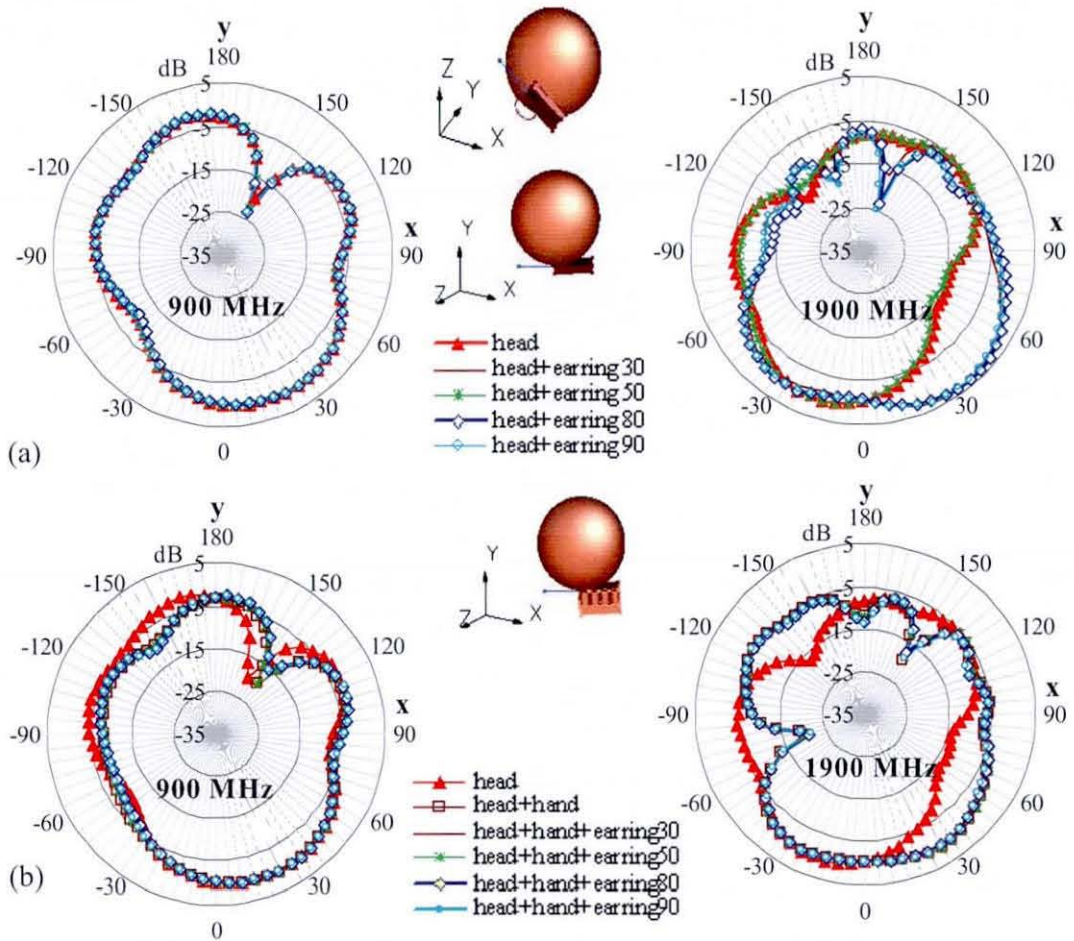
Figure B.3: Radiation patterns for a monopole antenna at 900 MHz (left) and 1900 MHz (right) when placed close to the spherical head. Metallic earrings attached on the right hand side of the head (a) without the hand, (b) with the hand (xy-plane).
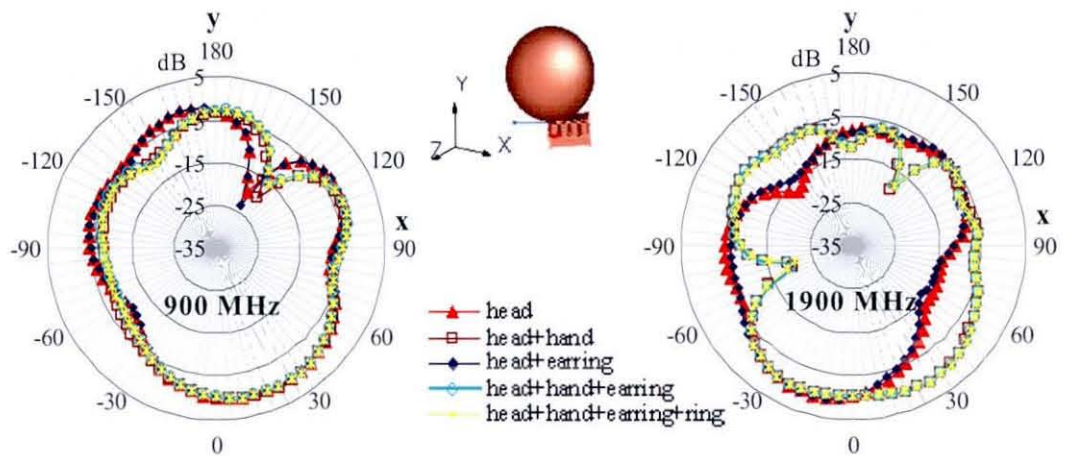

Figure B.4: Radiation patterns for a monopole antenna at 900 MHz (left) and 1900 MHz (right) when placed close to the spherical head. In this simulation, the effect of the combination of the earring and ring were investigated (xy-plane).

Appendix C

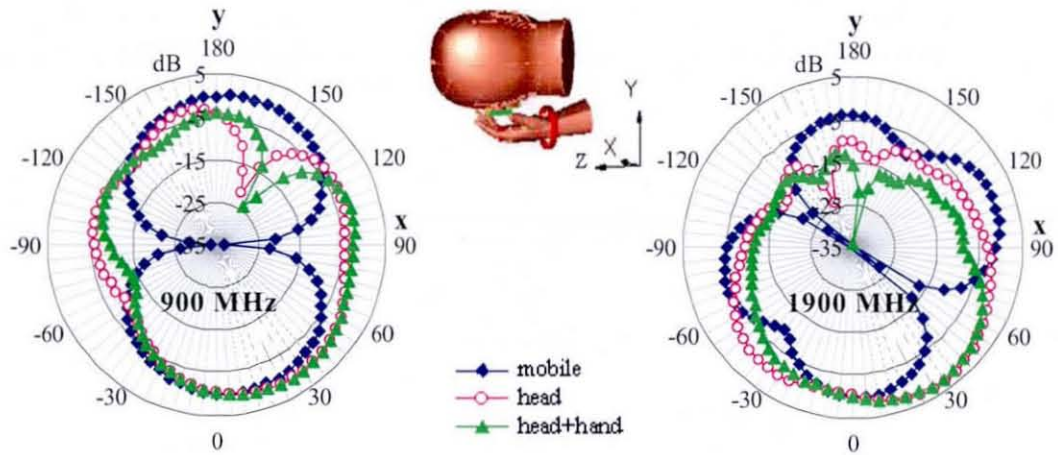## C.1 Radiation patterns for a monopole antenna (xy-plane) (Chapter 5)

Figure C.1: A monopole antenna radiation patterns at 900 MHz (left) and 1900 MHz (right) with and without the head and the hand (xy-plane).

Figure C.2: A monopole antenna radiation patterns at 900 MHz (left) and 1900 MHz (right) with and without the head and the hand worn a ring (with and without the bangle) (xy-plane).

Figure C.3: Radiation patterns for a monopole antenna at 900 MHz (left) and 1900 MHz (right) when place close to the SAM head (xy-plane). The earrings penetrate the earlobe in the model (a) without the hand, (b) with the hand and (c) with the hand wearing a ring and the bangle.

C.2 Radiation patterns for a PIFA antenna (xy-plane)

(Chapter 5)
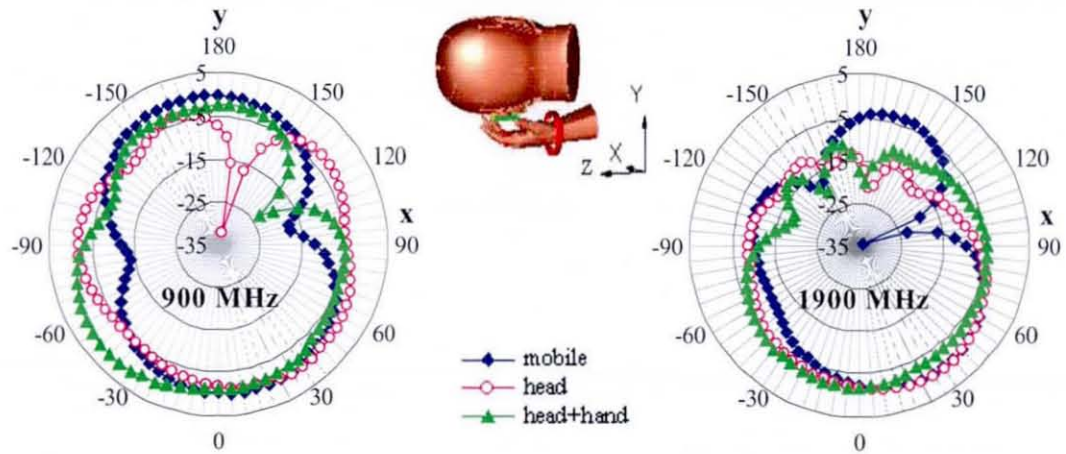
Figure C.4: A PIFA radiation patterns at 900 MHz (left) and 1900 MHz (right) with and without the head and the hand (xy-plane).
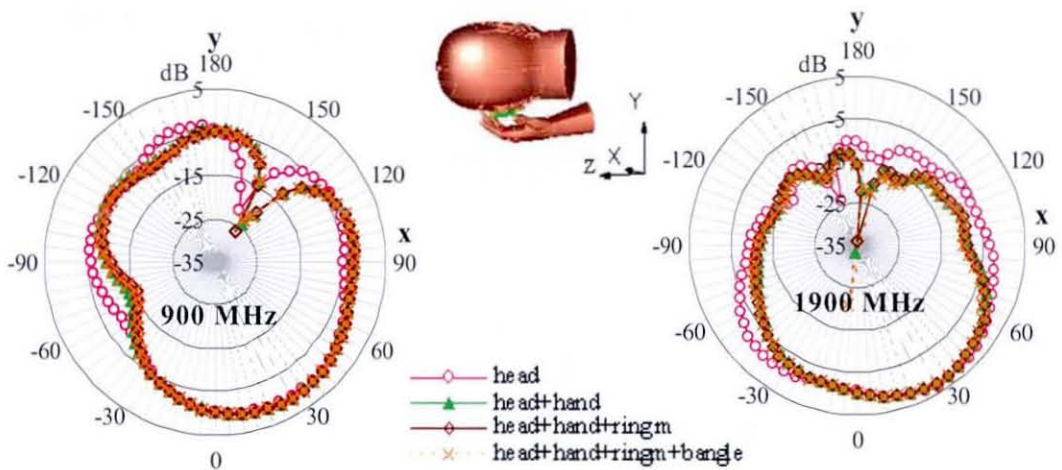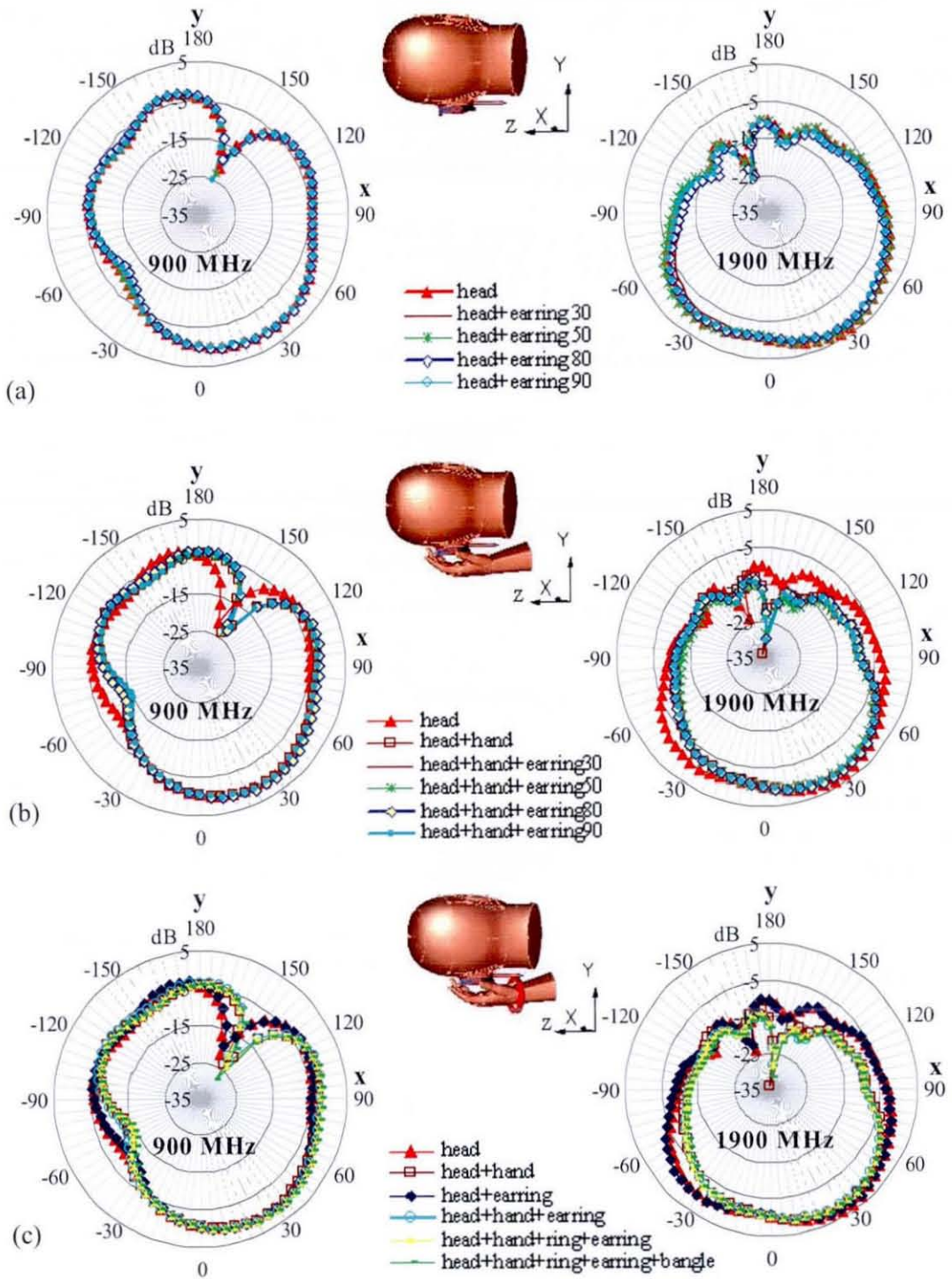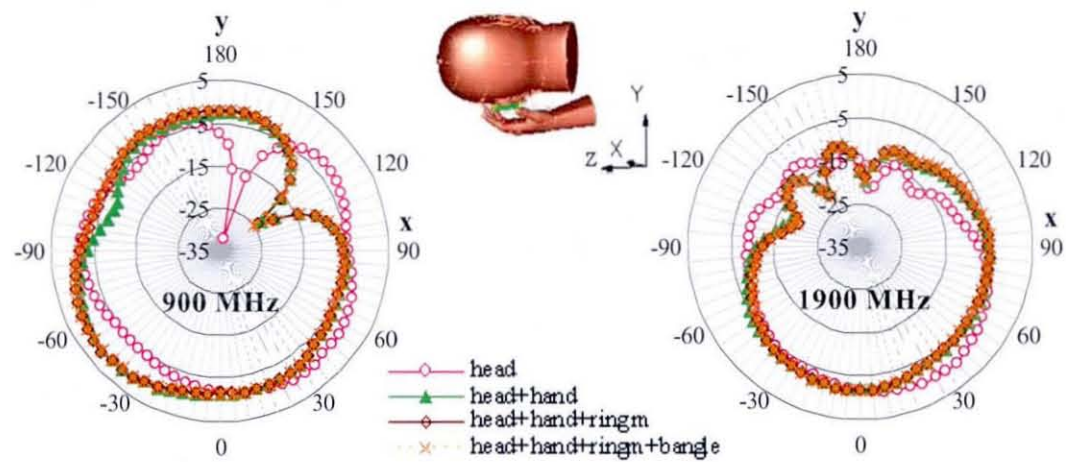

Figure C.5: A PIFA radiation patterns at 900 MHz (left) and 1900 MHz (right) with and without the head and the hand worn a ring (with and without the bangle) (xy-plane).

Figure C.6: Radiation patterns for a PIFA antenna at 900 MHz (left) and 1900 MHz (right) when place close to the SAM head (xy-plane). The earrings penetrate the earlobe in the model (a) without the hand, (b) with the hand and (c) with the hand wearing a ring and the bangle.
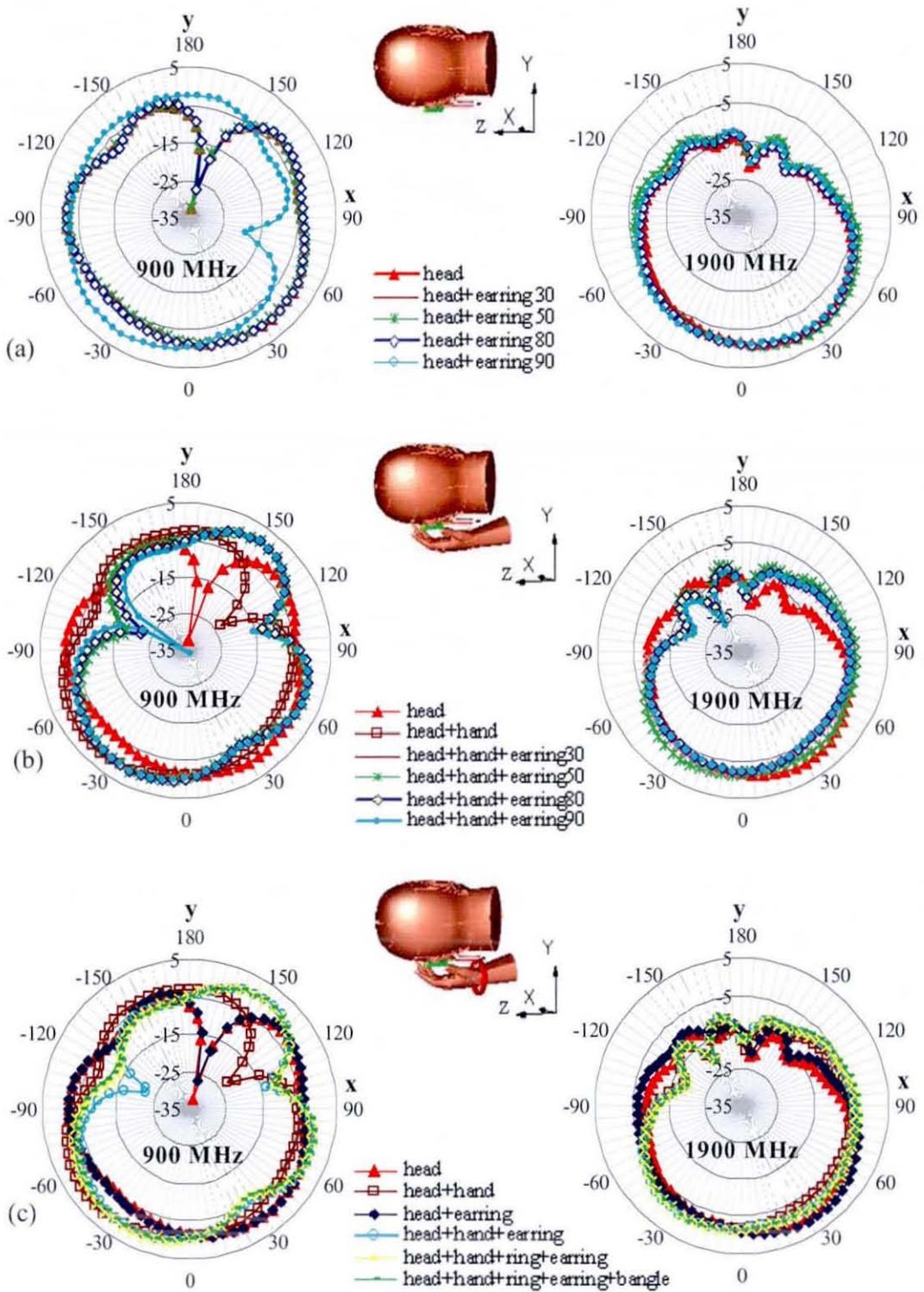
Appendix D

D.1 Hand and fingers dimensions

Table D.1: The hand and finger length of 15 people selected randomly from the locality.

| Person	length (mm)	l1	l2	l3	r1	r2	r3	m1	m2	m3	i1	i2	i3	t1	t2
								(mm)							
1	177	22	18	21	26	23	29	26	25	30	25	22	24	30	24
2	170	23	19	15	23	22	22	27	22	24	23	19	23	28	18
3	194	23	19	20	29	29	29	28	29	31	30	29	30	29	30
4	181	25	14	15	30	20	23	31	22	25	30	19	22	35	16
5	183	24	20	18	26	26	25	32	24	23	28	22	21	31	21
6	186	27	18	15	30	23	27	31	25	26	29	29	28	38	18
7	188	22	12	19	27	19	26	29	25	26	33	18	20	37	16
8	188	28	13	19	30	20	32	28	25	33	27	21	28	33	22
9	183	23	20	22	26	27	29	28	26	28	27	22	26	30	18
10	203	30	19	19	31	23	29	29	30	29	31	29	27	33	22
11	181	27	18	14	28	23	22	26	29	25	29	23	23	34	20
12	198	21	24	23	27	29	28	27	28	28	22	30	22	35	25
13	184	25	18	17	26	26	27	29	26	27	29	24	28	30	17
14	212	27	24	22	30	31	26	30	36	30	31	30	27	37	29
15	195	25	17	19	28	26	25	27	26	29	29	24	24	32	23

The person who had his hand cast
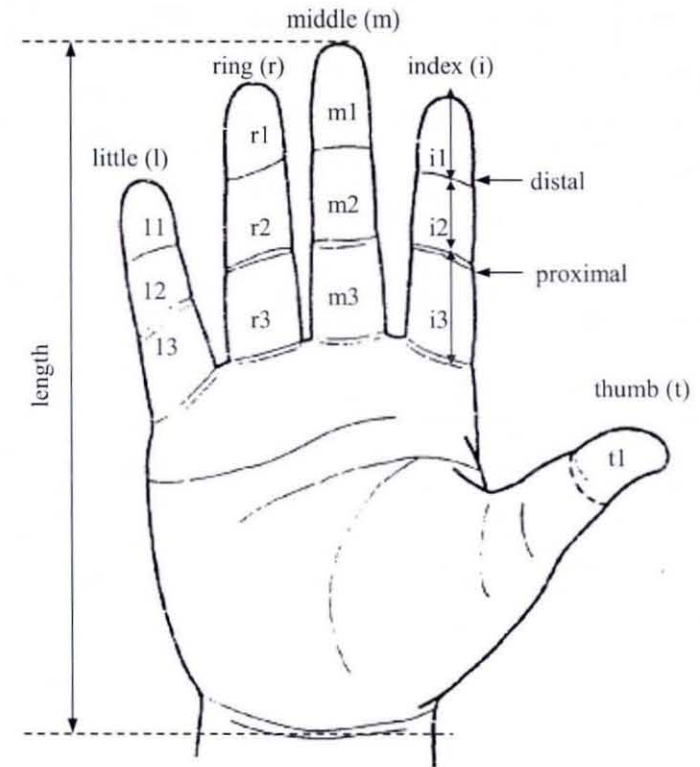
Table D.2: The hand and finger breadth of 15 people selected randomly from the locality.

Person	palm	Little		ring		middle		index		thumb
	(mm)	distal	proximal	distal	proximal	distal	proximal	distal	proximal	distal
1	76	14	15	14	17	15	17	17	18	20
2	70	12	15	15	17	16	18	15	17	19
3	85	15	18	16	20	17	19	18	20	20
4	83	13	15	15	19	17	19	18	20	21
5	86	15	17	18	20	18	21	20	22	21
6	88	15	17	16	19	18	20	19	21	21
7	86	17	19	16	19	18	21	18	20	22
8	82	15	17	16	19	18	21	18	21	21
9	89	16	18	16	18	17	19	18	21	20
10	97	16	18	19	21	20	24	20	22	24
11	83	15	17	16	19	17	20	18	21	20
12	92	16	19	18	21	20	24	20	23	21
13	84	13	15	14	17	15	19	16	18	20
14	100	19	20	19	22	20	23	20	23	24
15	85	17	19	17	19	19	21	18	21	20

The person who had his hand cast

middle (m)

ring (r) index (i)

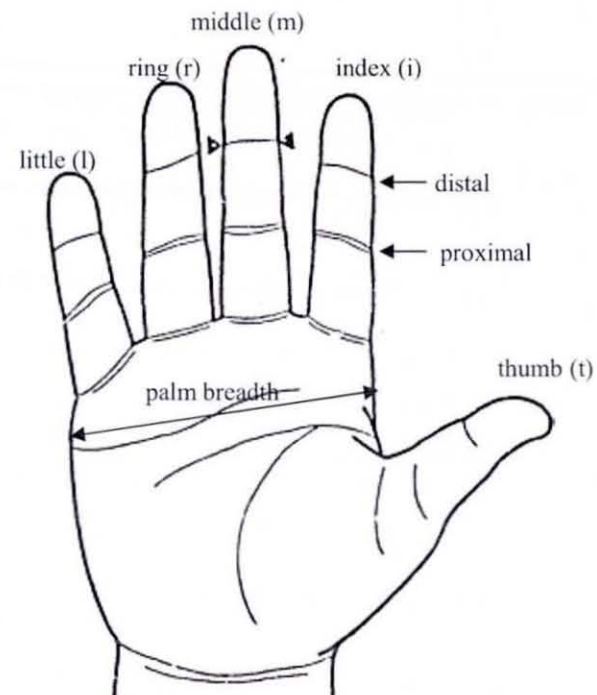little (l)

distal

proximal

thumb (t)

palm breadth

Table D.3: Comparison between the hand and finger dimension of an individual selected from the group of 15 to the U.S. Army anthropometric data (1991)[*]

Hand dimension		Length (mm)			
		US Army	Person15	Dti	
				Right	Left
hand	Length	194.3	195.0	176.5	175.6
little	l1	27.3	25.0		
	l2	17.5	17.0		
	l3	19.9	19.0		
ring	r1	29.6	28.0		
	r2	24.3	26.0		
	r3	25.3	25.0		
middle	m1	28.4	27.0		
	m2	26.4	26.0		
	m3	29.0	29.0		
index	i1	28.4	29.0		
	i2	22.6	24.0		
	i3	24.3	24.0		
thumb	t1	34.5	32.0		
	t2	21.1	23.0		
	t3	14.0			

Hand dimension		Length (mm)			
		US Army	Person15	Dti	
				Right	Left
palm	breadth	83.0	85.0	90.5	89.9
little	distal	17.4	17.0	15.7	15.1
	proximal	19.2	19.0	17.7	16.9
ring	distal	18.5	17.0	16.9	16.4
	proximal	21.4	19.0	20.2	19.3
middle	distal	19.8	19.0	18.0	17.6
	proximal	22.5	21.0	21.2	20.8
index	distal	20.1	18.0	18.3	18.1
	proximal	23.0	21.0	21.0	20.9
thumb	distal		20.0	21.6	21.8

[*] T. M. Greiner. (Dec. 1991, Hand anthropometry of U.S. army personnel. *Army Natick Research Development and Engineering Center MA* [http://handle.dtic.mil/100.2/ADA244533].

D.2 Moulding process[†]

Six part of water to one alginate was used for this hand phantom construction

Measure the water and put into a container

Weigh the alginate

Add the alginate a bit at a time. Keep mixing until the mix gets very smooth

Mixing

The hand is moistened before putting it in. Insert the hand slowly and work it around in the alginate to minimize air bubbles. Strike the intended pose

Put the hand in

Wait for the alginate to set. Pull the hand out slowly

Mix the plaster as per the directions indicated by the manufacturer

Mix the plaster and pour slowly into the mold

Wait overnight for the plaster to set up

Remove the alginate, using a wooden stick to remove the smaller pieces

Remove the mold from the container-break the mold

[†] Full instruction and figures can be found here: http://www.bnglifecasting.com/diy/hand/index.html
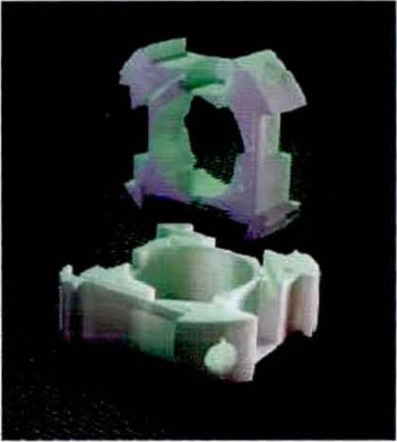
D.3 *DuraForm Polyamide (PA)*$^{\psi}$

DuraForm Polyamide (PA) descriptions and technical data, nylon material used to manufacture the hand phantom employed in this thesis.

DuraForm® PA & GF plastic
for use with all SLS® systems

3D SYSTEMS

Automatically produce durable, high-quality thermoplastic parts for functional use and testing with DuraForm material and an SLS system — from 3D Systems

BENEFITS

Outstanding functional performance
DuraForm PA and DuraForm GF plastics are used with SLS systems to produce rugged thermoplastic parts that withstand aggressive functional use in both rapid manufacturing and prototyping applications. In addition to rugged durability, DuraForm PA and GF materials also produce high quality, complex parts with excellent surface finish and feature detail.

DuraForm PA material is also USP Level VI certified for brief in-vivo exposure; it can be used for modeling and testing surgical devices, and can be sterilized with an autoclave.

APPLICATIONS

- Complex production or prototype plastic parts
- Form, fit or functional prototypes
- Applications where stiffness is required
- Heat and chemical resistance testing
- Snap-fit assemblies
- Durable patterns for sandcasting & silicone tooling
- USP Level VI certified for brief in-vivo exposure
- Parts requiring machining, welding, or joining with glue

Choose DuraForm GF material for adverse testing conditions.
DuraForm GF material's increased stiffness, heat resistance, and mechanical integrity make it a perfect material for extreme testing conditions. As an example, a connector with snap fits, hinges and locking cams produced with DuraForm GF recently withstood temperatures up to 100°C and an electrical charge of 460 Amps (twice the amperage withstood by the final production part).

Eliminate tooling and enjoy the many benefits of rapid manufacturing
Companies worldwide are realizing the benefits of rapid manufacturing, and producing economical batch-quantities of DuraForm PA plastic parts with their SLS systems for a variety of production applications. Producing batch-quantities of plastic parts on an SLS system is an economical, fast, and beneficial manufacturing method - and eliminates tooling time and cost, reduces inventory holding costs, and reduces or eliminates labor for assembly operations compared to previous traditional manufacturing methods. With tool-less manufacturing, design changes can be incorporated up to the last minute — without the normal penalty for associated tooling.

3D SYSTEMS CORPORATION

(**TRANSFORM YOUR PRODUCTS**)

$^{\psi}$ source: http://www.acucast.com/pdf/DS-DuraForm_LS_mat-US_Engl_0405.pdf

DuraForm PA and **Duraform GF** plastic

For use with all SLS systems

TECHNICAL DATA

Powder Properties

PROPERTIES	CONDITION	UNITS	TEST METHOD	PA	GF
Density	Tap	g/cm^3	ASTM D4164	0.59	0.84
Particle Size Average [1]		μm	Laser Diffraction	58	48
Particle Size Range [1]	90%	μm	Laser Diffraction	25-62	15-96
Specific Gravity	23 °C		ASTM D792	0.97	1.40
Moisture Absorption	23 °C	%	ASTM D570	0.41	0.30

Thermal Properties

PROPERTIES	CONDITION	UNITS	TEST METHOD	PA	GF
Melting Point:	T_m	°C	DSC	184	185
D UL	0.45 MPa	°C	ASTM D648	177	175
DTUL	1.82 MPa	°C	ASTM D648	86	110

Mechanical Properties

PROPERTIES	CONDITION	UNITS	TEST METHOD	PA	GF
Tensile Strength		MPa	ASTM D638	44	38.1
Tensile Modulus		MPa	ASTM D638	1600	5910
Tensile Elongation at Break		%	ASTM D638	9	2
Flexural Modulus		MPa	ASTM D790	1285	5500
Impact Strength	Notched Izod	J/m	ASTM D256	214	96
	Unnotched Izod	J/m	ASTM D256	420	101

Surface Finish

PROPERTIES	CONDITION	UNITS	TEST METHOD	PA	GF
Facing	As Processed (R_a)	μm		8.5	6.2
	After Polishing (R_a)	μm		0.13	1.0

Chemical Resistance

PROPERTIES	CONDITION	UNITS	TEST METHOD	PA	GF
	Alkalines, hydrocarbons, fuels and solvents				

Electrical Properties

PROPERTIES	CONDITION	UNITS	TEST METHOD	PA	GF
Volume Resistivity	22°C, 50% RH, 500V	ohm x cm	ASTM D257-93	3.1x10^{14}	2.06Ex10^7
Surface Resistivity	22°C, 50% RH, 500V	ohm x cm	ASTM D257-93	3.0x10^{14}	2.3Ex10^7
Dielectric Constant	22°C, 50% RH, 500V		D150 95	2.9	3.7
Dielectric Strength		v/mm	D149-95a	1.6x10^4	1.5Ex10^7
Comparative Tracking Index		V	D5289-92	595, TI-Cu and/or IEC Standard	TDD <1mm depth

(1) Results are based upon volume distribution of particles.

Data was generated from the testing of parts produced with the DuraForm material under typical processing conditions. (New materials processed at 4 watts laser power, 16mm/sec scan speed, 0.1 mm scan spacing, 0.1 mm layer thickness on a Sinterstation° 2500 SLS system. Expected shelf life of this material is at least twelve months, when stored in dry conditions at ambient temperature.